Quantum Corpuscular Approach to Solutions in Gravity and Field Theory

Tehseen Rug

München 2016

Quantum Corpuscular Approach to Solutions in Gravity and Field Theory

Tehseen Rug

Dissertation
an der Fakulät für theoretische Physik
der Ludwig–Maximilians–Universität
München

vorgelegt von
Tehseen Rug
aus München

München, den 25. Februar 2016

Erstgutachter: Prof. Dr. Gia Dvali
Zweitgutachter: Prof. Dr. Stefan Hofmann
Tag der mündlichen Prüfung: 18. April 2016

Contents

List of Figures

Zusammenfassung

Wir formulieren eine Quantentheorie von Lösungen in Gravitation und Feldtheorie basierend auf einer großen Anzahl von Konstituentenfreiheitsgraden. Solch eine Beschreibung wird auf zwei verschiedene Arten realisiert.

Im ersten Teil stellen wir die sogenannte Hilfsstrombeschreibung vor. Die grundlegende Idee besteht darin, den wahren quantenmechanischen Zustand der Lösung die man betrachtet, durch einen multilokalen zusammengesetzten Operator der Felder der mikroskopischen Theorie zu representieren. Obwohl dieser Ansatz komplett allgemein ist, werden wir hauptächlich daran interessiert sein, schwarze Löcher als gebundene Gravitonzustände aufzufassen. Wir zeigen, dass die Masse des schwarzen Lochs mikroskopisch gesehen ein kollektiver Effekt von N Gravitonen ist, welche das schwarze Loch zusammensetzen. Um dies zu demonstrieren, berechnen wir Observablen, welche mit dem Inneren des schwarzen Lochs in Zusammenhang stehen, wie die Konstituenten- oder die Energiedichte von Gravitonen. Als nächster Schritt wird gezeigt, wie diese Observablen in S-Matrix Prozesse eingebettet werden können. Insbesondere wird gezeigt, dass ein Beobachter außerhalb des schwarzen Lochs Zugang zu dessen Innerem hat indem er Streuexperimente durchführt. Durch Messung des Wirkungsquerschnittes für die Streuung von Teilchen am schwarzen Loch, ist ein außenstehender Beobachter sensitiv auf die Verteilung von Gravitonen im schwarzen Loch. Mögliche Implikationenen dieses Resultates im Bezug auf das Informationsparadoxon werden diskutiert. Schließlich zeigen wir, wie geometrische Konzepte, und insbesondere die Schwarzschild-Lösung, sich als effektive Beschreibung aus unserer Konstruktion herleiten lassen.

Im zweiten Teil wird in alternativer Ansatz basierend auf kohärenten Zuständen präsentiert. Zuerst wenden wir diese Logik auf Solitonen in Feldtheorie an. Insbesondere zeigen wir explizit, wie wohlbekannte Eigenschaften von Solitonen zum Beispiel deren Wechselwirkung, Zerfall des falschen Vakuums, oder Erhaltung topologischer Ladung als simple Konsequenz der grundlegenden Eigenschaften von kohärenten Zuständen folgen. Darauf folgend entwickeln wir ein ähnliches quantenmechanisches Bild von Instantonen. Da Instantonen als Solitonen in einer weiteren räumlichen Dimension verstanden werden können, welche sich in euklidischer Zeit entwickeln, impliziert eine Beschreibung von Solitonen, basierend auf kohärenten Zuständen, dass Instantonen auf eine ähnliche Weise beschrieben werden sollten. Darauf aufbauend entwickeln wir ein neuartiges quantenmechanisches Verständnis im Bezug auf die Physik von Instanton-induzierten Übergängen und dem Konzept von "Resurgence". Zum Schluss betrachten wir Solitonen in supersymmetrischen

Theorien. Es wird gezeigt, dass die korpuskulären Effekte zu einem neuen Supersymmetriebrechungsmechanismus führen, welcher niemals in der semi-klassischen Behandlung gesehen werden kann.

In letzten Abschnitt der Arbeit lösen wir Anti-de Sitter (AdS) als kohärenten Zustand auf. Einerseits werden wir erklären, wie wohlbekannte holographische und geometrische Eigenschaften einfach verstanden werden können durch die Besetzungszahl von Gravitonen im Zustand. Andererseits berechnen wir explizit korpuskuläre Korrekturen zum skaralen Propagator in AdS. Zusätzlich wird gezeigt, dass korpuskuläre Effekte zu Abweichungen der Thermalität führen, die ein Unruh-Beobachter in AdS misst.

Abstract

We formulate a quantum theory of classical solutions in gravity and field theory in terms of a large number of constituent degrees of freedom. The description is realized in two different ways.

In the first part we introduce the so-called auxiliary current description. The basic idea is to represent the true quantum state of the solution one considers in terms of a multi-local composite operator of the fields of the microscopic theory. Although the approach is completely general, we will be mostly interested in representing black holes as bound states of a large number of gravitons. We show how the mass of the black hole arises microscopically as a collective effect of N gravitons composing the bound state. For that purpose we compute observables associated to the black hole interior such as the constituent density of gravitons and their energy density, respectively. As a next step, it is shown how these observables can be embedded within S-matrix processes. In particular, it is demonstrated that an outside observer has access to the black hole interior doing scattering experiments. Measuring the cross section for the scattering of particles on black holes, the outside observer is sensitive to the distribution of gravitons in the black hole. Possible implications concerning the information paradox are discussed. Finally, we show how geometric concepts, and in particular the Schwarzschild solution emerge as an effective description derived from our construction.

In the second part, an alternative approach based on coherent states in presented. First, we apply our reasoning to solitons in field theory. In particular, we explicitly show how well-known properties of solitons such as interactions, false vacuum decay or conservation of topological charge follow easily from the basic properties of coherent states. Secondly, we develop in detail a similar quantum picture of instantons. Since instantons can be understood in terms of solitons in one more spatial dimension evolving in Euclidean time, a coherent state description of the latter implies a similar description of the former. Using the coherent state picture we develop a novel quantum mechanical understanding of the physics of instanton-induced transitions and the concept of resurgence. Finally, we consider solitons in supersymmetric theories. It is shown that the corpuscular effects lead to a novel mechanism of supersymmetry breaking which can never be accounted for in the semi-classical approach.

In the last part of the thesis we resolve anti-de Sitter (AdS) space-time as a coherent state. On the one hand, we explain how well-known holographic and geometric properties can easily be understood in terms of the occupation number of gravitons in the state. On

the other hand, we explicitly compute corpuscular corrections to the scalar propagator in AdS. Furthermore, it is shown that corpuscular effects lead to deviations from thermality an Unruh observer in AdS measures.

Chapter 1

Introduction

1.1 Classicality versus Quantumness

In recent years the standard models of particle physics and cosmology were tested with a precision which had not been seen before. While the Large Hadron Collider provides striking evidence for the quantum nature of fundamental interactions [1], observations from Planck and WMAP indicate that inflation could be the true mechanism of generation of density perturbations [2]. In particular, the measurement of the spectral index substantiates the prediction that these perturbations are due to quantum fluctuations in the early universe which are stretched to macroscopic scales via an epoch of inflationary expansion.

While these experiments show that nature operates according to the laws of quantum field theory at the fundamental level, it is still common wisdom to approximate physical reality by (semi)-classical calculations. The question whether such an approximation is valid is of course related to the typical length scales that we probe in an experiment. In particular, one would assume a classical calculation to be a good approximation to physical reality as long as its action is much larger than Planck's constant $\hbar$. Namely, in such a situation only the classical path effectively contributes to the functional integral of the system one considers.

A different situation where a semi-classical computation is supposed to give an accurate result is connected to the physics of bound states or condensates. Such systems are usually characterized by the occupation number N of microscopic degrees of freedom. If this number is large, quantum effects are usually suppressed as powers of $1/N$. Formally speaking, in the limit $N \to \infty$, there is no difference between creation and annihilation operators for the microscopic degrees of freedom. Therefore, operators can be safely replaced by c-numbers giving rise to classical physics.

Let us, for example, consider the electric field of a laser. At a microscopic level it is clear that the system can be described as a coherent state of a large number N of longitudinal and temporal photons in one mode. Due to the large occupancy, one usually neglects the effects related to finiteness of N. Technically, this amounts to replacing the quantum coherent state by a classical electric field of high intensity giving rise to an action much larger than $\hbar$. This example already indicates that when going from quantum to semi-classical we no longer take the microscopic structure of the system into account. In other words, the limit $N \to \infty$ does no longer allow for a resolution of the underlying micro-physics.

Notice, however, that as long as $\hbar$ is finite quantum effects are not completely decoupled. In particular, one can still consider quantum fluctuations in the fixed background electric field. Such considerations, for example, let to the discovery of the famous Schwinger pair creation effect [3]. Thus, although backreaction on the background field is neglected as we take $N \to \infty$, finiteness of $\hbar$ still allows for non-trivial quantum effects. In other words, one is working at the level of semi-classicality. Only if we take $\hbar \to 0$ the system becomes truly classical and all possible quantum effects vanish.

Let us now consider a different example where one would naively expect a classical or semi-classical description to capture the relevant physics, namely large black holes. For simplicity let us look at asymptotically flat Schwarzschild black holes. The action of this

solution in $3+1$ dimension scales as $(r_g/l_p)^2$ with r_g the Schwarzschild radius and l_p the Planck length. For a large black hole we have $r_g \gg l_p$. Thus, in such a situation, a semi-classical saddle-point analysis should be a rather good approximation. In other words, such a black hole can be taken as a classical background field. Taking finiteness of $\hbar$ into account then leads to the famous result of Hawking [4], namely, that a black hole gradually emits particles which are measured by an outside observer at null infinity. These particles are distributed thermally with a temperature set by the inverse size of the black hole. Notice that qualitatively this effect is somewhat similar to the Schwinger effect in the sense that virtual particles can materialize due to the presence of a large background field.

Looking closer at Hawking's analysis, however, reveals a very deep conceptual problem. Starting with the collapse of a pure state into a black hole and subsequently waiting for it to evaporate completely, one ends up with a perfect mixture of radiation [5]. Therefore, the process seems to violate one of the principles of quantum mechanics, namely unitary time evolution. This breakdown of unitarity is the essence of the so-called information paradox which will be explained in more detail in later parts of the thesis. Thus, even though we expect a semi-classical analysis to be valid when considering large black holes, we end up with a puzzle which so far has no proper resolution.

Notice that within Hawking's computation and even beyond it no attempt has been made which aims at resolving the microscopic structure of the black hole[1]. In particular, if nature is truly quantum, the black hole itself should have a description in terms of microscopic degrees of freedom of the underlying field theory valid at large distances, i.e. gravitons. The situation is thus somewhat similar to our discussion of the field of a laser. As explained before, at the full quantum level, the electric field should be replaced by a coherent state of a large number of longitudinal and temporal photons. Being motivated by the information paradox, one of the major goals of this thesis is to develop a similar fundamental quantum theory of black holes in terms of a large number of gravitons. In particular, we will explain that in the case of black holes finite N effects could be the underlying microscopic origin of restoration of unitarity in the process of black hole evaporation.

Taking the point of view that **all of nature is quantum at a fundamental level**, we will further apply our logic to other solutions in gravity as well as in field theory. In particular, we construct microscopic theories for AdS space-time as well as solitons and instantons. As a persistent phenomenon we find that for all these systems the microscopic structure leads to deviations from semi-classicality in terms of $1/N$ effects with N the typical number of constituents. In this sense, classical solutions are reinterpreted in the language of many-body physics with the limit $N \to \infty$ corresponding to a mean-field approximation.

[1] Of course, there are microscopic theories of black holes in the context of string theory, most notably based on counting of BPS states [6] or fuzzballs [7]. These models, however, heavily rely on physics in the deep UV, where string theoretic effects are important. The point we want to make is that the physics of large black holes should not be sensitive to the details of UV physics according to the laws of effective field theory. Rather, it should be possible to describe large black holes in terms of the microscopic degrees of freedom of the effective field theory of Einstein gravity expanded around flat space-time.

Note that while effects of finite N might be negligible for the physics of a laser, they become crucial in the case of black hole physics and for solitons and instantons in supersymmetric theories. In particular, as already mentioned before, these effects could be the microscopic origin of purification of Hawking radiation. Furthermore, within the context of supersymmetric solitons and instantons, such quantum corrections lead to departures from the BPS condition subsequently leading to a novel mechanism of supersymmetry breaking as we will explain in detail.

In order to realize the ideas outlined above, we explicitly construct two frameworks which aim at a quantum mechanical resolution of classical solutions. The first approach is based on a so-called auxiliary current description (ACD). The method is inspired by techniques used in quantum chromodynamics (QCD) which allow to represent hadrons in terms of their quark and gluon content. Roughly speaking, the true quantum state of the system we want to describe is represented by a local composite operator constructed from the microscopic degrees of freedom of the underlying theory. When acting on the vacuum this operator should create a state with the same quantum numbers as the object we want to describe. In that case, it is possible to rewrite the true quantum state in terms of fields of the microscopic Lagrangian. Having achieved such a representation, correlation functions can be computed using the standard machinery of QFT. Although the framework is completely general, we will mostly apply the ACD to the physics of black holes understood as composites of a large number of gravitons.

The second approach is based on resolving classical solutions in terms of quantum coherent states. These state are constructed in a self-consistent way such that a proper semi-classical limit is guaranteed. In other words, when evaluated in such a state, the one-point function of the field operator reduces to the classical profile. In order for such a construction to be possible, the coherent state is constructed as a linear combination of number eigenstates of the fully interacting theory. Since the corresponding quanta can in general not be identified with asymptotic states, we shall refer to these particles as corpuscles throughout the thesis. The program is explicitly developed for the physics of AdS as well as solitons and instantons.

The outline of the thesis is as follows. In the rest of this chapter we review some background material needed for later parts of the thesis. We will focus on aspects which will be most important for later chapters. For more detailed presentations of the material, we refer the reader to the literature whenever necessary. In the second chapter, we introduce the ACD following our original work [8,9]. First, we give a detailed discussion of the generic construction. Subsequently, we apply our logic to black holes physics. In this context, we construct and compute observables connected to the black hole interior such as the number and energy density of gravitons in the black hole. Using these results allows to derive a scaling relation for the black hole mass in terms of the number of gravitons composing the black hole. In addition, we show how these observables can be embedded naturally in the context of S-matrix theory. In particular, we consider the scattering of a probe scalar field on a black hole represented as a N-graviton system. Our findings suggest that contrary to semi-classical expectation, an outside observer has access to the black hole interior doing scattering experiments. More precisely, it is shown that the cross section can be expressed

in terms of the density of gravitons in the black hole. Thus, measuring the cross section the outside observer can reconstruct the internal structure of a black hole in terms of graviton distribution functions. Although we mostly restrict our analysis to the partonic level (free gravitons inside the black hole) and to tree-level processes, we think that we already capture some of the most relevant aspects of the full theory. Furthermore, we explain how higher-order corrections as well as multiple graviton exchanges can be taken into account. Finally, we explain how geometry emerges as an effective phenomenon from an underlying quantum description defined with respect to a flat space-time vacuum. In particular, the Schwarzschild solution is obtained in the limit of infinite black hole mass. In addition, we explicitly derive corrections to that result (i.e. corrections due to the finiteness of the mass of a real black hole). It is shown that this correction can be understood as a novel type of black hole wave function renormalization which is intrinsically related to the quantum bound state structure of the black hole.

In the third chapter, we introduce the coherent state representation of classical solutions. As a first example, we consider kinks in $1+1$ dimensions. We first show how well-known properties of kinks such as energy, conservation of topological charge or interaction among two kinks follow easily from the basic properties of coherent states following our paper [10]. In order to clearly disentangle the quanta responsible for energy from those that account for the topological properties we further represent the kink as a convolution between the two sectors. This representation makes manifest the fact that topology is related to corpuscles of infinite wavelength supporting the momentum flow in one direction. In contrast, it shows that the corpuscles responsible for the energy are of a completely different nature. Indeed, these corpuscles have wavelength set by the size of the kink. In order to give a self-contained discussion we confront the coherent state picture of topological solitons with that of non-topological solitons. Indeed, we find that the quanta contributing to the energy of the non-topological soliton are similar to those accounting for the energy of the topological soliton. For the non-topological soliton, however, the topological sector can be represented trivially. In other words, at the corpuscular level, absence of topological stability is related to the fact that the occupation number of infinite wavelength quanta is finite for the non-topological soliton. In turn, this finiteness explains the instability of the vacuum with respect to creation of non-topological solitons at the quantum level.

We proceed with a discussion of the corpuscular theory of instantons. Since the physics of instantons in d Euclidean dimensions can be understood in terms of solitons in $d+1$ dimensions evolving in Euclidean time, a representation of the latter in terms of coherent states gives us an idea how to quantize the former. We shall explicitly develop the dictionary in full generality. In order to illustrate our idea, we shall consider various examples in great detail. Among others, these include topological and non-topological instantons in quantum mechanics as we as Yang-Mills instantons. It is shown how the coherent state picture correctly accounts for the physics of instanton-induced transitions. Furthermore, we investigate the implications of our construction for the concept of resurgence.

Having established the coherent state picture of solitons and instantons, we consider their embeddings in supersymmetric theories. In the case of a Wess-Zumino model in $1+1$ dimensions, we explicitly show how corpuscular $1/N$ effects (by N we denote here the

number of corpuscles which account for the energy) lead to a new mechanism of supersymmetry breaking. While the topological sector is protected from quantum corrections (infinite wavelength corpuscles are not subject to quantum fluctuations), the energetic part is affected. This mismatch is reflected in a violation of the BPS condition leading to supersymmetry breaking. It is argued that the nature of the corpuscular correction is encoded in loops of corpuscles and the subsequent need for regularization and corpuscular renormalization.

Finally, we develop the coherent state portrait of AdS space-time. In this context we explain how concepts such as holography or geometry of AdS can naturally be reinterpreted in the corpuscular language. Indeed, all the well-known properties of AdS map into the occupation of gravitons constituting parts of AdS. In addition, we explicitly compute corpuscular corrections to the scalar propagator in AdS. It is shown that these corrections can be summed up explicitly in terms of a Dyson series. Thus, the corpuscular corrections effectively shift the mass pole of the scalar. Furthermore, we study the Unruh effect in AdS in the coherent state approach. We explicitly show that, when resolved quantum mechanically, an Unruh observer in AdS cannot experience a perfectly thermal spectrum as expected semi-classically.

In the last chapter of the thesis we summarize our findings and give an overview over possible new research directions.

1.2 General Relativity and QFT in Curved Spacetime

In view that a large part of the thesis will be devoted to a novel quantum mechanical description of black holes, we will here first of all review the relevant properties of black holes within classical general relativity as well as QFT in curved space-time. For simplicity, the discussion will be mostly restricted to Schwarzschild black holes.

1.2.1 Classical General Relativity

Within classical general relativity, space-time is a dynamical quantity. This is explicitly encoded in the Einstein-Hilbert action,

$$S = \frac{1}{16\pi G_N} \int d^4x \sqrt{-g}(R + g_{\mu\nu} T^{\mu\nu}). \tag{1.1}$$

Here G_N is the Newton's constant, $g_{\mu\nu}$ the metric and g its determinant. R and $T_{\mu\nu}$ denote the Ricci scalar and a collection of all possible energy-momentum sources gravity is coupled to, respectively. Notice that this coupling is universal. In other words, gravity interacts with all forms of energy democratically.

Varying (1.1) with respect to the metric one obtains the famous Einstein equations,

$$R_{\mu\nu} - \frac{1}{2} g_{\mu\nu} R = 8\pi G_N T_{\mu\nu}, \tag{1.2}$$

where $R_{\mu\nu}$ is the Ricci tensor. This equation has a very suggestive physical interpretation. Any form of energy or momentum (right-hand side of the equation) will curve space-time (left-hand side of the equation). In turn, since space-time is curved, it will influence the motion of arbitrary energy-momentum sources such that they follow geodesics.

There are numerous tests confirming this theory on various lengthscales ranging from millimeters to the solar system up to the size of the observable universe. Nevertheless, on purely theoretical grounds, it is clear that the range of applicability of general relativity is limited. First of all, in the deep UV the theory becomes perturbatively strongly coupled suggesting that the theory must be completed in some way at high energies . Secondly, the nature of dark energy, and correspondingly the smallness of the cosmological constant are mysteries which motivate physicists to modify gravity at the largest observable scales as well. Finally, it seems that as soon as one considers quantum fluctuations around classical solutions of general relativity, one encounters inconsistencies such as the information paradox which we will recapitulate later. Since this paradox is persistent for black holes of arbitrary size, one might be tempted to reconsider the way we think about black holes. Since developing such a new understanding of black holes which circumvents apparent paradoxes will be one of the major goals of the thesis, let us briefly review the standard approach to black hole physics.

1.2.2 Classical Black Holes

Taking as an energy-momentum tensor a point source of mass M, one finds the Schwarzschild solution from (1.2):

$$ds^2 = g_{\mu\nu}dx^\mu dx^\nu = -\Big(1-\frac{r_g}{r}\Big)dt^2 + \frac{1}{\Big(1-\frac{r_g}{r}\Big)}dr^2 + r^2 d\Omega^2, \tag{1.3}$$

where $r_g = 2G_N M$ is the Schwarzschild radius of the source and $d\Omega^2$ the volume element of the two-sphere. The physical meaning of the Schwarzschild radius is as follows. Suppose you have a spherically symmetric gravitating source of mass M. Squeezing that mass onto the scale r_g, the resulting system becomes a black hole. Furthermore, r_g marks the so-called event horizon of a Schwarzschild black hole. In other words, the spatial hypersurface $r = r_g$ seperates two regions of space-time, one from which events can escape the black hole ($r > r_g$) and the other one from which this is no longer possible ($r < r_g$) as will be discussed below.

Notice that this metric has two singular points, one at $r = r_g$ and the other at $r = 0$. The first one, however, is merely a coordinate artifact. In other words, the Schwarzschild metric covers only the exterior of the source. Performing suitable coordinate transformations to cover the space-time globally reveals that there is no physical singularity at $r = r_g$. In particular, all curvature invariants remain finite at $r = r_g$. The second point $r = 0$, however, is a true singularity with all the curvature invariants blowing up[2]. Classically, all

[2]Quantum mechanically, it is clear that we should not trust the solution for $r \leq l_p$ with l_p the Planck

future directed geodesics inside the black hole will reach the singularity at a finite time. This behaviour becomes also apparent from Figure (1.2.2), which shows the light-cone structure of the full space-time in Kruskal coordinates.

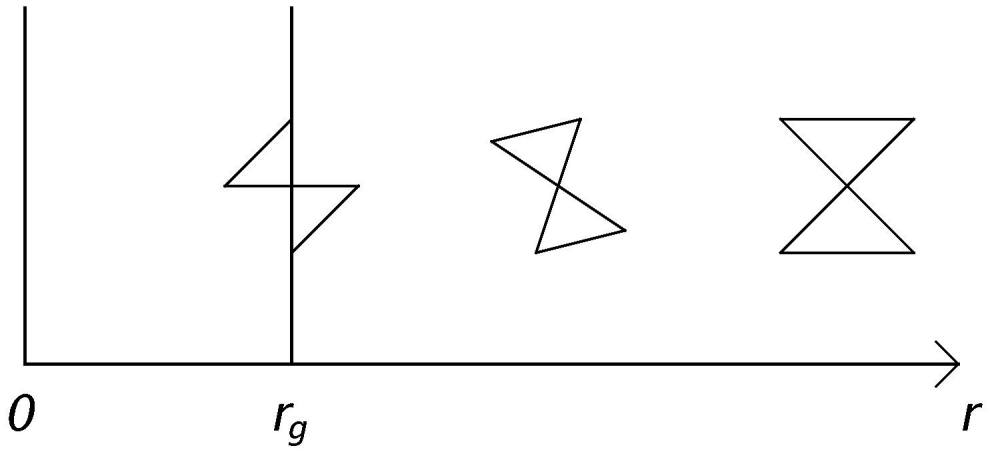

Figure 1.1: The structure of light-cones in a black hole space-time in Kruskal coordinates. At large distances, the light-cone structure is that of flat space-time. Approaching the black hole horizon at $r = r_g$, the light-cone flips and all future directed events point inside the black hole.

One can see that the space-time looks flat for $r \gg r_g$. Approaching the horizon, however, the light-cone flips and finally completely turns over at r_g. Thus, any event entering the black hole interior can no longer escape from it at the classical level.

Note that this behaviour already indicates that a black hole should carry entropy. Since the black hole is only characterized by its mass (which is a macroscopic quantity)[3], it looses memory about its formation history. In fact, Bekenstein argued that the entropy of a black hole should be determined by its area A [12]. Taking into account that quantum mechanically a black hole can radiate, it was shown that the precise relation is given as $S = A/(4l_p^2)$ [4] as we will explain in more detail in the next section. First, however, we want to mention that a scaling of entropy with the area is very peculiar. In particular, for other thermodynamic systems, one expects a growth of the entropy with the volume of the system. The fact that black holes behave differently thus lead to the advent of the holographic principle [13, 14] which was most explicitly realized within the context of AdS/CFT duality [15–17].

length. In particular, from an EFT point of view, it is clear, that new UV physics should be integrated in at $r \sim l_p$. This new physics should then lead to a mechanism which allows for a resolution of the singularity. Note, however, that the results of [11] indicate that already at the semi-classical level, the singularity is a void concept, because quantized probes can never probe it.

[3] The most general black hole solution, the Kerr-Newman black hole can further be characterized by its electric charge and angular momentum. This fact leads to the so-called classical no-hair theorems which say that a black hole is only characterized by the charges that can be measured at infinity using the Gauss law. We will come back to this point later when discussing a quantum mechanical portrait of black holes.

1.2.3 QFT on Curved Space-Time

As explained in the last section, at the classical level nothing can escape from a black hole. We will now briefly review how this story changes when one takes quantum fluctuations of fields in the classical background space-time into account. In other words, a brief overview is given concerning the semi-classical ideas used within QFT in curved space-time subsequently leading to Hawking radiation [4].

The basic idea of QFT on curved space-time is to keep the background metric classical, but to quantize all particles which propagate in that background. Thus, schematically

$$g_{\mu\nu} \to g_{\mu\nu}, \quad \Phi \to \hat{\Phi}. \tag{1.4}$$

Here Φ could be any field coupled to gravity and $\hat{\Phi}$ denotes the associated quantized field operator satisfying standard commutation relations (in what follows we will omit the hat again). Notice that such a replacement effectively corresponds to a decoupling of background and fluctuations. For example, for a black hole such a replacement only holds in the idealized semi-classical limit, $M \to \infty$, $l_p \to 0$ with r_g fixed. Note, however, that this limit should give a rather good approximation for real gravitating sources as long as these are characterized by a large curvature scale $R \gg l_p$. Nevertheless, we will later argue that such an approximation leads to paradoxes which have no resolution within this standard semi-classical approach. Before, however, we will briefly review the original arguments given by Hawking concerning particle production in the presence of black holes.

Hawking Radiation

While in flat space-time there is a unique vacuum state this is no longer true in a curved space-time. In particular, different observers disagree on what they call vacuum. Thus, what looks like a vacuum state to one observer, i.e. a state containing no particle excitations, might look like a highly excited state to a different observer. Technically speaking this is related to the fact that the wave equation for a field in a curved background does not allow for a unique choice of the mode function $u(t)$. Therefore, there is no invariant meaning of what observers call positive frequency modes, i.e. particles, with respect to their preferred vacuum.

Let us make these statements more precise. For simplicity, consider a quantized scalar field Φ moving in some fixed, classical background geometry $g_{\mu\nu}$. The dynamics of this field is governed by the corresponding wave equation,

$$g^{\mu\nu} \bigtriangledown_\mu \bigtriangledown_\nu \Phi = 0, \tag{1.5}$$

where $\bigtriangledown_\mu$ is the covariant derivative. Suppose there are two different sets of functions u and v satisfying (1.5). Then the field operator can be expressed in two different ways:

$$\begin{aligned} \Phi &= \textstyle\sum_i (u_i \hat{a}_i + u^* \hat{a}_i^\dagger), \\ &= \textstyle\sum_i (v_i \hat{b}_i + v^* \hat{b}_i^\dagger). \end{aligned} \tag{1.6}$$

Here the $\hat{a}_i$'s ($\hat{a}_i^\dagger$'s) and $\hat{b}_i$'s ($\hat{b}_i^\dagger$'s) represent two different sets of annihilation operators (creation operators) corresponding to the mode functions u_i and v_i, respectively. As a consequence, there is no invariant meaning of vacuum. In particular, while one observer defines his Fock vacuum via $\hat{a}_i|0_a\rangle = 0$ for all i, another observer chooses the vacuum state $|0_b\rangle$ such that $\hat{b}_i|0_b\rangle = 0$ for all i.

It can be shown easily that the operators are related by a so-called Bogoliubov transformation in the following way,

$$\hat{b}_i = \sum_j (\alpha^*_{ij}\hat{a}_j - \beta^*_{ij}\hat{a}_j^\dagger), \tag{1.7}$$

where α_{ij} and β_{ij} are the Bogoliubov coefficients.

From (1.7) it becomes transparent that what looks like a vacuum to one observer can look like an excited state to another observer. In particular, the number of $\hat{b}$ particles in mode i in the $\hat{a}$-vacuum is given by

$$\langle 0_a|\hat{b}_i^\dagger\hat{b}_i|0_a\rangle = \sum_j |\beta_{ij}|^2. \tag{1.8}$$

Thus, in order to quantify in what way observers disagree on the flux of particles they measure, one needs to determine the coefficients β_{ij}. Notice that in Minkowski space-time we have $u_i = v_i \Rightarrow \hat{a}_i = \hat{b}_i \Rightarrow \beta_{ij} = 0$. Thus, as expected, in this case there is a unique notion of particle excitation.

While the above reasoning is very general, Hawking applied it to the specific case of asymptotically flat black hole space-times. In particular, he considered space-times subject to spherical collapse of infalling matter. Such a situation allows to relate vacua at past null infinity and future null infinity. Determining the mode functions asymptotically, Hawking managed to determine the coefficients β. His findings show that within the semi-classical approximation, outgoing particles are distributed thermally with a temperature $T \sim 1/r_g$. Thus, for an observer at future null infinity, a black hole looks like a black body gradually emitting particles. Notice, this result was the key for establishing black hole thermodynamics in full glory. In particular, it allows to identify the precise coefficient in front of the black hole area law for the entropy, $S = A/4l_p^2$.

Let us now try to understand black hole evaporation from a different, more intuitive point of view. Although (1.3) does not cover the full Schwarzschild black hole space-time, it nevertheless shows that this space-time cannot have a globally defined time-like Killing vector field ∂_t. In particular, for $r < r_g$, the radial direction becomes time-like and the time-like direction becomes spatial. Therefore, in the interior of the black hole space-like hypersurfaces correspond to constant r rather than constant t. Thus, although the exterior of the black hole is static, the full space-time, including the black hole interior is dynamical. In other words, the Hamiltonian describing time-evolution in the interior is not conserved. In turn, this is the origin of particle creation in a black hole space-time. What looks like a lowest energy eigenstate of the Hamiltonian at some initial time t_0 no longer minimizes the Hamiltonian at a later time t_1 Therefore, the initial vacuum appears to be a state populated with particles at time t_1.

Finally, we want to give a heuristic, but very intuitive picture of Hawking radiation. Due to vacuum fluctuations at the horizon virtual particle-antiparticle pairs are created. Due to the presence of the gravitational field these particles can materialize to become propagating degrees of freedom[4]. While positive energy particles just outside the horizon can escape to infinity, negative energy particles created in the black hole interior evolve towards the singularity. This behaviour is captured by the Hamiltonian time evolution outside and inside of the black hole, respectively.

Information Paradox

As mentioned in the last subsection, the spectrum of particles emitted by a black hole is exactly thermal in the semi-classical limit. Although Hawking's result shows some of the fascinating aspects of black hole physics, it also reveals some severe conceptual problems.

Consider the evolution of the infalling matter described by a pure state and observed by a semi-classical observer. After collapsing into a black hole, the system carries no hair. In other words, the black hole looses memory of its microscopic origin. As such, this would be no problem. Rather, since an outside observer has no access to the black hole interior he would describe the collapse as a dissipative process. In that way no information is lost, but rather hidden in the black hole interior.

The situation changes as soon as the observer realizes that the black hole emits particles. Due to the evaporation, an outside observer can no longer attribute the apparent loss of information to dissipation. Rather, if information were to be preserved, the observer should be able to reconstruct the initial state data making enough measurements on the emitted Hawking quanta. Unfortunately, however, the spectrum of quanta is exactly thermal. This means that the outside observer can only use a density matrix for a mixed state to describe the physics of the emitted particles. As a consequence, the semi-classical observer witnessed a pure state evolving into a perfect mixture and concludes that information is lost.

Thus, it seems that in the presence of black holes time evolution is not unitary and the principles of quantum mechanics are violated.

Being puzzled by this observation, one might think that quantum gravity effects at the Planck scale or effects due to the back-reaction on the geometry could circumvent the problem of information loss. Both of these approaches, however, do not seem to offer the key for understanding the resolution of the information paradox. First of all, quantum gravity in the deep UV should only affect the latest stages of the evaporation. Therefore, only a few modes could severely be affected by Planck scale quantum gravity. It thus seems very unlikely that these few quanta carry all the information so that the mixed state can be turned into a pure state. Secondly, in a semi-classical treatment, corrections to thermality are exponentially suppressed as $e^{-S_{BH}}$ where S_{BH} is the black hole action. Since for massive black holes S_{BH} is very large, the corrections to perfect semi-classicality seem to be negligibly small. In particular, such corrections are not expected to lead to a purification of Hawking radiation.

[4]As discussed before, an example of a similar pair creation process is the Schwinger effect [3]. In that case vacuum fluctuations can be materialized by a strong external electric field.

It is worth mentioning that the information paradox is not the only mysterious feature of black hole physics. Since $T \sim 1/r_g$ the black hole has a negative heat capacity meaning that the smaller a black hole is, the hotter it becomes. This property makes the black hole rather different from other thermodynamic systems. Furthermore, very generic, non-perturbative arguments imply that global charges such as baryon number or lepton number are inevitably violated in the presence of the black hole [18].

All these features seem to indicate that there is something very deep missing in our description of large black holes. Thus, developing a novel understanding of the physics of black holes which circumvents these paradoxes will be one of the main motivations of the thesis.

We want to conclude our discussion by mentioning an attempt aiming at a resolution of the information paradox. Within the semi-classical approach, the principle of black hole complementarity was introduced in [19]. In a nutshell, assuming unitary time evolution as well as the equivalence principle, it was argued that there are no paradoxes in black hole physics if one takes into account that an outside observer cannot communicate with an observer in the black hole interior. In this way, the principle of complementarity managed to nullify some apparent paradoxes surrounding black hole physics (see e.g. [20]).

Recently, however, Almheiri et al. [21] considered a gedankenexperiment that severly questions the validity of black hole complementarity. In particular they argued that within the semi-classical approach not all the principles of complementarity can hold at the same time. Sticking to unitarity, the authors thus concluded that the equivalence principle breaks down at the horizon. Thus, instead of entering smoothly the black hole interior an infalling observer encouters a firewall and burns up at the horizon. Since this work a lot of arguments have been given in the literature either for or against black hole complementarity. This plethora of paper, in my opinion however, seems to simply indicate that when restricting to semi-classical arguments, one cannot circumvent all paradoxes, be it the information paradox or firewalls.

Page's Argument

Following the spirit that the semi-classical treatment cannot lead to the purification of Hawking radiation, Page [22] presented a non-perturbative, information theoretic argument indicating that information should actually be preserved in the process of black hole evaporation. Since Page's argument serves as a motivation for constructing a microscopic model of black holes, we will briefly review the basic ingredients and results of his approach. As a starting point consider the combined system of black hole and radiation as a generic quantum mechanical system described by a pure state. Assume that the dimensionality of the black hole Hilbert space is given by $n \sim e^{s_h}$ and that of the radiation by $m \sim e^{s_r}$. Now define the reduced density matrices of both subsystems,

$$\rho_r = \mathrm{tr}_h \rho_{rh}, \quad \rho_h = \mathrm{tr}_r \rho_{rh}, \tag{1.9}$$

where ρ_{rh} is the pure state density matrix of the combined system. As usual, the corresponding entanglement entropy is defined as

$$S_r = -\mathrm{tr}_r(\rho_r \ln \rho_r) = -\mathrm{tr}_h(\rho_h \ln \rho_h) = S_h \tag{1.10}$$

where the equality reflects a generic property of the entanglement entropy of two subsystems. In order to measure how much information is carried by the subsystems, and in particular by radiation, one should consider deviations from the entanglement entropy from its maximum which is given by the number of microstates of the corresponding Hilbert space. Thus, define the amount of information carried by the subsystems as

$$I_r = \ln m - S_r, \quad I_h = \ln n - S_h. \tag{1.11}$$

Analyzing the amount of information carried by the Hawking quanta as a function of time, Page discovered that the following picture emerges. During the initial stages of evaporation, the entanglement of the entropy increases and no information is released in these quanta. As soon as $n \sim m$, however, the entanglement decreases and information is carried away by the Hawking quanta. The turning point at which information release becomes efficient is known as the Page time and it corresponds to the time scale where the black hole lost half of its entropy. Note that the argument is entirely based on non-perturbative physics assuming that some kind of microscopic quantum mechanical description of the black hole exists. In other words, the purification of Hawking radiation seems to be connected to quantum processes which can never be uncovered in any order by order perturbative analysis around the black hole saddle point. Thus it seems that a resolution of the information paradox requires physics that leads to deviations from thermality larger than the exponentially suppressed effects one obtains when performing a perturbative, semi-classical saddle point analysis. Later in this thesis, we will discuss explicit field theoretical models of black holes incorporating these ideas.

1.2.4 Anti-de Sitter Spacetime

Since we will develop a microscopic understanding not only of black holes, but also of AdS space-time we will briefly recapitulate the semi-classical picture of this space-time. In particular, the geometry of AdS and some coordinate systems covering that space-time (or parts of it) are introduced.

The Geometry of AdS

AdS in d space-time dimensions can be defined as the embedding of an hyperboloid satisfying

$$-X_0^2 + \sum_{i=1}^{d-1} X_i^2 - X_d^2 = -\rho^2 \tag{1.12}$$

into $(d+1)$-dimensional flat space-time,

$$ds^2 = -dX_0^2 + \sum_{i=1}^{d-1} dX_i^2 - dX_d^2, \tag{1.13}$$

where ρ is the curvature radius of AdS. From equation (1.12) one can see that the group leaving the hyperboloid invariant is $SO(d-1,2)$. Since the naive embedding contains closed time-like curves, one usually considers the universal cover of AdS with topology of R^d. One can show that this space-time can be obtained as a maximally symmetric solution of Einstein's equation with a negative cosmological constant. Thus, just as Minkowski or de Sitter (dS), it possesses the maximal number of Killing vector fields, which in $d+1$ dimensions is given by $1/2(d+1)(d+2)$.

A natural coordinate system for AdS are global, hyperbolic coordinates (τ, R, w_j),

$$\begin{aligned} X_0 &= R\cosh(R)\sin(R), \\ X_i &= R\sinh(R)w_i, \\ X_d &= R\cosh(R)\cos(\tau), \end{aligned} \tag{1.14}$$

where $0 \leq \tau < \infty$, $0 \leq R < \infty$ and w_j are coordinates on the $(d-2)$ unit sphere $S^{(d-2)}$. In these coordinates the metric takes the form

$$ds^2 = \rho^2[-\cosh^2(R)d\tau^2 + dR^2 + \sinh^2(R)d\Omega^2_{(d-2)}], \tag{1.15}$$

where $d\Omega^2_{(d-2)}$ denotes the metric on $S^{(d-2)}$.

Another parametrization of AdS which we shall use later in the thesis is given by the so-called static coordinates which are obtained from global, hyperbolic coordinates when performing the following transformations:

$$\begin{aligned} r &= \rho\sinh(\rho), \\ t &= \rho\tau. \end{aligned} \tag{1.16}$$

In these coordinates the line element becomes

$$ds^2 = -\Big(1 + \frac{r^2}{\rho^2}\Big)dt^2 + \Big(1 + \frac{r^2}{\rho^2}\Big)^{-1} dr^2 + r^2 d\Omega^2_{(d-2)}. \tag{1.17}$$

Notice that this metric does not depend on time. Since the coordinates cover the full space-time, we see that AdS possesses a global time-like Killing vector field ∂_t; hence the name static coordinates. Another coordinate system which shall be used later is the so-called Poincaré patch. These coordinates are obtained as follows. First we define

$$\begin{aligned} X_{(d-1)} + X_d &= u, \\ X_{(d-1)} - X_d &= v, \\ X_i &= \frac{u}{\rho} x_i. \end{aligned} \tag{1.18}$$

Next, we introduce the coordinate z via $z = \rho^2/u$. The resulting metric finally takes the form

$$ds^2 = \frac{\rho^2}{z^2}(dz^2 + \eta_{\mu\nu}dx^\mu dx^\nu), \tag{1.19}$$

with $\eta_{\mu\nu}$ the Minkowski metric. Note that these coordinates cover only a part ($z > 0$) of the AdS space-time. Furthermore, the metric has two special point. At $z \to \infty$ the metric vanishes. Thus, there is a particle horizon at this point. At $z \to 0$ the metric blows up and becomes ill-defined. This point corresponds to the boundary of AdS space-time which plays a prominent role in the context of AdS/CFT duality. Close to this boundary, all modes are highly blue-shifted for an observer inside AdS. Finally, the metric is conformally flat. It is this property which makes (1.19) our preferred choice when discussing the corpuscular theory of AdS. Finally, there is one more coordinate system which we already want to introduce at this point. It is based on a so-called non-factorizable geometry described by a warp factor. The line element takes the form:

$$ds^2 = e^{y/\rho}\eta_{\mu\nu}dx^\mu dx^\nu + dy^2, \tag{1.20}$$

where $y \in (-\infty, \infty)$. Using this coordinate system will be particularly useful in the case of five-dimensional AdS and when discussing the corpuscular theory of a related space-time, the so-called Randall-Sundrum 2 (RS2) set-up.

1.3 Black Holes Quantum N Portrait

Having reviewed the standard textbook treatment of classical solutions within general relativity, we will now proceed by presenting new ideas concerning the physics of black holes and other gravitational backgrounds. First, we will present an intuitive picture of black holes viewed as quantum bound states of weakly coupled gravitons first proposed in [23]. Next, we will discuss how this approach circumvents problems of the semi-classical treatment such as the information paradox or the absence of global quantum numbers in the presence of black holes [24]. Finally, similar ideas are applied to other gravitational backgrounds following [23, 25]. A more detailed discussion, however, can be found in the original works [25].

1.3.1 Black Holes Quantum N Portrait - Basics

Although quantum mechanical fluctuations can never be switched off in nature, the standard lore is that large objects such as heavy black holes should behave classically to a very good approximation as already mentioned in the introduction. In particular, one would naively expect that quantum corrections should be completely negligible as long as $M \gg M_p$ with M the black hole mass and $M_p = l_p^{-1}$. As explained before, corrections to the classical field equation coming from back-reaction on the geometry are assumed to be

exponentially suppressed. These effects are due to loop corrections on a fixed background. These assumptions are at the heart of quantum field theory on curved space-time.

Taking the point of view that quantum mechanics is truly fundamental, however, suggests that one should also take the quantum nature of black holes seriously. In particular, within the Quantum N Portrait a black hole is reinterpreted as a large-N bound state of weakly coupled longitudinal gravitons on flat space-time. In this sense, the black hole is somewhat similar to the electric field of a laser which, when resolved quantum mechanically, represents a coherent state of longitudinal photons of large occupation number in one momentum mode. Let us explain this statement for black holes in more detail. For that purpose consider a large black hole (i.e. $r_g \gg l_p$). Furthermore, notice that the effective dimensionless gravitational coupling $\alpha = l_p^2/\lambda^2$ depends on the Compton wavelength of the momentum transfer of a given scattering process. Since r_g is the only scale characterizing the black hole, we expect the typical wavelengths of the gravitons in the black hole to be set by that scale, $\lambda \sim r_g$. Then the typical coupling between individual gravitons inside the bound state is given by $\alpha \sim l_p^2/r_g^2$ which is extremely weak for large black holes. Thus, the physics of the bound state should be describable within the effective QFT of Einstein gravity expanded around flat space.

Let us now estimate how the number of gravitons is related to the mass of the black hole. We will give a simple derivation which, however, can be made more precise using the virial theorem as in the original work [23]. Since individual gravitions are extremely weakly coupled, we can approximate the total energy of the black hole by the sum of kinetic energies of the N gravitons. Thus, we have $M \sim N\lambda^{-1} \sim Nr_g^{-1}$ up to corrections of order l_p^2/r_g^2. Expressing the mass of the black hole in terms of its Schwarzschild radius, we immediately arrive at the following relations of the black hole parameters to leading order:

$$M \sim \sqrt{N} M_p, \quad r_g \sim \sqrt{N} l_p, \quad \alpha \sim \frac{1}{N}. \tag{1.21}$$

Therefore, all properties of a Schwarzschild black hole are characterized by a single number N.[5]

Notice first that while individual gravitons in the black hole are indeed extremely weakly coupled they nevertheless feel a large collective effect due to the presence of all other gravitons. Introducing the effective 't Hooft-like coupling $\lambda = N\alpha \sim 1$, it becomes obvious that the physics of black holes interpreted as bound states on Minkowski space-time mimics a mean-field type situation. Secondly, a similar analysis could have been performed for other spherically symmetric sources of geometric radius larger then their associated Schwarzschild radius. For such systems one obtains $\alpha < 1/N$ and therefore $\lambda < 1$ [23]. In other words, these objects are weakly coupled individually as well as collectively. In contrast, the black hole represents a maximally packed source at the point of strong collective coupling. Finally, we want to mention that the semi-classical limit is understood as the limit

$$N \to \infty, \quad M_p \to \infty, \quad r_g \text{ fixed}. \tag{1.22}$$

[5] Notice that similar scaling relations were proposed earlier in the context of matrix models [26]

Thus, in order for the portrait to make any sense, it should reproduce standard results of QFT in curved space-time in that limit. In the next part, we will first argue that this is indeed the case and secondly, we will discuss the implications of departures of that limit.

1.3.2 Black Holes Quantum N Portrait - Physical Implications

Having discussed the basic ideas and scaling relations underlying the Black Hole Quantum N Portrait, we will now proceed by reviewing some of its physical implications. We will mainly focus on the existence of quantum $U(1)$ hair and the physics of information release in black hole evaporation [24]. In addition, a short discussion of black hole criticality [27–29] and scrambling will be included [28]. For recent aspects of quantum criticality and information processing see also [30–32]. Other aspects of the Black Hole N Portrait are for example discussed in [33, 34].

Hawking Radiation

In the usual (semi-classical) approach, Hawking radiation can be interpreted as a vacuum process. As such, a virtual particle-antiparticle pair is created by quantum fluctuations at the horizon and pulled apart due to the gravitational field of the black hole. Subsequently, one particle falls into the black hole while the other one escapes to future null infinity.

Within the corpuscular approach to black hole physics there is no such interpretation of Hawking radiation. Rather, since black holes are viewed as bound states of weakly interacting gravitons on flat space-time, it is natural to expect that black hole evaporation should be understood as scattering process. Indeed the evaporation is due to rescattering of two gravitons in the condensate with one of them gaining energy large enough to leave the bound state. The final state of the scattering process then corresponds to a black hole with one graviton less and the other one escaping to infinity (see Figure (1.2)). In order to see that this process can truly be interpreted as Hawking radiation, let us estimate the typical decay rate for the process.

From the interaction vertices there will be a factor α^2. To leading order, however there are $\sim N^2$ pairs of gravitons which can interact. Finally, since the rate has dimensionality of mass, we should multiply with the typical energy of the process set by the inverse Schwarzschild radius. Thus, to leading order

$$\Gamma \sim \alpha^2 N^2 r_g^{-1} \sim r_g^{-1}. \tag{1.23}$$

Already at this point it is worth mentioning that corrections to this result scale as $1/N$. These are due to the precise combinatoric factor associated to the diagram as well as to processes involving more gravitons. Thus, we see that the corpuscular portrait of black holes reveals quantum corrections which are much larger than expected in the standard semi-classical approach[6]. We will elaborate on the physics of these effects below. First,

[6] Notice that such corrections are typical for other large-N systems such as $SU(N)$ baryons or Bose-Einstein condensates as well.

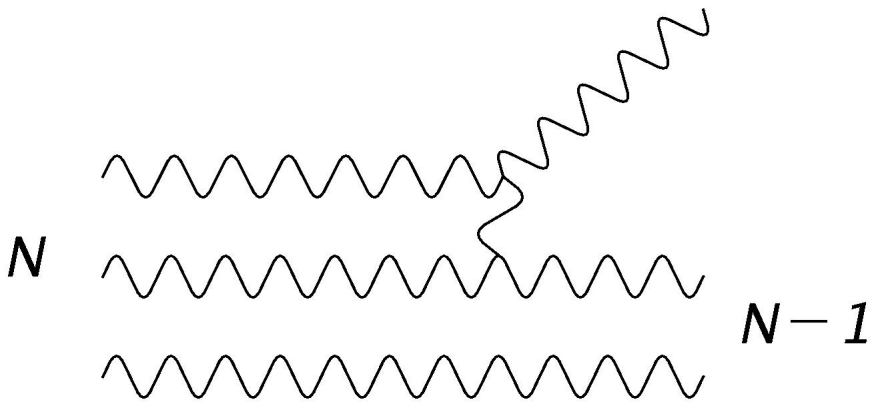

Figure 1.2: Hawking radiation as rescattering of two graviton constituents in the black hole quantum bound state. One of the particles escapes to infinity and is observed as Hawking quantum. The other constituent rescatters into the bound state. Thus, schematically, the process corresponds to $\langle N-1, k|N\rangle$ with k the momentum of the emitted Hawking quantum.

however, we want to show how the standard evaporation rate and the black hole half life-time are recovered in the strict $N \to \infty$ limit. For that purpose notice that from (1.23) it follows that the characteristic time-scale for the process is set by r_g. During that time the change of the black hole mass is given by the energy of the emitted graviton which is order r_g^{-1}. Thus,

$$\frac{dM}{dt} \sim -\frac{1}{r_g^2} \sim -\frac{1}{N l_p^2}, \tag{1.24}$$

where the minus sign follows from the fact that the black hole emits gravitons. Using (1.21) this equation can be immediately rewritten in the form of an evaporation law for N. Intergrating the resulting differential equation and defining $T = 1/(\sqrt{N} l_p)$, one finds the black hole half life-time:

$$\tau \sim \frac{M_P^2}{T^3}. \tag{1.25}$$

Notice that this expression is just the familiar Hawking result. It is important to remember, however, that the bound state itself has no temperature. Rather, it emits particles by rescattering which seem to be distributed according to a thermal spectrum to an observer at infinity. In other words, the concepts of temperature and perfect thermality only arise as an effective phenomenon for an outside observer in the limit of infinite occupation number of gravitons. Notice furthermore that a negative heat capacity is captured in the minus sign in (1.24). Thus, negative heat capacity is a simple consequence of the emission of gravitons by the bound state.

Conservation of Global Charge and Information Release

Let us now proceed by discussing the physical origin of conservation of global charge and information release within the Black Hole Quantum N Portrait. For that purpose, consider the specific situation of a black hole endowed with some amount of $U(1)$ charge B carried by fields Φ. One could, for example, imagine to throw B units of Φ fields into the black hole each carrying one unit of charge. Classically, once the charge is swallowed by the black hole, an outside observer has no longer access to that charge because of classical no-hair theorems. At this level, however, no problem arises. The reason is that the charge is simply hidden beyond the event horizon of the black hole. Taking into account the effect of Hawking radiation, however, there is no way that the charge can be conserved. As explained before this is due to the fact that no information about that charge can be encoded in the Hawking quanta accessible to the outside observer. From Page's argument, it should nevertheless be clear that information retrieval and thus conservation of the global charge should be guaranteed in any sensible microscopic model of the black hole.

Let us now explain, how this precisely works in the Black Hole Quantum N Portrait. Since the black hole now consists of gravitons as well as Φ quanta, it can emit either of these particles. In order for an outside observer to measure the global charge, one of the Φ's needs to be depleted, measured by the observers detector and subsequently rescattered into the condensate. Suppose now that $B \ll N$ and denote the interaction vertex of Φ with the detector by g. Then the rate can be estimated as

$$\Gamma_\Phi \sim g \frac{B}{N^{3/2} l_p} + \mathcal{O}(B/N). \tag{1.26}$$

Notice that the result is consistent with semi-classical no hair theorems because (1.26) vanishes in the limit (1.22). For finite N, however, the rate is suppressed compared to the depletion rate of gravitons as B/N for $B \ll N$, instead of exponentially. It is this effect that ensures conservation of global charge. Let us explain this statement in more detail. At the beginning of the emission process, the black hole prefers to emit gravitons with enhancement factor N/B as compared to the emission of Φ quanta. Indeed, according to [24] one finds that in this regime the number of black hole constituents is given by

$$N(\tau) = (\tau_* - \tau)^{2/3} N(0), \quad B(\tau) = (1 - \tau/\tau_*)^{2/3} B(0), \tag{1.27}$$

with $\tau = \frac{2t}{3l_p}$. These equations explicitly demonstrate that B decreases very slowly in the beginning, but starts to catch up with the depletion of gravitons as soon as $\tau \sim \tau_*$. This tendency continues until $B \sim N$ where one needs to take higher order corrections to (1.27) into account. Notice that at this point emission of the $U(1)$ charge becomes as probable as the emission of gravitons. In other words, deviations from thermality become 100 percent important and semi-classical arguments concerning non-conservation of global charge based on thermality and no-hair do not longer apply. Therefore, when viewed as a bound state of weakly coupled constituents, black holes are perfectly compatible with global symmetries.

Finally, we want to mention that the general argument of Page concerning information release during black hole evaporation applies in particular to the model under consideration. Since the black hole represents a system of N gravitons, one naturally has a finite dimensional Hilbert space for the black hole and the radiation. But then Page's argument can directly be applied suggesting that the release of information becomes efficient after the Page time. Let us note that physically it should also be clear that there cannot be a problem with unitarity in the Black Hole Quantum N Portrait. Since the black hole is a bound state with respect to Minkowski space-time it is subject to the rules of the EFT of general relativity expanded around flat space-time. From this point of view the existence of a global time-like Killing vector field is guaranteed and no loss of information is to be expected.

1.3.3 Quantumness and Scrambling

It is worth mentioning some other possible features of the Black Hole Quantum N Portrait which were investigated in a simple toy model first proposed in [27]. The authors consider a model of N non-relativistic bosons in a box of size R in $3+1$ space-time dimensions subject to an attractive delta function interaction,

$$H = -\hbar L \int d^3x \Psi^\dagger \triangle \Psi - g \int d^3x \Psi^\dagger \Psi \Psi^\dagger \Psi, \tag{1.28}$$

where L is a parameter of length dimensionality, $\triangle$ the Laplacian, Ψ the field operator and g a coupling. Notice that the potential is chosen to be attractive in order to compare to gravity. Without going into the details, we will state the basic findings of [27]. Expanding around a mean-field, the Hamiltonian describing fluctuations around the condensate can be diagonalized by virtue of a Bogoliubov transformation. The spectrum of fluctuations is then found to be

$$E(\mathbf{k}) = \sqrt{\mathbf{k}^2(\mathbf{k}^2 - \alpha N)}, \tag{1.29}$$

where $\alpha = \frac{4gR^2}{\hbar V L}$, V is the spatial volume and $\mathbf{k}$ denotes a dimensionless spatial momentum of the Bogoliubov modes taking values in the positive integers (for a derivation the reader is referred to the original work). From (1.29) one can see that the spectrum only depends on the effective coupling αN which is the analogue of the 't Hooft-like coupling in the Black Hole Quantum N Portrait. While N is a fixed parameter, one can tune α and analyze how the spectrum responds to such a tuning. As long as $\alpha N < 1$, there is a mass gap between the ground state and the first excited state. Notice that the gap vanishes exactly for $\alpha N = 1$ which coincides with the value of the 't Hooft coupling which is supposed to be relevant for black holes. For $\alpha N > 1$ the $k = 1$ mode becomes tachyonic signaling an instability of the ground state. Indeed, for $\alpha N < 1$, the ground state of the system is given by a homogeneous Bose-Einstein condensate, while for $\alpha N > 1$, the ground state corresponds to a so-called bright soliton. Thus, there is a phase transition at $\alpha N = 1$. Since this transition happens at zero temperature, it is driven solely by quantum

fluctuation. Therefore, making contact to the N Portrait, the authors propose that the black hole is at the critical point of a quantum phase transition. Thus, these findings would indicate, that despite the black hole being a macroscopic object, quantum effects can never be neglected. In particular, in [28] the properties of the quantum critical point were further investigated in a $1+1$-dimensional analogue of (1.28). Indeed, in this work it is shown, that the mean-field description can never account for the properties of the system at the critical point. In the language of quantum correlators, these findings suggest that higher order correlation functions become as important as the background mean-field. Assuming that the toy model captures some of the features of gravity, one could conclude that a description of a black hole in terms of a classical metric is rather doubtful (see also the discussion in [35]). These claims were further investigated in related work [30], where it was argued that due to the instability of a black hole, generation of entanglement between subsystems of the black hole becomes maximally efficient. It was shown that this effect should be related to the breakdown of semi-classical time-evolution after a logarithmic time scale $t_{\text{break}} \sim r_g \log(N)$. Although the analysis is restricted to the $1+1$-dimensional version of (1.28), the findings might indicate what the microscopic origin of fast scrambling of information by black holes as first proposed in [36] could be.

1.3.4 Other Space-Times

It is worth noting that a similar picture was proposed for other space-times such as dS or AdS as well [25]. Note that these space-times are not asymptotically flat. Nevertheless, in [25] it was proposed to understand these space-times as bound states of weakly coupled gravitons on Minkowski space-time as well. First, one should notice that similar to black holes, dS and AdS are also characterized by their curvature radius ρ. Then the typical wavelength of constituent gravitons should be set by exactly that scale.

In particular, in the case of four space-time dimensions, the typical number of gravitons constituting (A)dS is given by $N \sim \rho^2/l_p^2$. In addition, the curvature radius and the coupling expressed in terms of N satisfy scaling relations reminiscent of that of the black hole, $\rho = \sqrt{N} l_p$, $\alpha \sim 1/N$. Thus, just as in the case of a black hole, the maximally symmetric space-times, dS and AdS, are at the point of strong collective coupling, $\alpha N \sim 1$. There is an important difference as compared to black holes. For black holes, r_g appears as an integration constant. Thus, it is not fixed by the underlying theory which implies that it can take arbitrary values. In other words, there are black holes for arbitrary $r_g \gg l_p$. Consequently, by emitting a particle, the black hole can readjust its size from $\sqrt{N}$ to $\sqrt{N-1}$ in Planck units. This is not true for dS or AdS. For these space-times the curvature scale is set by the cosmological constant. Therefore, for a given cosmological constant, N is a fixed parameter in the quantum portraits of the maximally symmetric space-times.

Later in this thesis, we will propose an explicit formalism to realize the corpuscular theory of AdS in terms of coherent states. In the case of dS, it is worth mentioning the work of [25]. There it is shown that the classical metric of dS can be reproduced order by order in terms of scattering processes of probes on the gravitons constituting AdS. Furthermore,

in the same paper, the logic of understanding space-time in terms of condensates was applied to inflationary backgrounds. In particular, understanding gravitational as well as inflaton backgrounds as quantum bound states, the authors showed how the correct power spectrum is obtained in the large N limit. On top, taking effects of finite N into account, the picture could have important implications for eternal dS and the cosmological constant problem (for related work see also [37]).

1.4 Semi-classical Picture of Solitons and Instantons

Following the logic that classical solutions only approximate a more fundamental quantum mechanical description, we will not only develop a microscopic model for gravitational backgrounds in this thesis, but also for solitons an instantons within field theory. In order to give a self-contained presentation, we will first of all briefly review the standard approach to the physics of solitons and instantons. Although we will discuss some generic features of these objects, we will mostly consider specific examples which will be most relevant in later parts of the thesis[7]. For more general and complete discussions on the physics (and mathematics) of solitons and instantons we recommend standard textbooks such as [38,39]. In the first subsection, we will discuss topological solitons using as an example the kink in $1+1$-dimensional scalar field theory. We proceed by discussing properties and results concerning instanton physics. In order to illustrate the physics of instantons and for later convenience, we will focus on two specific examples, instantons in a quantum mechanical double well potential on the one hand, and instantons in Yang Mills theory on the other hand. Finally, we consider solitons and instantons in the context of supersymmetric field theories. In particular, we will emphasize the importance of so-called BPS configurations in supersymmetric theories. As we will discuss, the configurations preserve parts of the original supersymmetries. We carefully chose to review these topics because later, when discussing the corpuscular theory of solitons and instantons, we will steadily refer of the material covered here.

1.4.1 Solitons

Solitons are defined as stable, localized, finite energy solutions to the classical equations of motion. There are two types of solitons, topological and non-topological. In this thesis we will mostly be interested in topological solitons. Nevertheless, in order to test the corpuscular theory, we will later also develop a coherent state approach to non-topological solitons. This allows to extract common as well as differing features of topological and non-topological solitons from the corpuscular point of view as we shall explain in detail in later parts of the thesis. In this part, however, we want to restrict ourselves to a

[7] Within the corpuscular theory, we will discuss even more examples than the ones presented here. These, however, will be introduced in the corresponding section in a self-contained way. Here, we will only try to highlight some of the features which are common to arbitrary solitons and instantons using some well-known examples.

discussion of the properties of topological solitons in the semi-classical approach. These objects correspond to solutions of the classical equations of motion which are stabilized by boundary conditions at spatial infinity. Consequently, a topological charge can be associated to these configurations. This charge is somewhat analogous to an electric-type charge in the sense that it is conserved. Physically, however, it is not associated to a long-range field, but rather related to a topologically non-trivial structure of the vacuum manifold of a theory. For a given topological charge, there is a special configuration, the so-called BPS configuration which minimizes the Hamiltonian in that topological sector. These configurations are of particular interest in supersymmetric theories because they preserve parts of supersymmetry. Before discussing supersymmetric solitons, however, let us elaborate on the physics of solitons using a specific example, the kink in $1+1$-dimensional scalar field theory.

An Example-The Kink

The simplest example of a topological soliton is a so-called kink in $D = 1+1$ dimensions. This object is a solution of the theory described by a Lagrangian involving a real scalar field ϕ only,

$$\mathcal{L} = \frac{1}{2}\partial_\mu\phi\partial^\mu\phi - V(\phi), \tag{1.30}$$

where $V(\phi)$ is the classical potential for the field ϕ. Considering static solutions[8], the Hamiltonian (energy) of the system can be written as

$$H = \int dx\Big(\frac{1}{2}(\partial_x\phi)^2 + V(\phi)\Big) = \frac{1}{2}\int dz\Big(\partial_x\phi \pm \sqrt{2V(\phi)}\Big)^2 \mp \int dx(\partial_x\phi)\sqrt{2V(\phi)}. \tag{1.31}$$

Since the first term on the right-hand side of (1.31) is a perfect square, we immediately conclude that the energy of any configuration is bounded from below by the second term. Let us now consider the specific example $V(\phi) = (m^2/g - g\phi^2)^2$, where m is a parameter of mass dimension and g is the coupling. This theory has two degenerate vacua at $\phi = \pm m/g$. Minimizing the energy corresponding to this potential, we find the so-called kink solution,

$$\phi_{sol}(x) = \frac{m}{g}\tanh((x - x_0)m), \tag{1.32}$$

where x_0 is a constant of integration. Notice that this solution interpolates between the two vacua, i.e. it approaches $-m/g$ at $x = -\infty$ and m/g at $x = +\infty$. Furthermore, the profile changes significantly only on a lengthscale given by m^{-1}. In other words, the kink stores most of its energy density on the scale m^{-1} around its center at x_0. Finally, we can define a trivially conserved current $j_\mu = 1/2\epsilon_{\mu\nu}\partial^\nu\phi$. Note that the corresponding charge $1/2\int dx\partial^x\phi = 1/2(\phi(+\infty) - \phi(-\infty)) = m/g$ is non-vanishing because of the non-trivial boundary conditions of the solution. Thus, there is a charge connected to the properties

[8] Time-dependent solution can be obtained by Lorentz boosting.

of the kink at infinity, a so-called topological charge, which stabilizes the field. It can be shown that this charge is directly related to the energy of the configuration via the so-called BPS condition which we shall explain in much more detail below. There is another solution given simply by $-\phi_{sol}$. This is the so-called anti-kink which has opposite topological charge to the kink. Notice that in contrast the constant solution, $\phi = m/g$, has topological charge 0. In other words, due to conservation of topological charge, it is not possible to deform the kink solution to the constant solution. This can be understood easily from a more physical point of view. Deforming the kink to the constant solution would cost an infinite amount of energy and is consequently excluded. To summarize, while energy is stored on the scales determined by $\Delta x \sim m^{-1}$, topology follows from global properties of the solution. Nevertheless, the BPS condition connects the two in a non-trivial way as we shall discuss in the context of supersymmetric versions of (1.30) in more detail. In the corpuscular theory, however, we will argue that this relation cannot be maintained. Indeed, understanding the physics of the violation of the BPS condition from the point of view of a microscopic quantum theory, will be one of the major goals in later parts of the thesis.

At a mathematical level, the existence of such topologically non-trivial solutions is also guaranteed by homotopy theory. The interested reader, however, is referred to the literature for a mathematical classification of topological solitons (and instantons).

Fluctuations

Let us elaborate a little bit more on the physics of the kink which will be important in later chapters of the thesis. In the standard semi-classical treatment, one is usually interested in fluctuations around the classical background. Thus, one expands in small fluctuations around the background, $\phi = \phi_{sol} + \phi_q$. Inserting this ansatz in into the classical equation of motion leads to a differential equation for the field ϕ_q in the background of the kink. This equation in turn determines the spectrum of fluctuations in terms of mass eigenstates. It should be clear that there is a zero-mode corresponding to a Goldstone boson of spontaneously broken translational invariance along the x-direction. On top, there is a tower of massive states. Furthermore, if the field ϕ is coupled to fermions, one can show that the kink also supports fermionic zero modes [40][9]. Having determined the spectrum of fluctuations, one can then proceed as usual and consider the QFT of the fluctuations in the kink background. We will have to say more on this point later when discussing supersymmetric theories with solitons.

The Moduli Space

For now, we briefly want to mention that the number of zero-modes in a given solitonic (or instanton) background is closely connected to the so-called moduli space. This space is defined as the set of all physically inequivalent vacua. In other words, moving in the moduli space, we change the physical parameters of the theory (such as e.g. renormalized masses or couplings). It can be shown that the dimensionality of this space also determines the

[9] Note that the existence of the fermionic zero modes is guaranteed by the index theorem [39].

number of zero modes in the background of the soliton (instanton). Roughly speaking, the moduli space is spanned by all possible values of the parameters which explicitly appear in the soliton (instanton) solution and which break certain symmetries. Since there are goldstone bosons for each symmetry, the number of zero modes should coincide with the dimensionality of the moduli space. Of course, this is only a very qualitative argument. Nevertheless, it captures the main idea. For a more rigorous discussion on the connection of moduli and zero modes we refer, for example, to [39].

1.4.2 Instantons

Let us now proceed and discuss some of the most important properties of instantons. In contrast to solitons which are objects in real time, an instanton describes a tunneling process in imaginary time between some initial and final state. In other words, an instanton corresponds to a quantum mechanical tunneling through a potential barrier. Of course, for the process to have non-vanishing probability, the energy of the final state should not exceed that of the initial state[10]. Since instantons describe transition amplitudes in imaginary rather than in real time, one should define them as solutions of the Euclidean equations of motion of finite Euclidean action S_E. Notice that solutions of infinite Euclidean action cannot correspond to non-vanishing tunneling probability by default because in the saddle-point approximation (which one usually studies in the semi-classical treatment) we have $\langle f|in\rangle = e^{-S_E} = 0$, where $|in\rangle$ and $|f\rangle$ are the initial and final states, respectively. Furthermore, just as in the case of solitons, there are topological as well as non-topological instantons. For topological instantons, there is a trivially conserved current and, correspondingly, a topological charge stabilizing the instanton. Similar to solitons, the solution which minimizes the Euclidean action in a given topological sector obeys the BPS condition. It is special because if embedded in a supersymmetric theory, it preserves part of the supersymmetry as we will dicuss. For non-topological instantons, there is no topological charge and the instanton has finite probability to decay into the ground state of the theory.

In later parts of the thesis, among others, we will be interested in particular in the corpuscular theory of instantons in a quantum mechanical double well potential and in the context of Yang Mills theory. Therefore, let us briefly review some of the features of these configurations within the semi-classical theory. For more exhaustive discussions on instantons in the double well and in Yang Mills theory, the reader is referred to [39,41–43].

Instantons in the Double Well Potential

In this part we wish to review some of the properties of instantons in the simple example of a quantum mechanical double well potential. The theory is defined classically by the following Lagrangian,

$$\mathcal{L} = (\partial_t \phi)^2 - g^2(\phi^2 - m^2/g^2)^2. \tag{1.33}$$

[10] We restrict our discussion to field theories at zero temperature.

Notice first that although we work in quantum mechanics, we adopted a field theoretic notation for later convenience. In other words, we view the theory (1.33) simply as a $0+1$-dimensional QFT. Secondly, the model (1.33) has exactly the same form as the theory for the kink described above in one more spatial dimension (of course, this implies that the mass dimensionality of the coupling differs in the two theories). Since the kink corresponds to a static solution of the equations of motion while the instanton solves the Euclidean equations of motion obtained when varying a Wick-rotated version of (1.33), there already seems to be a connection between the two. The general dictionary that clearly allows to identify the physics of the two configurations, however, shall be established in much more detail later when discussing the corpuscular theory of instantons. As expected from the previous discussion, the instanton solution takes on a form similar to that of (1.32),

$$\phi_{ins} = \pm\frac{m}{g}\tanh(tm), \tag{1.34}$$

where we set the instanton center to zero, $t_0 = 0$. This solution describes the tunneling from one of the vacua, $\pm m/g$ at $t = -\infty$ to the other vacuum $\mp m/g$ at $t = +\infty$. The Euclidean action of this solution is easily found to be $\frac{8m^3}{3g^2}$. Note already at this point, that this result coincides with the energy of the kink in one more spatial dimension introduced before if we identify the couplings in the two theories in terms of a lengthscale relating the action of the instanton and the mass of the soliton. This is no coincidence, but rather has a clear physical interpretation which we shall uncover when presenting the quantum theory of instantons.

Furthermore, (1.34) plays an important role in the context of instanton-induced transitions [43]. Using standard semi-classical methods, the amplitude for transitions of excited states in one of the vacua to an excited state in the other vacuum was computed in [43]. Using a saddle-point approximation for the S-matrix combined with the LSZ reduction formula for the in-states and out-states, the authors showed that the amplitude (neglecting the contribution of zero modes) is given by[11]

$$\mathcal{A}_{n\to n} = \exp\Big(-\frac{4}{3}\frac{m^3}{g^2}\Big)\frac{1}{n!}\Big(16\frac{m^3}{g^2}\Big)^n, \tag{1.35}$$

where n means that we are looking at the n-th excited level. Notice that the result is valid only for $n \ll m^3/g^2$, i.e. much below the potential barrier m^4/g^2. For $n \gg m^3/g^2$, the amplitude grows unbounded, thereby signaling a breakdown of the expansion used. In later parts of the thesis, we will show how the result (1.35) can be easily understood fully quantum mechanically using a coherent state resolution of the instanton profile (1.34). Furthermore, we discuss a possible unitarization mechanism in terms of asymptotic states constructed from corpuscles of the kink in $1+1$ dimensions.

A related question concerning the model (1.33) is connected to the idea of resurgent trans-series [41, 42, 44, 45]. As it is well known, a naive perturbative expansion around

[11] Note that we rewrote their result such that it matches with our conventions.

the trivial saddle-point has zero radius of convergence. This problem can often be circumvented by performing a Borel resummation of the series. In case that the resulting series is alternating, perturbation theory leads to unambiguous and well-defined results. Suppose, however, that the theory has degenerate vacua. Then it often happens that the Borel-series is non-alternating. This leads to ambiguities (imaginary parts contributing to real observables) in defining the series expansion properly [41]. In such a situation, however, one should also take into account the effect of instantons. In other words, since instantons contribute to the functional integral of the theory with finite Euclidean action, one should take the perturbative expansion around the instanton solution seriously when defining observables. Taking all instanton saddles as well as the saddles due to instanton-anti-instanton solutions into account leads to the concept of resurgent trans-series. The important point is that this series expansion is believed to give unambiguous results [44,45]. Although not proven, the validity of resurgence was demonstrated in several examples in quantum mechanics [44, 45], QFT [46, 47] as well as in string theoretic models [48, 49] and is subject of ongoing research. Let us try to illustrate the idea. Suppose you are working on the naive perturbative vacuum. Then, as explained above, the Borel resummation will lead to an ambiguous part which is purely imaginary. By conservation of topological charge such a contribution can only be canceled when expanding around other saddles which are topologically trivial. These are exactly the saddles connected to a solution describing an equal number of instantons and anti-instantons (since their topological charge is opposite). The interaction of instantons and anti-instantons (which we shall reproduce later using coherent states) then leads to complex logarithms which induce an imaginary part exactly canceling the one appearing after Borel resumming the expansion around the trivial saddle. Resurgence now states that such a cancellation should take place within all the sectors of a given topological charge.

Although it is sensible that such a mechanism takes place, the literature to our knowledge still lacks a proper quantum mechanical understanding of this phenomenon. Using the corpuscular approach to instanton physics we will try to give such an explanation. Having a full quantum description, we will later argue that the mechanism of cancellation of imaginary parts in observables, i.e. the concept of resurgence, is a simple consequence of the optical theorem. In other words, possible imaginary parts generated on the trivial saddle must inevitably be canceled by intermediate states corresponding to instantons and anti-instantons viewed as coherent states.

Yang-Mills Instantons

Let us now consider instantons in pure $SU(N)$ Yang-Mills theory in $d = 4$ Euclidean dimensions. The Euclidean action is given by

$$S_E = \int d^4x \frac{1}{4} G^a_{\mu\nu} G^a_{\mu\nu} \tag{1.36}$$

Here $G^a_{\mu\nu} = \partial_\mu A^a_\nu - \partial_\nu A^a_\mu + g\epsilon^{abc} A^b_\mu A^c_\nu$ is the non-abelian field strength and A^a_μ the corresponding gluon field. Completing the square in (1.36), we can rewrite the Euclidean action

(we will only consider self-dual systems in what follows);

$$S_E = \frac{1}{8}\int d^4x \big(G^a_{\mu\nu} - \tilde{G}^a_{\mu\nu}\big)^2 + Q\frac{8\pi^2}{g^2}, \tag{1.37}$$

where $\tilde{G}^a_{\mu\nu} = 1/2\epsilon_{\mu\nu\alpha\beta}G^a_{\alpha\beta}$ is the dual field strength, g is the Yang-Mills coupling and Q the topological charge given by

$$Q = \frac{g^2}{32\pi^2}\int d^4x G^a_{\mu\nu}\tilde{G}^a_{\mu\nu}. \tag{1.38}$$

Notice that $G^a_{\mu\nu}\tilde{G}^a_{\mu\nu} = \partial_\mu K_\mu$, where K_μ is the topological Chern-Simons current,

$$K_\mu = 2\epsilon_{\mu\nu\alpha\beta}(A^a_\nu\partial_\alpha A^a_\beta + \frac{g}{3}f^{abc}A^a_\nu A^b_\alpha A^c_\beta), \tag{1.39}$$

with f^{abc} the $SU(N)$ structure constants.
Note that the Euclidean action is minimized for self-dual configurations, $G = \tilde{G}$, which corresponds to the BPS condition in the case of the Yang-Mills instanton. Let us focus on the $SU(2)$ instanton with topological charge $Q = 1$ in four Euclidean dimensions (the so-called BPST instanton [50]). The classical profile is obtained as a solution to the classical BPS condition $G = \tilde{G}$ that follows from (1.37):

$$A_{a\mu} = \frac{2}{g}\eta_{a\mu\nu}\frac{x_\nu}{(x-x_0)^2+\rho^2}, \tag{1.40}$$

where x_0 denotes the instanton center, ρ is the scale modulus (typical size) of the instanton and $\eta_{a\mu\nu}$ are the so-called 't Hooft symbols (for a definition of the 't Hooft symbols we refer the reader to Shifman's book [39]). Notice that (1.40) is only one representative of a family of gauge equivalent solutions. In this thesis, however, we will only work with this choice. Since this solution has topological charge $Q = 1$, we can infer from equation (1.37) that its Euclidean action is given as $S_E = 8\pi^2/g^2$. We thus see that the action is independent of the modulus ρ. In other words, instantons in four Euclidean dimensions come in arbitrary sizes without affecting the action. Physically this makes sense because in this case Yang-Mills theory contains no lengthscale at the level of the classical action. In other words, scale invariance of the classical theory implies that the instanton action should be independent of ρ[12].

Let us briefly discuss the moduli of the solution (1.40). Obviously, there are four moduli corresponding to the position x_0 in four-dimensional Euclidean space and the scale modulus ρ. Furthermore, one can obtain new solutions by acting with global $SU(2)$ rotations acting on the internal indices. Since $SU(2)$ has three generators we find that the BPST instanton

[12] Of course, considering loops of fluctuations in the instanton background leads to a breaking of scale invariance via dimensional transmutation. These effects, however, can be fully absorbed in a redefinition of a coupling so that it runs as a function of ρ.

in $SU(2)$ has eight moduli in total. Thus, it supports eight bosonic zero modes. In general, one can show that the moduli space of self-dual instantons of topological charge k in $SU(N)$ Yang-Mills theory is given by $4Nk$. It is worth mentioning that the moduli space metric becomes singular as we take $\rho \to 0$. This suggests that new physics resolving this singular point is needed if we consider instantons of vanishing size. While this fact is puzzling at the classical level (Yang-Mills in four dimensions is scale-invariant classically and asymptotically free at short distances at the quantum level), the singularity has a clear and simple interpretation in the corpuscular theory as we shall explicitly show.

1.4.3 Supersymmetry

Before discussing the role of solitons and instantons in supersymmetric field theories, let us briefly review some of the most important aspects of supersymmetry. The main idea of supersymmetry is to enlarge the Lorentz group in a non-trivial way. By the Coleman-Mandula theorem [51] such an enhancement is only possible if the new generators are fermionic. The resulting algebra is called super-Poincaré algebra. The implications of this algebra are extremely profound as we shall briefly discuss. The explicit form of the $\mathcal{N} = 1$ supersymmetry algebras in two and four space-time dimensions (including central charges) can be found in [39]. As a consequence of this algebra, one can immediately derive the following properties of supersymmetric theories:

- If supersymmetry is unbroken then the energy corresponding to an arbitrary state is always positive. In particular, in a theory without central extension, Z, the energy of the vacuum vanishes. If a theory has a non-trivial central extension, the vacuum energy coincides with this central extension. It will be this latter property that we will study in detail in the corpuscular approach.

- If supersymmetry is unbroken, all particles belonging to an irreducible representation of the supersymmetry algebra have the same mass.

- The number of degrees of freedom of bosons and fermions in a given supermultiplet (irreducible representation) coincide.

Notice that the first property tells us that the energy of the vacuum is zero without the need of normal ordering. This is completely different in non-supersymmetric theories, where we usually subtract an infinite (unphysical) contribution to set the vacuum energy to zero. The reason why supersymmetry does not need normal ordering can roughly be understood as follows: By the second and third property, there are always the same number of physical fermions and bosons in the spectrum of a supersymmetric theory. Furthermore, since in a given multiplet bosons and fermions have the same masses, both satisfy the same dispersion relation. Expressing the Hamiltonian as usual in terms of creation and annihilation operators of the fields, there will be divergent contributions when acting on the vacuum state. There are, however, contributions of bosons and fermions having the same dispersion. Since bosons are governed by commutation relations, fermions

must fulfill the corresponding anti-commutation relations. As a consequence, the divergent contributions cancel. Note that this is the first example of a non-renormalization theorem in a supersymmetric theory. Another important non-renormalization theorem which we shall review briefly is that of the so-called superpotential (for a discussion concerning superfields and superspace the reader is referred to [52]). The superpotential basically describes the interaction part of a supersymmetric field theory. It has the remarkable property that it receives no quantum corrections, for example, in four space-time dimension. Notice that this is an exact statement which holds to all orders of perturbation theory. The proof of this non-renormalization theorem basically relies on the properties of R-symmetry and holomorphicity and was first given in [53]. Notice that this is no longer true e.g. in two space-time dimensions. In that case, fermions are in a real (Majorana) representation of the super-Poincaré algebra and propagate only one degree of freedom. In order for the theory to be supersymmetric, bosonic components of supermultiplets must be real. Therefore, instead of being holomorphic, the superpotential which combines fermions and bosons is real. Reality, however, is not as restrictive as holomorphicity. Thus, the superpotential for such theories is in general not protected from quantum corrections. Nevertheless, in the case of supersymmetric kinks, quantum corrections to the superpotential act in such a way that the BPS condition is still obeyed to all orders of perturbation theory. We will briefly come back to this point in the next subsection.

Thus, in conclusion we see that supersymmetry has some remarkable properties which are not present in ordinary QFT's. In the next part, we combine our knowledge to discuss topological defects in supersymmetric theories.

1.4.4 Supersymmetric Solitons and Instantons

Solitons and instantons saturating the BPS bound are of particular interest in supersymmetric theories. The reason is that such solutions preserve a part of the supersymmetry. In contrast, solutions in the same topological sector, but with energy larger than BPS configurations inevitably break supersymmetry completely. As a consequence, topological defects played a major role in the literature on dynamical breaking of supersymmetry [54]. Since a large part of the thesis will be devoted to quantum mechanical deviations from the BPS condition, let us briefly recall why BPS saturated solitons and instantons preserve parts of the supersymmetry in the semi-classical treatment. For illustrational purposes let us consider as an example the kink in $1+1$ space-time dimensions. Similar arguments can be generalized to more complicated solitons and in particular also to instantons in supersymmetric Yang-Mills theory.

First of all it is obvious that any soliton breaks translational invariance. By the super-Poincaré algebra ($\{Q, \bar{Q}\} \propto P$) this in general implies that supersymmetry is completely broken on the background of the soliton. There are, however, special configuration, namely the BPS saturated solitons. Indeed, in the case of a static configuration in $1+1$ dimensions,

the supercharges take the form

$$Q_1 \propto \partial_x \Phi + \partial_\Phi \mathcal{W}$$
$$Q_2 \propto \partial_x \Phi - \partial_\Phi \mathcal{W}. \tag{1.41}$$

Here $\mathcal{W}$ denotes the superpotentail and Φ is a chiral superfield combining scalar and fermionic component fields. Note that these conditions are exactly the (anti)-BPS conditions rewritten in terms of the superpotential. Now consider a kink obeying the BPS condition. In this case, the second line in (1.41) vanishes identically. Thus, we immediately see that the configuration preserves half of the original supersymmetries. The other supercharge Q_1, however, does not vanish. Thus, Q_1 corresponds to a broken generator. Similarly to the Goldstone theorem, it can be shown that a broken supersymmetry generator is accompanied by the appearance of a massless particle, a goldstino. Notice that there is also a bosonic zero mode due to breaking of translational invariance. These fields pair up as a supermultiplet with respect to the unbroken generators Q_2. If we had considered a profile which breaks all supersymmetries, there would be an additional goldstino zero mode corresponding to Q_2. Therefore, the bosonic and fermionic spectra no longer match which is consistent with the fact that the theory is no longer supersymmetric. Let us focus on the configurations which preserve half of the supersymmetry. It can be shown that the classical energy of such configurations is given by the central extension of the superalgebra which in turn is determined by the topological charge of the kink [39]. One might wonder whether such a statement still holds when considering quantum fluctuations in the kink's background. In $1+1$ space-time dimension the analysis is a little bit subtle. Since the superpotential receives quantum corrections in this case, it is not at all obvious that the relation between mass and topological charge will hold to arbitrary orders in perturbation theory. Nevertheless, after a long debate in the literature (for a summary see [55] and references therein), the equality was established to all orders. In other words, the central extension is renormalized in the same way as the energy of the profile. Notice that this statement is extremely non-trivial. Indeed, as discussed before, since topology is determined by global properties, i.e. the boundary conditions at spatial infinity one imposes on the solution, energy is determined by the gradients of the solution which are non-trivial only on lengthscales given by the inverse mass of the field. Therefore, naively one could expect that topology and energy are independent quantities. Nevertheless, BPS-saturated solitons are special in the sense that the former is directly given by the latter. In the corpuscular treatment, however, we will show that such a relation can no longer be maintained. The reason is that corpuscles contributing to topology have zero momentum and are thus not subject to quantum corrections. In contrast, the quanta accounting for the energy have finite wavelength of the order of the size of the soliton and are thus not protected from quantum fluctuations. We shall show in detail in this thesis that this is the origin of quantum violations of the BPS condition and subsequently the reason of quantum mechanical breaking of supersymmetry. We thus once again see that the corpuscular effects are of a completely different nature than the usual loops effects due to fluctuations in the presence of a fixed background. While the latter will never lead to departures from the

kink being BPS-saturated, the former will inevitably lead to corrections. In other words, restoration of supersymmetry is only achieved in the limit where one sends the number of corpuscles contributing to the energy of the soliton to infinity, i.e. in the semi-classical limit in which a resolution of the profile is no longer possible.

1.5 Conventions

Before representing the findings of our research, let us briefly set the conventions. We will work mostly in units where $c = \hbar = 1$. Whenever convenient, however, we will explicitly restore powers of $\hbar$.

Following the standard conventions used in the literature, we choose to work with a "mostly +" metric in the context of gravity. Within quantum field theory, however, the metric convention will be "mostly −".

Finally, we will put "hats" on all creation and annihilation operators. Considering field operators, however, we will omit hats.

Chapter 2

Auxiliary Current Approach

In this chapter we introduce the method of auxiliary currents as a tool of representing classical solutions as quantum bound states of a large number of constituents. In the first section, we will present the general construction and explain how it can be used to describe black holes and space-times with perturbations in terms of elementary graviton fields and possibly other degrees of freedom. Subsequently the formalism will be applied to address concrete questions black hole physics. In particular, we construct and compute observables connected to the black hole interior such as constituent density and energy density of constituent gravitons inside the black hole. Explicit results are obtained at lowest order (partonic level) in the limit $M, N \to \infty$ with M/N fixed, where M denotes the mass of the black hole and N the typical number of constituents. Notice that, although we work at the partonic level mostly, the results are nevertheless non-trivial in the sense that large collective effects are parametrized in terms of condensates as will be explained in detail. Furthermore, it is possible to trace back the effects of finite N. In particular, for finite N, quantum corrections naturally appear as powers of $1/N$. Thus, our formalism can be viewed as an explicit field theoretic realization of the ideas put forward in the Black Hole Quantum N Portrait.

Further, we show how these observables can be embedded within S-matrix processes. One of our key findings is that an outside observer can have access to the black hole interior doing scattering experiments. By measuring the cross section of the particle which is scattered on the black hole information about the density of constituents inside the bound state can be obtained. Notice that these findings immediately suggest that our formalism could shed new light on the information paradox and related problems connected to black hole physics.

As a final application, we show how the Schwarzschild metric emerges from our description as an effective phenomenon. For that purpose we develop a quantum mechanical understanding of the black hole viewed as a source within the auxiliary current approach. We argue that microscopically, this source must be understood in terms of the energy-momentum tensor of gravitons in the black hole which we will already compute to leading order in the next subsection. At this level, it is shown that our construction indeed correctly accounts for the exterior Schwarzschild geometry. Furthermore, quantum corrections

due to the finiteness of the black hole mass will be computed explicitly. These can be interpreted rather naturally as a renormalization of the black hole wave function.

2.1 Auxiliary Currents for Bound States

In the first part of this chapter we want to introduce the general formalism for describing bound states in the context of relativistic field theory. We will show that a generic bound state in the spectrum of a Hamiltonian can be represented in terms of fields which appear in the microscopic theory. Using this representation, one can use standard field theoretical methods in order to compute correlation functions connected to the bound state of interest. In the first subsection, we will present the general construction which will subsequently be applied to black holes. It is shown that this construction reduces to LSZ-type formulas for local, composite operators in the asymptotic framework of the S-matrix. Finally, we show how to generalize the auxiliary current construction in such a way that arbitrary space-times including perturbations can be represented as quantum bound states on Minkowski space-time.

2.1.1 Generic Construction

Let us start by constructing general quantum mechanical bound states in terms of constituent degrees of freedom. Before deriving an exact expression for the quantum state, let us first recall how bound states enter the spectrum of the Hamiltonian of a given theory and how such a state can be represented in terms of Fock basis states.

Spectral Decomposition of the Two-Point Function

For that purpose let us remind the reader of the Kallen-Lehmann (spectral) representation of the two point function of elementary fields in a QFT following [56]. Let us for simplicity consider an interacting scalar field theory in $(3+1)$ space-time dimensions [1]. Label the eigenstates of the corresponding Hamiltonian by $|\lambda_{\mathbf{p}}\rangle$, where $\mathbf{p}$ denotes the three-momentum of the state. Note that we can always obtain a state of a given momentum $\mathbf{p}$ by Lorentz boosting the corresponding eigenstate with vanishing three-momentum, $|\lambda_0\rangle$. In order to analyze the spectral properties of the two-point function, we shall make use of the completeness relation for the full Hilbert space of the theory,

$$\mathbb{I} = |\Omega\rangle\langle\Omega| + \sum_{\lambda} \int \frac{d^3\mathbf{p}}{(2\pi)^3 2E_\lambda(\mathbf{p})} |\lambda_{\mathbf{p}}\rangle\langle\lambda_{\mathbf{p}}|, \tag{2.1}$$

where $E_\lambda(\mathbf{p}) = \sqrt{\mathbf{p}^2 + m_\lambda^2}$ denotes the energy of the eigenstate $|\lambda_{\mathbf{p}}\rangle$, m_λ its mass and $|\Omega\rangle$ is the unique ground state in Minkowski space-time. Inserting (2.1) into the two-point

[1] Generalizing the arguments given here for other fields is straightforward. For higher spins, however, one needs to introduce several spectral functions.

function (assuming $x_0 > y_0$) and performing some standard manipulations using Lorentz invariance yields

$$\langle\Omega|\phi(x)\phi(y)|\Omega\rangle = \sum_\lambda \int \frac{d^4p}{(2\pi)^4} \frac{1}{p^2 - m_\lambda^2 + i\epsilon} e^{-ip(x-y)} |\langle\Omega|\phi(0)|\lambda_0\rangle|^2, \tag{2.2}$$

where p is the four-momentum of the state. Performing a similar analysis for the case $y_0 > x_0$ we arrive at the Kallen-Lehmann spectral representation of the time-ordered two-point function of the full theory,

$$\langle\Omega|\phi(x)\phi(y)|\Omega\rangle = \int_0^\infty \frac{dM^2}{2\pi} \rho(M^2) \Delta_F(x-y; M^2), \tag{2.3}$$

where $\Delta_F(x-y; M^2)$ is the Feynman propagator with "mass" M and

$$\rho(M^2) = \sum_\lambda (2\pi)\delta(M^2 - m_\lambda^2) |\langle\Omega|\phi(0)|\lambda_0\rangle|^2 \tag{2.4}$$

is the so-called spectral density. Notice that the spectral density contains information about the full spectrum of the theory. In particular, in a general theory, one-particle states, multi-particle states as well as bound states contribute to the spectral density. Therefore, the full two-point function can be interpreted as a propagation from a point x to y dressed with intermediate multi-particle states and bound states. Note that the intermediate multi-particle states have the obvious interpretation of virtual particles running in loops. By energy-momentum conservation, there is a threshold for production of such particles. Beyond that threshold, however, these multi-particle states can run in the loop with arbitrary energy. Therefore, there is a continuum of such states contributing to the two-point function as soon as p is large enough. In contrast, one-particle states and bound states contribute to the spectral density in the form of isolated mass poles.

Let us illustrate the spectral decomposition in the simple example of quantum electrodynamics (QED) with only electrons, positrons and photons. The single particle states correspond to physical particles such as electrons. These contribute an isolated pole to the spectral density at $p^2 = m_e^2$, where m_e denotes the renormalized, physical mass of the electron. Furthermore, the free propagator is corrected by loops of photons, electrons and positrons leading to the continuum contribution in the Kallen-Lehmann spectral decomposition. Finally, there are bound states such as positronium leading to a poles. The positions of these poles are determined by the binding energies of positronium. Note that the construction can easily be generalized to higher-order correlation functions revealing the full analytic structure of the S-matrix of the theory. Indeed, the bound state poles of a two-particle bound system appear as an infinite resummation of contributions to the four-point contribution to the S-matrix.

Fock Space Representation of Bound States

Having discussed the spectral properties of the two-point function in an interacting theory, let us have a closer look at the bound state spectrum. First of all, a given bound state

transforms according to certain representations of the symmetry groups of the underlying QFT. Secondly, given a bound state, we are usually interested in its composition in terms of microscopic degrees of freedom. At a theoretical level we thus expand a given bound state in terms of a Fock basis of multi-particle states consistent with the transformation properties of the bound state[2].

To illustrate this point, let us consider the example of bound states in QCD. In this case, bound states are characterized by flavour content, electrical charge, isospin and transformation properties with respect to the Lorentz Group. Furthermore, due to confinement, all hadrons should be color singlets. Therefore, a given hadron can be expanded in a basis of quark and gluon states transforming accordingly. Of course, in general there are infinitely many such states $|\mathrm{i}\rangle$ having non-vanishing overlap with the true quantum state of the hadron. Thus, schematically we can expand the state of the hadron $|\mathrm{H}\rangle$ as

$$|\mathrm{H}\rangle = \sum_{\mathrm{i}} \alpha_{\mathrm{i}} |\mathrm{i}\rangle \tag{2.5}$$

where $|\alpha_{\mathrm{i}}|^2$ is the probability of detecting the hadron in the Fock state $|\mathrm{i}\rangle$. One then might ask for example: "Why is it appropriate to represent a proton in term of two up-quarks and one down-quark when studying deep inelastic scattering in the Bjorken limit? From (2.5) this should only be a good approximation as long as $\alpha_{uud} \simeq 1$ with all other coefficients close to zero. Why is this assumption justified?" The answer to this question is in principle already encoded in the question itself. The reason is that the question singles out a specific kinematic regime corresponding to infinite momentum transfer in the scattering process. In other words, the coefficients in general depend on the scale at which we perform an experiment. Due to asymptotic freedom, QCD in the Bjorken limit becomes a theory of free quarks with respect to the strong interactions. Therefore, in this limit, a representation of the proton in terms of two up-quarks and one down-quark leads to sensible predictions for cross sections matching the parton level results. At lower energies, however, the running of the QCD coupling should be taken into account. In explicit computations, this running can be related to a running of the distribution functions of quarks and gluons inside the proton [57]. In other words, computing the distribution functions as a function of the renormalization scale gives information on "how much a proton looks like a state $|\mathrm{i}\rangle$" as a function of the renormalization scale μ.
Thus, although in general a bound state has non-vanishing overlap with a plethora of states there are kinematical regimes which single out a preferred Fock eigenstate of the Hamiltonian. Understanding when a kinematical regime allows for a good description in terms of a given eigenstate requires either experimental input and subsequent renormalization group evolution as in QCD or physical arguments and insight like it is the case in the Black Hole Quantum N Portrait, where a large black hole of given mass is represented as a bound state of N gravitons. Notice that in the latter picture the label N is a good

[2]Note that this statement is consistent with the fact mentioned earlier concerning the appearance of bound state poles in terms of an infinite resummation. In other words, if we properly want to take bound states into account, it is necessary to consider infinitely many Fock eigenstates.

approximation, because the individual constituents are weakly interacting. There is no principle, however, which forbids the black hole to have overlap with a state composed out of $N' \neq N$ gravitons. As long as we cannot rely on experimental data, one should thus parametrize physical observables in terms of constants characterizing the overlap between the true black hole state and a N-graviton state as we shall do when discussing the auxiliary current description of the black hole.

Auxiliary Current Representation of Bound States

Before explaing how bound states can be naturally embedded in the framework of the S-matrix, we shall first of all derive a generic expression for the bound state in terms of the microscopic degrees of freedom of the underlying theory which is independent of any asymptotic construction. Indeed, when computing observables connected to the interior of the black hole we will make heavy use of this non-asymptotic construction.

As explained before, at the kinematical level all quantum states are identified by their quantum numbers. In particular, from the point of view of representing a bound state in terms of Fock eigenstates constructed from the weakly coupled degrees of freedom appearing in the microscopic Lagrangian, it is clear that only those Fock states have non-vanishing overlap with the bound state which carry the same quantum numbers as the latter. In other words, these states should have quantum numbers in accordance with the intrinsic symmetries at work (such as gauge symmetries), and with the isometries characterizing bound states in Minkowski space–time. Furthermore, the state has to be characterized according to the Casimir operators of Minkowski, i.e. mass squared and spin. Including all these quantum numbers, collectively denoted as $\mathcal{L}$, leads to a complete kinematic characterization of the bound state in question.

In Minkowski space-time there is a unique ground state $|\Omega\rangle$ which supports all quantum numbers $\mathcal{L}$ in the bound state spectrum. In particular, bound states can be created using appropriate auxiliary currents $\mathcal{J}$ acting on $|\Omega\rangle$. These currents should contain the field content associated with the bound state at hand. Furthermore, the current should be subject to the same transformation properties as the bound state itself. For example the current for the ρ–meson is given by $\mathcal{J}^{\mu}_{\rho} = 1/2(\bar{u}\gamma^{\mu}u - \bar{d}\gamma^{\mu}d)$ [58], where u and d are the up and down quark fields, respectively. Notice that this current has the correct isospin, charge and colour quantum numbers to represent a ρ–meson. This ensures that the overlap with the true state of the ρ–meson is non–vanishing, thus allowing to express the true state $|\rho\rangle$ in terms of $\mathcal{J}^{\mu}_{\rho}$. Notice that, as explained before, choices of the current with different field content, but the same transformation properties under the symmetries of the theory also lead to non-trivial overlap. In particular, introducing gauge invariant combinations of the non-abelian gauge field in the current in addition to the quark fields will generate a quantum state when acting on the vacuum which gives another well-defined representative for the ρ–meson. As discussed previously, the concrete current we will work with in explicit computations will be motivated by physical considerations. As another example consider positronium of zero spin in quantum electrodynamics (QED). Kinematically, the bound state corresponds to a state of zero electric charge and mass $2m_e$ with m_e the electron

mass. Thus, a sensible auxiliary current in this case could be $\mathcal{J}_{pos} = e^+e^-$ with e^+ and e^- the electron and positron field operators, respectively and their spins anti-aligned.

In our case the current should be composed out of N gravitons. Such a choice allows to make contact with the ideas put forward in the context of the Black Hole Quantum N Portrait. Since a Schwarzschild Black Hole is characterized by its mass M and spin $S = 0$, the current needs to couple gravitons in such a way that the total spin of the current is zero. Furthermore, it has to satisfy the constraint that in the rest frame of the black hole, the mass of the bound state must be given by the sum of energies of its constituents. We will come back to the explicit form of the current later in this section.

First we derive the representation of a generic bound state $|\mathcal{B}\rangle$ in Minkowski space–time with quantum numbers encoded in $\mathcal{J}$. For that purpose consider

$$\langle\Omega|\mathcal{J}(x)|\mathcal{B}\rangle = \int \frac{\mathrm{d}^3\mathrm{P}}{(2\pi)^3}\mathcal{B}(P,\mathcal{Q})\mathrm{e}^{-\mathrm{iPx}}\underbrace{\langle\Omega|\mathcal{J}(0)|P\rangle}_{\Gamma_{\mathcal{B}}}. \tag{2.6}$$

Here we inserted a complete set of on-shell momentum eigenstates $|P\rangle$ and used translational invariance of the vacuum state. $\mathcal{B}(P,\mathcal{Q})$ is the wave function of the bound state in momentum space carrying information about possible gauge quantum numbers and isometries encoded in $\mathcal{Q}$. Thus we identify the complete set of quantum numbers $\mathcal{L} = \{P,\mathcal{Q}\}$. It is important to note already at this point, that our construction works in a similar way when working with off-shell momentum eigenstates. When performing explicit computations, however, we will use the representation which is most convenient for the question under investigation. Furthermore, it is worth mentioning that our construction links macroscopic properties of the black hole ($P^2 = -M^2$) with microscopic ones (via the explicit choice of the current). In other words, the momentum of the bound state P is directly related to the energies of the particles created when acting with the current on the vacuum. Note that the matrix element on the right hand side defines a non–trivial decay constant $\Gamma_{\mathcal{B}}$. Comparing to our previous discussion concerning the Fock state representation of a bound state, we see that $\Gamma_{\mathcal{B}}$ should be proportional to the expansion coefficient $\alpha_{\mathcal{J}}$. As explained before this construction is analogous to definitions of decay constants in the framework of QCD [58].

Expanding $|\mathcal{B}\rangle$ and $\mathcal{J}(x)|\Omega\rangle$ separately in momentum eigenstates and using the definition of $\Gamma_{\mathcal{B}}$ we arrive at the auxiliary current representation of an arbitrary quantum state[3] and, in particular, a bound state

$$|\mathcal{B}\rangle \;=\; \frac{1}{\Gamma_{\mathcal{B}}}\int \frac{\mathrm{d}^3P}{(2\pi)^3}\,\mathcal{B}(P,\mathcal{Q})\int \mathrm{d}^4x\;\mathrm{e}^{\mathrm{i}P\cdot x}\mathcal{J}(x)|\Omega\rangle\;. \tag{2.7}$$

Notice that $\mathcal{B}(P,\mathcal{Q})$ localizes the information encoded in $\mathcal{J}$ in $|\mathcal{B}\rangle$. It is intrinsically non–perturbative and can be related to the distribution of gravitons inside the bound

[3]Later, for example, we will explain how this construction reduces to the Lehmann-Symanzik-Zimmermann formula in the context of perturbative S–matrix theory.

state as we will discuss in more detail later. In particular, (2.7) gives a representation of the black hole which is independent of perturbative S-matrix theory. Therefore, $|\mathcal{B}\rangle$ is not restricted to be an asymptotic state. Physically, it should be clear that such a local description of a bound state should exist. Indeed, when measuring the density of particles in some bound state, one can in principle perform a local measurement independent of scattering theory[4]. Nevertheless, we will later show that (2.7) can nicely be embedded into the S-matrix as in-state or out-state. This is also perfectly reasonable since arbitrary states can contribute to the S-matrix, either elementary or bound. In particular, within relativistic field theory, one often extracts observables connected to bound states indirectly. Indeed, when talking about, for example, the wavefunction of a hadron in terms of gluons and quarks, one usually reconstructs it experimentally by measuring the scattering angle of a probe lepton after interacting with the hadron. Thus, although the observables should have a local description, one often extracts them indirectly via information at spatial and temporal infinity. We will later show in detail how this works in the case of a black hole bound state.

Finally, one might wonder why we restricted our presentation to local currents. Since the current will depend on powers of the fields of the microscopic Lagrangian, in general one could take the fields at different space-time points. In particular, for a black hole which is characterized by the Schwarzschild radius, one expects that the fields can be located anywhere within the interior of the black hole. Notice, however, that the qualification of a field being at a special point is to be understood rather as a bookkeeping device. In particular, within quantum theory the size of a bound state should be set by the characteristic wavelength of its constituents. Therefore it is plausible that a macroscopic scale such as r_g could be derivable in terms of local, composite operators. Nevertheless, it is still interesting to start from a multi-local construction and then check consistency of the results. Although we shall show that at the level of scattering theory, i.e. asymptotically, consistency of the two descriptions can be established (there will be a well-defined limit which reduces multi-local currents to local ones), it remains to be seen whether a similar construction works in the non-asymptotic description of the bound state corresponding to (2.7).

In any case, thinking in terms of quantum numbers only, a non-vanishing overlap should be guaranteed in bothe cases, i.e. when working with composite, local currents, as well as when considering multi-local currents. For practical reasons we thus choose to work with local, composite operators in explicit computation.

2.1.2 Auxiliary Currents for Black Holes

Since in our construction spherically symmetric, gravitating sources are understood as bound states on flat space–time, one characterization is given by the Casimir operators of

[4]One could for example imagine to measure the number of particles in a non-interacting Bose-Einstein condensate. Note that the condensate could be modeled using a current consisting of bosons which are all in the ground state. As such, also the Bose condensate can be interpreted as a bound state subject to an auxiliary current description.

Minkowski. In particular, we have $P^2 = -M^2$ and $S = 0$ for a Schwarzschild black hole. Thus our generic derivation applies here as well. Since we consider Schwarzschild black holes there are no gauge quantum numbers associated to it. Therefore, in this discussion we do not need to take gauge quantum numbers into account[5].

Let us now specify the current $\mathcal{J}$ for the question at hand. The current $\mathcal{J}$ carries isometry information of black hole quantum bound states appropriate for the kinematical description. Note that these isometries are not due to any geometrical concept. Instead, they are a consequence of the explicit breaking of certain Lorentz symmetries in the presence of bound states.

Black holes can be modelled using bound states of N gravitons by means of the following local, composite operator,

$$\mathcal{J}(x) = \mathcal{M}(\underbrace{h, \ldots, h}_{N})(x) \; . \tag{2.8}$$

Here $\mathcal{M}$ denotes a Lorentz covariant tensor coupling N gravitons h in accordance with the bound state isometries archived in $\mathcal{Q}$. Note that for simplicity we omitted the tensorial indices. In particular, using (2.8) and remembering the Fock state representation of bound states we are effectively projecting $|\mathcal{B}\rangle$ on a N-graviton Fock basis state. Let us stress once more that our choice is motivated by the proposal of Dvali and Gomez [23]. The idea, that gravitons are weakly interacting individually, suggests that currents with a number of fields differing substantially from N should generate an exponentially suppressed overlap with the true quantum state of the black hole at least in the limit of large N.

Note that for simplicity we displayed only graviton couplings, but other degrees of freedom can be included in the current description. In fact, this will be necessary when gravitons are coupled to other fields. We shall come back to this issue later.

Let us now explain how the isometries of a given background can be encoded in our construction. Considering a specific solution of Einstein's theory, one might ask how the isometries of that solution can be implemented in the auxiliary current description of the corresponding quantum bound state. In order to answer this question, we first note that within the quantum theory, isometries of a given classical background should be reflected in the invariance of the quantum bound state $|\mathcal{B}\rangle$ under the action of the corresponding symmetry generators. At the same time, since a bound state generically breaks some of the symmetries of Minkowski space-time explicitly, it should transform non-trivially under the action of the broken generator. Therefore, denoting collectively the unbroken generators by $\mathcal{G}$ and the broken ones by $\mathcal{H}$ respectively, we have

$$\begin{aligned} \mathcal{G}|\mathcal{B}\rangle &= |\mathcal{B}\rangle, \\ \mathcal{H}|\mathcal{B}\rangle &= |\mathcal{B}'\rangle, \end{aligned} \tag{2.9}$$

where $|\mathcal{B}\rangle \neq |\mathcal{B}'\rangle$. Let us now try to understand how these transformation properties are realized at the level of auxiliary currents. Using the expansion of the state $|\mathcal{B}\rangle$ in terms

[5]These, however, could be implemented easily. In the case of electrically charged black holes one could choose the current in such a way that it contains $U(1)$ fields as well as gravitons.

of auxiliary currents, we need to consider the action of the generators on $\mathcal{J}(x)|\Omega\rangle$. Since the vacuum is invariant under all generators of the Poincaré group, the transformation properties of the bound state are captured in the space-time dependence of the auxiliary currents. In particular, denoting infinitesimal transformations by $\mathcal{G} \simeq 1+\delta_{\mathcal{G}}$ and $\mathcal{H} \simeq 1+\delta_{\mathcal{H}}$ respectively, we have

$$\begin{aligned} \delta_{\mathcal{G}}\mathcal{J}(x) &= [\mathcal{G}, \mathcal{J}(x)] = 0, \\ \delta_{\mathcal{H}}\mathcal{J}(x) &= [\mathcal{H}, \mathcal{J}(x)] \neq 0. \end{aligned} \tag{2.10}$$

The right-hand side of (2.10) can be translated into a differential equation determining the space-time dependence of the auxiliary currents for a given background. In this way it is guaranteed that the classical background isometries of a given space-time are implemented in terms of a quantum mechanical auxiliary current description of the corresponding quantum state.

So far, our arguments are completely general. Let us now apply our reasoning to spherically symmetric space-times and, in particular, to Schwarzschild black holes. When viewed as bound states on Minkowski space-time, such solutions are clearly invariant under spatial rotations and time-translations. The corresponding generators can be represented as $\mathcal{G}_{ij} = x_i\partial_j - x_j\partial_i$ and $\mathcal{G}_t = \partial_t$, respectively. Here $i, j = 1, 2, 3$ denote spatial coordinates and t is the Minkowski time coordinate. Using (2.10), we conclude that the auxiliary current representing a black hole effectively only depends on the spatial distance $|\mathbf{r}|$. Furthermore, representing $\mathcal{J}$ explicitly in terms of its graviton field content, the dependence on spatial distance is realized at the level of individual field operators.

Notice that while such symmetry restrictions are expected physically, it would be desirable to perform explicit calculations in a fully Lorentz covariant way and impose the isometries at the end. Fortunately, we can indeed proceed in exactly such a way by virtue of Ward's identity. Using the invariance of the state $|\mathcal{B}\rangle$, Ward's identity leads to

$$0 = \langle\mathcal{B}|\partial_\mu j^\mu|\mathcal{B}\rangle = \langle\mathcal{B}|\delta_{\mathcal{G}}\mathcal{O}|\mathcal{B}\rangle = \delta_{\mathcal{G}}\langle\mathcal{B}|\mathcal{O}|\mathcal{B}\rangle. \tag{2.11}$$

Here, j denotes a conserved current corresponding to an isometry (this should not be confused with the auxiliary current $\mathcal{J}$). In practice, (2.11) implies that observables can be calculated in a fully Lorentz covariant way and it suffices to impose the symmetry constraints in the end.

The coupling tensor $\mathcal{M}$ is further constrained by the condition $S = 0$. The simplest auxilliary current realizing this constraint is given by $\mathcal{J} = (\mathrm{tr}h)^N(|\mathbf{r}|)$. For notational simplicity we represent the bound state gravitons by massless scalars, $\mathcal{J} = h^N$. This is completely justified at the partonic level, where gravitons are non-interacting. Let us explain this point in more detail. Due to the degeneracy of the choice of currents explained before, it is possible to take the graviton current to be of the form $\mathcal{J} = (h^\mu_\mu)^N$. Working in harmonic gauge, $\partial_\mu h^\mu_\nu = 1/2\partial_\nu h^\mu_\mu$, graviton propagators in momentum space take the following form:

$$\tilde{\Delta}_{\mu\nu\alpha\beta}(p^2) = \tfrac{1}{2}\tilde{\Delta}^{(0)}(p^2)(\eta_{\mu\alpha}\eta_{\nu\beta} + \eta_{\nu\alpha}\eta_{\mu\beta} - \eta_{\mu\nu}\eta_{\alpha\beta}). \tag{2.12}$$

Here $\tilde{\Delta}^{(0)}(p^2)$ is the propagator of a massless scalar field. We see that the evaluation of observables leads to contractions of the tensor structures in (2.12) giving rise to numerical prefactors and scalar propagators. Since we are primarily interested in scaling relations of observables, we will not be interested in keeping track of those numerical factors. Thus, at the parton level, we can work with massless scalars, $h(x)$ without changing our main conclusions and results. Later we will explain in detail that this statement is no longer true when interactions are considered which is completely reasonable, because the derivative structure of gravity is rather special.

2.1.3 Asymptotic Construction

In this part we want to show how the generic construction of representing black holes in terms of auxiliary currents reduces to LSZ-type formulas when embedded in the S-matrix following [59,60] where a similar construction was applied to mesonic bound states. Although we will not need this construction directly in the computations and applications which follow, we think that there are several reasons to present this construction anyway. First of all, we thing that such a presentation is helpful in order for the reader to have a complete discussion concerning the physics of bound states. Furthermore, we are currently investigating how this approach can be used to obtain similar results as in section (2.2.6) where we explain how geometry emerges from our description.

We will explain in detail that from the point of view of in-states or out-states a bound state pretty much behaves as an ordinary one-particle state with the difference that it is normalized differently when expressed through auxiliary currents. Before giving a detailed technical derivation of these statements, let us first of all give an intuitive explanation why this should be the case. For that purpose, let us first of all remind ourselves of the basic ideas of the LSZ construction without bound states. In this case, particles are prepared as in-states or out-states at temporal and spatial infinity. In addition, these individual particles must be well separated at infinity. In other words, one can prepare them as wavepackets with vanishing overlap. As such, the different particles do not interact. Consequently, at infinity, they are described by free, propagating waves fulfilling a standard free wave equation. Furthermore, it can be shown that there exists a well-defined limit in which the wavepacket can be replaced by a plane wave. This makes sense because these states solve the free wave equation by construction. Physically, it is also clear that this limit should exist. Since the particles are prepared at spatial infinity, they look like point-particles to a local observer. Therefore, finite-width effects captured in the variance of the wavepacket are negligible.

Let us now consider bound states in the framework of S-matrix theory. In order to give a well-defined expression for such states in terms of field operators, these states must also be considered at infinity. Furthermore, the bound state must be localized. Thus, effectively, i.e. at infinity, it should also satisfy a wave equation with the mass appearing in the Klein-Gordon equation identified with the bound state's mass. But then the construction works similar as in the case of elementary particles. In other words, at infinity, bound states can be described in terms of a free effective field theory. Although at this level the

corresponding field might be treated as fundamental, its microscopic structure must be taken into account as soon as one considers actual scattering. The reason is that particle exchange probes the bound state structure locally. Thus, despite the fact that the field can be represented as a fundamental degree of freedom at infinity, an embedding of the corresponding state into the S-matrix requires a microscopic resolution of that state. As a consequence, the state can be represented as a composite operator from the point of view of the microscopic theory. Since the overlap of that operator with the bound state is determined by the Fock representation of the bound state, it will in general differ from that of elementary particles with the field operator acting on the vacuum. Therefore, we expect a different normalization factor in the LSZ formula when bound states are included (in the case of one-particle states this overlap is determined by the wavefunction renormalization). Furthermore, although in general one could take the current to be multi-local, also the bound state at infinity looks like a point particle. Thus, we expect that there exists a limit where the auxiliary current can be taken as a local, composite operator. We want to stress, however, that the non-trivial structure of the bound state can still be appreciated by measuring cross sections for the scattering of a particle on the bound state. This follows from the fact that the interaction happens locally. Therefore, by measuring the scattering angle, one should be sensitive to the local character of the bound state as we will show in detail later.

Having this intuitive argument in mind, let us now proceed and give a detailed derivation of the statement given above. Consider gravitons described by a rank-2 Lorentz-tensor field $h(x)$ and demand that the principle of microscopic causality holds, and that the spectral condition is obeyed. For simplicity we assume there is only one spin-zero bound state $|\mathcal{B}\rangle$ with mass M, and $\langle\Omega|h(x)|\Phi\rangle \neq 0$ if $|\Phi\rangle$ is a momentum eigenstate corresponding to vanishing mass and spin, but $\langle\Omega|h(x)|\mathcal{B}\rangle \equiv 0$ and $\langle\Omega|h(x_1)\cdots h(x_N)|\mathcal{B}\rangle \neq 0$.[6] In other words, we assume that the spectrum consists of a one-particle state, i.e. a graviton and a bound state, the black hole. In order to describe the gravitational bound state $|\mathcal{B}\rangle$, we introduce the multi-local auxiliary current centered around x,

$$\mathcal{J}(x,\zeta) = \mathrm{T}\mathcal{C}^{\mu_1\nu_1\cdots\mu_N\nu_N} h_{\mu_1\nu_1}(x+\zeta_1)\cdots h_{\mu_N\nu_N}(x+\zeta_N)\ , \quad \sum_{a=1}^{N}\zeta_a = 0\ , \tag{2.13}$$

where $\zeta \equiv (\zeta_1,\ldots,\zeta_N)$ and $\mathcal{C}$ denotes the coupling tensor. Asymptotic fields are given by

$$\begin{aligned} h^{\mathrm{asy}}_{\mu\nu}(x) &= h_{\mu\nu}(x) + \int \mathrm{d}^4y\ G_{\mu\nu}{}^{\lambda\sigma}(x-y)T_{\lambda\sigma}(y)\ , \\ \mathcal{J}^{\mathrm{asy}}(x,\zeta) &= \mathcal{J}(x,\zeta) + \int \mathrm{d}^4y\ \mathcal{G}(x-y)\mathcal{T}(y)\ , \end{aligned} \tag{2.14}$$

with $G, \mathcal{G}$ denoting the retarded and advanced Green functions for the incoming and out-

[6] Of course, there are multi-particle states corresponding to virtual loop contributions as usual. Since the effect can be completely absorbed in a redefinition of the parameters of the theory at low energies as usual, we will not explicitly consider loop effects in the following discussion.

going fields, respectively, with the source operators

$$\begin{aligned} T_{\mu\nu}(x) &= \mathcal{E}_{\mu\nu}{}^{\alpha\beta} h_{\alpha\beta}(x) \;, \\ \mathcal{T}(x) &= \left(\Box - M^2\right) \mathcal{J}(x) \;. \end{aligned} \tag{2.15}$$

Here, $\mathcal{E}$ denotes the wave operator for the gravitons. Clearly,

$$\begin{aligned} \mathcal{E}_{\mu\nu}{}^{\alpha\beta} h^{\text{asy}}_{\alpha\beta}(x) &= 0 \;, \\ \left(\Box - M^2\right) \mathcal{J}^{\text{asy}}(x,\zeta) &= 0 \;. \end{aligned} \tag{2.16}$$

Notice that these equation simply formalize the intuitive picture we discussed above, namely that when viewed asymptotically, all states must be well-localized and subsequently subject to free propagation. As a consequence of (2.16) and the covariance properties of the asymptotic field operators, their expectation value with respect to the ground state vanishes, $\langle\Omega|h^{\text{asy}}(x)|\Omega\rangle = 0$ and $\langle\Omega|\mathcal{J}^{\text{asy}}(x,\zeta)|\Omega\rangle = 0$. This is not surprising due to the following reasoning. Again, since viewed at infinity, elementary particles as well as bound states can be expanded in terms of creation and annihilation operators of free bosonic fields. Using this expansion and the definition of the Minkowski vacuum, it is obvious that these conditions must hold for the asymptotic operators. Furthermore, h^{asy} and $\mathcal{J}^{\text{asy}}$ satisfy the usual asymptotic conditions, for instance

$$\lim_{x_0\to\pm\infty} \int_{\Sigma_{x_0}} \mathrm{d}^3x \; \mathcal{J}(x,\zeta) \overleftrightarrow{\partial_0} F^*(x) = \int \mathrm{d}^3x \; \mathcal{J}^{\text{asy}}(x,\zeta) \overleftrightarrow{\partial_0} F^*(x) \;, \tag{2.17}$$

for any normalizable solution F of the free Klein-Gordon equation, and $\overleftrightarrow{\partial_0} \equiv \partial_0 - \overleftarrow{\partial_0}$ with $\overleftarrow{\partial_0}$ acting to the left. The label Σ_{x_0} denotes the spatial hypersurface at time x_0 according to an inertial observer, while the right hand side of (2.17) is time independent.

The commutators of the incoming and outgoing fields coincide and are c-numbers. We focus on the bound state. It is convenient to expand $\mathcal{J}$ and $\mathcal{J}^{\text{asy}}$ with respect to a complete orthonormal system $\{F_{\mathbf{k}}(x)\}$ of positive frequency solutions of $(\Box - M^2)F(x) = 0$:

$$\begin{aligned} \mathcal{J}(x,\zeta) &= \int \frac{\mathrm{d}^3k}{2k_0} \; \left(F_{\mathbf{k}}(x)\mathcal{J}_{\mathbf{k}+}(x_0,\zeta) + F_{\mathbf{k}}{}^*(x)\mathcal{J}_{\mathbf{k}-}(x_0,\zeta)\right) \;, \\ \mathcal{J}^{\text{asy}}(x,\zeta) &= \int \frac{\mathrm{d}^3k}{2k_0} \; \left(F_{\mathbf{k}}(x)\mathcal{J}^{\text{asy}}_{\mathbf{k}+}(x_0,\zeta) + F_{\mathbf{k}}{}^*(x)\mathcal{J}^{\text{asy}}_{\mathbf{k}-}(x_0,\zeta)\right) \;. \end{aligned} \tag{2.18}$$

The coefficients are given by

$$\mathcal{J}_{\mathbf{k}\pm}(x_0,\zeta) = \mp\mathrm{i} \int_{\Sigma_{x_0}} \mathrm{d}^3x \; \mathcal{J}(x,\zeta) \overleftrightarrow{\partial_0} F_{\mathbf{k}\mp}(x) \;, \tag{2.19}$$

where $F_{\mathbf{k}-} \equiv F_{\mathbf{k}}$ and $F_{\mathbf{k}+} \equiv F^*_{\mathbf{k}}$, and similar expressions for $\mathcal{J}^{\text{asy}}_{\mathbf{k}\pm}$. Notice that all of the previous formulas are the obvious analogues of the LSZ construction when applied to

one-particle states. In order to show that $[\mathcal{J}^{\text{in}}(x,\zeta),\mathcal{J}^{\text{in}}(y,\eta)]$ and $[\mathcal{J}^{\text{out}}(x,\zeta),\mathcal{J}^{\text{out}}(y,\eta)]$ coincide, we start from

$$\begin{aligned}&\int d^4x\, \mathrm{d}^4y\; F^*_{\mathbf{k}}(x)F_{\mathbf{q}}(y)(\Box_x - M^2)(\Box_y - M^2)\mathrm{T}\mathcal{J}(x,\zeta)\mathcal{J}(y,\eta) = \\ &\int d^4y\, \mathrm{d}^4x\; F^*_{\mathbf{k}}(x)F_{\mathbf{q}}(y)(\Box_x - M^2)(\Box_y - M^2)\mathrm{T}\mathcal{J}(x,\zeta)\mathcal{J}(y,\eta)\;. \end{aligned} \tag{2.20}$$

Using Green's theorem as well as (2.15), it follows that

$$\begin{aligned}&-\mathrm{i}\int \mathrm{d}^4y\; F_{\mathbf{q}}(y)(\Box_y - M^2)T\mathcal{J}(x,\zeta)\mathcal{J}(y,\eta) \\ &= -\mathrm{i}\int \mathrm{d}y_0\partial_0 \int \mathrm{d}^3y\; \mathrm{T}\mathcal{J}(x,\zeta)\mathcal{J}(y,\eta)\overleftrightarrow{\partial_0}F_{\mathbf{q}}(y)\;. \end{aligned} \tag{2.21}$$

But this is just $\mathcal{J}(x,\zeta)\mathcal{J}^{\text{in}}_{\mathbf{q}-}(\eta) - \mathcal{J}^{\text{out}}_{\mathbf{q}-}(\eta)\mathcal{J}(x,\zeta)$, where $\mathcal{J}^{in} = \mathcal{J}|_{y_0=-\infty}$ and $\mathcal{J}^{+} = \mathcal{J}|_{y_0=+\infty}$. Proceeding in the same way with the x-integration, we find for the left hand side of (2.20)

$$\begin{aligned}&\int d^4x\, \mathrm{d}^4y\; F^*_{\mathbf{k}}(x)F_{\mathbf{q}}(y)(\Box_x - M^2)(\Box_y - M^2)\mathrm{T}\mathcal{J}(x)\mathcal{J}(y) = \\ &\mathcal{J}^{\text{out}}_{\mathbf{q}-}(\eta)\mathcal{J}^{\text{out}}_{\mathbf{k}+}(\zeta) - \mathcal{J}^{\text{out}}_{\mathbf{q}-}(\eta)\mathcal{J}^{\text{in}}_{\mathbf{k}+}(\zeta) - \mathcal{J}^{\text{out}}_{\mathbf{k}+}(\zeta)\mathcal{J}^{\text{in}}_{\mathbf{q}-}(\eta) + \mathcal{J}^{\text{in}}_{\mathbf{k}+}(\zeta)\mathcal{J}^{\text{in}}_{\mathbf{q}-}(\eta)\;. \end{aligned} \tag{2.22}$$

For the right hand side, we find a similar expression. As a result, (2.20) implies

$$\left[\mathcal{J}^{\text{in}}(x,\zeta),\mathcal{J}^{\text{in}}(y,\eta)\right] = [\mathcal{J}^{\text{out}}(x,\zeta),\mathcal{J}^{\text{out}}(y,\eta)]\;. \tag{2.23}$$

In order to determine the commutator, we calculate its expectation values with respect to the ground state. For this purpose, consider first the matrix elements of $\mathcal{J}^{\text{asy}}$ between the ground state and an arbitrary state. Let $|\mathbf{k}\rangle$ be a momentum eigenstate with eigenvalue components k_μ and rest mass given by $k^2 = -M^2$. Then,

$$\langle\Omega|\mathcal{J}(x,\zeta)|\mathbf{k}\rangle = (2\pi)^{-3/2}\exp(\mathrm{i}k\cdot x)F_{\mathbf{k}}(\zeta)\;, \tag{2.24}$$

by translation invariance. Note that the amplitude $F_{\mathbf{k}}(\zeta)$ depends on the relative coordinates $\zeta_1,\ldots,\zeta_N$ with respect to the center x,

$$F_{\mathbf{k}}(\zeta) = (2\pi)^{3/2}\langle\Omega|\mathrm{T}\mathcal{C}^{\mu_1\nu_1\cdots\mu_N\nu_N}h_{\mu_1\nu_1}(\zeta_1)\cdots h_{\mu_N\nu_N}(\zeta_N)|\mathbf{k}\rangle\;, \tag{2.25}$$

and the sum over all relative coordinates vanishes by definition. Clearly,

$$\left(\Box_x - M^2\right)\langle\Omega|\mathcal{J}(x,\zeta)|\mathbf{k}\rangle = 0\;. \tag{2.26}$$

From this and the definition of the asymptotic bound state it follows that $\langle\Omega|\mathcal{J}^{\text{asy}}(x,\zeta)|\mathbf{k}\rangle = \langle\Omega|\mathcal{J}(x,\zeta)|\mathbf{k}\rangle$. On the other hand, if $|\mathbf{k}\rangle$ is a momentum eigenstate with eigenvalue components k_μ but rest mass $k^2 \neq -M^2$, then $(k^2+M^2)\langle\Omega|\mathcal{J}^{\text{asy}}(x,\zeta)|\mathbf{k}\rangle = -(\Box -$

$M^2)\langle\Omega|\mathcal{J}^{\text{asy}}(x,\zeta)|\mathbf{k}\rangle = 0$. As a consequence, $\langle\Omega|\mathcal{J}^{\text{asy}}(x,\zeta)|\mathbf{k}\rangle = 0$ in this case. Physically, this simply reflects the fact that when acting on the vacuum, the chosen current must must create a state which has the same eigenvalues of the Casimirs on Minkowski as the bound state itself. Therefore,

$$\begin{aligned}\langle\Omega|\mathcal{J}^{\text{asy}}(x,\zeta)\mathcal{J}^{\text{asy}}(y,\eta)|\Omega\rangle &= \int \tfrac{\mathrm{d}^3k}{2k_0}\ \langle\Omega|\mathcal{J}^{\text{asy}}(x,\zeta)|\mathbf{k}\rangle\langle\mathbf{k}|\mathcal{J}^{\text{asy}}(y,\eta)|\Omega\rangle \\ &= \int \tfrac{\mathrm{d}^3k}{2k_0}\ \exp\left(\mathrm{i}k\cdot(x-y)\right)F_{\mathbf{k}}(\zeta)F_{\mathbf{k}}(\eta)\ . \end{aligned} \tag{2.27}$$

Introducing the Fourier-transform $\mathcal{J}^{\text{asy}}(k,\zeta)$ of the asymptotic auxiliary currents by

$$\mathcal{J}^{\text{asy}}(x,\zeta) = \int \tfrac{\mathrm{d}^4k}{(2\pi)^{3/2}}\ \exp\left(\mathrm{i}k\cdot x\right)\delta^{(1)}(k^2+M^2)\mathcal{J}^{\text{asy}}(k,\zeta)\ , \tag{2.28}$$

as well as emission and absorption operators, $\mathcal{J}^{\text{asy}}_{\pm}(\mathbf{k},\zeta) \equiv \mathcal{J}^{\text{asy}}(\mp k,\zeta)$ for $k_0 = \pm\sqrt{\mathbf{k}^2+M^2}$, we find the usual commutation relations,

$$[\mathcal{J}^{\text{asy}}_{+}(\mathbf{k},\zeta),\mathcal{J}^{\text{asy}}_{-}(\mathbf{q},\eta)] = F_{\mathbf{k}}(\zeta)F_{\mathbf{q}}(\eta)2k_0\delta^{(3)}(\mathbf{k}-\mathbf{q})\ , \tag{2.29}$$

and all other commutators vanish. Similarly, we can show that commutators between emission/absorption operators of elementary fields and auxiliary currents vanish. Again, the interpretation of this result is obvious. Since asymptotically both gravitons and bound states are free, on-shell quantization implies similar commutation relations for both. The only difference is that, since the current still depends on the relative positions, this dependence should also be captured in the commutators. Using (2.18) then fixes this dependence completely.

For the asymptotic framework used within S-matrix theory we are only interested in the center of mass coordinates of the auxiliary currents. It suffices to construct local field operators representing the bound states by taking the limit $\zeta \to 0$ of the multi-local auxiliary current $\mathcal{J}(x,\zeta)$. We assume the existence of

$$\mathcal{J}(x) \equiv \lim_{\zeta\to 0}\frac{\mathcal{J}(x,\zeta) - \langle\Omega|\mathcal{J}(0,\zeta)|\Omega\rangle}{(2\pi)^{3/2}\langle\Omega|\mathcal{J}(0,\zeta)|\Phi_{\text{rest}}\rangle}\ , \tag{2.30}$$

where $|\Phi_{\text{rest}}\rangle$ denotes the bound state at rest. The local auxiliary current $\mathcal{J}(x)$ transforms covariantly with respect to the inhomogeneous Lorentz group, and $[\mathcal{J}(x),\mathcal{J}(y)] = 0$ for $\|x-y\|^2 > 0$. Furthermore, it satisfies the asymptotic conditions, i.e.

$$\lim_{x_0\to\pm\infty}\int_{\Sigma_{x_0}}\mathrm{d}^3x\ \mathcal{J}(x)\overleftrightarrow{\partial_0}F^*(x) = \int \mathrm{d}^3x\ \mathcal{J}^{\text{asy}}(x)\overleftrightarrow{\partial_0}F^*(x)\ , \tag{2.31}$$

for normalizable solutions F of the free Klein-Gordon equation. Note that the right hand side is time independent.

In summary, the local auxiliary current $\mathcal{J}(x)$ transforms covariantly under the inhomogeneous Lorentz transformation, respects causality and satisfies the asymptotic conditions

exactly in the same way as the local fields representing elementary particles. Hence, the Lehmann-Symanzik-Zimmermann reduction formalism can be used to get the usual expansion of the scattering matrix:

$$\begin{aligned} S &= \sum_{m,n\in\mathbb{N}} \tfrac{(-\mathrm{i})^{m+n}}{m!n!} \int \mathrm{d}^4x_1 \cdots \mathrm{d}^4x_m \int \mathrm{d}^4y_1 \cdots \mathrm{d}^4y_n \, \Box_{x_1} \cdots \Box_{x_m} \\ &\quad \langle\Omega|\mathrm{T}h(x_1)\cdots h(x_m)\mathcal{J}(y_1)\cdots\mathcal{J}(x_n)|\Omega\rangle \left(\overleftarrow{\Box}_{y_1} - M^2\right) \cdots \left(\overleftarrow{\Box}_{y_n} - M^2\right) \\ &\quad :h^{\mathrm{in}}(x_1)\cdots h^{\mathrm{in}}(x_m)\mathcal{J}^{\mathrm{in}}(y_1)\cdots\mathcal{J}^{\mathrm{in}}(y_n): \, . \end{aligned} \tag{2.32}$$

There is one important difference between fields representing elementary particles and auxiliary currents representing bound states. If $\mathcal{J}(x)$ is the local auxiliary current corresponding to a bound state composed of N gravitons described by rank-2 Lorentz tensors h, it is possible to represent $\mathcal{J}(x)$ as a monom in h,

$$\mathcal{J}(x) = \mathcal{N}^{-1/2} \left(\mathcal{J}(x,0) - \mathcal{V}\right) \, , \tag{2.33}$$

with the renormalisation constants

$$\begin{aligned} \mathcal{N} &= -\mathrm{i} \int \mathrm{d}x_0 \, \exp\left(-\mathrm{i}Mx_0\right) \langle\Omega|\mathrm{T}\mathcal{J}(0,0)\mathcal{J}(x,0)|\Omega\rangle \\ \mathcal{V} &= \langle\Omega|\mathcal{J}(0,0)|\Omega\rangle \, . \end{aligned} \tag{2.34}$$

Notice that the reason for normalizing $\mathcal{J}$ as in (2.33) again relates to the Fock space expansion of bound states. Indeed, since $\langle\mathcal{B}|\mathcal{J}(0)|\Omega\rangle = \alpha_{\mathcal{J}} \sim \Gamma_{\mathcal{B}}$ already at tree level, we need to normalize $\mathcal{J}$ properly when deriving the LSZ reduction formula for bound states!

2.1.4 Inclusion of Perturbation

In this part we want to generalize the auxiliary current description to arbitrary solutions of Einstein's field equations. In particular, it should be possible to describe classical backgrounds with small fluctuations in terms of quantum bound states living in an appropriate Hilbert space. Although we will not present applications of the generalized auxiliary current description in this thesis, we think that it is important to explain the general construction. Explicit examples can then be studied using the techniques discussed in this part in future work. Notice that a general background does not have the property of being asymptotically flat. Thus, P^2 is no longer a good label of the state.

Knowing the exact quantum state of a general space-time $|\mathcal{G}\rangle$ is definitely not possible. It is possible, however, to store kinematical data in a quantum state in such a way, that its overlap with $|\mathcal{G}\rangle$ is non-vanishing. Since in our picture the "would-be" classical geometry should be understood as bound state of the (weakly interacting) elementary degrees of freedom of the underlying EFT, we again use an auxiliary current J to represent the state (note that we changed the notation for the current to distinguish it from the one we used to construct black hole quantum bound states).

This current has to respect the isometries of a given background. In general the associated symmetries will be broken softly by small fluctuations. In order to have a complete quantum description we also need to incorporate these fluctuation in the construction of $J(x)$. This implies that the state $J(x)|\Omega\rangle$ is no longer invariant under the action of the symmetry group of the background. The isometries, however, must be recovered in the case of vanishing fluctuations. Since we consider only small fluctuations which should not destabilize the background, this idea can be understood as a realization of the mean–field idea within the auxiliary current description.

Let us now explain how $|\mathcal{G}\rangle$ can be expressed in terms of $J(x)|\Omega\rangle$ and how to compute observables in this state. First of all, we can think of $|\mathcal{G}\rangle$ as a quantum superposition of states representing classical geometries subject to fluctuations,

$$|\mathcal{G}\rangle = \sum_i \alpha_i |\mathcal{G}_i\rangle. \tag{2.35}$$

Here $|\mathcal{G}_0\rangle$ corresponds to the classical background solution and the other $|\mathcal{G}_i\rangle$ correspond to fluctuations around it with i counting the order of fluctuation. Note that in a standard semi-classical treatment (2.35) would amount to an expansion around a classical saddle point including all interaction terms of fluctuations. Of course, in practice, one would truncate the sum at some finite order. The different basis states are weighted with coefficients α_i. Notice that in order to realize a mean–field description in this framework, we should assume that $|\alpha_0| \simeq 1$ while all the other α_i are close to zero. In this sense, we could think of the α_i as being determined by the magnitude of the effective operators appearing in the Lagrangian when expanding in small fluctuations around the "classical" background. Furthermore, we will see that $\langle \mathcal{G}_i|\mathcal{G}_j\rangle = \delta_{ij}$ (at least at the parton level).

Let us now explain how $|\mathcal{G}\rangle$ can be expressed in terms of $J(x)$. Let us define $|\mathcal{L}(\mathcal{G})\rangle = \int d^4x F_{\mathcal{L}}(x) J(x)|\Omega\rangle$, where $|\mathcal{L}(\mathcal{G})\rangle$ is a state of quantum numbers compatible with $|\mathcal{G}\rangle$ and $F_{\mathcal{L}}(x)$ is a weight function. Inserting a complete set of such states we can formally write

$$|\mathcal{G}\rangle = \sum\!\!\!\!\!\!\int_{\mathcal{L}(\mathcal{G})} \mathcal{G}(\mathcal{L}) \int \mathrm{d}^4x\, F_{\mathcal{L}}(x) J(x)|\Omega\rangle. \tag{2.36}$$

Here $\mathcal{G}(\mathcal{L})$ is the wavefunction of $|\mathcal{L}(\mathcal{G})\rangle$ in the basis $|\mathcal{L}\rangle$. Note that we cannot simply substitute a plane wave for $F_{\mathcal{L}}(x)$, because as explained before, for a non-asymptotically flat space-time P^2 is no longer a sensible label of the state. Decomposing the current in terms of a background and fluctuations,

$$J(x) = J_0(x) + \delta J(x) \equiv \sum_{j=1}^{max(j)} \delta_{(j)} J(x) \tag{2.37}$$

leads to

$$|\mathcal{G}\rangle = \sum_{j=0}^{max(j)} \sum\!\!\!\!\!\!\int_{\mathcal{L}_j(\mathcal{G}_j)} \mathcal{G}_j(\mathcal{L}_j) \int \mathrm{d}^4x\, F_{\mathcal{L}_j}(x) \delta_{(j)} J(x)|\Omega\rangle. \tag{2.38}$$

A few comments concerning this equation are in order. As we have already discussed, $|\mathcal{G}\rangle$ should be understood as quantum superposition. Equation (2.38) gives an explicit realization of this idea. The different basis states are represented by different wavefunctions $\mathcal{G}_i(\mathcal{L}_i)$ and currents $\delta_{(i)}J(x)$. For the zeroth order $\delta_{(0)}J(x) = J_0(x)$ holds where $J_0(x)$ only consists of background fields. Therefore, $J_0(x)$ should be invariant under the background isometries. This induces $J_0(x) = J_0(\tilde{x})$, where $\tilde{x}$ are coordinates which manifestly respect the symmetries of the bound state[7] . The $\delta_{(i)}J(x)$ correspond to geometries containing i fluctuating fields while all other fields provide an effective background geometry for these fluctuations. Furthermore, the functions $F_{\mathcal{L}_i}(x)$ display the relative weights of different quantum geometries constituting $|\mathcal{G}\rangle$. At the level of mean-field Lagrangians, (2.36) can be interpreted in the following way. Working with $|\mathcal{G}_0\rangle$ only amounts to evaluating the classical action at its saddle point value. Taking $1/N$ effects due to the bound state structure of the background into account, however, $|\mathcal{G}_1\rangle$ then represents a correction to this result which is of order $\hbar$. In other words, the resulting $1/N$-corrected classical background geometry receives an extra quantum correction due to loops of fluctuations. At the level of functional integrals, these correspond to the Gaussian approximation for the fluctuating fields and subsequent evaluation of the one-loop functional determinant. Finally, all the $|\mathcal{G}_i\rangle$ with $i \geq 2$ represent non-Gaussian contributions, i.e. at the level of the action, such terms are interpreted as interactions among the fluctuations. Thus, our construction takes into account two types of quantum effects. One is connected to $\hbar$ effects due to fluctuations, the other corresponds to finiteness of N.
Notice that the background $|\mathcal{G}_0\rangle$, when resolved in terms of its constituent degrees of freedom, can be interpreted as non–perturbative condensation process of fields with proper quantum numbers in the current $J_0(x)$ on Minkowski space–time. The fluctuations, however, are perturbative in nature. Effectively, this tells us that all background fields create states in the bound state spectrum of the theory. In contrast, for the fluctuations, the condensed background behaves as a vacuum. Roughly speaking, the fluctuations are represented as single-particle states with a modified dispersion originating from the non-trivial background. Since the background itself is quantum, the dispersion relations for fluctuations should also receive $1/N$ corrections[8].
Now one can make an ansatz for a current consisting of M different types of fields. In order to have an explicit model in mind, we might imagine to couple gravity to $M-1$ species. Therefore, we split $\delta_{(j)}J(x)$ in a background and a fluctuating part where the index (j) represents the number of fields in the current.

$$\delta_{(j)}J(x) = J^b_{\sum_{l=1}^{M} N_l - j_l}\delta_{(j)}\tilde{J} \tag{2.39}$$

Here $N_l - j_l$ is the number of background fields of type l and j_l the corresponding number of fluctuations with $j = \sum_{l=1}^{M} j_l$. Now it is easy to see that $\langle\mathcal{G}_i|\mathcal{G}_j\rangle = \delta_{ij}$ at the parton level.

[7] In particular, $J_0(x) = J_0$ for the maximally symmetric de Sitter space-time.

[8] Indeed, in the context of the coherent state approach, we will explicitly compute these corrections in the case of scalars in AdS as well as bosonic and fermionic fluctuations in a domain wall background in a $1+1$-dimensional Wess-Zumino model.

Indeed, since at the parton level there are no interactions, contributions with differing number of fluctuating and background fields can not mix. Thus, such terms must vanish. Restricting ourselves to a partonic description, let us prove this statement more rigorously.

Using the auxiliary current representation, terms of the form

$$\langle\Omega|\delta_{(i)}J(x)\delta_{(j)}J(x)|\Omega\rangle = \langle\Omega|J^b_{\sum_{l=1}^M N_l - i_l}\delta_{(i)}\tilde{J}J^b_{\sum_{l=1}^M N_l - j_l}\delta_{(j)}\tilde{J}|\Omega\rangle \tag{2.40}$$

contribute. If $i_l \neq j_l$, because of the factorization property, we need to evaluate the overlap of two different effective backgrounds multiplied with a matrix element describing the overlap between an i_l and a j_l particle state. These contributions vanish simply by virtue of the standard commutation relation for the fluctuating fields. Therefore $i_l = j_l \ \forall l$ has to hold. From this it automatically follows that $j = i$. Notice that this argument can also be applied for any observable $\mathcal{O}(x_1, x_2, \ldots, x_L)$ consisting of fluctuations only. In practice this tells us that only "diagonal" elements contribute to $\langle\mathcal{G}|\mathcal{O}(x_1, x_2, \ldots, x_L)|\mathcal{G}\rangle$. Schematically, $\langle\mathcal{G}|\mathcal{O}(x_1, x_2, \ldots x_L)|\mathcal{G}\rangle = \sum_i |\alpha_i|^2\langle\mathcal{G}_i|\mathcal{O}(x_1, x_2, \ldots x_L)|\mathcal{G}_i\rangle$.

Before finishing this section, let us discuss possible applications of the generalized auxiliary current description. Of course, there is a plethora of interesting questions one could address. Two applications which we are investigating currently are dS as well as inflationary backgrounds. In the former case, it would be interesting to understand the implications of our approach with respect to the cosmological constant problem. In the latter scenario, a derivation of the power spectrum and possible deviations could be of major phenomenological interested. In particular, CMB measurements might be sensitive to $1/N$ effects, because these could accumulate during the expansion history of the universe. We hope that we can report on explicit results concerning these questions in future publications.

2.2 Application: Black Holes

Having developed the general construction which allows to represent a bound state in terms of constituent degrees of freedom, we now wish to apply the formalism to explicit questions in black hole physics. We shall construct observables which are directly related to the black hole interior such as the constituent density and the energy of gravitons inside the black hole. Our discussion will be restricted mostly to the partonic level, i.e. non-interacting gravitons inside the black hole. As explained above, in this case it suffices to work with scalars instead of gravitons, because the scaling relation we will find will only be affected by an order one prefactor. Although we work at lowest order, our results will be non-trivial. This is due to the condensate structure and will be explained in more detail below. At the end, we will outline how higher order corrections can be taken into account in a gauge invariant way. In order to make the idea transparent, we shall compute corrections to the constituent density due to curvature terms. We proceed by discussing scattering of a probe scalar on a black hole quantum bound state. It is shown explicitly that within our framework, the cross section for the process can be expressed in terms of the constituent density of gravitons composing the black hole. Notice that this is very similar to deep inelastic scattering in QCD where the cross section for scattering on a hadron can

be expressed in terms of partial cross sections corresponding to scattering on the quarks inside the hadron. Our result shows that, contrary to the standard lore, in our approach an outside observer can access the black hole interior measuring the scattered probe particle. Thus, we expect our framework to circumvent the usual mysteries surrounding black hole physics such as non-conservation of global symmetries or the information paradox. We conclude this section by giving an overview over possible new research directions.

2.2.1 The Role of Condensates

One might wonder why our results should be non-trivial at the parton level. The logic is as follows. Being motivated by the ideas put forward in the context of the Black Hole Quantum N Portrait, we assume that, while individual constituents are weakly interacting, there is nevertheless a large collective effect. In other words, although we effectively work with non-interacting gravitons, we still want to include the large collective effect. In turn, this guarantees that our results are non-trivial. In some sense, a single free graviton propagates in the background of all the other gravitons. Thus, the motion of a single graviton is affected by in-medium modifications[9]. Furthermore, already at this level we can trace the origin of the $1/N$ corrections which are crucial for the resolution of the information paradox as explained above. In order to take into account the large collective effect, we are motivated by mean-field physics. This can be achieved by postulating the existence of so-called condensates which correspond to normal-ordered contributions in correlation functions. These condensates act like an effective background source on flat space-time with respect to which individual gravitons propagate. As we shall show, these ideas will become very transparent when presenting explicit computations. Before doing so, however, let us explain the physics of condensates in more detail.

Condensation as a Vacuum Property

A condensate is ultimately related to the vacuum structure of a given theory. That is, a condensate is simply a non-vanishing vacuum expectation value of a field operator or a product of field operators. Of course, such a condensate needs to respect Lorentz invariance in a relativistic QFT. Therefore, only a relativistically invariant combination of fields can form a condensate[10]. In general, understanding the condensation process dynamically is a very difficult task and there are only a few cases where such an understanding has been

[9] In order to illustrate the idea, consider the motion of a light ray through a medium with refractive index > 1. On the one hand, using geometric optics arguments, we know that the effective propagation speed of light in such a medium is lower than the speed of light c. On the other hand, at a microscopic level it is clear that the proper way to describe the motion of the ray is in terms of the vertices of QED. Of course in practice, due to the large number of rescatterings (large collective effect) of the photons, a proper QED computation is not feasible. There is a way, however, to account for the large collective effect field theoretically. This is achieved by treating the large number of vertices as an effective background which in turn changes the propagator of single photons. In this way, an effective mass is generated which leads to an effective propagation speed lower than that of light traveling in the vacuum.

[10] We do not consider Lorentz-violating theories in our presentation.

established. The most prominent example of a condensate within a relativistic QFT is the Higgs condensate within the standard model. It is well known that this condensate acts as a medium (mean-field) with respect to which particles propagate. In other words, the effect of the condensate is to modify the propagator of the particles the Higgs is coupled to in such a way that a mass pole is generated.

Another condensate which is of immediate phenomenological interest is the chiral condensate in QCD which spontaneously breaks an approximate chiral symmetry of the QCD Lagrangian. The condensation of quark-antiquark pairs is the underlying reason for the generation of a mass gap in QCD and the observed spectrum of hadrons. Although we still lack a proper understanding of the dynamics of condensation, it is fair to say that the basic picture should be clear. Due to confinement the QCD coupling is a relevant parameter in the IR. Looking at the renormalization group flow, an effective potential in the effective action should be generated which allows the quarks to condense (see e.g. [61]).

While this mechanism of generation of the chiral condensate in QCD is basically established, one expects that QCD should have a much richer vacuum structure. In particular, relying again on the relevance of the QCD coupling in the IR, one expects generation of condensation of a whole tower of operators including gauge condensates such as $\langle G^a_{\mu\nu} G^{a\mu\nu} \rangle$ or four quark condensates.

It is exactly this expectation which is at the heart of the analytic, non-perturbative approach to resonance physics which is known as SVZ sum rules [58]. The basic idea of this approach is to determine observables at low energies such as couplings or masses of hadrons in terms of these condensates. Although the value of the condensates is in general not known theoretically, these parameters can be determined experimentally. Predictivity of the sum rules then follows from the universality of the condensates. i.e. the same condensates contribute to the resonance properties of all hadronic resonances. Although we think that the sum rule method is not directly applicable to gravity, let us review its essence[11]. We think that such a discussion is useful, because it shows how condensates enter physical observables from a technical point of view in the familiar example of QCD. Having presented the sum rule approach, we will move to gravity and explain why we assume that in this context there should be condensates as well.

SVZ Sum Rules

The starting point of QCD sum rule calculations is based on the idea of quark-hadron duality [62]. The duality states that it is possible to express hadronic quantum states in a basis of quark and gluon Fock space states of appropriate quantum numbers and vice versa. By appropriate we mean that the basis states should have the same transformation properties as the state one expands. In turn, this allows to represent certain physical quantities either directly in terms of hadrons or in terms of quarks and gluons. An important example of such a quantity is the vacuum polarization graph. On the one hand, the intermediate loop can be interpreted as exchange of a meson between gluons, on the other

[11] We will only present the basic ideas inherent to the sum rule approach. For a much more detailed exposition we refer the reader to the original work [58].

hand we may identify it with production and subsequent annihilation of a quark-antiquark pair. Therefore, let us schematically write

$$\Pi_{\text{hadronic}}(q^2) = \Pi_{\text{quark-gluon}}(q^2), \tag{2.41}$$

where q denotes the momentum of the virtual gluon in the corresponding diagram and Π denotes the Lorentz-invariant contribution to the full vacuum polarization. Thus, there are two ways of representing the vacuum polarization. On the hadronic (phenomenological) side, one represents the correlator in terms of a Kallen-Lehmann representation for the bound state contributions. Notice that as long as there is no determination of the hadronic spectrum from first principles, one needs to model the spectral density based on phenomenological grounds. On the quark-side, we can write the same quantity as a correlation function of local operators composed of quark fields. This correlation function can be computed using standard QFT techniques such as Wick's theorem and the operator product expansion (OPE). Matching both results then leads to predictions for physical observables related to hadronic resonances such as e.g. couplings, masses or form factors.

Let us discuss the quark-gluon side of the computation in more detail. Notice that we are interested in energy scales of order of the mass of the resonance we want to describe. Since such energy scales are not much larger than the QCD confinement scale, a purely perturbative expansion truncated at a certain order becomes a rather inaccurate description. In other words, confining effects suggest that we should take the non-perturbative character of QCD seriously. This is exactly the point were the condensates enter. As explained before, at low energies, one expects effective potentials to be generated which allow for the condensation of a tower of operators in QCD. Thus, at energies of the order of the mass of the hadron, one should take the confining structure of the QCD vacuum into account. This is achieved on purely phenomenological grounds in the sum rule approach by parametrizing non-perturbative effects in terms of non-vanishing vacuum condensates. At a technical level this simply means that the vacuum expectation value of normal-ordered products of fields no longer vanish[12]. Applying Wicks theorem to the quark-gluon side of the polarization diagram, we thus get contributions from all possible contractions as well as from normal-ordering. Coming back to the mean-field idea, contraction thus leads to a propagation in the background of the condensates. Of course, an expansion in terms of power corrections within the OPE in general introduces an infinite tower of such condensates. There is, however, a well-defined way of truncating the expansion keeping only the

[12]Note that the condensates effectively act as a new background in which quarks and gluons propagate. In this way, the condensates parametrize effects which one would expect to see in a purely perturbative expansion only at high orders of perturbation theory. This is also clear from the fact that condensates are assumed to be directly related to the so-called IR-renormalons (for a recent discussion see [63]). In other words, the sum rule approach can be viewed as an effective theory which, when derived from first principles would require a complicated resummation of diagrams. This is kind of reminiscent to a very different situation in QCD, namely scattering at fixed momentum transfer, but at very high energies. One finds that a sensible description is only feasible when one resums a whole series of diagrams leading to the famous BFKL equation [64,65]. Alternatively, one can parametrize the same effect in terms of an effective classical background gluon field as is done in the context of the so-called Color Glass Condensate (for a review see, for example, [66]).

effect of a few condensates [58]. Unfortunately, there is so far no first principles determination of the values of the condensates. Thus, in practice the condensates such as gluon or higher-order quark condensates need to be matched with given data. With this matching, however, predictivity concerning other observables follows as discussed above.

Condensates in Gravity

In the context of gravity, there is so far no proof of condensation of gravitons in the vacuum. Nevertheless, our starting assumption when computing observables related to black holes is the existence of such condensates. In this part we will try to motivate this postulate physically. Already at the classical level, we can understand a black hole as a relevant deformation of the Minkowski metric in the following sense. Given an arbitrary metric which is asymptotically flat, we can always decompose it as $g_{\mu\nu} = \eta_{\mu\nu} + h_{\mu\nu}$ with $\eta_{\mu\nu}$ the Minkowski metric. Usually, such a decomposition is a useful tool when studying small perturbations around flat space-time. Such a small perturbation corresponds to $|h_{\mu\nu}| \ll 1$. Given that this condition holds, one is usually interested in the dynamics of scattering of gravitational waves order by order in classical perturbation theory.

In the case of a black hole, however, the fluctuation becomes as large as the flat space-time background itself. Therefore, in order to account for the physics of black holes properly within perturbation theory, a resummation of an infinite number of tree diagrams on flat space-time is required [67]. Of course, instead of performing such a complicated resummation, one usually recognizes that one should instead consider the Schwarzschild metric as a new background. In either case, the physics such as geodesics are of course the same. From the point of view of the field theory computation, however, the description of black holes in terms of a classical Schwarzschild metric, is most naturally interpreted only as an effective theory derived from a microscopic theory of gravitons on flat space-time[13]. In other words, since classically the Schwarzschild solution is obtained as a solution of Einstein's equations in the presence of a point-like massive source, it should be viewed as some kind of coherent state of longitudinal gravitons from the QFT point of view. The situation is in some sense reminiscient of high-energy scattering at fixed momentum transfer in QCD. In particular, the regime of interest is as follows, $s \gg q^2 \gg \lambda_{QCD}^2$ with s the squared center-of-mass energy and λ_{QCD} the confinement scale. In this kinematic regime (which is also called small-x regime), the coupling is still small. Nevertheless, there are large logarithms multiplying the coupling so that the effective expansion parameter is of order one. Consequently, a resummation of an infinite tower of diagrams (the so-called BFKL ladder diagrams) is needed from the point of view of fundamental QCD [64, 65]. The physical origin of this resummation is encoded in the phenomenon of gluon saturation. The saturation takes place when gluon fusion and splitting inside a given hadron balance each other. Technically speaking, gluon saturation corresponds to the point in the renormalization group evolution (with

[13] In this way, geometry can be interpreted as an effective phenomenon. A similar situation occurs within geometrical optics. At large distances, we use an effective description to describe, for example, the motion of light rays. Microscopically, however, it is clear that the geometric interpretation is not fundamental. Instead, the motion of the ray is dictated by the rescattering of coherent photons on a given medium.

respect to small x), where the gluon distribution becomes maximally packed. Since this point corresponds to a critical point in the flow equation, the phenomenon is universal for arbitrary hadrons. Remembering our discussion about the scale dependence of the Fock space representation of a hadron, this result tells us that at that point all hadrons basically look like a dense state of gluons. As such the hadron could be represented as a coherent state of longitudinal gluons which at the classical level of the description is replaced by a classical field configuration, i.e. a classical color background [66]. Notice that the coherent state can be represented as some kind of condensate from the QFT's persective. Since there is a large number of quanta of characteristic wavelength given by the inverse typical mass scale of the kinematic regime one considers, the classical background simply corresponds to a high flux of particles of the underlying microscopic theory in a given momentum mode, i.e. a condensate. Taking this analogy seriously we might be tempted to interpret gravitational backgrounds in a similar way. There is, however, one more input that we need. While Duff's computation of the Schwarzschild metric in terms of tree level processes [67] seems to be somewhat analogous to the BFKL resummation, there is still an important difference. While in QCD the internal structure of a hadron in terms of quarks and gluons is taken into account explicitly, this is not the case in Duff's computation. Instead, he considers the scattering on a classical external source with no internal dynamics. It is exactly this type of internal dynamics which we need in order to postulate the existence of condensates in gravity. In particular, we saw that an interpretation of a hadron in terms of a condensate of gluons heavily relies on the distribution function of gluons inside the hadron. Using additional input from the Black Hole Quantum N portrait, the analogy to QCD in the small-x regime becomes more appropriate. In particular, since black holes are maximally packed systems of N gravitons of typical wavelength set by the Schwarzschild radius there is a high graviton flux concentrated in the black hole which we interprete as condensation process with respect to flat space-time.

There are two comments in order. First, from the point of view of the microscopic theory, the computation of Duff using external sources should be understood as scattering on individual graviton constituents at a fundamental level. Indeed, in section (2.2.6) this statement will be made explicit. Replacing a classical spherically symmetric source by the energy-density of individual gravitons making up the bound state, it is shown how geometric concepts such as the motion in a Schwarzschild metric are recovered quantum mechanically (at least at next-to-leading order in non-linearities). Furthermore, in this context, we will show how novel quantum $1/N$ corrections can be included in all orders in Newton's constant. Secondly, this discussion suggests that a classical background can be understood as a certain resummation of field theory diagrams on flat space-time. As such, the classical background represents a relevant deformation of the theory which cannot simply be captured by perturbation theory. Therefore, either a full resummation is needed or a parametrization in terms of non-perturbative parameters representing the high density of particles in the perturbative expansion. It is exactly these non-perturbative parameters which we identify as condensates with respect to the Minkowski vacuum and which we shall use in explicit computations.

2.2.2 Composite Operator Renormalization at Parton Level

As we have discussed before, it is always possible to represent a black hole state in terms of local composite operators when resolved as a quantum bound state. Considering in particular the process of scattering of a probe particle on a black hole quantum bound state, the corresponding cross section factorises into a perturbatively calculable part (Wilson coefficient) and the distribution function of gravitons, $\langle\mathcal{B}|\mathrm{T}h(x_1)h(x_2)|\mathcal{B}\rangle$, inside the bound state [9]. One of the purposes of this thesis is to compute this distribution function non-perturbatively in terms of non-vanishing vacuum condensates of gravitons at the parton level.

Using the auxiliary current description, an evaluation of the distribution function effectively amounts to a computation of a correlator of the following form (the explicit form of the distribution function will be derived in the next Section):

$$\mathcal{M}(x_1,x_2;x,y)=\langle\Omega|\mathcal{J}(x)h(x_1)h(x_2)\mathcal{J}(y)|\Omega\rangle. \tag{2.42}$$

In the case of a black hole, $\mathcal{J}$ is a local monomial of graviton fields. Subsequently, in order to give meaning to (2.42) a proper renormalization procedure needs to be imposed. Actually, we will encounter the same obstacle when computing an arbitrary observable $\mathcal{O}(x_1,x_2,\ldots,x_k)$ inside the black hole state (e.g. the energy density of gravitons inside the black hole which we shall calculate later as well). Thus, in order to give a well-defined computation scheme, let us discuss the renormalization of composite operators at the parton level before presenting our actual computations. Fortunately, at the partonic level, following [68], a proper definition of composite operators can be given straight forwardly. Let us first consider a situation where we want to define a composite operator $\mathcal{F}(x)$ which is an arbitrary functional of the field $h(x)$. Of course, in explicit applications, we will identify the functional with the auxiliary current introduced before. The renormalization prescription, however, is more general. For example, the functional could be constructed from derivatives of fields as well. Let the degree of $\mathcal{F}(x)$ (power of field operators) be N. In order to give a renormalized expression for the functional, it suffices to properly define the matrix elements $\langle\Omega|\mathrm{T}h(y_1)\ldots h(y_s)\mathcal{F}(x)|\Omega\rangle$ [68]. These elements can be computed using the standard Feynman diagram expansion. Due to the local nature of the composite operator there will be diagrams which contain self-loops at the position x. Of course, integrating over the momentum running in the loop leads to a divergence as usual. In the context of free field theory (which we are considering when working at the parton level), there is an easy way to circumvent this problem. Indeed, imposing the composite operator to be normal-ordered removes all divergencies leading to well-defined expressions for all correlation functions. Notice that this normal-ordering prescription simply corresponds to composite operator renormalization at the level of a free theory with the renormalization scheme chosen so that a possible ambiguous finite part is set to zero.

In our applications, we will be interested not only in correlation function involving one composite operator, but rather in expressions of the form $\langle\Omega|\mathrm{T}\mathcal{F}(x)\mathcal{O}(x_1,\ldots,x_k)\mathcal{F}(y)|\Omega\rangle$ with $\mathcal{O}$ an observable constructed from graviton field operators and possibly derivatives. In order to remove the divergences originating from closed loops at x and y we should first

of all normal-order both composite operators seperately. Furthermore, using the Feynman diagram expansion, we will now encounter contributions from loops connecting the points x and y. The divergences which occur in such computations can be regulated using standard techniques such as dimensional regularization.

Notice that we might be interested in a kinematic limit in which the intermediate propagators in such diagrams shrink to a point. In such cases, we again encounter a situation where we effectively only need to renormalize self-loops. In other words, in principle there could be a certain kinematic limit where the two local operators are effectively evaluated at one point. Given such a situation, it is most natural to define the renormalized matrix elements as $\langle\Omega|\mathrm{T}\,{:}\mathcal{F}(x)\mathcal{O}(x_1,\ldots,x_k)\mathcal{F}(y){:}\,|\Omega\rangle$, where :: denotes the normal ordering operation.

As we will explain in detail, in the limit where we send the mass of the bound state to infinity, the diagrammatic expansion of the observables we calculate will exactly reduce to this class of effective diagrams. Therefore, in this article, it suffices to impose normal ordering on all correlation functions in order to define observables properly.

The cautious reader might worry about triviality of the renormalized results for observables as soon as $2N > k$. Indeed, using the renormalization procedure described above, a purely perturbative computation (neglecting normal-ordered contributions in Wick's theorem) would lead to trivial results. In other words, at the perturbative partonic level all observables vanish as soon as $2N > k$. This may sound puzzling, because even at the level of free constituents inside a bound state of infinite mass, it should be possible to compute non-trivial observables such as the density of constituents or their typical energy. The important point is that despite working at the partonic level, the large-N nature of the systems we want to describe, implies that there are large collective effects which can only be captured properly when non-perturbative effects are taken into account. In particular, applying Wick's theorem, observables in large-N systems receive non-trivial contributions from normal-ordered products of operators evaluated in the vacuum. These vacuum condensates parametrize the non-perturbative many-body dynamics in terms of mean-field physics. As such, the condensates should be regarded as non-trivial background sources creating an effective collective potential to which individual gravitons are sensitive. In order to capture the physics we want to describe properly, we should therefore take normal-ordered contributions seriously. In turn, these contributions lead to non-trivial results for observables even at the partonic level as expected physically. Thus, the appearance of condensates can already be anticipated in our approach simply by requiring non-triviality of observables.

2.2.3 Constituent Density and Energy Density

Having presented the necessary theoretical background which we shall use, we will now discuss applications in the context of black holes viewed as bound states of a large number of gravitons. We begin with the construction of the constituent density on the light-cone[14].

[14]Note that this will be the gravitational analogue of the so-called Ioffe-time distribution in QCD [69,70].

In the next part, this observable as well as the distribution of energy of constituents inside the black hole will be computed explicitly. Having obtained these results allows us to derive a scaling relation for the mass of the black hole in terms of the number of fields composing the auxiliary current. This relation will be obtained at the parton level and in the double scaling limit $M \to \infty$, $N \to \infty$ with N/M fixed. We will see that the result allows for an interpretation of the condensate as the typical energy of constituents inside the black hole. We proceed by explaining how higher-order corrections due to condensation of Ricci scalars can be taken into account in a manifestly gauge invariant way. In order to illustrate these ideas, we explicitly compute one such contribution to the constituent distribution. Based on these results, we study the scattering of a probe scalar on a black hole quantum bound state. It is shown that the cross section can directly be expressed in terms the distribution of gravitons inside the black hole. This result shows that our description allows an outside observer to reconstruct the internal structure of a black hole by measuring the scattering angle of the scattered probe scalar. It furthermore suggests that no loss of information is expected in our approach. Finally, we show how classical concepts such as a metric emerge from our description when considering the field produced by a black hole quantum bound state.

Preliminaries

In this section we review the construction of the constituent density at the parton level (free constituents), as well as in the interacting theory. This amounts to construct an operator that measures the distribution of particles inside the bound state $|\mathcal{B}\rangle$.

At the parton level, it suffices to consider scalar constituent densities corresponding to a field h. The difference to a faithful graviton distribution is just a numerical prefactor as explained in Section (2.1.2).

Later we will discuss distribution functions within an interacting theory. For simplicity we will couple fundamental scalars Φ to a background gravitational field[15]. This corresponds to gravitational bound states consisting of both, scalars and gravitons. In particular, we construct the distribution of scalars in the bound state in a gauge invariant way. Notice that this is reminiscent of QCD and pure Yang-Mills theory, respectively. In the latter you only need to consider gluon distribution functions, while in the former quark distributions need to be taken into account in a gauge invariant way, as well. This is explicitly realized by inserting a Wilson line operator into the definition of the distribution functions [71].

The occupation number density n of a free scalar field h is proportional to the field intensity, $n \propto |h(\mathbf{k})|^2$, corresponding to a Fourier–transform of the bi–local operator $\mathcal{O}^{(0)}(x,y) := h(x)h(y)$.

The constituent number density in a state $|\mathcal{B}\rangle$ is the momentum occupation $n(\mathbf{k})$ of that state, in the absence of any interactions. Expanding $|\mathcal{B}\rangle$ in momentum eigenstates

[15] In principle, we could also take the back reaction on the gravitational field due to graviton fluctuations into account. This, however, is rather technical. In order to make the presentation transparent, we thus restrict ourselves to scalars coupled to gravity.

$|P\mathcal{Q}_\mathcal{B}\rangle$ and denoting the associated on-shell momentum wave function by $\mathcal{B}(P)$,

$$\langle\mathcal{B}|(\zeta^3 n)(\mathbf{k})|\mathcal{B}\rangle = \int \mathrm{d^3P}\ |\mathcal{B}(P)|^2 \int \tfrac{\mathrm{d}^3 r}{(2\pi)^3}\ \mathrm{e^{ik\cdot r}}\ \langle P\mathcal{Q}_\mathcal{B}|\mathcal{O}^{(0)}(r,0)|P\mathcal{Q}_\mathcal{B}\rangle. \tag{2.43}$$

Here, $\mathcal{Q}_\mathcal{B}$ denotes a set of quantum numbers compatible with those of the bound state $|\mathcal{B}\rangle$ and $\zeta(\mathbf{k}) := 1/\sqrt{(2\pi)^3 2k^0(\mathbf{k})}$ is the characteristic size of a momentum eigenstate in phase space. The definition (2.43) is therefore manifestly Lorentz-invariant. Notice that we explicitly work on the mass shell of the black hole. The fact that we work on-shell suggests that all observables are effectively evaluated on a spatial hypersurface. This will be reflected in the appearance of delta-functions restricting the time dependence of the constituent number density[16].

Provided the bound state is in a regularised momentum eigenstate, $|\mathcal{B}\rangle = |P_\mathcal{B}\mathcal{Q}_\mathcal{B};\vartheta\rangle$, the P–integration becomes trivial. The regularisation parameter ϑ normalises the variance around $P_\mathcal{B}$.

Associating the number density of constituents with a space–time configuration requires an auxiliary current description for $|\mathcal{B}\rangle$ (see also Section (2.1.2)). This allows to interpret $\mathcal{O}^{(0)}$ as a measurement device. The corresponding process is incorporated by the connected component of the time–ordered product $\mathrm{T}\mathcal{J}(x)\mathcal{O}^{(0)}(y;r/2)\mathcal{J}(0)$, where $\mathcal{J}$ denotes the auxiliary current representing the quantum bound state, and
$\mathcal{O}^{(0)}(y;r/2) := h(y+r/2)h(y-r/2)$ in the absence of interactions[17]. It can be shown that the fixed-order operator product can be replaced by a time–ordered product, $\mathcal{O}^{(0)}(y;r/2) := \mathrm{T}h(y+r/2)h(y-r/2)$, without changing the value of the constituent number density. This fact is obvious, because our construction guarantees that all observables are evaluated at the same spatial hypersurface where the auxiliary currents are inserted. Note that the origin of the coordinate system is chosen such that it makes the external scale r of the diagnostic device manifest.

Diagrammatically, the diagnostic process corresponds to a triangular–like graph, with one vertex point–split to accommodate the diagnostic scale r. Connectedness requires either at least one correlation bridging the currents space–time locations, or a condensation process merging the two events. In principle, however, multiple connections are possible, depending on the auxiliary current and the ground state. We will come back to this issue in much more detail later. Indeed, using composite operator renormalization at the parton level as explained above, we shall see that all diagrams with loops can be renormalized to zero.

Since the constituent number is, in the absence of interactions, tied to the occupation number, a Fock–space description in agreement with the interpretation for $\mathcal{O}^{(0)}(y;r/2)$ can be expected. The mode expansion of h can simply be inverted to give the annihilation and

[16]Of course, instead we could have worked in a fully covariant way without affecting our main results. In particular, in later parts of the thesis, when we reconstruct the classical Schwarzschild metric from our description, we will find it more convenient to work in a four-dimensional notation. The on-shell condition will then be understood implicitly in terms of the P_0 integration as usual.

[17]Note that we chose the space-time dependence of $\mathcal{O}^{(0)}$ symmetrically. This choice is not special, but rather for later convenience.

creation operators, using the time independence of the symplectic product:

$$\hat{a}(\mathbf{k}) = 2k_0(\mathbf{k})\zeta(\mathbf{k}) \int \mathrm{d}^3x \; \mathrm{e}^{-\mathrm{i}k\cdot x} h(x). \tag{2.44}$$

The distinction between annihilation and creation operators is made by the sign in the argument of the exponential. Following the logic of equal–time quantisation, k_0 is on–shell.

The occupation number density n with respect to the covariant momentum measure is given by $n(\mathbf{k}) = \mathrm{d}\mathcal{N}_\mathrm{c}/(\mathrm{d}^3k\; \zeta(\mathbf{k}))$, where $\mathcal{N}_\mathrm{c}$ is the total constituent number. With respect to this measure, $n(\mathbf{k}) = (\zeta^{-1}\hat{a}^\dagger\hat{a})(\mathbf{k})$. Let us already at this point comment on the difference between N and $\mathcal{N}_c$. While N counts the number of free, transverse gravitons, $\mathcal{N}_c$ also counts virtual gravitons. These are accounted for in terms of the condensate contributions. The situation is again reminiscent of the analogous definitions in QCD. When we say, there are three quarks in a proton, we usually refer to the free valence quarks. These constitute the proton even in the regime of asymptotic freedom, i.e. where strong interaction can be neglected. As such, the valence quarks serve as a working analogue of the N gravitons used to define the auxiliary current. At lower energies, however, the effect of virtual quarks and gluons becomes important. These are not on the mass-shell and thus not transverse. Nevertheless, one counts these particles as well when defining the distribution of gluons and sea quarks. While this can be done in perturbation theory as long as the coupling is still smaller than one, these are accounted for in terms of condensates at energies of the order of the confinement scale. In the context of gravity, in contrast, we parametrize the large collective effects via condensates. In other words, effective strong interaction are taken into account. Thus, also here we expect the contribution of interacting, longitudinal gravitons to be important. In fact, we again want to stress that similar collective effects are present in QCD in the BFKL regime [64, 65]. As explained before, the large density of gluons in this situation can be accounted for either by resumming a proper class of diagrams, or by parametrizing the physics in terms of condensed gluons which are well approximated in terms of a strong classical color background field [66].

As advertised in the beginning of this section, we will now move on to the distribution function of scalars interacting with gravity. In the context of gauge theories, the constituent description requires a suitable generalisation to accommodate the related gauge symmetry. A gauge–invariant definition, in accordance with (2.43), is given by inserting a suitable path–ordered exponential of the gauge field, or a Wilson line.

For gravitational interactions, the gauge field $\mathcal{G}$ is given by the connection Γ, in components $\mathcal{G}_\mu = \Gamma^\lambda_{\lambda\mu}$. Treating $\mathcal{G}$ as an external gauge field,

$$(-\Box + \mathcal{G}\cdot\partial)\,\mathcal{O}(y; r/2) = \delta^{(4)}(r), \tag{2.45}$$

which follows from the action of a scalar Φ minimally coupled to gravity. The physical significance of the above equation from the point of view of auxiliary currents can be understood for example as follows. Considering the spherical collapse of a shell of massless scalars into a black hole, the gravitational field will start to produce a large number of

gravitons. At the point when the black hole is formed, there are scalars as well as gravitons inside the black hole. Subsequently, one has to take into account the distributions of both, scalars and gravitons in the black hole interior. Again, the situation is similar to the one in QCD, where quarks and gluons determine the internal structure of a hadron [71].

Equation (2.45) can be solved by iteration, for a detailed derivation we refer the reader to the appendix. The result is,

$$\mathcal{O}(y;r/2) = \mathcal{P}\exp\left(-\oint_C \mathrm{d}z^\lambda \mathcal{G}_\lambda(z)\right)\mathcal{O}^{(0)}(y;r/2), \tag{2.46}$$

where C denotes the contour given by the path $z:[0,1]\to\mathbb{R}^4$, $u\to z(u):=y-(1-2u)r/2$, and $\mathcal{P}$ refers to path ordering along this contour. Note that in this case $\mathcal{O}^{(0)}(y;r/2) = \mathrm{T}\Phi(y+r/2)\Phi(y-r/2)$.

Equation (2.46) shows a simple relation between the constituent number density in the presence and the absence of external gauge fields, respectively, holding to all orders in $\mathcal{G}$, provided the characteristic scale is close to the light–cone.

The observable can now be stated precisely: We are explicitly interested in calculating the constituent distribution

$$\mathcal{D}(r) := \int \mathrm{d}^3k\ \mathrm{e}^{-\mathrm{i}k\cdot r}\langle\mathcal{B}|(\zeta^3 n)(\mathbf{k})|\mathcal{B}\rangle, \tag{2.47}$$

where $|\mathcal{B}\rangle$ could be any bound state, and, in particular, the black hole quantum bound state constructed before. In explicit calculations presented below, we calculate the parton distribution of massless quanta constituting the bound state, the total constituent number and energy density inside the bound state. Since we are interested in a generic, theoretical framework, we will primarily be interested in calculating observables at the level of the free theory. Due to non-perturbative effects (tight to the large-N nature), however, the calculations lead to non-trivial results already at this level as advertised before. In section 2.2.4 we outline how gauge corrections can be taken into account based on existing external field methods. In order to illustrate the idea and method, we explicitly compute a specific diagram corresponding to a higher-order Ricci condensate correction. A systematic analysis concerning these higher-order terms, however, is beyond the scope of the thesis.

Parton-Level Results

In this section the calculation of $\mathcal{D}(r)$ is presented, using $\mathcal{J} = h^N$ with $N \gg 1$ as an auxiliary current representation of a black hole quantum bound state $|\mathcal{B}\rangle$, and $\mathcal{O}^{(0)}(y;r/2)$ as the operator probing the free constituent distribution inside the bound state at resolution scale r (as explained before, for a Schwarzschild black hole, this distribution will only depend on the spatial distance $|\mathbf{r}|$ by virtue of the isometries and Ward's identity). Let us first calculate the current normalisation. Using the auxiliary current description to represent $|\mathcal{B}\rangle$, the normalization condition $\langle\mathcal{B}|\mathcal{B}\rangle = 1$ becomes

$$\Gamma_B^2 = \int \mathrm{d}^3k\mathrm{d}^3p\ \mathcal{B}^*(k)\mathcal{B}(p)\int \mathrm{d}^3x\mathrm{d}^3y\ \tfrac{e^{-\mathrm{i}k\cdot x}}{(2\pi)^{3/2}}\tfrac{e^{\mathrm{i}p\cdot y}}{(2\pi)^{3/2}}\langle\Omega|\mathcal{J}(x)\mathcal{J}(y)|\Omega\rangle\ \delta_{\mathcal{B}}. \tag{2.48}$$

Here, $\delta_{\mathcal{B}}$ indicates that we are considering correlations at equal time[18]. In turn, we can evaluate (2.48) using Wick's theorem. It can be shown that all possible loops can be reduced to self-loops in the limit of large black-hole masses. We go through this exercise when calculating the distribution function. As explained in the section on composite-operator renormalization in free field theories, all such contributions can be safely set to zero at the parton level. The only non-trivial connected diagram is the one where a graviton is emitted at $\mathbf{x}$ and subsequently absorbed at $\mathbf{y}$, while all other fields condense. Thus, the expectation value in (2.48) reduces to $N^2\Delta(x-y)\langle\Omega|{:}\, h^{N-1}(x)h^{N-1}(y){:}\,|\Omega\rangle$. Fourier-transforming the propagator, we can shift the integration variable $q_0 \to q_0 + p_0 \sim M^2$, where in the last step the on-shell condition and the limit $M \to \infty$ have been used. The remaining integrations can now be performed trivially. This gives rise to a contact contribution, i.e. the condensate becomes local. Using translational invariance, we can shift the condensate to the origin. As a result, we find

$$\Gamma_B^2 \;=\; \left(\tfrac{N}{M}\right)^2 \langle\Omega|{:}h^{2(N-1)}(0){:}|\Omega\rangle \int \mathrm{d}^3p \;\; |\mathcal{B}(p)|^2 \;\; \delta_{\mathcal{B}} \; . \tag{2.49}$$

We proceed with the calculation of the constituent distribution $\mathcal{D}(x)$ within a composite object described by the local auxiliary current $\mathcal{J}(x)$. This amounts to calculating

$$\begin{aligned} \mathcal{D}(x) \;&=\; \int \mathrm{d}^3p \;\; |\mathcal{B}(p)|^2 \, \mathcal{A}(p,x) \; , \\ \mathcal{A}(p,x) \;&=\; \int_\Sigma \mathrm{d}^3z_1 \mathrm{d}^3z_2 \; \mathrm{e}^{-\mathrm{i}p\cdot(z_1-z_2)} \langle\Omega|\mathrm{T}\mathcal{J}(z_1)\mathcal{O}(x,0)\mathcal{J}(z_2)|\Omega\rangle \; , \end{aligned} \tag{2.50}$$

with $\mathcal{O}(x,0) = h(x)h(0)$. This bi-local operator is anchored in the hypersurface $\Sigma = \{P : y(P) = (0,\mathbf{y})\}$. The four-point correlation function in $\mathcal{A}$ can only be nontrivial if the auxiliary currents are localised on Σ. Hence, $\mathcal{A} = \mathcal{A}_\Sigma\delta_\Sigma$, and correspondingly for the constituent distribution $\mathcal{D} = \mathcal{D}_\Sigma\delta_\Sigma$, where δ_Σ indicates that all fields are localised on the spatial hypersurface Σ. Note, as we have already mentioned before, this fact a posteriori allowed us to directly express the observable $\mathcal{D}_\Sigma$ in terms of time-ordered correlators.

A connected component in $\mathrm{T}\mathcal{J}(z_1)\mathcal{O}^{(0)}(x,0)\mathcal{J}(z_2)$ requires $N \geq 2$. Before considering $N \gg 1$, it is instructive to calculate the minimal connected component corresponding to $N = 2$. This is a purely perturbative contribution. Wick expansion of the four-point correlation function gives the Feynman diagram shown on the left of Figure 2.1 (plus a term with x and 0 exchanged). We are interested in the limit $M/\mu \to \infty$, where μ denotes any other quantity of mass dimension one such as momenta flowing through propagators. This limit corresponds to a contact configuration of the two auxiliary currents. Including the term with x and 0 exchanged, we arrive at

$$\mathcal{D}_\Sigma^{[0]}(x)\Big|_{N=2} = \frac{2}{(2\pi)^5} \; \frac{1}{M^2} \frac{1}{\langle\Omega|{:}h^2(0){:}|\Omega\rangle} \; \frac{1}{|\mathbf{x}|^2} \; . \tag{2.51}$$

[18] Alternatively, we could work with time-ordered products at different times and use solely covariant integration measures. The on-shell condition is then understood implicitly and is realized as usual when performing the integration over the zero components of the momenta. The results are, of course, unaffected.

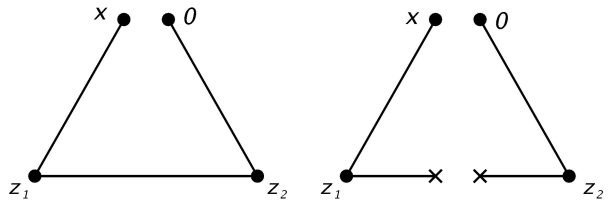

Figure 2.1: Diagrams contributing to the calculation of $\mathcal{D}(r)$ for $N = 2$. The first diagram represents a purely perturbative configuration. The second diagram depicts a condensation of space-time events originally located at z_1 and z_2. For $N = 2$, however, this diagram is disconnected.

Here, $\mathcal{D}^{[0]}(x)$ denotes the purely perturbative contribution to the constituent distribution, which in the context of a free theory refers to the absence of condensates. In other words, condensates in the perturbative contribution only appear in the denominator via the normalisation of Γ_B. In contrast, non-perturbative processes also generate condensates in the numerator (see below). The constituent distribution as a function of wavelength is found by Fourier-transforming (2.51) and setting $\lambda \equiv \sqrt{2\pi}/|\mathbf{k}|$,

$$\mathcal{D}^{[0]}_{\Sigma}(\lambda)\Big|_{N=2} = \frac{1}{(2\pi)^5}\,\frac{1}{M^2}\,\frac{1}{\langle\Omega|{:}h^2(0){:}|\Omega\rangle}\,\lambda\,. \tag{2.52}$$

As a result, we find that the constituent distribution depends linearly on the wavelength. In other words, the bound state $|\mathcal{B}\rangle$ is predominantly populated with soft gravitons. Although the case $N = 2$ is just of pedagogical interest, we will see the phenomenon of long wavelength dominance will persist even as we take N large. This shall be demonstrated explicitly in what follows.

An important question arising from the $N = 2$ case is whether a purely perturbative contribution is generic for $N \gg 1$. The answer is no. If the connectivity between the space–time events at x and 0 is increased by means of perturbative correlations (as opposed to condensation), then a contribution proportional to $\Delta^{(0)}(0)$ is inevitable in the limit $M/\mu \to \infty$, corresponding to a loop anchored at one of the auxiliary currents space–time location, as shown in Figures 2.2 and 2.3. The occurrence of self-loops can be understood

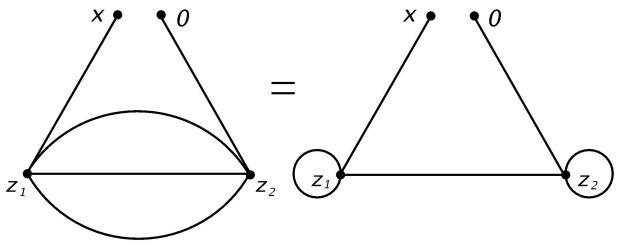

Figure 2.2: Purely perturbative contribution for $N = 4$. In the limit of large black-hole masses, both diagrams reduce to the same divergency class. Performing composite operator renormalization, these diagrams can be set to zero.

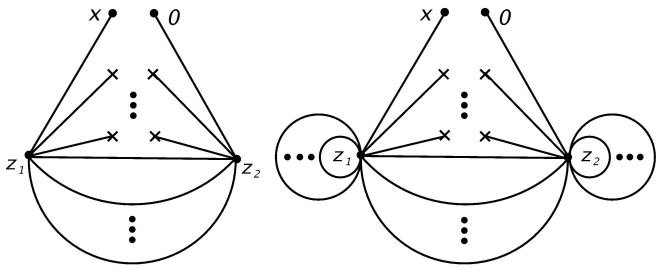

Figure 2.3: The generic situation corresponding to Figure 2.2 for N scalar fields constituting the auxiliary current. Shown are k condensate insertions and $l = N - k - 2 \neq 0$ loops connecting the space–time points x and 0. All diagrams with $l > 0$ vanish in the limit of large black-hole masses due to composite operator renormalization.

as follows. Consider a diagram with one loop connecting the positions of the auxiliary currents. This will generate a contribution of the form

$$\begin{aligned}
&\int \mathrm{d}^4x\ \mathrm{e}^{-\mathrm{i}p\cdot x} f(x)\Delta^{(0)}(x)\Delta^{(0)}(-x) \\
&= \int \tfrac{\mathrm{d}^4k}{(2\pi)^4}\ f(k) \int \tfrac{\mathrm{d}^4k}{(2\pi)^4}\ \Delta^{(0)}(q)\Delta^{(0)}(p-k-q) \\
&\overset{M/\mu\to\infty}{\longrightarrow} M^{-2} \int \tfrac{\mathrm{d}^4k}{(2\pi)^4}\ f(k) \int \tfrac{\mathrm{d}^4q}{(2\pi)^4}\ \Delta^{(0)}(q)\ . \qquad (2.53)
\end{aligned}$$

where p denotes the on-shell momentum of the black hole, $p^2 = -M^2$, and f is a generic diagram connected to the loop, which results from Wick expanding the four-point correlation function in the definition of $\mathcal{A}(p,r)$. For simplicity we have suppressed all arguments of f irrelevant for our discussion. Thus, the limit $M/\mu \to \infty$ results in an analytic structure of the diagrams that is indistinguishable from self-loops. As discussed in section (2.2.2), a proper renormalization prescription at the parton level amounts to setting these contributions to zero.

As a consequence, even in the general $N > 2$ cases, the connected component of $\mathcal{A}(p,x)$ is always minimally connected, i.e. the number of h-propagators is exactly the same as in the purely perturbative case for $N = 2$. For arbitrary $N > 2$, the standard Wick expansion of $\mathcal{A}(p,x)$ corresponds to the diagram shown in Figure 2.4 plus a diagram with $z_1 \leftrightarrow z_2$. We find

$$\begin{aligned}
\mathcal{A}(p,x) \;=\; (-\mathrm{i})^3\Gamma^{-2}\tbinom{N}{2}^2 \int_\Sigma \mathrm{d}^3z_1\mathrm{d}^3z_2\ \tfrac{\mathrm{e}^{-\mathrm{i}p\cdot(z_1-z_2)}}{(2\pi)^3}\langle\Omega|{:}h^{N-2}(z_1)h^{N-2}(z_2){:}|\Omega\rangle \\
\Delta(x-z_1)\Delta(z_1-z_2)\Delta(z_2) \qquad (2.54)
\end{aligned}$$

plus the exchange diagram. Inserting a complete set of momentum eigenstates $|k\rangle$ in the condensate, and Fourier-transforming the propagators, the integrals over the spatial positions of the auxiliary currents can be performed resulting in the momentum constraints: $\mathbf{q_2} = \mathbf{p} - \mathbf{k} + \mathbf{q_1}$, and $-\mathbf{q_3} = \mathbf{p} - \mathbf{k} + \mathbf{q_3}$, where q_1 is the four-momentum associated with

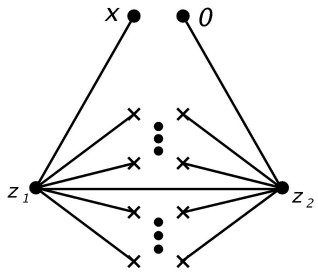

Figure 2.4: Typical diagram contributing to the constituent distribution of a bound state described by a local auxiliary current composed of $N \gg 1$ constituent fields. The four-point correlation function corresponds always to a minimal connected diagram. All remaining constituents end up in condensates that parametrise the background in which the perturbative degrees of freedom propagate.

$x - z_1$, q_2 with $z_1 - z_2$ and q_3 is associated with z_2. Shifting the energies of the propagators connecting the observable $\mathcal{O}(x,0)$ with the auxiliary currents, $(q_2)_0 \to (q_2)_0 + (p-k)_0$ and $(q_3)_0 \to p_0$, and taking the limit $M/\mu \to \infty$, we find (including the exchange diagram)

$$\mathcal{A}(\mathbf{x}) \;=\; \frac{2}{(2\pi)^5}\,\frac{\binom{N}{2}^2}{M^4}\,\frac{\langle\Omega|{:}h^{2(N-2)}(0){:}|\Omega\rangle}{\Gamma^2}\,\frac{1}{|\mathbf{x}|^2}\,\delta_{\mathcal{B}}\delta_{\Sigma}\;. \tag{2.55}$$

Fourier-transforming $\mathcal{A}(p,x)$ with respect to the difference vector $\mathbf{x}$ which connects the fields composing $\mathcal{O}(x,0)$ in the hypersurface $x_0 = 0$, the constituent distribution as a function of wavelength is given by

$$\mathcal{D}_{\Sigma}(\lambda) \;=\; \frac{1}{(2\pi)^5}\frac{(N-1)^2}{M^2}\frac{\langle\Omega|{:}h^{2(N-2)}(0){:}|\Omega\rangle}{\langle\Omega|{:}h^{2(N-1)}(0){:}|\Omega\rangle}\,\lambda\;, \tag{2.56}$$

where (2.48) has been used. The limit $M/\mu \to \infty$ considerably simplifies the calculations of correlation functions involving bound states of mass M. This raises the question whether (2.56) is trivial. The answer must be no, since there is no reason to expect that this distribution should be trivial, in particular for $M/\mu \to \infty$. But then M cannot be independent of N. Moreover, $M/(\mu N) \to$ constant in this limit, which really is a non-triviality condition and the second indication for $M \propto N$. This conclusion assumes that the condensate ratio appearing in (2.56) is N-independent. Relaxing from the limit $M/\mu \to \infty$, it is clear that $1/N$-corrections will be generated. Alternatively, the result (2.56) can be presented in terms of $\mathcal{D}$ (2.50). Since $\mathcal{D} \propto \delta_{\Sigma}$, only ratios of $\mathcal{D}$ evaluated at different length scales are sensible quantities. Denoting by r_s an arbitrary pivot scale, for instance the Schwarzschild radius which then enters as an external quantity, we have

$$\mathcal{D}(\lambda) \;=\; \mathcal{D}(r_s)\,\frac{\lambda}{r_s}\;. \tag{2.57}$$

Let us briefly recapitulate the physics corresponding to the limit of large mass. Form (2.54) we see that the correlation effectively reduces to a free propagator subject to a

multiplicative normalization in terms of non-vanishing vacuum condensates. Thus, we can really understand the distribution as a resulting from probing a non-trivial constant medium, the black hole, as advertised before.

While N counts the number of h-fields composing the auxiliary current or, equivalently, its mass dimension, the total constituent number $\mathcal{N}_{\rm c}$ is given by

$$\begin{aligned}\mathcal{N}_{\rm c} &= \int \mathrm{d}^3q\ \langle\mathcal{B}|n(\mathbf{q})|\mathcal{B}\rangle \\ &= \int \mathrm{d}^3q\ 2q^0 \int \mathrm{d}^3x\ \mathrm{e}^{\mathrm{i}q\cdot x}\ \mathcal{D}(x)\Big|_{q^0=|\mathbf{q}|}\ .\end{aligned} \tag{2.58}$$

Since $\langle\mathcal{B}|n(\mathbf{q})|\mathcal{B}\rangle = |\mathcal{B}(\mathbf{q})|^2$, and due to the on-shell condition, the momentum integral should be restricted to $|\mathbf{q}| \in [0, M]$. In the limit $M/\mu \to \infty$, $N \to \infty : M/(\mu N) \to$ constant, we find

$$\mathcal{N}_{\rm c} = \frac{1}{3\pi^2}\frac{N^2}{M^2}\frac{\langle\Omega|{:}h^{2(N-2)}(0){:}|\Omega\rangle}{\langle\Omega|{:}h^{2(N-1)}(0){:}|\Omega\rangle}\ M^3\ \delta_\Sigma\ . \tag{2.59}$$

As expected on physical grounds, the constituent number diverges as the mass dimension of the auxiliary current goes to infinity: In fact, for $N_1, N_2 \gg 1$, $\mathcal{N}_{\rm c}(N_1)/\mathcal{N}_{\rm c}(N_2) \propto (N_1/N_2)^3$. Note that this result is consistent with our earlier remark concerning $N \neq \mathcal{N}_c$, i.e. $\mathcal{N}_c$ counts the total number of constituents including virtual gravitons which in our formalism are accounted for in terms of condensates.

Given the above scaling behaviour, it is interesting to ask whether the energy density of black-hole constituents is a meaningful quantity in the limit $M/\mu \to \infty$, $N \to \infty$: $M/(\mu N) \to$ constant. At the parton level, it suffices to consider the following energy-momentum tensor: $\mathcal{T}_{\alpha\beta} = G_{\alpha\beta}{}^{\mu\nu}\partial_\mu h \partial_\nu h/2$, where G denotes the Lorentz-covariant generalisation of the Wheeler–DeWitt metric. Using the auxiliary current description, the standard Wick expansion of $\mathcal{E}(x) \equiv \langle\mathcal{B}|\mathcal{T}_{00}(x)|\mathcal{B}\rangle$ results in the type of Feynman diagrams shown in Figure 2.5. By the same reasoning as before when we calculated the distribution function, all loop corrections vanish in the limit $M/\mu \to \infty$. The remaining Feynman diagram is readily calculated to give

$$\mathcal{E}(\mathbf{x}) = \frac{|\mathcal{B}(\mathbf{x})|^2}{2\int \mathrm{d}^3p\ |\mathcal{B}(\mathbf{p})|^2}\ \delta_\Sigma\ . \tag{2.60}$$

Both, the total number of constituents as well as the energy density are defined on the spatial hypersurface Σ. In order to define a proper observable, we can consider the energy density per constituent $\mathcal{E}(x)/\mathcal{N}_{\rm c}$. While $\mathcal{E}(x)$ and $\mathcal{N}_c$ are temporal distributions proportional to δ_Σ, the ratio $\mathcal{E}(x)/\mathcal{N}_{\rm c}$ is a physical density that can be integrated over Σ to yield the energy per constituent[19] $\omega = \delta M$, with $\delta \equiv c\langle h^{2(N-1)}\rangle/\langle h^{2(N-2)}\rangle/(NM)^2 \ll 1$, where $c \equiv 2/(3\pi^2)$ and $\langle A\rangle \equiv \langle\Omega|:A:|\Omega\rangle$. This is in agreement with our earlier result

[19] This does not imply that the integral of $\mathcal{E}$ over Σ is M, since $\mathcal{E} \propto \delta_\Sigma$.

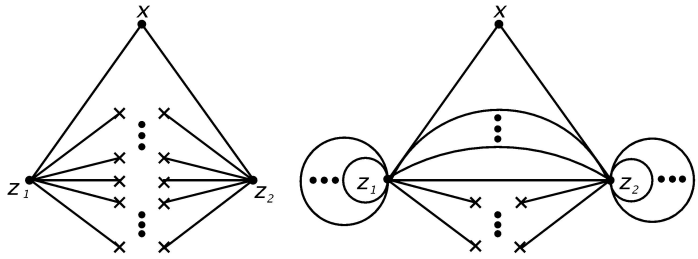

Figure 2.5: Diagrams contributing to the constituents energy-density inside a black hole represented by a generic auxiliary current. Only the diagram on the left is nontrivial. It corresponds to a condensation of all constituent fields not connected to the fields composing the observable $\mathcal{E}$. Increasing the connectivity between the space–time points z and y just by one propagator leads to a vanishing contribution in the limit $M/\mu \to \infty$ (upon imposing correlation functions to be normal-ordered).

that the black-hole interior is predominantly populated with quanta of the largest possible wavelength. Let us introduce the physical constituent number $N_{\rm c} \equiv \delta^{-1}$, which allows to establish a link between the macroscopic and microscopic description of black holes:

$$M^2 = \frac{2}{3\pi^2} \frac{\langle h^{2(N-1)} \rangle}{\langle h^{2(N-2)} \rangle} \frac{N_{\rm c}}{N^2} \, . \tag{2.61}$$

Defining $E^2 \equiv 2\langle h^{2(N-1)} \rangle / (3\pi^2 \langle h^{2(N-2)} \rangle N^2)$, the characteristic energy scale E can be related to the typical energy per condensed constituent. It depends on a condensate ratio that is a phenomenological input parameter. At this stage, at the parton level, we cannot make strong claims about the value of this ratio.

In terms of the characteristic energy scale E we find

$$M \;\; = \;\; \sqrt{N_{\rm c}} \, E \, . \tag{2.62}$$

This scaling relation shows that the limiting processes are self-consistent and capture the correct physics. The consistence and non-triviality requirements, as well as simplicity are all granted by the well-established benefits of field theories with a large number of constituents.

2.2.4 Beyond Parton-Level

There are various corrections to the results presented in the last section, which have been established in the large$-N$ limit of a free field theory. First, perturbative graviton exchanges give rise to a series in the gravitational coupling strength. Secondly, already at the parton level there are corrections to our earlier results which are due to finite N or equivalently finite mass effects. These corrections will be discussed in more detail in the section on the emergence of geometry from the auxiliary current description. Finally, non–perturbative contributions arise due to strong collective gravitational potentials experience

by individual constituents. Following the logic of the framework presented here, collective effects can be parametrised by condensates, i.e. for the case at hand by curvature condensates (corresponding to field-strength squared condensates in Yang-Mills theories). In this section, we sketch the general strategy for incorporating these corrections in a pragmatic fashion. Detailed calculations are left for future research.

Let us demonstrate the appearance of graviton condensates for the case of gravitational bound states containing scalars Φ as well as gravitons. For simplicity, we assume the scalar to be minimally coupled to gravity and restrict the discussion to the distribution function of the scalars. Note that at the parton level this contribution coincides with the result presented before. As discussed before, this exercise is not only of academic interest, but also of physical significance. If a shell of scalar matter collapses, it will source gravity. The resulting state then consists of both, scalars as well as longitudinal gravitons. Subsequently, distribution functions for both fields can be defined in accordance with gauge- invariance. Here we show how the distribution of scalars is affected by gravity. Note that the construction is reminiscent of quark distribution functions inside a hadron when interactions are switched on. Also there, the distribution of quarks is influenced non-trivially by the presence of gauge condensates. Having this physical situation in mind, let us now discuss our strategy for computing the scalar distribution in the presence of gravity.

In order to relate gravitons to curvature, the following gauge is useful:

$$x^\lambda x^\sigma \Gamma^\mu_{\lambda\sigma}(x) = 0 \,, \tag{2.63}$$

which is the exact analogue of the Fock–Schwinger gauge, originally proposed in electrodynamics and heavily employed in QCD. In gravity it corresponds to the choice of a well–known coordinate neighbourhood called a (pseudo-)Riemannian normal-coordinate system. Indeed, the Fock–Schwinger gauge is equivalent to $x^\mu g_{\mu\nu}(x) = x^\mu g_{\mu\nu}(0)$, which in combination with $g_{\mu\nu}(0) = \eta_{\mu\nu}$ defines a normal coordinate system anchored at 0. The geodesic interpretation is that straight lines through the origin parametrize geodesics in these coordinates. The Fock–Schwinger gauge allows to conveniently express the potential $\mathcal{G}_\mu \equiv \Gamma^\lambda_{\lambda\mu}$ in terms of the Ricci tensor,

$$\mathcal{G}_\mu(x) \;\; = \;\; -\tfrac{1}{3} x^\lambda R_{\lambda\mu}(0) + \cdots \,. \tag{2.64}$$

Terms suppressed in this expansion involve covariant derivatives and products of Riemann tensors. Although a closed formula for the Riemann normal coordinate expansion of $\mathcal{G}(x)$ in local operators can be given, it suffices to work with (2.64) to illustrate the main idea.

Consider a Φ–quantum emitted at the space–time point y and absorbed at x. The propagator $\Delta(x,y) \equiv \mathrm{i}\langle\Omega|\mathrm{T}\Phi(x)\Phi(y)|\Omega\rangle$ satisfies $(-\Box + \mathcal{G}\cdot\partial)\Delta(x,y) = \delta(x-y)$. Assuming

$\mathcal{G}$ to be small as compared to the free propagation scale $x-y$, $\Delta(x,y)$ can be expanded as

$$\begin{aligned}\Delta(x,y) &= \sum_{n=0}^{\infty}\Delta^{(n)}(x,y)\ ,\\ \Delta^{(n)}(x,y) &= \int \mathrm{d}^4z_1\cdots\mathrm{d}^4z_n\ (-1)^n\Delta^{(0)}(x-z_1)\\ &\quad\times\mathcal{G}\cdot\partial\Delta^{(0)}(z_n-y)\prod_{a=1}^{n-1}\mathcal{G}\cdot\partial\Delta^{(0)}(z_a-z_{a+1}),\end{aligned}\tag{2.65}$$

where $\Delta^{(0)}$ denotes the free propagator. This formula has a simple diagrammatic interpretation, shown in Figure 2.6. The free propagator $\Delta^{(0)}$ transforms invariant under space–time translations, while Δ is non–invariant, since $\mathcal{G}$ depends on the space–time location. Given that $\mathcal{G}$ is external and tied to the ground state properties, this space–time dependence is fictitious when the averaged ground state structure is considered. There is, however, a second reason for breaking translation invariance. Namely, once we choose Fock–Schwinger gauge for evaluating (2.65), the origin of the Riemann normal coordinate neighbourhood is distinguished. But this is simply due to choosing a coordinate system and bears no physical significance, provided all calculations are performed in these coordinates.

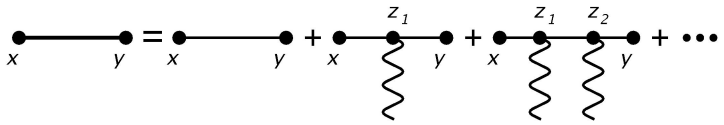

Figure 2.6: Diagrammatic representation of the scalar propagator in the external $\mathcal{G}$–field. The constituent scatters zero, one, two, ... times off the external potential $\mathcal{G}$, represented by the wavy lines. On the light–cone, the series of interactions can be summed up, resulting in a path–ordered exponential of the connection $\mathcal{G}$, in accordance with gauge invariance.

Having a bookkeeping procedure in mind such as the operator product expansion, there might be situations where we are only interested in the $R_{\mu\nu}$ contribution. Then, effectively, $\mathcal{G}_\mu(x) = -x^\lambda R_{\lambda\mu}(0)/3$. Other operators in the Riemann normal coordinate expansion of $\mathcal{G}$ cannot result in R–contributions to Δ. An elementary calculation using dimensional regularization and the modified minimal subtraction scheme gives

$$\Delta^{(1)}(x,y) = \tfrac{-\mathrm{i}}{96\pi^2}\ \langle R(0)\rangle\left\{\ln\left(\tfrac{y^2}{d^2}\right) - 1 - \tfrac{y^2-(x-y)^2}{(x-y)^2}\left[\ln\left(\tfrac{y^2-(x-y)^2}{y^2}\right)-1\right]\right\}.\tag{2.66}$$

Here, d denotes an arbitrary renormalization length scale. Note that (2.66) is exact up to condensates of operators with mass dimensions larger than two, which are not shown here. The Ricci condensate $\langle R(0)\rangle \equiv \langle\Omega|{:}R(0){:}|\Omega\rangle$ originates from the condensation of $\mathcal{G}$. This highlights the practical value of the external field method in Fock-Schwinger gauge for the non-perturbative description of bound states.

As an example for a gauge correction to the distribution of Φ-constituents, consider the diagram shown in Figure 2.7, which gives rise to a contribution proportional to the

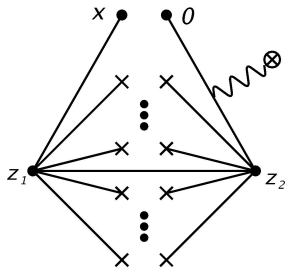

Figure 2.7: An example for a gauge correction to the constituent distribution, resulting in a Ricci condensate indicated by the wiggly line.

condensate $\langle\Phi^{2(N-2)}R\rangle \equiv \langle\Omega|:\Phi^{2(N-2)}R:|\Omega\rangle$. The amplitude is given by (compare to (2.54))

$$\begin{aligned}\mathcal{A}^{\mathrm{gc}}(p,r) &= \tfrac{1}{96\pi^2\Gamma^2}\binom{N}{2}\int_\Sigma \mathrm{d}^3x\mathrm{d}^3y\ \tfrac{\mathrm{e}^{-\mathrm{i}p\cdot(x+y)}}{(2\pi)^3}\Delta^{(0)}(x)\Delta^{(0)}(x-y_-)\\ &\quad\times\left[\ln\left(\tfrac{-(y_-)^2}{d^2}\right)-2\right]\left\langle\Phi^{N-2}(x)\left(\Phi^{N-2}R\right)(0)\right\rangle, \end{aligned}\tag{2.67}$$

where $y_- := y - r/2$. Expanding $\Phi^{N-2}(x)(\Phi^{N-2}R)(0)$ into local operators yields coefficients suppressed by powers of $p^2 = -M^2$. In the limit $M/\mu \to \infty$ (with μ denoting an arbitrary energy scale), the leading contribution is given by

$$\mathcal{A}^{\mathrm{gc}}(\mathbf{p},\mathbf{r}) = \tfrac{1}{96\pi^2\Gamma^2}\tfrac{\binom{N}{2}^2}{M^4}\,\mathrm{e}^{\mathrm{i}\mathbf{p}\cdot\mathbf{r}/2}\left[\ln\left(\tfrac{\mathbf{r}^2}{\mathbf{d}^2}\right)-2\right]\left\langle\Phi^{2(N-2)}R\right\rangle\delta_{\mathcal{B}}\delta_\Sigma\,. \tag{2.68}$$

The corresponding correction to the constituent distribution is given by

$$\mathcal{D}_\Sigma(\mathbf{r}) = \frac{1}{4}\frac{1}{96\pi^2}\frac{N^2}{M^2}\,\frac{\left\langle\Phi^{2(N-2)}R\right\rangle}{\langle\Phi^{2(N-1)}\rangle}\,\frac{|\mathcal{B}(\mathbf{r})|^2}{\int\mathrm{d}^3p\ |\mathcal{B}(\mathbf{p})|^2}\left[\ln\left(\tfrac{\mathbf{r}^2}{\mathbf{d}^2}\right)-2\right]\,. \tag{2.69}$$

This concludes our outlook, which was intended to show how gauge corrections can be incorporated. As systematic study of the physics of these corrections will be left for further investigations.

2.2.5 Scattering on Black Holes

In this part we will show how observables connected to the black hole interior such as the constituent distribution of gravitons can be embedded within scattering theory.

Considering black holes as external sources, i.e. not resolved in a physical Hilbert space, small–scale structure of their interior is a void concept. Scattering experiments allow to extract observables localized outside of the black hole. In particular, the $1/r$–potential can be recovered for $r > r_{\mathrm{g}}$, where $r_{\mathrm{g}} \equiv 2M/M_p^2$ is the Schwarzschild radius, with M_p denoting the Planck mass and M the black hole mass as before. Furthermore, resummation of tree scattering processes sourced by the external black hole give rise to

geodesic motion in the respective Schwarzschild background [67]. As explained before this allows for a reinterpretation of geometry as being emergent from an S-matrix defined on flat space–time. Note that in the next subsection we will show that such a resummation still correctly accounts for geometric features even when the source, i.e. the black hole is resolved quantum mechanically using the auxiliary current approach.

Following this logic and treating black holes as internal sources in the physical Hilbert space, we will first demonstrate that their interior quantum structure can be resolved by employing probes of sufficient virtuality, $-q^2 > r_{\mathrm{g}}^{-2}$. This can be described in a weakly coupled field theory provided $-q^2 < M_p^{\,2}$ holds. Notice, that these ideas depart from the semi-classical point of view. There, the existence of a horizon prohibits an observer outside of the black hole to get any information about the internal structure of the system. As explained before, the geometrical concept is not fundamental within our approach. Rather geometry and thus the existence of a horizon should be understood as effective phenomena. On the microscopic level, however, this description should break down and a resolution of the bound state becomes possible for an outside observer. From that point of view the black hole can be viewed as the gravitational analogue of the proton in the context of QCD. Also here, before developing a proper understanding of the nature of the strong interactions, protons were viewed as structureless quanta subject to electromagnetic interactions only. Of course, by now it is clear that this picture of the proton breaks down if we perform experiments at energies large enough to resolve the proton in terms of quarks and gluons. According to our philosophy, we want to develop a similar microscopic understanding of the black hole as a composite graviton bound state and extract this structure using the S-matrix.

In order to do so consider an ingoing scalar Φ outside of the black hole emitting a graviton with appropriate virtuality, which subsequently gets absorbed by another scalar in the black hole's interior[20]. This process is encoded in the linearized Einstein–Hilbert action coupled to the energy–momentum tensor of a massless scalar, $\mathcal{T} = \mathrm{d}\Phi \otimes \mathrm{d}\Phi - (\mathrm{d}\Phi, \mathrm{d}\Phi)\eta/2$:

$$S = \int \mathrm{d}^4x \left[\frac{1}{2} h_{\mu\nu} \epsilon^{\mu\nu}_{\alpha\beta} h^{\alpha\beta} + \frac{1}{M_{\mathrm{P}}} h_{\mu\nu} \mathcal{T}^{\mu\nu} \right] . \tag{2.70}$$

Here $\epsilon^{\mu\nu}_{\alpha\beta}$ is the standard linearized kinetic operator of general relativity expanded around flat space–time. Note that we can trust this effective action in the kinematic regime discussed above.

Before truncating ingoing and outgoing emitter legs, the one–graviton exchange amplitude for this process at tree level reads (see also figure (2.8))

$$a^{(2)}(x_1, x_2) = \tfrac{\mathrm{i}^2}{M_{\mathrm{P}}^{\,4}} \int \mathrm{d}^4z_1 \mathrm{d}^4z_2 \; \mathcal{P}^{\mu\nu}(z_1, z_2; x_1, x_2) \mathcal{N}_{\mu\nu}(z_2),$$

[20] We restrict our analysis to the scattering of a scalar on a black hole for notational simplicity. Of course, since gravity couples to all matter democratically, the analysis can easily be extended to other particles such as photons or gravitons scattering on the bound state.

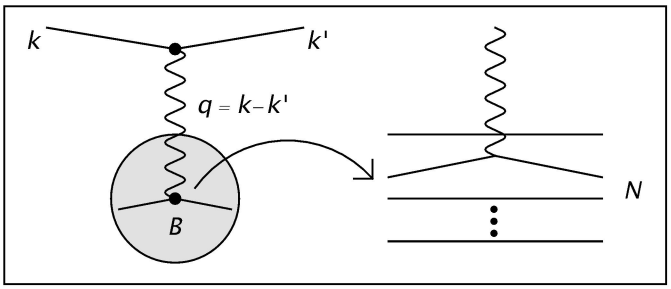

Figure 2.8: Feynman diagram for the scattering of a scalar on a black hole bound state at tree level. The wiggly line corresponds to the exchange of a virtual graviton. On the right hand side, the corresponding absorption is resolved into the microscopic constituents spectating and participating in the scattering process.

where $\mathcal{P}$ contains all perturbative correlations and $\mathcal{N}$ carries local, non-perturbative information about the black hole quantum state $|\mathcal{B}\rangle$:

$$\begin{aligned} \mathcal{P}^{\mu\nu} &= \langle\Omega|\mathrm{T}\Phi(x_2)\mathcal{T}_{\alpha\beta}(z_1)\Phi(x_1)|\Omega\rangle\ \Delta^{\alpha\beta\mu\nu}(z_1,z_2)\ , \\ \mathcal{N}_{\mu\nu} &= \langle\mathcal{B}'|\ {:}\mathcal{T}_{\mu\nu}{:}\,(z_2)|\mathcal{B}\rangle\ . \end{aligned} \tag{2.71}$$

Here Δ denotes the free graviton propagator, and $|\mathcal{B}'\rangle$ is the black hole quantum state after absorbing the graviton. Basically, $\mathcal{P}$ describes space–time events that originate outside the bound state, while $\mathcal{N}$ is localized in its interior. In other words, it corresponds to the effective vertex describing the interaction between the black hole with a graviton. We will have to say much more about this effective interaction in the next subsection.

Using the auxiliary current description, and provided that the bound state wave function $B(P)$ has a sufficiently compact support in momentum space, the graviton absorption event can be translated to the origin:

$$\mathcal{N}(z_2) \approx \mathrm{e}^{-\mathrm{i}(P'-P)\cdot z_2}\langle\mathcal{B}'|\ {:}\mathcal{T}{:}\,(0)|\mathcal{B}\rangle\ , \tag{2.72}$$

with P' and P denoting the black hole momentum after and before the graviton absorption, respectively, around which the corresponding wave function is peaked. The evaluation of $\mathcal{P}$ is straightforward. Truncating the ingoing and outgoing emitter legs using the standard LSZ prescription, the one–graviton exchange amplitude becomes

$$\begin{aligned} \langle\mathcal{B}'\Phi'|\mathcal{B}\Phi\rangle^{(2)} \quad &= -\mathrm{i}(2\pi)^4\delta(k'+P'-k-P)\ \alpha_{\mathrm{g}}{}^2 \\ &\quad\times\langle\mathcal{B}'|\ {:}\mathcal{T}_{\mu\nu}{:}\,(0)|\mathcal{B}\rangle\ \Delta^{\mu\nu\alpha\beta}(k'-k)\ G_{\alpha\beta\rho\sigma}\ \tfrac{k'^\rho k^\sigma}{k'^0 k^0}\ , \end{aligned} \tag{2.73}$$

where the coupling $\alpha_{\mathrm{g}} \equiv 1/(4\pi M_{\mathrm{P}}^2)$ has been introduced, and $G_{\alpha\beta\rho\sigma} = \eta_{\beta(\alpha}\eta_{\rho)\sigma} - \eta_{\beta\sigma}\eta_{\alpha\rho}$ is the Wheeler–DeWitt metric.

The total cross section $\sigma(\mathcal{B}'\Phi' \leftarrow \mathcal{B}\Phi)$ involves the absolute square of this amplitude and an integration over all intermediate bound states in the spectrum of the theory. Therefore, the differential cross section can be written as

$$k'^0\frac{\mathrm{d}\sigma}{\mathrm{d}^3k'} = \frac{2}{\mathcal{F}(\Phi)}\ |\alpha_{\mathrm{g}}\Delta(k'-k)|^2\ \mathcal{E}^{\alpha\beta\mu\nu}(k,k')\mathcal{A}_{\alpha\beta\mu\nu}(\mathcal{B};k,k')\ . \tag{2.74}$$

Here $\mathcal{F}$ denotes the ingoing flux factor and Δ the scalar part of the graviton propagator. The emission tensor $\mathcal{E}$ captures the virtual graviton emission outside of the black hole, and the absorption tensor $\mathcal{A}$ its subsequent absorption by a black hole constituent. The emission tensor $\mathcal{E} \equiv Q \otimes Q$ is build from

$$Q^{\mu\nu} = 4\pi^2 \, \Pi^{\mu\nu\alpha\beta}(k' - k) \, G_{\alpha\beta\rho\sigma} \, \tfrac{k'^\rho k^\sigma}{k'^0 k^0} \; , \tag{2.75}$$

with the graviton polarisation tensor $\Pi_{\mu\nu\alpha\beta}(q) \equiv \pi_{\mu(\alpha}\pi_{\beta)\nu} - \pi_{\mu\nu}\pi_{\alpha\beta}$, where $\pi_{\mu\nu} \equiv \eta_{\mu\nu} - \frac{q_\mu q_\nu}{q^2}$ is the transverse projector, and k, k' the on–shell momenta of the ingoing and outgoing scalar emitter, respectively. Notice that expressing the amplitude in terms of $\pi_{\mu\nu}$ makes conservation of energy and momentum manifest.

Graviton absorption is described as the energy momentum correlation of black hole constituents:

$$\mathcal{A} = \tfrac{1}{2\pi} \int \mathrm{d}^4x \; \mathrm{e}^{-\mathrm{i}(k'-k)\cdot x} \langle \mathcal{B} | \mathcal{T}(x) \otimes \mathcal{T}(0) | \mathcal{B} \rangle \; . \tag{2.76}$$

Clearly, $\mathcal{A}$ contains information about the black hole interior, which is not yet resolved in terms of time ordered subprocesses. For practical calculations, $\mathcal{A}$ will be related to the corresponding time ordered amplitude in the next section.

Time Ordering

Given that the graviton absorption tensor is not directly subject to time ordering, the question arises whether it can be deconstructed into time ordered correlations. The method to achieve this is very well-known in the context of scattering processes on bound states in QCD and will be adapted to the problem at hand in the following discussion.

As a first step, let us relate $\mathcal{A}$ to a tensor built from $[\mathcal{T}(x), \mathcal{T}(0)]$. Inserting a complete set of physical states in between the energy–momentum tensors at x and 0 in (2.76), and making use of space–time translations, we arrive at

$$\mathcal{A} = \tfrac{1}{2\pi} \sum\!\!\!\!\!\!\int_{\mathcal{B}'} (2\pi)^4 \delta(q + P - P') \langle B | \mathcal{T}(0) | \mathcal{B}' \rangle \langle \mathcal{B}' | \mathcal{T}(0) | \mathcal{B} \rangle \; ,$$

with $q \equiv k - k'$, P and P' denoting the central momenta of wave–packets corresponding to ingoing and outgoing black hole quantum states, respectively. Standard kinematical arguments[21] allow to replace (2.76) with

$$\mathcal{A} = \tfrac{1}{2\pi} \int \mathrm{d}^4x \; \mathrm{e}^{\mathrm{i}q\cdot x} \langle \mathcal{B} | [\mathcal{T}(x), \mathcal{T}(0)] | \mathcal{B} \rangle \; . \tag{2.77}$$

Using the optical theorem, the absorption tensor (2.77) is determined by the absorptive part of the Compton–like amplitude $\mathcal{C}$ for the forward scattering of a virtual graviton off

[21] The argument works similar to the one used in QCD when studying deep inelastic scattering, see e.g. [72].

a black hole,

$$\mathcal{C} = \mathrm{i}\int \mathrm{d}^4x \mathrm{e}^{\mathrm{i}q\cdot x}\langle\mathcal{B}|\mathrm{T}\,\mathcal{T}(x)\otimes\mathcal{T}(0)|\mathcal{B}\rangle\ . \tag{2.78}$$

In order to see this, let us make the discontinuity of $\mathcal{C}$ manifest repeating the steps that allowed to extract the kinematical support of $\mathcal{A}$, leading to

$$\mathcal{C} = \sum\!\!\!\!\!\!\int_{\mathcal{B}'} \tfrac{(2\pi)^3\delta(\mathbf{P}'-\mathbf{P}-\mathbf{q})}{P'^0-P^0-q^0-\mathrm{i}\varepsilon}\langle\mathcal{B}|\mathcal{T}(0)|\mathcal{B}'\rangle\langle\mathcal{B}'|\mathcal{T}(0)|\mathcal{B}\rangle\ . \tag{2.79}$$

Defining $\mathrm{Abs}\,\omega^{-1} \equiv [(\omega-\mathrm{i}\varepsilon)^{-1}-(\omega+\mathrm{i}\varepsilon)^{-1}]/(2\mathrm{i})$, it follows that $\mathrm{Abs}(P'^0-P^0-q^0-\mathrm{i}\varepsilon)^{-1} = \pi\delta(P'^0-P^0-q^0)$ and hence,

$$\pi\mathcal{A}(\mathcal{B};q) = \mathrm{Abs}\,\mathcal{C}(\mathcal{B};q)\ , \tag{2.80}$$

which allows to deconstruct $\mathcal{A}$ in terms of time ordered correlation functions.

Constituent representation of $\mathcal{A}$

In this part we want to give a physical interpretation of the absorption tensor in terms of constituent observables.

The time–ordered product of energy–momentum tensors in $\mathcal{C}$ gives rise to three contributions: The first corresponds to maximal connectivity between the tensors, resulting in a purely perturbative contribution without any structural information. The second represents a disconnected contribution. Finally, the third contribution allows for perturbative correlations between the energy–momentum tensors and, in addition, carries structural information. Dropping the contributions which do not conatin any structural information,

$$\mathrm{T}\,\mathcal{T}_{\alpha\beta}(x)\mathcal{T}_{\mu\nu}(0) = \tfrac{1}{4}G^{ab}_{\alpha\beta}G^{mn}_{\mu\nu}\,C_{bm}(x)\,\mathcal{O}_{an}(x,0)\ ,$$

where $C(x) \equiv 4\langle\Omega|\mathrm{T}\,\mathrm{d}\Phi(x)\otimes\mathrm{d}\Phi(0)|\Omega\rangle$ denotes the perturbative correlation with respect to the vacuum,

$$C(x) = -\frac{2}{\pi^2}\frac{x^2\eta - 4x\otimes x}{(x^2)^3} \tag{2.81}$$

in free field theory, and $\mathcal{O}(x,0) \equiv :\mathrm{d}\Phi(x)\otimes\mathrm{d}\Phi(0):$ is the bi–local operator allowing to extract certain structural information when evaluated in a quantum bound state.

In order to extract local observables, $\mathcal{O}(x,0)$ has to be expanded in a series of local operators. In principle, this amounts to a Laurent–series expansion of the corresponding Green's function. Let us first focus on its Taylor part:

$$\Phi(x) = \exp\left(x\cdot\partial_z\right)\Phi(z)|_{z=0}\ . \tag{2.82}$$

The ordinary partial derivative is appropriate in the free field theory context, otherwise $\mathcal{O}(x,0)$ requires a gauge invariant completion. Then,

$$\mathcal{O}(x,0) = \sum_{j=0}^{\infty} \tfrac{1}{j!}\, \mathcal{O}^{[j]}(0)\ , \tag{2.83}$$

with $\mathcal{O}^{[j]}(0) \equiv :(x\cdot\partial_z)^j \mathrm{d}\Phi(0)\otimes \mathrm{d}\Phi(0):$. Note that we suppressed the space–time point x appearing in the directional derivative in order to stress the local character of the operator expansion.

The fast track to relate $\mathcal{C}$ to constituent observables is to evaluate $\mathcal{O}(x,0)$ in a black hole quantum state using the auxiliary current description. We find for the local operators

$$\langle\mathcal{B}|\mathcal{O}^{[j]}(0)|\mathcal{B}\rangle = \kappa\,(x\cdot P)^j\,\langle\mathcal{B}|\Phi(r)\Phi(0)|\mathcal{B}\rangle P\otimes P\,. \tag{2.84}$$

Here, κ denotes a combinatoric factor. Note that a simple point–split regularisation has been employed ($r^2\to 0$). The operator appearing on the right hand side of (2.84) measures the constituent number density. Alternativeley, we could decompose $\langle\mathcal{B}|\mathcal{O}^{[j]}(0)|\mathcal{B}\rangle$ into irreducible representations of the Poincaré group, i.e.

$$\langle\mathcal{B}|\partial_{\mu_1}\ldots\partial_{\mu_j}\partial_a\Phi\partial_b\Phi|\mathcal{B}\rangle = P_{(\mu_1}\ldots P_{\mu_j)}P_aP_b+\ldots\,, \tag{2.85}$$

where the brackets denote symmetrization and the terms indicated as $\ldots$ correspond to terms involving traces and are thus subleading in the limit $M\to\infty$. Keeping only the leading term, we again arrive at (2.84). Hence, the absorptive part of the forward virtual graviton scattering amplitude $\mathcal{C}$ or, equivalently, the graviton absorption tensor $\mathcal{A}$ can be directly interpreted in terms of the black hole constituent distribution. In other words, (2.84) already indicates that an outside observer is sensitive to the black hole interior in the framework of the auxiliary current description when measuring the scattered scalar.

Analytic properties of $\mathcal{C}$

The Ward–Takahashi identity associated with the underlying gauge symmetry fixes the tensorial structure $\theta_{\alpha\beta\mu\nu}(q,P)\equiv\Pi^{ab}_{\alpha\beta}\Pi^{mn}_{\mu\nu}\eta_{bm}P_aP_n$ of the amplitude $\mathcal{C}(q,P)$ in accordance with source conservation. The Laurent–series expansion of $\mathcal{O}(x,0)$ in local operators gives to leading order up to $\mathcal{O}(q\cdot P/P^2)$

$$\mathcal{C}(q,P) \;=\; \langle\mathcal{B}|\Phi(r)\Phi(0)|\mathcal{B}\rangle\;\theta(q,P)\;\tfrac{-\mathrm{i}}{2\pi^2}\sum_{j=-\infty}^{\infty} C_j(q)u^j\ . \tag{2.86}$$

Here the coefficients C_j are calculable and turn out to be momentum independent, and the expansion parameter $u\equiv -P^2/q^2\gg 1$. Note that this parameter is the analogue of the inverse Bjorken scaling variable known from deep inelastic scattering. There is a profound difference between these two parameters, however. While in standard discussions of deep inelastic scattering in the infinite momentum frame one makes use of asymptotic freedom,

this is not possible in gravity. For the problem at hand, however, there is a natural limit and correspondingly an appropriate expansion parameter. Namely, considering black holes of large mass and momentum transfers smaller than $M_{\rm P}$ (which is needed in order to trust the perturbative expansion) we are naturally lead to the expansion parameter u.

The discontinuity of $\mathcal{C}$ for fixed $q^2 = -Q^2$ is at

$$u_* = \frac{M_{\mathcal{B}}}{2(M'_{\mathcal{B}} - M_{\mathcal{B}})} \left(1 - \frac{M'^2_{\mathcal{B}} - M^2_{\mathcal{B}}}{Q^2}\right) \gg 1 \ . \tag{2.87}$$

So $\mathcal{C}$ has an isolated pole at $u_* \gg 1$ and, in particular, no branch cut to the leading order, corresponding to the statement that $M'_{\mathcal{B}}/M_{\mathcal{B}} - 1 \approx 0$. Notice that this condition implies that we are neglecting the effect of back reaction on the state $|\mathcal{B}\rangle$ due to the scattering process. Of course, the presence of a branch cut beyond leading order poses no obstacle. On the contrary, it has an evident interpretation in terms of intermediate black hole excitations.

In order to project onto the Laurent–coefficients, a path enclosing $[-u_*, u_*] \subset \mathbb{R}$ in the complex u plane has to be chosen. This covers the physical u region, while the radius of

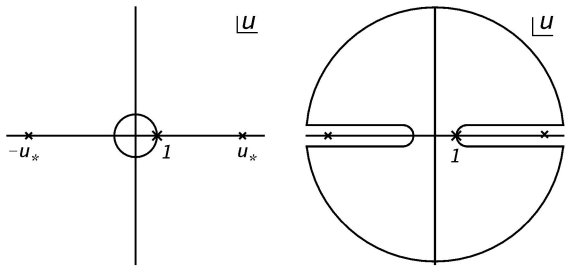

Figure 2.9: Integration contour in the complex u-plane. The left figure displays an integration contour corresponding to the radius of convergence. In order to relate this to the physical u-region ($P^2 > Q^2$) we perform a contour deformation (right figure). The radius of the circle is sent to infinity.

convergence of the corresponding Taylor series would only allow for unphysical $u \in [-1, 1]$ (see Figure 2.9). We find

$$\int_0^1 \mathrm{d}\zeta \ \zeta^{k-2} \mathcal{A}(q, P, \zeta) = \frac{C_{k-1}}{4\pi^2} \ \langle \mathcal{B}|\Phi(r)\Phi(0)|\mathcal{B}\rangle \ \theta(q, P) \ , \tag{2.88}$$

with $\zeta \equiv 1/u$ denoting the graviton virtuality relative to the black hole target mass. Hence, all moments of the absorption tensor with respect to ζ are directly proportional to the constituent distribution inside the black hole. This implies that $\mathrm{d}\sigma/\mathrm{d}^3k' \propto \langle \mathcal{B}|\Phi(r)\Phi(0)|\mathcal{B}\rangle$. Thus, black hole constituent distributions are observables that can be extracted from scattering experiments. In particular, in the limit of infinite black hole mass, the cross section is determined only by the $k = 2$ moment. Note that in contrast, for small mass of the bound state, one would need much more information (i.e. more moments) to properly reconstruct the cross section. Thus, we again see that the limit of large black hole mass greatly simplifies our problem.

2.2.6 Schwarzschild Solution from Tree-level Scattering

Having shown that within the auxiliary current construction it is indeed possible for an outside observer to probe the black hole interior, we shall now explain how geometry emerges from our description. Before discussing the full quantum description of the black hole, let us first review the semi-classical approach leading to a reconstruction of the Schwarzschild solution in terms of tree-level processes on flat space-time [67]. The basic idea is to compute the expectation value of metric fluctuations around Minkowski space-time in the presence of a classical massive background source. In pure gravity without including couplings to any stabilizing forces this source collapses under its own gravitational attraction. Assuming spherical collapse, the energy-momentum tensor can be taken as

$$T^{\mu\nu}_{\text{class}}(t,r) = \rho(t)\delta^{\mu}_{0}\delta^{\nu}_{0}\Theta(r_g(t)-r)\,, \tag{2.89}$$

where $\rho(t) = 3M/(4\pi r_g^3(t))$ denotes the energy density of the source of radius $r_g(t)$. As a consequence of the collapse, we can think of the final state of the source as a classical Schwarzschild black hole of fixed radius r_g. Since in this article we will only be interested in the metric produced by this final state, we will simply refer to the source as a static Schwarzschild black hole.

The question Duff addresses in [67] is how the Schwarzschild metric emerges from the tree-level S-matrix on flat space-time without referring to any geometric concepts. For that purpose one can decompose the metric as $g_{\mu\nu} = \eta_{\mu\nu} + \sqrt{16\pi G}h_{\mu\nu}$ with G the Newton constant and compute the vacuum expectation value of the fluctuation $h_{\mu\nu}$ in the presence of the classical black hole source:

$$\langle\Omega|h_{\mu\nu}|\Omega\rangle_T = \frac{\langle\Omega|\mathrm{T}\left[h_{\mu\nu}S_T\right]|\Omega\rangle}{\langle\Omega|S_T|\Omega\rangle}\,. \tag{2.90}$$

Here S_T denotes the S-matrix with interaction Lagrangian $\mathcal{L} \propto h_{\mu\nu}T^{\mu\nu}_{\text{class}}$. Expanding (2.90) leads to the diagrammatic expansion given in figure (2.10). Notice that we only display the leading order diagrams. The first diagram corresponds to the Newtonian approximation, while higher order tree-level diagrams give non-linear corrections. These diagrams include graviton self-couplings as well as multiple interactions between virtual gravitons and the black hole. For a more detailed discussion we refer the reader to the original work [67].

Deriving the expectation value, one can show that the fluctuations can be expressed in terms of the potential

$$V(x) = 4\pi G\int \mathrm{d}^4k \frac{\mathrm{e}^{\mathrm{i}kx}}{k^2}\tilde{T}_{00}(k)\,, \tag{2.91}$$

where $\tilde{T}_{00}(k)$ denotes the Fourier transform of the 00-component of the energy-momentum tensor given in (2.89). In particular, in de Donder gauge, the expectation values of the fluctuations to second order can be expressed in terms of the potential in the following

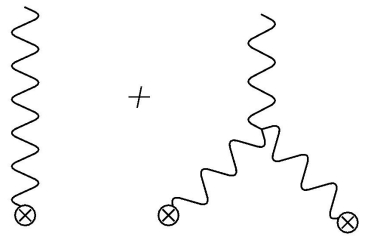

Figure 2.10: Leading order tree-level Feynman diagrams representing the metric produced by a classical source. The wiggly lines correspond to gravitons and the crosses display the classical background source.

way:

$$\begin{aligned}\kappa\langle h^{ij}\rangle_T &= \left(2V + \frac{4}{\nabla^2}\eta_{kl}\partial^k V\partial^l V\right)\eta^{ij} + \frac{4}{\nabla^2}\partial^i V\partial^j V \\ \kappa\langle h^{00}\rangle_T &= 2V - \frac{4}{\nabla^2}\eta_{kl}\partial^k V\partial^l V - \frac{8}{\nabla^2}V\nabla^2 V\ .\end{aligned} \tag{2.92}$$

Here $\kappa \equiv \sqrt{16\pi G}$, ∇^2 is the Laplace operator and $\langle A\rangle \equiv \langle\Omega|A|\Omega\rangle$ for any operator A. Let us already mention at this point that all the information about the metric fluctuations produced by the black hole is encoded in the potential which is evident from equation (2.92). This will become important later in the quantum analysis of the source.

From (2.92) it, indeed, follows that one correctly reproduces the Schwarzschild metric to this order:

$$\begin{aligned}\langle g^{00}\rangle &= -1 - \frac{r_g}{r} - \frac{r_g^2}{2r^2} \\ \langle g^{ij}\rangle &= \left(1 - \frac{r_g}{r} - \frac{3r_g^2}{4r^2}\right)\eta^{ij} - \frac{r_g^2}{4r}\frac{x^i x^j}{r^2}\ .\end{aligned} \tag{2.93}$$

Thus, even at this level one can see that geometry which is usually considered as fundamental in general relativity can be viewed as an emergent phenomenon encoded in the effective field theory of a massless spin 2 particle coupled to a classical source on flat space-time. In what follows, we will go a step further and propose a quantum treatment of the source based on the auxiliary current description as well.

Quantum Meaning of the Source

Having outlined the basic construction which allows to represent a black hole quantum mechanically in terms of constituent gravitons in earlier sections, we shall now address the question how to define the energy-momentum source of the black hole in our approach.

Representing the black hole as a quantum state, it is clear that within our formalism the concept of a classical source can only emerge in an appropriate limit (to be defined below). Fundamentally, however, a resolution of the black hole immediately implies that the source should be described by an observable represented by an operator evaluated in the corresponding black hole state.

Since in our approach the black hole is a bound state of N gravitons, this observable should be the energy-momentum tensor of individual gravitons constituting the quantum state of the black hole. Thus, in the quantum theory we should replace the classical energy-momentum tensor from equation (2.89) with fixed radius and energy density:

$$T^{\mu\nu}_{\text{class}}(x) = \rho\delta^\mu_0\delta^\nu_0\Theta(r_g - r) \to \langle B|T^{\mu\nu}(x)|B\rangle \ . \tag{2.94}$$

Here $T_{\mu\nu}$ is the energy-momentum tensor of gravitons inside the black hole,

$$T_{\mu\nu}(x) = \frac{1}{2}S_{\mu\alpha\nu\beta}\partial^\alpha h(x)\partial^\beta h(x) \ , \tag{2.95}$$

where we defined $S_{\mu\nu\alpha\beta} = \eta_{\mu\alpha}\eta_{\nu\beta} + \eta_{\mu\beta}\eta_{\nu\alpha} - \eta_{\mu\nu}\eta_{\alpha\beta}$. Notice first that this is exactly the energy-momentum tensor which have already computed to leading order in $1/N$ and at the parton level in section (2.2.3). Here, we will go a step further and also take effects due to the finiteness of the black hole mass into account. Furthermore, such a replacements also suggests that the effective coupling of gravitons to the source described by the interaction Lagrangian needs to be modified in the same way. In other words, the effective quantum coupling is given by $\mathcal{L}_{\text{eff}} \propto h_{\mu\nu}\langle B|T^{\mu\nu}|B\rangle$. This expression makes it clear that possible new quantum effects due to the bound state structure appear at all orders in Newton's constant. Therefore, we truly consider quantum features beyond semi-classicality. We shall discuss these new corrections in detail below.

Using the auxiliary current representation of the black hole state $|B\rangle$ (see equation (2.7)), the energy-momentum tensor can be evaluated explicitly. For black holes of large mass M, we can use this mass as an expansion parameter. Keeping terms up to order M_B^{-2} we arrive at the following result (for details the reader is referred to the appendix):

$$\begin{aligned}\langle B|T_{\mu\nu}(x)|B\rangle &= \delta^0_\mu\delta^0_\nu|\mathcal{B}(x)|^2\left(1 - \frac{4}{M^2}f(x)\right) \ ; \\ f(x) &= \left(\left(\partial_{z_0}\partial_{y_0} - \partial^2_{z_0} - \partial^2_{y_0}\right)\frac{\langle h^{N-1}(z)h^{N-1}(y)\rangle}{\langle h^{2N-2}(0)\rangle}\right)\Bigg|_{y,z=x} \ .\end{aligned} \tag{2.96}$$

Let us now explain the physical meaning of this result in detail.

First of all, one can see that for infinite M only the 00-component is non-vanishing[22]. This is expected, because in this limit, the source must be dominated by the energy density of the constituent gravitons. Secondly, one can see that the subleading terms consist of

[22]Note that for any large, but finite M, also the off-diagonal components contribute. In order to focus only on the most relevant aspects, we will not take these components into account (though we will consider finite mass effects in the 00-component).

a ratio of condensates. These condensates parametrize the non-trivial collective potential individual gravitons experience in the presence of all other gravitons in the black hole. Notice that this condensate structure can only be uncovered in a microscopic description of the black hole interior. For a more detailed discussion on the physics of these graviton condensates, we refer the reader to the previous sections. Finally, the wave function of the black hole in configuration space $\mathcal{B}(x)$ enters in the expression for the energy density. Since we are working in a quantum theory this is not surprising. Rather, such a dependence could have been anticipated on physical grounds solely. We will have to say more about the physical significance of this wave function concerning the reproduction of geometry as well as corrections to it in the next section.

2.2.7 Emergence of Geometry

Using the result for the energy-momentum tensor of constituent gravitons inside the black hole, we will now explain how to make contact to general relativity. Furthermore, we will discuss the physics of the new type of quantum corrections (condensate terms) which arise in our approach. In particular, in the first subsection we show how our result consistently reproduces Duff's description of the emergence of space-time geometry to leading order. Following this discussion we will analyze the physical significance of quantum corrections which appear as inverse powers of M.

Newton Potential and Schwarzschild Metric

Before discussing quantum corrections, let us explain how our formalism consistently accounts for classical results. Notice that the classical limit effectively amounts to taking $M \to \infty$, because only in that case one can strictly neglect backreaction. Therefore, the energy density can be taken as $\langle B|T_{00}(x)|B\rangle = |\mathcal{B}(|\mathbf{x}| = r)|^2$. Note that the dependence on the spatial distance only follows as a consequence of the isometries of the problem and Ward's identity as explained above. Before discussing the non-linear structure revealed in Duff's computation, let us for simplicity first demonstrate how Newton's potential emerges from our description. Using equation (2.91), the potential can be written as

$$V(r) = 4\pi G \int \mathrm{d}^3k \frac{\mathrm{e}^{\mathbf{ikr}}}{\mathbf{k}^2} \widetilde{|\mathcal{B}(\mathbf{k})|^2} \,, \tag{2.97}$$

where $\widetilde{|\mathcal{B}(\mathbf{k})|^2}$ denotes the Fourier transform of $|\mathcal{B}(x)|^2$. Notice that the wave function should be localized on the support of the source. Taking the Newtonian limit, $r \gg r_g$, we can effectively neglect finite size effects of the wave function profile. This amounts to the replacement

$$|\mathcal{B}(r)|^2 \to \frac{M_B}{4\pi r^2}\delta(r) \,. \tag{2.98}$$

Thus, we recover the usual Newtonian potential, $V(r) \propto r_g r^{-1}$ in this limit.

In order to make contact with Duff's computation, we should take the finite extension of the source into account. Notice that in the limit $M_B \to \infty$, this leads to the replacement

$$|\mathcal{B}(r)|^2 \to \rho\Theta(r_g - r) \; . \tag{2.99}$$

Obviously, in that case, we trivially recover all results of Duff simply performing the steps explained in section 2.

Let us explain in more detail why the replacements (2.98) and (2.99) are justified starting from the quantum point of view. Due to the uncertainty relation, taking a δ- or Θ-function source must correspond to an idealized limit. Let us try to understand the physical meaning of this idealized situation. First of all, we consider a very massive black hole. As a consequence, the de-Broglie wavelength is much smaller than the Planck length. In turn, this tells us that the wave function must be localized on the Schwarzschild radius of the black hole with uncertainties smaller than the Planck length l_p. Since $l_p \ll r_g$, these uncertainties can be neglected to leading order. Furthermore, as explained above, if one considers the potential at distances $r \gg r_g$ we can neglect the extension of the source. Thus, there are well-defined limits, in which the quantum description of the source reduces to θ- as well as δ-functions, respectively.

Note that in principle, we could also simply rely on Birkhoff's theorem. Since also the quantum version of the source respects spherical symmetry and couples to all matter democratically, one can already anticipate from these facts that the only consistent metric which can be produced in our description is the Schwarzschild geometry.

To summarize, we can see that our formalism is capable of reproducing the known classical, geometric properties of black holes from an underlying quantum theory of black hole bound states on flat space-time to leading order.

Quantum Corrections

Having discussed how classical geometric concepts emerge from the auxiliary current approach to black hole physics, we will now go a step further and discuss quantum corrections to it. As explained before, these effects are beyond semi-classical reasoning. As shown above, they arise as a consequence of the quantum structure of the black hole. Indeed, from equation (2.96) it is clear, that these effects are due to the finiteness of M, or, equivalently, due to the finiteness of N.

The question which we want to address now is how these corrections can be interpreted physically. First of all, there is a standard uncertainty due to the wave function of the black hole appearing in (2.96). Secondly, the corrections in M^{-2} always appear in combination with $|\mathcal{B}(x)|^2$. Note that the condensates in $f(x)$ explicitly depend on the space-time location. Indeed, the space-time dependence has the natural interpretation of a wave function renormalization. This becomes even more transparent if we think about this correction in Fourier space. The derivatives appearing in equation (2.96) as well as the space-time dependence of the condensates translate into an energy scale dependence of the effective energy momentum tensor. This can be absorbed into a redefinition of the black hole wave function.

In contrast to the standard running which is induced by quantum loops on top of a background, the renormalization of the wave function found here is ultimately related to the bound state structure of the black hole. Thus, we are uncovering a novel effect which can not be accounted for in any semi-classical approach. In other words, on top of the usual semi-classical expansion leading to exponentially suppressed quantum corrections which also renormalize the wave function, we find a second source of quantum effects which are only suppressed as inverse powers of M. Thus, in the full quantum treatment, there are two independent expansion parameters, the gravitational coupling in a given background on the one hand and the finiteness of N on the other hand.

Let us say a few more words on the meaning of wave function renormalization due to compositeness of the black hole. Just as in standard renormalization, we need to introduce a new parameter, in our case the ratio of condensates. This ratio can then be understood as the analogue of the renormalization constant needed to define perturbation theory at loop level. Just as in this case, the condensate ratio has to be measured at a given scale. Having performed such a measurement, predictions can be made in terms of the renormalization group evolution of the wave function. Notice that since the wave function of the black hole depends on M, this running can naturally be interpreted as a running of the black hole mass.

As a consequence of this running, there will be corrections to the Newtonian potential as well as the Schwarzschild metric depending on the distance at which we are probing the black hole. In other words, since the potential can be expressed in terms of the energy density, the quantum effects which we are uncovering translate directly into an effective quantum corrected potential. Thus, to leading order in r/r_g we find departures from Newton's force law! In addition, since non-linear effects can always be expressed in terms of this corrected potential, our results implies that also geodesics and related non-linear effects will receive the same type of corrections.

To summarize this section: We saw that a quantum resolution of a black hole source necessarily leads to novel quantum effects which can not be discovered in the standard semi-classical approach. While there is a well-defined limit which allows us to recover classical geometry as an emergent phenomenon, quantum corrections lead to novel effects such as running of the black hole mass. In turn, the correction can be absorbed in terms of a quantum corrected Newtonian potential. Since this enters also at the non-linear level, we find that the auxiliary current description naturally leads to deviations from predictions of general relativity in terms of $1/M^2$-effects.

2.2.8 Summary and Outlook

In this section we want to briefly recapitulate our construction which allows for a representation of bound states in terms of elementary fields and our major findings in the field of black hole physics. Furthermore, we will give an overview over new possible research directions.

Our proposal was motivated by ideas first put forward in [23]. In order to realize these ideas field theoretically, we suggested to represent black holes (or other solutions of

general relativity or other field theories) in terms of so-called auxiliary currents. These are local, composite operators constructed from the fields appearing in the fundamental, microscopic action. In addition, the field content of the current has to be chosen in a way which is compatible with the quantum numbers of the true state one wants to study. Having constructed such a current one can compute observables connected to the state one is interested in.

In the case of a black hole, we calculated the light-cone distribution and energy density of gravitons in the black hole. We restricted our analysis mostly to infinitely massive black holes and non-interacting gravitons. The results are nevertheless non-trivial. The reason is that despite the fact that gravitons are weakly interacting individually, they experience a large collective effect due to the mean-field created by the other gravitons. This mean-field was modeled in terms of non-vanishing vacuum condensates. We found that consistency of our results in the large mass limit inevitably suggests that we should take $N \to \infty$ at the same time with M/N fixed. Having computed the energy density and constituent density further allowed to relate the mass directly to the number N. In particular, we found $M \propto N$ with the constant of proportionality determined by a ratio of large N vacuum condensates of gravitons. Since we expect that at the parton level physical quantities should scale extensively with the number of fields, this condensate ratio could be identified with the typical energy of individual constituents of the black hole. Subsequently, we argued how higher order corrections can be taken into account in a gauge invariant way. Although we illustrated the construction by computing a specific higher order diagram, a systematic study of corrections to the parton level result remains to be done in future work.

In the following, it was shown how the constituent density can be embedded naturally in to the S-matrix. Considering the scattering of a probe particle on a black hole resolved in terms of gravitons, we explicitly showed that the differential cross section can be expressed directly in terms of this distribution. Note that this result could have some profound implications. It demonstrates that an outside observer actually has access to the black hole interior by measuring the scattering angle of the probe scalar. This result directly sheds a new light on the semi-classical black hole mysteries such as the no-hair theorems or the information paradox. Indeed, since an outside observer has access to the internal structure of the black hole, no loss of information is expected.

Finally, we explained how classical concepts such as a metric description emerge as a simple consequence of our framework. Indeed, since the black hole is understood as a bound state of gravitons, the energy and momentum that it sources must be understood as a collective effect of these gravitons. In turn, at the quantum level, the black hole source should be replaced by the energy-momentum sources of individual gravitons. We explicitly showed that to leading order in $1/N$ this construction guarantees an effective metric description. Furthermore, we explained that for finite mass, there are corrections to the metric description which have the natural interpretation of a black hole wave function renormalization. These corrections are intrinsically related to the bound state structure of the black hole and appear to all orders in Newton's constant. As such, any semi-classical treatment can never uncover these effects.

Having summarized our major findings, let us now discuss possible applications of the

auxiliary current construction which should be studied in the future. Of course, the list is not exhaustive. Rather, it summarizes current research directions of the author.

- Higher order corrections:

  We already explained how higher order corrections can be included and exemplified our ideas by calculating a specific diagram. It would be important to study a wider class of diagrams. In particular, the effect of curvature condensates might become important if the whole tower of diagram is included.

- Hawking radiation and Black Hole Entropy:

  Hawking radiation within our approach should be understood in terms of scattering processes. Intuitively, one should consider processes of the type $\langle \mathcal{B}', k_1, \ldots, k_j | \mathcal{B} \rangle$, where $|\mathcal{B}\rangle$ and $|\mathcal{B}'\rangle$ denote the black hole state before and after evaporating j Hawking quanta with momenta $k_1, \ldots, k_j$, respectively. Note that $j = 1$ should correspond to the leading process giving rise to a thermal spectrum in the semi-classical limit (compare to Figure (1.3.2)) in the context of the Black Hole Quantum N Portrait. Corrections to this result should be of order $1/N$ due to combinatorics and higher order diagrams.

  A question closely related to the emergence of Hawking radiation is the one of the microscopic origin of black hole entropy. Notice that whenever we used the auxiliary current description to represent a black hole as a bound state of gravitons, we restricted ourselves to a specific microstate. In order to take different microscopic realizations of a given macroscopic black hole state into account, one could modify the framework in such a way that one represents the true quantum state in term of density matrices. Such a construction would amount to constructing a density operator in terms of graviton field operators in such a way that its overlap with the black hole density matrix is non-vanishing in an appropriate operator norm. Whether such a description is feasible on the one hand, and if it is, whether it can account for the entropy of the black hole on the other hand, remains to be seen.

- Multiple graviton exchanges:

  In our discussion concerning the scattering of a scalar on the black hole state, we restricted our analysis to the one-graviton exchange amplitude. Of course, the chosen approximation was sufficient to demonstrate the conceptual point that an outside observer can access the interior of the black hole. Nevertheless, a proper description might requires multiple graviton exchanges to be included in the computation. In other words, making again contact to the Black Hole Quantum N Portrait, one could consider the scattering for fixed size of the bound state as a function of the effective coupling αN. Then, according to the N Portrait, something special should happen

at $\alpha N = 1$, i.e. when the probe scatters on a full-fledged black hole. From the point of view of QFT, such a point might be identified with a critical point of the flow of the distribution of gravitons as a function of αN. Such a behaviour of the flow equation would then have the natural interpretation of graviton saturation, i.e. at that point the rate for graviton splitting and recombination balance each other. This phenomenon would then resonate with the ideas of the N Portrait, namely that a black hole represents a maximally packed system of gravitons. Let us mention that these statements are motivated by an observation made in QCD. If one considers scattering of a probe on a hadron at fixed momentum transfer larger than the QCD scale, but at high energies, one finds that an infinite tower of diagrams, the so-called BFKL ladder diagrams need to be resummed [64, 65]. These diagrams involve the exchange of intermediate gluon lines. One can then show that there is a critical energy at which the distribution of gluons inside a hadron is saturated. In other words, there is a critical point in the flow equation at which any hadron basically looks like a dense state of gluons.

Of course, at this point it is rather speculative whether a similar phenomenon can be observed in gravitational scattering. Nevertheless, we think that it is worth investigating this question. If one really finds such a behaviour, one could give a non-perturbative field theoretical definition of a black hole as a state at the point of graviton saturation.

- Applications to other space-times:

In the last chapter we explained how our approach can in principle be applied to other space-times. Possible applications of the framework which are of immediate interest include dS as well as inflationary backgrounds. On the one hand, reproducing known results at leading order in $1/N$ would be an important theoretical test of our methods. On the other hand, possible deviations might be relevant for CMB physics or the mystery of the cosmological constant.

Chapter 3

Coherent State Formulation of Classical Solutions

Having discussed the auxiliary current construction and its applications to black hole physics in detail, we now wish to introduce another possible theoretical framework which allows to replace classical solutions by composite quantum systems. The main idea is to represent the classical solution as the expectation value of the field operator in a coherent state constructed from number eigenstates of particles constituting the object we want to study. As we shall explain in detail, in order to represent the quantum version of the classical profile, these particles must be fully interacting. As a consequence, the quanta should not be confused with the free, propagating particles of the theory under consideration. Therefore, in what follows, we shall call the particles constituting the classical solution corpuscles. In order to give a self-contained presentation, we will first of all explain our general strategy which is based on representing classical solutions in terms of coherent states. The following sections are devoted to explicit applications of our proposal. In particular, in the the second section, the coherent state picture is applied to solitons within field theory. We start by explaining the basics of the coherent state approach to soliton physics in detail. We identify which quanta contribute to the topological charge of the soliton on the one hand, and which quanta account for its energy on the other hand. We then proceed and argue that a coherent state quantization of a soliton immediately implies that a similar coherent state picture must be applied to instantons as well in the next section. The reason is that an instanton can always be understood as a higher-dimensional soliton evolving in Euclidean time. This correspondence is developed in detail for various examples such as topological and non-topological instantons in quantum mechanics, Polyakov-type instantons and instantons in Yang Mills theory. Having identified the quantum structure of an instanton, we argue that the concept of resurgence follows as a simple consequence of the unitarity of the S-matrix. Finally, in the fourth section, we apply our construction to solitons in supersymmetric theories. It is shown that due to corpuscular corrections, the BPS condition can never be fulfilled. Therefore, supersymmetry is inevitably broken in the presence of solitons. This program is explicitly carried out in the case of a Wess-Zumino model in $1+1$ dimensions. Our results, however, should be more general. Indeed, similar

effects of supersymmetry breaking are also expected in the case of other objects which are classically BPS saturated such as the Yang Mills instantons.

Finally, in the fifth section, we again turn to gravity and apply our reasoning to AdS space-time. We start by discussing how well-known holographic and geometric properties of AdS can be understood easily in terms of the corpuscular language to leading order. As a next step, we turn our attention to higher order quantum corrections due to the compositeness of AdS. It turns out that, when considered as a coherent state, there are corpuscular corrections to observables which scale as the typical inverse number of corpuscles. We explicitly compute these corrections for the scalar propagator in an AdS space-time and show that the corpuscular corrections lead to deviations from thermality of the spectrum an Unruh observer in AdS measures. This result suggests that a similar corpuscular breaking of thermality happens in black hole radiation which could be the key for purification of Hawking radiation.

3.1 The Proposal

Hystorically, coherent states were first introduced by Schrödinger as states of the quantum mechanical harmonic oscillator which minimize the uncertainty relation. Therefore, the coherent states are the quantum states which are closest to being classical, i.e. evaluated in a coherent state the dynamics of the quantum oscillator is closest to its classical counterpart. The first systematic study of the properties of coherent states was performed by Glauber [73]. His aim was to study classical electric fields using coherent states.

Let us now explain quantitatively in what sense we propose to resolve solutions in field theory quantum mechanically using coherent states. For that purpose consider a generic classical solution $\phi_c(x)$ in a QFT in $d+1$ space-time dimensions. Notice that we can always expand any such solution in a Fourier basis in Minkowski space-time,

$$\phi_c(x) = \int \frac{d^d x}{\sqrt{(2\pi)^d 2\omega_k}} (\alpha_k e^{ikx} + \text{h.c.}), \tag{3.1}$$

where α_k are classical expansion coefficients, h.c. denotes the hermitian conjugated (complex conjugated at the classical level) and ω_k is the dispersion relation whose form is dictated by the equation of motion ϕ_c obeys classically. Had we started from a free theory, on-shell quantization of the field would amount to replace the classical Fourier coefficients by creation and annihilation operators fulfilling $[\hat{a}_k, \hat{a}_p^\dagger] = \delta^d(k-p)$. Notice, however, that such a quantization prescription holds in more general situations. In particular, as a starting point of our approach, we want to promote the classical field ϕ_c which in general solves a non-linear field equation to a quantum operator. Then, the $\hat{a}_k$ and $\hat{a}_k^\dagger$ have the natural interpretation of operators annihilating/creating corpuscles inside the would-be classical solution. So far, we did not specify how we want to represent this quantum operator in terms of coherent states. From our previous discussion it is clear that the coherent state $|\text{coh}\rangle$ should be constructed in such a way that we reproduce the classical solution when we evaluate the field operator corresponding to that solution in the coherent state. This

requirement immediately fixes the form of the coherent state. In particular, since the coherent state should be an eigenstate of the annihilation operator, i.e. $\hat{a}_k|\text{coh}\rangle = \alpha_k|\text{coh}\rangle$, we find

$$|\text{coh}\rangle = \prod_k e^{-N_k/2} \sum_{n_k} \frac{N_k^{n_k/2}}{\sqrt{n_k!}} |n_k\rangle \tag{3.2}$$

with $\alpha_k = \sqrt{N_k}$ and $\hat{a}_k^\dagger \hat{a}_k |n_k\rangle = n_k |n_k\rangle$. Thus, the $|n_k\rangle$ are eigenstates of the number operator of corpuscles inside the field of momentum k. Notice that we used a notation for the classical Fourier coefficients which makes our corpuscular picture more transparent. Classically, α_k denotes the amplitude (square root of the intensity) of the field in the mode k. In a quantum theory, the intensity is most naturally replaced as the density of particles in the given mode. Therefore we adopt the notation N_k. Notice that the coherent state (3.2) represents a distribution of occupation numbers in different modes weighted with a prefactor $\prod_k e^{-N_k/2} \frac{N_k^{n_k/2}}{\sqrt{n_k!}}$. Now assume that the classical solution is characterized by some lengthscale L. Then it is natural to expect that the peak of the distribution is set by exactly that scale. Indeed, we will show that this is true in the case of solitons and instantons. To be more precise, it will be shown that the corpuscles contributing most to the energy of the soliton (Euclidean action of the instanton) are those which occupy the mode $k = L^{-1}$. We will in particular argue that one needs to distinguish between those quanta and the ones accounting for the topological charge which correspond to infinite wavelength corpuscles.

So far the reader might wonder how corrections to classical results are obtained. Indeed, so far we only explained how our construction guarantees the correct classical results. The origin of quantum corpuscular corrections are actually encoded in higher point correlation functions. Consider for example an operator of the form ϕ_c^N, $N \geq 2$. Expanding the operator acccording to (3.1) and evaluating in (3.2) the quantum corrections are simply encoded in the ordering of the creation and annihilation operators[1]. Thus, the corpuscular effects originate in the non-trivial commutation relations of the corpuscular creation and annihilation operators. Subsequently, these effects naturally occur at order $\hbar/N_{L^{-1}}$. Therefore the corpuscular corrections simply parametrize deviations from the mean-field which by construction is given by the classical solution.

3.2 Quantum Theory of Solitons - Topology and Energy

In this section we develop a dictionary that allows to replace solitons in terms of coherent states. A careful distinction is made between the corpuscles carrying information about

[1] As we will discuss in the context of scattering on AdS in the next section, there can be quantum corrections to the one point function if we take backreaction on the background due to non-trivial momentum transfer into account.

the topology on the one hand, and the corpuscles determining the configuration's energy. Subsequently, we give a microscopic definition of topological charge in terms of the former quanta and energy in terms of the latter. Using simple examples such as kinks, we demonstrate that the quantum mechanical explanation of the conservation of topological charge is encoded in an infinite occupation of infinite wavelength topological corpuscles. Thus, topological charge emerges as the momentum flow of these quanta at the quantum level. In order to give a self-contained presentation, we confront the quantum portrait of the topological kink with the one of a non-topological soliton in a slightly deformed theory. We shall find that, while the quanta accounting for the energies of the two configurations are rather similar, no infinite occupation of zero momentum corpuscles is found in the case of the non-topological soliton. On the one hand, this gives a microscopic explanation of the fact that the non-topological soliton has zero topological charge. On the other hand, the finiteness of the occupation number leads to the possibility of decay of the vacuum via bubble nucleation. We further investigate consistency of our approach by studying the kink-anti-kink system. It is shown, how the standard result for the interaction energy is reproduced in terms of matrix elements on the one hand, and by defining a corpuscular Hamiltonian on the other hand. The computations do not rely on the notion of classical Lagrangian, but are instead consequences of the coherent state formulation of solitons.

3.2.1 Motivation

From the very early days of soliton physics it has been suspected that quantum solitons should be thought of as some sort of quantum coherent states. As quantum coherent states they are many quanta systems with an average number of quanta N that scales as the inverse of the relevant coupling. Therefore, in the strong coupling regime this picture of the soliton as a quantum coherent state looses its meaning and we are forced to think of the quantum soliton as a fundamental particle of a potential dual theory. This is, for instance, the case in two dimensions, where Thirring fermions are the strong coupling version of Sine Gordon solitons [74, 75]. In this case what we identify as topological charge in the weak coupling, becomes simply fermion number in the strong coupling.

An obvious difficulty in identifying the quantum soliton state lies in understanding the quantum meaning of the topological charge that is normally introduced in purely classical terms. In the weak coupling, where we expect to have a good quantum coherent state representation of the soliton, it is *a priori* not clear how to distinguish the quanta accounting for the topological charge from those that account for the energy.

Intuitively it is clear that, if solitons were to admit some quantum coherent state description, the dominant contribution to the energy should come from the constituents of the wavelength comparable to the Compton wavelength (m^{-1}) of the quanta of the theory, with their mean occupation number scaling as inverse of the coupling. At the same time, we should expect that a very different type of quanta is responsible for the topology. Indeed, making contact to the classical picture, this can already be anticipated when remembering that topological charge is encoded in the boundary conditions at spatial infinity. Thus, within the quantum description, one could expect that the quanta accounting for the

topological charge should be aware of the global structure. Those quanta are the ones which have infinite wavelength.

In the present paper, we shall clarify this distinction by developing a coherent state picture of topological and non-topological solitons in $1+1$-dimensional theory. We shall follow the general strategy outlined in [76], in which the coherent state is constructed by using the classical Fourier-expansion data of the soliton. However, we shall carefully identify and separate topological and energetic ingredients.

We show that the contribution to the soliton mass indeed comes from the quanta of wavelength $\sim m^{-1}$ with the mean occupation number given by the inverse coupling. At the same time, we observe that the origin of the topological charge is dramatically different. Namely, it comes from the *infinite* wavelength quanta with the net momentum flow in one direction. The occupation number of these topology-carriers is *infinite*. In other words, the mean-occupation number of the coherent state constituents, N_k, as a function of momentum k exhibits a pole in zero momentum limit, $N_{k\to 0} \sim 1/k$. This divergence in the occupation number of infinite wavelength quanta with net momentum flow is the quantum origin of topology. We can think of it as a *Bose sea* of such quanta.

The conservation of the topological charge then trivially follows from the basic properties of coherent states. Namely, from the property that the projection of an infinite occupation number coherent state on any finite-number state vanishes. Due to this, the topological soliton has zero overlap with any state from the topologically-trivial vacuum sector, since such states have no singularities in net occupation numbers[2].

This divergence is absent for non-topological solitons, and correspondingly their overlap with the vacuum is non-zero, but exponentially small. This overlap can be viewed as a coherent state description of the false vacuum instability.

In order to make the distinction between the topological and energetic constituents manifest, it will further be useful to describe the soliton as a *convolution* of the two sectors, i.e.,

$$\text{soliton} = (\text{ topology }) \star (\text{ energy }) \quad .$$

This way of thinking allows to represent a soliton coherent state as a tensor product of two states, $|sol\rangle = |t\rangle \otimes |E\rangle$, one ($|t\rangle$) describing the topology and the other ($|E\rangle$) the energy. This representation allows to directly observe that the key difference between topological and non-topological solitons is encoded in the nature of the $|t\rangle$-state.

We perform different consistency checks, and show that certain known properties of solitons, e.g., the exponentially weak interaction among separated solitons can be nicely understood from basic properties of coherent states.

[2]Let us already mention at this point that we will unravel similar structures in later parts of the thesis in the case of higher dimensional solitons when discussing the quantum structure of instantons. In order to highlight the main points of our approach, however, we will restrict our discussion to $1+1$ dimensions in this section.

3.2.2 Coherent State Picture of Non-Topological Solitons

In order to clearly identify the role of topology, we confront corpuscular resolutions of non-topological and topological solitons. We start with non-topological solitons.

Consider a $1+1$-dimensional theory of a classical field $\phi(x_\mu)$ ($x_0 = t, x_1 = x$) with the Lagrangian

$$\mathcal{L} \;=\; (\partial_\mu \phi)^2 \;-\; m^2\phi^2 \;+\; g^2\phi^4\,, \tag{3.3}$$

where $m^2, g^2 \;>\; 0$. This theory has a classically-stable vacuum at $\phi \;=\; 0$, but becomes unstable for large field values. Correspondingly, there is a static soliton solution which describes a local (in x) excursion of the field from the point $\phi = 0$ to the point $\phi = m/g$ and back.

If we think of the coordinate x as time, the soliton configuration describes a classical evolution of the field in the inverted potential. The field starts at $\phi = 0$ at $x = -\infty$, reaches the point $\phi = m/g$ at $x = 0$ and bounces back reaching the point $\phi = 0$ at $x = +\infty$. The soliton solution is given by

$$\phi_{sol}(x) \;=\; \frac{m}{g}\mathrm{sech}(mx)\,, \tag{3.4}$$

which, as said above, describes an excursion of the field across the barrier and back. The energy of the configuration is

$$E_{non-top} \;=\; \frac{2m^3}{3g^2}. \tag{3.5}$$

Expanding the classical solitonic field in Fourier space ($2\pi R$ is the regularized volume of space),

$$\phi_{sol}(x) \;=\; \sqrt{R}\int \frac{dk}{\sqrt{4\pi|k|}}\,(e^{ikx}\alpha_k \;+\; e^{-ikx}\alpha_k^*)\,, \tag{3.6}$$

the α_k and α_k^* are c-number functions of momentum k that satisfy

$$\alpha_k^*\alpha_k \;= \pi\frac{|k|}{2R}\frac{1}{g^2}\mathrm{sech}^2\left(\frac{\pi k}{2m}\right)\,. \tag{3.7}$$

Using this representation, the classical energy of the soliton takes the form,

$$E_{non-top} \;=\; \int_k |k|\alpha_k^*\alpha_k\,, \tag{3.8}$$

where $\int_k \equiv R\int dk$.

We now wish to represent the soliton as a quantum coherent state, $|sol\rangle$. The natural way of doing this is to identify the Fourier expansion coefficients of the classical field, α_k, with the expectation values of Fock space operators $\hat{a}_k, \hat{a}_k^\dagger$,

$$\langle sol|\hat{a}_k|sol\rangle \;=\; \alpha_k\,, \tag{3.9}$$

satisfying the creation-annihilation algebra

$$[\hat{a}_k, \hat{a}^\dagger_{k'}] = \delta_{k,k'}\,, \tag{3.10}$$

for momenta k, k'.[3]

It then follows from the general properties of coherent states, that $|sol\rangle$ must be a tensor product of coherent states for different k,

$$|sol\rangle \;= \prod_{\otimes k} |\alpha_k\rangle\,, \tag{3.11}$$

where $|\alpha_k\rangle$ is a coherent state for momentum mode k,

$$|\alpha_k\rangle = e^{-\frac{1}{2}|\alpha_k|^2} e^{\alpha_k \hat{a}^\dagger}|0\rangle \;=\; e^{-\frac{1}{2}|\alpha_k|^2} \sum_{n_k=0}^{\infty} \frac{\alpha_k^{n_k}}{\sqrt{n_k!}}|n_k\rangle\,. \tag{3.12}$$

Here $|n_k\rangle$ are number eigenstates of corpuscles with momentum k.

Defining the particle number operator in the standard way, $\hat{N}_k \equiv \hat{a}^\dagger_k \hat{a}_k$, it is clear that the quantity, $N_k \equiv \langle sol|\hat{a}^\dagger_k \hat{a}_k|sol\rangle = \alpha^*_k \alpha_k$ counts the mean occupation number of corpuscles of momentum k in the state $|sol\rangle$. Correspondingly, the quantity

$$N \;\equiv\; \int_k N_k \;=\; \int_k \alpha^*_k \alpha_k \tag{3.13}$$

is the total mean occupation number. Using (3.7) and (3.8), we find that the total mean occupation number of corpuscles and the energy of the soliton are given by

$$N \;=\; \int_k N_k \;=\; \frac{m^2}{g^2}\left(\frac{8\log(2)}{2\pi}\right) \tag{3.14}$$

and

$$E_{non-top} \;=\; \int_k |k| N_k \;=\; \frac{2m^3}{3g^2}\,, \tag{3.15}$$

respectively.

Thus, the dominant contribution both to the number N as well as to the mass of the soliton comes from the corpuscles of momentum $k \lesssim m$. They also set the size of the soliton as $\sim m^{-1}$. The fact that the number (3.14) is finite for non-topological solitons has very important consequences for the quantum description. This finiteness is the reflection of the fact that the non-topological soliton carries no conserved quantum number. Correspondingly, the vacuum is not protected against the instability of soliton-creation! In fact, this instability reflects the fact that the vacuum $\phi = 0$ is not a true vacuum of the theory and decays via bubble-nucleation [77]. We shall discuss this in the next section.

[3] The operators $\hat{a}^\dagger_k, \hat{a}_k$ should not be confused with creation and annihilation operators of asymptotic propagating quanta of the theory. Rather, they create and destroy solitonic constituents, which have very different dispersion relation as compared to the free quanta. A more detailed discussion on the nature of these constituents will be given below.

3.2.3 Consistency Check: Quantum Nucleation of Non-Topological Soliton and Vacuum Decay

Let us evaluate the amplitude of quantum fluctuations that create a soliton out of the vacuum state. This amplitude is given by the overlap between the vacuum $|0\rangle$ and the soliton $|sol\rangle$. In the coherent-state picture this overlap is equal to

$$\langle 0|sol\rangle \;=\; e^{-\frac{N}{2}}\,. \tag{3.16}$$

Notice, that this expression is universal for any coherent state. The difference is only in the number N.

For a non-topological soliton, using (3.14) and restoring powers of $\hbar$, we obtain the following scaling of the exponential amplitude

$$\langle 0|sol\rangle \;=\; e^{-\frac{m^2}{\hbar g^2}}\,, \tag{3.17}$$

where we have ignored the order one numerical coefficient of (3.14). This amplitude is zero only in the classical limit, in which $\hbar \to 0$ and m, g are kept finite[4].

This result has a very interesting physical meaning and amounts to the fact that quantum-mechanically the vacuum $\phi = 0$ is unstable. In this respect, the possibility of non-topological soliton-creation reflects the instability of the $\phi = 0$ vacuum at the quantum level.

Notice, that in the semi-classical limit, in which the classical field configuration is not resolved as a coherent state, the decay goes through the nucleation of a critical bubble which must have the same classical energy as the vacuum $\phi = 0$, and thus, cannot be static. This "bubble" is a configuration that interpolates between $\phi = 0$ and $\phi = \phi_* > m/g$ in order to have zero total energy. But quantum-mechanically the decay can go through the intermediate creation of other coherent states, such as the above static soliton, since none of them is a true energy eigenstate[5].

Only in the classical limit ($N \to \infty$), the non-topological soliton becomes an energy eigenstate and correspondingly the amplitude (3.16) vanishes in this limit. This is a very important result concerning the way the coherent state picture tells us about the instability of the vacuum. In other words, the moment we declare that the static soliton exists and is represented as a coherent state of finite occupation number, it can be nucleated out of the vacuum and lead to its instability.

[4]In our notations, m is the frequency of a classical field oscillation and it is non-vanishing in the limit $\hbar = 0$. The mass of a quantum excitation (energy of a one-particle state) is $\hbar m$ which consistently vanishes in the classical limit.

[5]Notice, that the channel of decay through static soliton nucleation is not necessarily a new channel, since we never proved that this coherent state and the one corresponding to the critical bubble of zero classical energy are orthogonal. To resolve the latter as a coherent state is a bit more complicated because of the lack of the exact classical solution. It would be interesting to study this issue further.

3.2.4 Coherent State Picture of Topological Soliton

The next example we want to consider is a soliton with non-zero topological charge. For this we have to slightly modify the Lagrangian describing the non-topological soliton in order to create two degenerate stable minima. The new Lagrangian reads

$$\mathcal{L} \,=\, (\partial_\mu \phi)^2 \,-\, g^2(\phi^2 \,-\, m^2/g^2)^2\,. \tag{3.18}$$

Note that this is the theory which we already discussed in the introductory chapter. Nevertheless, in order to give a self-contained discussion, let us briefly review its most important aspects with respect to solitons. This theory has two degenerate minima at $\phi \,=\, \pm m/g$ and there is a solution that connects the two. Again, this soliton corresponds to the motion of a particle in an inverted potential in time x. The particle starts at $\phi \,=\, \pm m/g$ at $x \,=\, -\infty$ and reaches $\phi \,=\, \mp m/g$ at $x \,=\, +\infty$. The solution is described by a kink or an anti-kink,

$$\phi_c(x) \,=\, \pm\,\frac{m}{g}\tanh(xm)\,. \tag{3.19}$$

Repeating exactly the same construction as in the case of the non-topological soliton, we shall now represent the kink as a coherent state (3.11) with the occupation number data N_k fixed by matching it with the coefficients of the Fourier expansion of the soliton field (3.6). For the topological soliton (3.19) this matching gives

$$N_k \,=\, \alpha_k^*\alpha_k \,=\pi\frac{|k|}{R}\frac{1}{g^2}\mathrm{csch}^2\left(\frac{\pi k}{2m}\right)\,. \tag{3.20}$$

The mass of the soliton to leading order in $1/N$ is correspondingly

$$E_{top} \,=\, \int_k |k| N_k \,=\, \frac{8m^3}{3g^2}\,. \tag{3.21}$$

Notice, that unlike the non-topological case, the occupation number N_k exhibits a $1/k$-type singularity for small k. This singularity is very important and is the quantum mechanical manifestation of the topological charge. Due to it, in case of the topological soliton, the total number N exhibits a logarithmic divergence for small k,

$$N \,=\, \int_{k_0} dk N_k \,\sim\, \log(k_0)|_{k_o\to 0} \to \infty\,. \tag{3.22}$$

Notice, that the quanta with $k \to 0$ contributing to this divergence do not contribute to the energy of the soliton (3.21) to which the contribution from small k-s vanishes. The infrared quanta only contribute to the topological charge. This divergence ensures that topological charge is conserved in a full quantum theory.

In particular, creation of a topological soliton out of the vacuum, unlike the non-topological one, is impossible in the quantum theory. The coherent state corresponding to this soliton, even for finite $\hbar$, has *infinite* occupation number of zero momentum modes.

Correspondingly, the soliton-creation amplitude vanishes already at the quantum level. To see this it is enough to substitute in (3.16) the expression (3.22). We get

$$\langle 0|sol\rangle \;=\; e^{-\frac{1}{\hbar}\infty}\,. \tag{3.23}$$

Although the zero momentum modes give vanishing contribution to the soliton mass (3.21), they play the crucial role for the conservation of the topological charge, as it is clear from (3.23).

Thus, the following quantum picture emerges. Classically, the topological charge of the soliton comes from the boundary behaviour of the field which asymptotes to different constant values for $x = \pm\infty$. Correspondingly, in quantum description this charge is determined entirely by the infinite-wavelength corpuscles. The occupation number of $k = 0$ modes is infinite which ensures that topological charge is *not* subject to quantum fluctuations.

In contrast, the mass of the soliton gets the dominant contribution from $k \lesssim \hbar m$ modes. The mean occupation number of such modes is finite ($N_m \sim \frac{m^2}{\hbar g^2}$) [6]. Because of their finite number the contribution of these modes to physical processes is in general subject to quantum fluctuations. Consequently, the quantities that are determined classically by the mass of the soliton are expected to be subjected to quantum corrections in the quantum picture. Later, in the context of supersymmetric solitons, we will explicitly demonstrate that this is indeed the case.

3.2.5 Topology-Energy Decomposition: Topological Soliton as Convolution

The diverse roles of the quanta contributing into the energy and topology can be nicely visualized in a picture in which the soliton is defined as a *convolution* between topology and energy, i.e.,

$$\text{soliton} = (\text{ topology }) \star (\text{ energy }) \quad .$$

The quantum mechanical meaning of the above decomposition is based on the fundamental theorem of convolution, namely that the Fourier-transform – which is the tool we need in order to promote classical c-numbers into creation and annihilation operators – of the convolution of two functions is just the product of the Fourier-transforms. This will convert the former classical relation into

$$|sol\rangle = |t\rangle \otimes |E\rangle,$$

where $|t\rangle$ and $|E\rangle$ are coherent states constructed out of quanta carrying information about topology and energy, respectively.

[6] We mean that the contribution of the modes with momentum $0 \leqslant k < \epsilon$ to the mass of the soliton is $\sim \epsilon$ and is negligible for $\epsilon \ll m$. Whereas, the contribution of the same modes to the topological charge is dominant no matter how small ϵ is.

To illustrate this program explicitly, consider the kink solution (3.19). In order to disentangle the topology from the energy at the classical level we use the relation

$$\text{sign}(x) \star f(x) = +\frac{1}{2}\int_{-\infty}^{x} f(x')dx' - \frac{1}{2}\int_{x}^{\infty} f(x')dx' \,, \tag{3.24}$$

with $\text{sign}(x)$ being the sign function. Using this expression, we easily get

$$\phi_{sol}(x) = \frac{m}{g}\Big(\text{sign} \star \text{sech}^2\Big)(mx) \,, \tag{3.25}$$

where the sign part represents the topology, whereas the sech^2 represents the energy component. It is important to note already at this level that the energy component has the profile of the square of the non-topological soliton (3.4) for the inverted potential. This tells us that this component has no knowledge about the topology.

In order to move to quantum mechanics, we first define the Fourier-transform slightly changing the parametrization with respect to (3.6),

$$\phi_{sol}(mx) = \frac{1}{2}\int \frac{d(\frac{k}{m})}{\sqrt{4\pi(\frac{k}{m})}}\Big(\alpha_k e^{i(\frac{k}{m})xm} + \text{h.c.}\Big) \,. \tag{3.26}$$

Using now the fundamental convolution theorem, we get

$$\alpha_k = \frac{m}{g\sqrt{\pi}}\sqrt{\frac{k}{m}}[F(\text{sign})](k/m)[F(\text{sech}^2)](k/m) \,, \tag{3.27}$$

with F representing the Fourier-transform,

$$F(\text{sech}^2) = \pi\frac{k}{m}\text{csch}\Big(\frac{\pi k}{2m}\Big) \tag{3.28}$$

and

$$F(\text{sign}) = \frac{im}{k} \,. \tag{3.29}$$

The expressions (3.28) and (3.29) carry information about the energetic and the topological composition of the soliton. Notice the pole at $k = 0$ in (3.29). This pole encodes quantum information about the topology of the soliton. Namely, as before, topology comes from the infinite occupation number of zero-momentum corpuscles that support the momentum-flow in one direction. The only novelty in the convolution picture is that the pole is clearly attributed to one side (t-sector) of the decomposition. On the other hand, no such divergent part appears in (3.28). The contribution to this expression mainly comes from modes with momentum spread $|\Delta k| \sim m$ and zero net momentum. This is the reflection of the fact that such modes contribute to the energy of the soliton without contributing to the topology. They do not support momentum flow in any direction.

The above results lead us to the following representation for α_k,

$$\alpha_k = t_k \, c_k \,, \tag{3.30}$$

where

$$c_k \equiv \sqrt{\pi m}\frac{k}{g}\mathrm{csch}\Big(\frac{\pi k}{2m}\Big) \tag{3.31}$$

and

$$t_k \equiv \frac{i}{\sqrt{k}}\,. \tag{3.32}$$

We now define two sets of creation-annihilation operators $\hat{t}_k^\dagger, \hat{t}_k$, and $\hat{c}_k^\dagger, \hat{c}_k$, which satisfy the standard algebra, $[\hat{t}_k, \hat{t}_{k'}^\dagger] = \delta(k-k')$ and $[\hat{c}_k, \hat{c}_{k'}^\dagger] = \delta(k-k')m^2$ and all other commutators vanishing. Next, we construct the corresponding coherent states,

$$\hat{c}_k|c_k\rangle = c_k|c_k\rangle \tag{3.33}$$

and

$$\hat{t}_k|t\rangle = t_k|t_k\rangle\,, \tag{3.34}$$

where c_k and t_k are given by (3.31) and (3.32), respectively. Since the operators $\hat{c}_k$ and $\hat{t}_k$ act on different Fock spaces, we can write the coherent state representing the soliton in the following form:

$$|sol\rangle \;=\; |t\rangle \otimes |E\rangle, \tag{3.35}$$

where $|t\rangle \equiv \prod_k |t_k\rangle$ and $|E\rangle \equiv \prod_k |c_k\rangle$.

The quanta $\hat{c}_k$ are not different from the constituents of non-topological solitons built on the zero topological sector. The state $|E\rangle$ is defined as a quantum coherent state relative to these quanta. The state $|t\rangle$ is just the coherent state $|\mathrm{sign}(x)\rangle$.

Let us pause and make a couple of comments on the meaning of the above coherent states.

Formally, as a coherent state of t-quanta the state $|t\rangle$ is characterized by an infinite occupation number of zero momentum modes $\hat{t}_0|t\rangle = \infty|t\rangle$ and can be interpreted as a sort of *Bose sea*. On the other hand note, that as a convolution the non-topological soliton can be trivially represented as $\delta(x) \star \mathrm{sech(x)}$ and therefore we can proceed as we have done with the topological soliton and associate to it a quantum state $|t\rangle \otimes |E\rangle$ with $|E\rangle$ exactly the type of coherent state associated to the non-topological soliton considered earlier. This makes clear that from the energetic point of view topological and non-topological solitons are the same sort of coherent states. However, in the non-topological case the state $|t\rangle$ is trivially defined by $\hat{t}_k|t_{nt}\rangle = |t_{nt}\rangle$ instead of $\hat{t}_k|t\rangle = \frac{i}{\sqrt{k}}|t\rangle$. We can thus think about the topological charge as of the order n of the pole at $t_{k=0}$. Naturally, $n = 0$ holds for the non-topological soliton. Under these conditions the topological stability reduces simply to the conservation of n. The coherent state understanding of this conservation lies in the fact that a non-vanishing n requires an infinite Bose sea of quanta.

Secondly, we have to note, that operators defined as $\hat{a}_k = \hat{t}_k \hat{c}_k$ no longer satisfy the standard creation-annihilation algebra. This a priory is not necessarily a fatal problem, since the solitonic constituents are not propagating asymptotic degrees of freedom anyway[7]. They only exist in form of the bound-state and are off-shell relative to their asymptotic counterparts. This is already clear from their dispersion relations. In particular, they have zero frequencies, while having non-zero momenta. Such a dispersion relation is only possible for the interaction eigenstates. Among the free-particles, such a dispersion relation is exhibited by tachyons of momentum exactly equal to the absolute value of their mass. Or equivalently, tachyons moving at an *infinite* speed. Thinking of the solitonic constituents as of tachyons has certain appeal in the following sense. First, the tachyons cannot be the asymptotic S-matrix states. They cannot exist in the free state, but only within the bound-state in form of the soliton, similarly to quarks that can only exist inside hadrons. Secondly, at the same time the zero-frequency tachyons move at infinite speed. That is, they create an instant momentum flow between the two spatial infinities and this is why they "smell" topology. However, the particular interpretation of the nature of constituents is not affecting the physical consequences of the coherent state picture. Therefore, we shall not insist on any of them.

3.2.6 Orthogonality of Vacua with Different Topologies

Again, the above construction automatically accounts for the fact that the soliton of topological charge different from 0 has vanishing overlap with any state with zero topological charge. Indeed, the scalar product of this coherent state with the vacuum is given by

$$|\langle 0|sol\rangle|^2 \;=\; e^{-\int dk|\alpha_k|^2}\,. \tag{3.36}$$

Note now that according to (3.34) for the coherent state $|t\rangle$, we have $\alpha_k = t_k$, and because of (3.32) the integral $\int dk|\alpha_k|^2 \;=\; \int dk/|k|$ diverges. Thus, computing the overlap of the topologically-trivial vacuum with the topological coherent state we get

$$|\langle 0|t\rangle|^2 \;=\; e^{-\int dk t_k^* t_k} = 0\,. \tag{3.37}$$

Obviously, by the same reason the overlap between the topological soliton and any other state constructed about the topologically-trivial vacuum is also zero. For the coherent state $|E\rangle$ the average number of energy quanta can be defined as

$$N = m^{-1}\int d(k/m)\langle E|\hat{c}_k^\dagger \hat{c}_k|E\rangle \;=\; \frac{8m^2}{3g^2}\,, \tag{3.38}$$

which is of the same order as the number of quanta in the case of the non-topological soliton (3.14) obtained earlier.

[7]Assuming that the topological quanta fulfill a Cuntz algebra with only one generator at $k = 0$, it is easy to show that the $\hat{a}_k$ indeed satisfy a standard creation/annihilation algebra when evaluated in the solitonic state.

3.2.7 Energy and Topological Charge

We shall define the normalized topological number, i.e. the one representing the different homptopy classes in π_0 of the vacuum manifold in terms of the topological *quanta* as simply the order of the pole of t_k at $k = 0$ or equivalently by the Cauchi principal value,

$$|Q| = \frac{1}{\pi}\text{ImPV}\int dk\langle t|\hat{t}_k^\dagger \hat{t}_k|t\rangle\,. \tag{3.39}$$

As explained above, the pole in t_k at $k = 0$ implies the existence of a Bose sea with an infinite number of zero momentum t quanta and, therefore, with zero overlap with states defined by regular t_k at $k = 0$ [8].

The energy is instead given by

$$E_s = \int d(k/m)\langle E|\hat{c}_k^\dagger \hat{c}_k|E\rangle\,. \tag{3.40}$$

and it is equal to $\frac{8m^3}{3g^2}$. Note, that we can understand the energy of the soliton as a collective effect of $N = \frac{8m^2}{3g^2}$ quanta, each contributing a portion m to the energy.

Since the energy only depends on the corpuscular quanta $\hat{c}_k$ we can define it as the expectation value of a corpuscular Hamiltonian $H(\hat{c}_k, \hat{c}_k^\dagger)$ in the coherent state $|E\rangle$. At leading order in $1/N$ the *corpuscular Hamiltonian* H can be approximated as

$$H = \sum_k \hat{c}_k^\dagger \hat{c}_k\,. \tag{3.41}$$

It is instructive to view the corpuscular structure of the soliton in the light of many-body physics. A generic corpuscular Hamiltonian can schematically be visualized as

$$H \;=\; \sum_k \hat{c'}_k^\dagger \hat{c'}_k \;+\; \text{interaction terms}\,, \tag{3.42}$$

where prime indicates that in general we are taking $1/N$ effects into account. The "interaction terms" stands for up-to-quartic momentum-conserving contractions (e.g., $\sum_{k_1,k_2,k_3} \hat{c'}_{k_1}\hat{c'}_{k_2}^\dagger \hat{c'}_{k_3}\hat{c'}_{k_1+k_2-k_3}^\dagger + ...$). Then the soliton corresponds to a state with distributions of c_k-numbers over which the Hamiltonian is effectively diagonal and takes up the form (3.41), up to $1/N$ corrections.

[8] In general, we can use the convolution to define the topological charge as follows. Given a solitonic classical field configuration we look for a non-trivial representation of type $f \star g$, where neither f nor g are delta functions and where one of the two functions, let us say g, is a gradient. In these conditions topology is associated with f. Denoting F_k its Fourier coefficients, the *topological charge* is determined by the singularity of F_k at $k = 0$. Moreover the role of the *vacuum* in the topologically non trivial Hilbert space is played by the *Bose sea* coherent state defined by $F_{k=0}$. This reasoning will be applied later to an example more complicated as the kink. Indeed, we will show that a similar decomposition can be constructed for a magnetic monopole in 5 dimensions.

Later, when discussing the corpuscular portrait of instantons (as well as when computing higher-order corrections) we will outline how to construct the corpuscular Hamiltonian from two different points of view. On the one hand, using a Bogoliubov approximation, we can explicitly parametrize quantum fluctuations of the typical occupation number of a classical profile in terms of quadratic fluctuations of Bogoliubov modes. Furthermore, the construction explicitly guarantees, that the classical mean field results such as the energy of the profile are recovered to leading order in $1/N$. On the other hand, we can write down the corpuscular Hamiltonian directly in terms of full-fledged corpuscular creation and annihilation operators without performing a mean-field split. As we will explain in detail, while the classical results are captured in the normal-ordered part of any quantum operator, quantum corrections arise from the non-trivial commutators of creation and annihilation operators. In configuration space, these commutators are interpreted as loops which renormalize the classical background date. Although the former way of constructing the Hamiltonian has a simple physical interpretation, we choose to work with the latter when explicitly computing quantum effects. While intuitively it makes sense that there should be a correspondence between both approaches, the explicit mapping still needs to be worked out.

Finally, let us discuss the zero mode from the corpuscular point of view. This mode corresponds to translations of the soliton profile in the x-direction and it is the Nambu-Goldstone mode of broken translations. At the corpuscular level such a transformation simply amounts to redefining the corpuscular operators by a phase, $\hat{c}_k \to e^{ikb}\hat{c}_k$, where b is the displacement of the profile along the x-direction. Clearly, (3.41) is invariant under this $U(1)$ transformation, as it should be.

3.2.8 Quantum Meaning of Soliton-Anti-Soliton Interaction

Let us now understand the corpuscular meaning of soliton-anti-soliton interaction using the language of coherent states. The soliton-anti-soliton configuration solving the classical equations of motion is not known exactly. In general, such a configuration is not static. However, we can ignore this complication and estimate the interaction between the solitons using the classical Lagrangian. The natural question raised by the previous quantum representation of the soliton lies in understanding the quantum corpuscular meaning of interaction energy *without* directly using the Lagrangian information.

Let us start with the soliton-anti-soliton classical configuration which we shall approximate by two static solutions separated by a finite distance, $a \gg m^{-1}$,

$$\phi_{s,\bar{s}} = \frac{m}{g}\Big(\tanh(m(x+a/2)) - \tanh(m(x-a/2)-1\Big) . \tag{3.43}$$

This configuration can be viewed as a "bubble" of the $\phi = +m/g$ vacuum of size $\sim a$ surrounded by the $\phi = -m/g$ asymptotic vacuum. The coherent state data corresponding to this configuration is,

$$\alpha_k = \sqrt{\pi m}i\frac{\sqrt{k}}{g}\mathrm{csch}\Big(\frac{\pi k}{2m}\Big)\left(1-\mathrm{e}^{-iak}\right) . \tag{3.44}$$

The pole at $k = 0$ is removed, which immediately implies that the topological charge of this configuration vanishes.

Since the soliton-anti-soliton system has zero topological charge, the interaction energy can be estimated from the overlap of the energy parts of the coherent state. We can derive the exponential suppression of the soliton-anti-soliton potential by estimating the matrix element

$$\langle E|H|E\rangle_a \,, \tag{3.45}$$

where $|E\rangle_a$ stands for the energy part of the displaced anti-soliton which is the same as the one of the soliton. This matrix element can be easily estimated by taking into account the following facts. First, the soliton differs from the anti-soliton by the reflection of the sign.

Secondly, as noticed before, the translation amounts to the phase shift change $\hat{c}_k \to e^{iak}\hat{c}_k$. Moreover, the soliton and anti-soliton at large separation are approximately eigenstates of the Hamiltonian. Thus, the interaction among the solitons amounts to the overlap of the two sets of coherent states with $|c_k\rangle$ and $|e^{iak}c_k\rangle$ which from the well-known properties of coherent states gives

$$|\prod_k \langle c_k|e^{iak}c_k\rangle|^2 \;=\; e^{-2\int dk\,|c_k|^2(1-\cos(ak))}\,. \tag{3.46}$$

Taking into account the expression for c_k, we get

$$|\prod_k \langle c_k|e^{iak}c_k\rangle|^2 = \exp\big(-2E_s + 32\frac{m^3}{g^2}(am)e^{-2am}\big)\,, \tag{3.47}$$

where E_s is given in equation (3.40). This expression is in agreement with the standard Lagrangian computation.

The alternative way of estimating the interaction energy is the following. From the energetic point of view we can associate with the soliton and the anti-soliton two corpuscular algebras $\hat{c}_k, \hat{c}_k^\dagger$ and $\hat{\bar{c}}_k, \hat{\bar{c}}_k^\dagger$. In the limit of large a the soliton-anti-soliton quantum state can be defined as

$$|s, \bar{s}\rangle = |sol\rangle \otimes |\bar{sol}\rangle \tag{3.48}$$

with $\hat{c}_k|s,\bar{s}\rangle = (|t_s\rangle \otimes c_k|E_s\rangle) \otimes (|t_{\bar{s}}\rangle \otimes |E_{\bar{s}}\rangle)$ and $\hat{\bar{c}}_k|s,\bar{s}\rangle = (|t_s\rangle \otimes |E_s\rangle) \otimes (|t_{\bar{s}}\rangle \otimes \tilde{c}_k|E_{\bar{s}}\rangle)$ leading to

$$\hat{c}_k|s,\bar{s}\rangle = e^{iak/2}\sqrt{\frac{m^3}{\pi}}\frac{\pi k}{gm}\mathrm{csch}\Big(\frac{\pi k}{2m}\Big)|s,\bar{s}\rangle \tag{3.49}$$

and

$$\hat{\bar{c}}_k|s,\bar{s}\rangle = -e^{-iak/2}\sqrt{\frac{m^3}{\pi}}\frac{\pi k}{gm}\mathrm{csch}\Big(\frac{\pi k}{2m}\Big)|s,\bar{s}\rangle\,. \tag{3.50}$$

The corpuscular Hamiltonian in this approximation becomes simply

$$H = \int d(k/m)\Big(\hat{c}_k^\dagger\hat{c}_k + \hat{\bar{c}}_k^\dagger\hat{\bar{c}}_k + \hat{c}_k^\dagger\hat{\bar{c}}_k + \hat{\bar{c}}_k^\dagger\hat{c}_k\Big)\,, \tag{3.51}$$

where the interaction piece is manifest in the crossed terms between the two types of quanta $\hat{c}$ and $\hat{\bar{c}}$. Evaluated on the state $|s,\bar{s}\rangle$ we get

$$H = 2E_s - \frac{8m^3}{g^2}(-1 + (am)\coth(am))\mathrm{csch}^2(am)\,. \tag{3.52}$$

For large a we obtain

$$2E_s - 32\frac{m^3}{g^2}(am)e^{-2am}\,, \tag{3.53}$$

which fully agrees with (3.47). Replacing E_s by N we can estimate when the interaction among the solitons becomes order one, i.e., when the effect of the interaction is equivalent to replacing $2N$ by $2N-1$. This happens for $am \sim \ln(N)$. As it is well known this fact underlies the logarithmic corrections in the soliton anti-soliton sector [41].

At this point we shall briefly make a few remarks on the a-dependence of the interaction. In contrast to an isolated soliton, for which the energy is translationally invariant, for the soliton-anti-soliton the interaction term $-32\frac{m^3}{g^2}(am)e^{-2am}$ occurs. This term simply reflects the fact that the effective potential between the soliton and anti-soliton is attractive. The distance a between them determines the interaction strength. Due to this a-dependent interaction the energy is no longer invariant under the change of the relative position. Thus, there exists a quasi zero mode (a pseudo-Goldstone boson), which only becomes a true Goldstone mode in the limit $a \to \infty$. At the level of the corpuscular Hamiltonian (3.51), it is easy to see that the breaking of translational invariance is due to the interference terms $\hat{c}_k^\dagger \hat{\bar{c}}_k$ that are mixing corpuscles of both solitons. As explained before, shifting of the soliton profile corresponds to a phase shift of the corpuscular operators. Thus, shifting both operators in the opposite direction by an amount b changes the energy by an amount $\Delta H = \int dk(e^{ik2b}\hat{c}_k^\dagger \hat{\bar{c}}_k + \text{h.c.})$. In contrast shifting both profiles in the same direction will not change the energy of the system. Therefore, the interference terms explicitly break the symmetry $U(1)_S \times U(1)_{\bar{S}} \to U(1)_{diag}$, resulting in the existence of one zero mode and one quasi zero mode.

Let us briefly summarize our basic construction and results. We have displayed an attempt of uncovering the quantum origin of topology at the microscopic level. For this purpose we have developed a coherent state representation of both topological and non-topological solitons and confronted them with each other. This construction allowed us to clearly identify the quantum origin of topological charge in terms of the singularity in the occupation number of infinite wavelength corpuscles with net momentum flow in one direction. After this identification, many properties of solitons, such as conservation of topological charge or false vacuum instability via nucleation of non-topological solitons (bubbles), nicely follow from the basic properties of the coherent states.

Our results can be straightforwardly generalized to higher co-dimension cases. In each case, the topological charge is related to the singularity in occupation number of infinite wavelength quanta with the net non-zero Noether quantum number, such as, e.g., momentum or angular momentum. This shall be demonstrated explicitly in various situations in the next section.

3.3 Quantum Theory of Instantons

As a next step, we will argue that the quantization of the soliton presented in the previous section, immediately implies that instantons should be quantized as well. In particular, for an instanton in d Euclidean dimensions, there is always a soliton described by the same field configuration in $d+1$ space-time dimensions. Therefore, the quantization of the soliton translates directly into the quantization of the corresponding instanton. This connection allows to relate the fundamental parameters of the theory describing the instanton with the ones describing the soliton in one more dimension. Having established a general correspondence between the physics of solitons and instantons in terms of coherent states, we show how to reproduce the well-known instanton physics in terms of a coherent state description of solitons as developed earlier in higher dimensions. Applications of the formalism include a derivation of the instanton action as well as transition amplitudes. In order to make our discussion transparent, we shall construct explicit models which show that instanton effects observed by a d-dimensional observer Alice, can be mapped to a passing by soliton of a theory of Bob in $d+1$ dimensions. Furthermore, we discuss the physics of resurgence from the of the corpuscular point of view. Having a full quantum description, we will recognize that the non-trivial cancellation of ambiguous imaginary parts appearing in the expansion around perturbative and non-perturbative saddles follows as a simple consequence of the optical theorem.

3.3.1 Physical Meaning of Instanton Constituents

As discussed above, we want to develop a coherent state approach to instanton physics in terms of higher-dimensional solitons. Therefore, we should first of all try to explain what we mean when we talk about coherent states for instantons. Thus, let us discuss the physical meaning of the instanton constituency. Since an instanton describes a *tunneling process* rather than an object in real time, it is natural to think that the elementary constituents of the instanton are the elementary processes. Let us be more precise. An instanton describes a transition between some initial and final states, $|in\rangle \to |f\rangle$. In particular, these states can be the vacua corresponding to different values of some topological number. However, the transition process may be much more general. Usually, the term"instanton" is applied when the initial and final states are well-described semi-classically. Thus, the composite nature of the instanton is intimately linked with the corpuscular structure of a semi-classical system the Euclidean time evolution of which it describes.

For understanding the corpuscular structure of an instanton, we shall establish the following correspondence. Consider an instanton of some d-dimensional field theory. It is described by a classical Euclidean field configuration, which schematically we can denote by $\phi^{(d)}_{inst}(x)$. Then, there always exists a static soliton described by the identical field configuration in a $d+1$-dimensional theory. The latter theory is obtained by lifting the original d-dimensional theory into one more space dimension. This fact is obvious, since the static field equations of the lifted $d+1$ theory are identical to the Euclidean equations of motion of the original d-dimensional theory.

Notice, such lifting necessarily involves a fundamental length scale L that relates fields and coupling constants of the two theories. In particular, the coupling constants of the two theories are related as (for convenience, $d+1$ dimensional parameters will be endowed with a tilde in this section)

$$\frac{L}{\tilde{g}^2} \;=\; \frac{1}{g^2_{(d)}}. \tag{3.54}$$

The same scale enters in the relation among the fields, so that we have,

$$\phi^{(d)}_{inst}(x) \;= \sqrt{L}\,\tilde{\phi}^{(d+1)}_{sol}(x)\,. \tag{3.55}$$

Similarly, the action of the d-instanton is related to the static energy of the $d+1$-soliton as,

$$S^{(d)}_{inst} \;=\; L\,M^{(d+1)}_{sol}\,. \tag{3.56}$$

The physical meaning we give to this relation is that the right hand side must also be interpreted as the action of a process. This process describes the evolution of a $(d+1)$-dimensional soliton over the Euclidean time interval L.

Thus, an instanton of a d-dimensional field theory is in one to one correspondence with an Euclidean time evolution of a soliton of a $d+1$-dimensional theory.

This correspondence allows us to understand the corpuscular quantum structure of instantons in terms of the quantum structure of the corresponding soliton. Namely, quantum-mechanically we describe solitons as coherent states of some elementary quanta. Their mean occupation number N defines the number of constituents of the corresponding instanton in terms of N elementary processes. These elementary processes describe the Euclidean time evolution of solitonic corpuscles over the Euclidean time interval set by the same scale L that related the couplings of the two theories through (3.54).

Thus, we relate the mean occupation number of the coherent state describing a $d+1$-dimensional soliton and the Bohr-Sommerfeld quantum number of an d-dimensional instanton action.[9]

As a supporting evidence of the corpuscular picture, let us see, how the coherent state description reproduces the correct instanton amplitude in the large-N limit. Since the result follows from model-independent fundamental properties of coherent states, we shall first give a general discussion and later illustrate it on concrete examples.

[9]We must stress, that in our description, since an instanton is a coherent state rather than a number-eigenstate, its action is not strictly quantized in terms of $\hbar$. Rather, N describes only the mean number. The actual number is subject to quantum fluctuations that take us away from the classical saddle point values. Such excursions account for new type of quantum corrections that, among other things, lead to quantum violation of the BPS condition as we will discuss in detail below.

As before, let us represent a $d+1$-dimensional soliton state as a coherent state,

$$|sol_{(d+1)}\rangle \equiv |N_{(sol)}\rangle = \prod_k |N_k\rangle = \prod_k e^{-\frac{N_k}{2}} \sum_{n_k=0}^{\infty} \frac{N_k^{\frac{n_k}{2}}}{\sqrt{n_k!}} |n_k\rangle, \tag{3.57}$$

where the $|n_k\rangle$ are number eigenstates of corpuscles with d-momentum vectors k and the product is taken over all possible k-s[10]. This Fock space is constructed by the set of operators $\hat{a}_k, \hat{a}_{k'}^\dagger$ satisfying a creation and annihilation algebra,

$$[\hat{a}_k, \hat{a}_{k'}^\dagger] = \delta_{k,k'} \,, \tag{3.58}$$

for d-momentum vectors k, k'.

Thus, by construction $\hat{a}_k|N_{(sol)}\rangle = \hat{a}_k|N_k\rangle = \sqrt{N_k}|N_k\rangle$. Correspondingly, the total mean-occupation number is given by

$$N = \langle N_{(sol)}| \int_k \hat{a}_k^\dagger \hat{a}_k |N_{(sol)}\rangle = \int_k N_k \tag{3.59}$$

where $\int_k \equiv \frac{V^{(d)}}{(2\pi)^d} \int d^d k$ and $V^{(d)}$ denotes the volume of d-dimensional space. The soliton mass is given by the expectation value of the Hamiltonian, $\hat{H}$,

$$\langle N_{(sol)}|\hat{H}|N_{(sol)}\rangle = M_{sol} \,. \tag{3.60}$$

The mean-momentum k, i.e. the one contributing most dominantly to the soliton mass, set the characteristic inverse size of the soliton. This size, call it ρ, may be fixed by the mass scale of the theory, or may be a modulus (the latter is the case for the soliton in $4+1$ space-time dimensions (see below)). However, in each case the dominant role in soliton physics is played by the corpuscles of momenta $k \sim \rho^{-1}$.[11]

Although the coherent state is not an energy eigenstate for finite N, it becomes such for $N \to \infty$. At finite-but-large N it is an approximate energy eigenstate, up to $1/N$-corrections.

Correspondingly for short time scales $\tau \ll \rho$ the soliton coherent state evolves as

$$|N_{(sol)}, t+\tau\rangle = e^{iH\tau}|N_{(sol)}, t\rangle \simeq e^{iM_{sol}\tau}|N_{(sol)}, t\rangle \,. \tag{3.61}$$

[10] Of course, we could instead again work with a coherent state constructed from the direct product of topological and energetic quanta. As explained in the last section, our results will not depend on such a split. Thus, in order to focus on the connection with the instanton, we will use only one set of creation and annihilation operators in the following discussion. Later, however, we shall again make use of the topology/energy construction.

[11] Another important role is played by the quanta of zero momentum flow. As discussed in the last section, these account for the conservation of the topological charge of the soliton. Since an instanton is directly related to the corresponding soliton in one more spatial dimension, the infinite wavelength quanta also account for the topology associated with the instanton. Since we will be mostly interested in questions related to the instanton action in this section, we will however focus on the corpuscules of wavelength given by the typical size of the configuration.

Let us briefly pause at this point and make an important remark. In order to give a well-defined meaning to (3.61), we need to know the form of the time evolution operator H. Notice that so far, however, we did not specify the explicit form of the Hamiltonian. Rather, to leading order in $1/N$, there are various choices which satisfy the expectation value equation (3.60) such as $H = M_{sol}$ or $H = \int_k k a_k^\dagger a_k$. While in the former case, the coherent state is a true energy eigenstate, this is not true in the latter situation. Note, however, that although both choices lead to the same expectation value, the time evolution of both only coincides for small time scales. This makes sense, because the second possible form of the Hamiltonian matches the momentum operator. Thus, evolution generated by this operator, might just as well be interpreted as a spatial translation of the soliton. Since we are interested in giving some prescription which allows to map the instanton on an evolving soliton, both forms of the Hamiltonian can in principle be used to leading order in $1/N$ at least for small time scales.

If one were to include $1/N$ corrections, however, a proper way of deriving the Hamiltonian is to start with the microscopic theory. Then one should expand the full Hamiltonian (before performing a BPS completion) in Fourier space (i.e. insert the expansion of the field operator which we have given several times) and demand that when acting on the soliton state, the annihilation operator reduces to its classical value α_k plus small fluctuations accounting for $1/N$ deviations from a mean field situation. Note that this approach is usually used in the context of many-body physics. Indeed, keeping fluctuations up to quadratic order and diagonalizing the Hamiltonian describing the small fluctuations via Bogoliubov transformation, the quanta which account for deviations from the mean-field are naturally interpreted as quasi-particle excitations of the soliton. We shall come back to this point briefly when discussing corpuscular effects in the case of supersymmetric solitons. Thus, from the point of view of many-body physics, we see that the proper choice of the Hamiltonian at leading is simply M_{sol}[12].

In order to establish the connection with the d-instanton amplitude, we must evaluate a soliton-soliton transition matrix element for the separation over an Euclidean time interval $\tau = iL$. This gives

$$\langle N_{(sol)}|e^{iH\tau}|N_{(sol)}\rangle \simeq e^{-M_{sol}L}\,. \tag{3.62}$$

Notice, that since at finite N, the soliton is not an energy eigenstate (as explained before), the above relation is only a leading order relation. Taking into account (3.56), equation (3.62) reproduces the well-known semi-classical instanton amplitude, $e^{-S^{(d)}_{inst}}$.

We thus observe that the matrix element describing the Euclidean time evolution of

[12]Of course, it is not necessary to split the corpuscular creation and annihilation operators into a mean field value part and fluctuations around it. Indeed, for convenience we will work with full quantum operators below when discussing supersymmetric solitons. As we will show, the semi-classical part of the Hamiltonian then corresponds to the normal-ordered part of the time evolution operator and fluctuations around the classical background are encoded in non-trivial loops of corpuscles attached to the mean-field. Although it is clear that both approaches capture the same physics, a precise dictionary between the two still needs to be established.

the coherent state $|N_{(sol)}\rangle$ matches the instanton amplitude,

$$\langle N_{(sol)}|e^{iH\tau}|N_{(sol)}\rangle|_{t=iL} \;=\; e^{-S_{inst}}\,. \tag{3.63}$$

Below we shall obtain this relation for concrete examples that allow to read off the k-dependence of N_k explicitly. As we shall see, this explicit form allows to give a clear interpretation to the compositeness of the instanton action, in terms of a collection of elementary corpuscular actions.

3.3.2 Example: $1D$ Instanton and $2D$ Soliton

Let us consider a simple example. We shall establish an explicit correspondence between the instanton of a $0+1$-dimensional theory and a soliton of $1+1$-dimensional theory.

Consider a $0+1$-dimensional theory of a classical field $\phi(t)$, with the Lagrangian

$$\mathcal{L}_{0+1} \;=\; (\partial_t\phi)^2 \;-\; m^2\phi^2 \;+\; g^2\phi^4\,, \tag{3.64}$$

where $m^2, g^2 \;>\; 0$. This theory has a classically-stable vacuum at $\phi \;=\; 0$, but becomes unstable for large field values. Correspondingly, there is an instanton describing the tunneling process. The instanton configuration describes a classical evolution of the field in the inverted potential. The field starts at $\phi = 0$ at $t = -\infty$, reaches the point $\phi = m/\sqrt{2}g$ at $t = 0$ and bounces back reaching the point $\phi = 0$ at $t = +\infty$. The instanton solution is given by

$$\phi_{inst}(t) \;=\; \frac{m}{g}\mathrm{sech}(mt)\,. \tag{3.65}$$

The instanton describes an Euclidean excursion of the field across the barrier and back. Its Euclidean action is given by

$$S^{(1)}_{inst} \;=\; \frac{2m^3}{3g^2}. \tag{3.66}$$

We now wish to understand this instanton as an evolving soliton of the theory obtained by lifting the original theory into one more space dimension. That is, consider a $1+1$-dimensional theory of a classical field $\tilde{\phi}(t,x)$ with the similar Lagrangian,

$$\mathcal{L}_{1+1} \;=\; (\partial_t\tilde{\phi})^2 - (\partial_x\tilde{\phi})^2 \;-\; m^2\tilde{\phi}^2 \;+\; \tilde{g}^2\tilde{\phi}^4\,. \tag{3.67}$$

Notice that this is exactly the same theory describing a non-topological soliton which we studied in detail in the last section. In order to give a self-contained presentation concerning its connection to the corpuscular theory of the instanton, we will nevertheless review some of the important properties of the non-topological soliton. The mass parameter m is the same in two theories, but the couplings g^2 and $\tilde{g}^2$ have different canonical dimensionalities. Thus, lifting necessarily requires an introduction of a fundamental scale L that relates the two couplings

$$\frac{L}{\tilde{g}^2} = \frac{1}{g^2}. \tag{3.68}$$

The new theory has a static soliton solution,

$$\tilde{\phi}_{sol}(x) \;=\; \frac{m}{\tilde{g}}\mathrm{sech}(mx)\,, \tag{3.69}$$

which has exactly the same form as the instanton of the lower dimensional theory (3.65), except the argument is a Minkowski space coordinate x. Hence, the soliton describes a local field excursion across the barrier, but in a real coordinate space. This soliton is not topologically stable, because there is no stable vacuum on the other side of the barrier. But this is not important for our analysis. The soliton mass is given by,

$$M^{(2)}_{sol} \;=\; \frac{2m^3}{3\tilde{g}^2}. \tag{3.70}$$

Taking into account (3.68), it is obvious that the soliton mass and the instanton action satisfy the relation (3.56).

Now it is evident how the corpuscular structures of solitons and instantons are related. If we resolve the soliton as a coherent state, we must resolve the instanton as well. The soliton is a coherent state (3.57) of elementary quanta of characteristic momentum $\sim m$ and mean occupation number $N \sim \frac{m^2}{\tilde{g}^2}$. Then, the instanton is a collective process consisting of the same mean-number of elementary processes. Each elementary process describes an Euclidean time-evolution of some solitonic constituent over a time-interval L.

Indeed, using the relations (3.7), (3.13) as well as (3.15), we shall now see how the well-known instanton action follows from the above discussion concerning corpuscular resolution of the corresponding soliton. We can explicitly check that we can consistently choose the small-enough time interval $\tau = iL$, so that the coherent state evolves as energy eigenstate according to (3.62). Indeed, we can fix mL arbitrarily small, while keeping $N = m^2/\tilde{g}^2$ arbitrarily large. In this limit the hamiltonian can be taken as $\hat{H} = \int_k |k|\hat{a}^\dagger_k\hat{a}_k$. Then,

$$\langle N_{(sol)}|e^{iH\tau}|N_{(sol)}\rangle \;=\; \prod_k e^{-N_k(1-e^{i|k|\tau})}\,. \tag{3.71}$$

For $\tau \ll m^{-1}$, we can safely assume that $|k|\tau \ll 1$. The reason is that for $|k| \gg m$, the occupation numbers are exponentially-suppressed, $N_k \sim N\frac{|k|}{m}e^{-\pi\frac{k}{m}} \ll 1$, and such modes do not contribute. Expanding the exponent we get, $\prod_k e^{-N_k(1-e^{i|k|\tau})} \simeq e^{i\int_k N_k|k|\tau} = e^{iM_{sol}\tau}$, which for $\tau = iL$ gives (3.62).

We thus reproduce the relation (3.63). Using the expression of the soliton mass in terms of occupation numbers (3.15), we can display the corpuscular structure of the instanton action explicitly. Indeed, using relation (3.56) and (3.15) we can write the instanton action in the form,

$$S_{inst} \;=\; \int_k N_k\, L|k|\,. \tag{3.72}$$

This form makes the physical meaning of the corpuscular nature very transparent. Indeed, N_k plays the role of a "spectral" density for the instanton action. A corpuscle of momentum

k contributes into the instanton action the amount $L|k|$ weighted by the corresponding occupation number N_k.

The next example we want to consider is the correspondence between a $1D$-instanton and a $2D$-soliton with non-zero topological number. For this we have to slightly modify the Lagrangian in order to create two degenerate stable minima. The new Lagrangian reads,

$$\mathcal{L}_{0+1} \;=\; (\partial_t\phi)^2 \;-\; g^2(\phi^2 \;-\; m^2/g^2)^2\,. \tag{3.73}$$

This theory has two degenerate minima at $\phi = \pm m/g$ and there is an instanton solution describing tunneling between the two. The instanton corresponds to the motion of a particle in an inverted potenial. The particle starts at $\phi = \pm m/g$ at $t = -\infty$ and reaches $\phi = \mp m/g$ at $t = +\infty$. The solution is described by a kink or an anti-kink

$$\phi_{ins}(t) \;=\; \pm\,\frac{m}{g}\tanh(tm)\,. \tag{3.74}$$

Correspondingly, there is a soliton in a lifted $1+1$ dimensional theory,

$$\mathcal{L}_{1+1} \;=\; (\partial_t\tilde{\phi})^2 - (\partial_x\tilde{\phi})^2 \;-\; \tilde{g}^2(\tilde{\phi}^2 \;- m^2/\tilde{g}^2)^2\,. \tag{3.75}$$

The soliton is the static solution connecting the two degenerate vacua,

$$\phi_{ins}(x) \;=\; \pm\,\frac{m}{\tilde{g}}\tanh(xm)\,. \tag{3.76}$$

Notice that this is simply the kink of topological charge 1 which we studied in detail in the last section and in the introduction.

Using the results obtained there and the relation between the couplings, action and mass of the theories for the kink and the instanton, respectively, and studying the time-evolution for a small Euclidean time interval as we did in the case of non-topological soliton and instanton, it is again obvious that we reproduce the well-known instanton transition amplitude in this situation as well.

Thus, we again see that the corpuscular picture of an instanton is in $1:1$ correspondence with the one of the soliton with identical field configuration in one more spatial dimension.

Notice furthermore that since the kink exhibits a pole in the occupation number of zero momentum corpuscles, the same pole also occurs in the occupation number of instanton constituents according to our dictionary. Therefore, we can anticipate that also an instanton has vanishing overlap with any state of finite occupation number constructed on the topologically trivial vacuum state. In other words, conservation of topological charge in instanton physics follows as a direct consequence of the corpuscular resolution of the corresponding soliton in one more spatial dimension.

3.3.3 Instanton as Tunneling-Through Soliton

We are now fully prepared to visualize explicitly how the evolution of the soliton state in $1+1$ dimensions is viewed as an instanton transition from the $0+1$-dimensional point of

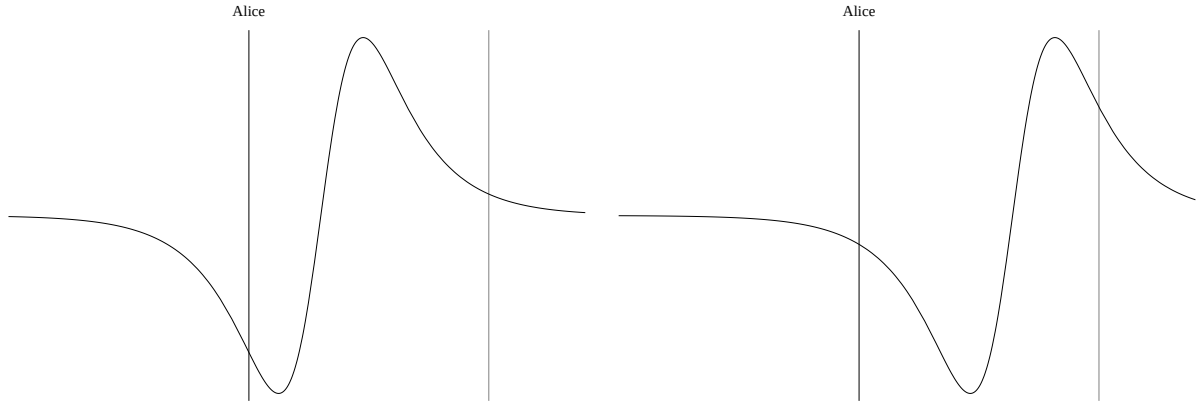

(a) Emergence of the Soliton on the left side of Alice's region from the vacuum.

(b) Soliton passing through Alice's region and discharging into the vacuum on the right side.

Figure 3.1: Soliton evolution as viewed by Alice who is restricted to live on the world volume of the χ-kink which is localized on the scale L (distance between the straight lines). Outside of this kink, the vacuum expectation value of the field $\tilde{\phi}$ vanishes. The Euclidean time evolution of $\tilde{\phi}$ can be interpreted as a "passing-through" virtual soliton. This is interpreted as an instanton induced transition in Alice's effective theory.

view. For this we need to give a setup in which the $0+1$-dimensional theory of an observer Alice is embedded in $1+1$-dimensions. We shall refer to this $1+1$-dimensional theory as Bob's theory. Such a construction will allow us to explicitly identify the length-scale L relating the couplings of both theories and also visualize the connection between the $0+1$-instantons and $1+1$-solitons. We start by considering the following theory of Bob,

$$\begin{aligned}\mathcal{L}_{1+1} \quad &= \partial_\mu\chi\partial^\mu\chi + \partial_\mu\tilde{\phi}\partial^\mu\tilde{\phi} - f^2\Big(\chi^2 - \frac{\mu^2}{f^2}\Big) \\ &+\frac{\tilde{g}^2}{2}\tilde{\phi}^4 + M^2\tilde{\phi}^2 - \beta^2\chi^2\tilde{\phi}^2 \ , \end{aligned} \tag{3.77}$$

where all parameters are chosen positive. This theory allows for kink solutions of the field χ,

$$\chi(x) = \pm\frac{\mu}{f}\tanh(\mu x) \ . \tag{3.78}$$

Let us now study the spectrum of $\tilde{\phi}$ quanta in the background of the kink. For that purpose, consider the linearized equation of motion for $\tilde{\phi}$,

$$\Big(\partial_\mu\partial^\mu + (\beta^2\chi(x)^2 - M^2)\Big)\tilde{\phi} = 0 \ . \tag{3.79}$$

Note that in the decoupling limit, $\beta \to 0$, $\frac{\mu}{f} \to \infty$ with $\beta\frac{\mu}{f}$ fixed, the back reaction on χ from $\tilde{\phi}$ can be ignored and we can look for the solutions for $\tilde{\phi}$ in the fixed χ-background.

Choosing $\frac{\beta^2}{f^2}\mu^2 - M^2 > 0$, we make sure that away from the kink (i.e., for $x \to \pm\infty$), the classical vacuum is at $\tilde{\phi} = 0$. Then the asymptotic states of the $1+1$-dimensional theory of $\tilde{\phi}$ are the $\tilde{\phi}$-quanta of effective positive mass squared given by $M^2_{\tilde{\phi}} = \frac{\beta^2}{f^2}m^2 - M^2$. However, for a wide range of parameters, there also exist modes that are localized on the χ-kink. Indeed, decomposing $\tilde{\phi}(x,t) = \psi(x)\phi(t)$ such that $\partial_t^2\phi(t) = -m^2\phi(t)$, the equation for $\psi(x)$ becomes

$$\left(\partial_x^2 - \left(\beta^2\frac{\mu^2}{f^2}\tanh^2(\mu x) - M^2 - m^2\right)\right)\psi(x) = 0\,. \tag{3.80}$$

For the range of parameters, this equation admits a localized finite norm solution. In particular, for $\frac{\beta^2}{f^2} = 6$ the solution takes the form,

$$\psi(x) = \sqrt{\frac{3\mu}{2}}\sinh(\mu x)\cosh^{-2}(\mu x)\,, \tag{3.81}$$

where the coefficient is chosen in such a way that the norm is $\int dx\psi(x)^2 = 1$. The corresponding mass of the localized mode is

$$m^2 \;=\; 5\mu^2 - M^2\,. \tag{3.82}$$

Furthermore, using equation (3.80), and integrating over x, we arrive at Alice's effective theory,

$$\mathcal{L}_{0+1} = (\partial_t\phi)^2 - m^2\phi^2 + \frac{g^2}{2}\phi^4\,, \tag{3.83}$$

where $g^2 = \tilde{g}^2/L$ and L is determined by the profile of $\psi(x)$ as follows:

$$\frac{1}{L} = \int dx\psi(x)^4 = \frac{9}{35}\mu\,. \tag{3.84}$$

Now notice, that choosing $5\mu^2 < M^2 < 6\mu^2$, we can render $m^2 < 0$, without destabilizing the $\tilde{\phi} = 0$-vacuum outside of the χ-kink. In this way, we achieve the situation in which the z_2 symmetry $\tilde{\phi} \to -\tilde{\phi}$ is spontaneously broken (at the classical level) only in Alice's effective $0+1$-dimensional theory on the kink world-volume, and is unbroken in the $1+1$-dimensional bulk theory of Bob.

In Alice's theory the $0+1$-dimensional field ϕ develops an expectation value, $\phi = \pm\frac{m}{g}$. Thus, the model, indeed, correctly accounts for instanton effects in Alice's theory.

The nice thing about this setup is that it explicitly allows to visualize the $1+1$-dimensional solitonic origin of $0+1$-dimensional instantons. The physical origin is very transparent. In order to see this, notice, that the vacuum outside of the kink corresponds to the phase in which $\tilde{\phi}$-quanta are not condensed. From the solitonic point of view this is the vacuum in which we have a condensate of $\tilde{\phi}$-solitons. Contrary, the world-volume theory of the χ-kink realizes the opposite phase, in which the $\tilde{\phi}$-quanta are condensed,

but solitons are not. Of course, the small thickness $\sim L$ of the χ-kink does not allow the existence of long-lived $\tilde{\phi}$-solitons, because they cannot fit within the world-volume of the χ-kink. However, they can virtually tunnel-through. Consider a tunneling process in which a topological $\tilde{\phi}$-kink emerges from the condensate on one side of the χ-kink, traverses through it and "discharges" in the condensate on the opposite side. This tunneling process in Alice's $0+1$-dimensional theory is seen as instanton transition that changes the sign of the vacuum expectation value (VEV) of ϕ. This is illustrated in figure 3.1. Now we understand in simple terms the physical origin of the instanton amplitude in the soliton language. Indeed, for a virtual soliton to be able to make it across the χ-kink, it must "survive" at least the Euclidean time interval given by the thickness of the kink $L \sim \mu^{-1}$. This is precisely the scale that relates the cutoff of Alice's effective $0+1$-dimensional theory and sets the relation between the coupling of the two theories! The resulting amplitude is given by (3.63).

3.3.4 Gauge Instanton as Tunneling Monopole

Let us consider a different example, in which the $2+1$-dimensional instanton represents a magnetic monopole tunneling through the world-volume of a $2+1$-dimensional domain wall. This domain wall realizes an embedding of a $2+1$-dimensional $U(1)$-gauge theory in $3+1$ dimensions via the gauge field localization mechanism of [78]. The instanton-monopole connection in this setup is relatively well-studied [79–81] and is therefore directly applicable for illustrating our ideas. The $3+1$-dimensional Lagrangian describes an $SU(2)$ gauge theory coupled to a Higgs triplet Φ^a, $a = 1, 2, 3$, in the adjoint representation and has the following form

$$\mathcal{L}_{SU(2)} \;=\; |D_\mu \Phi^a|^2 \;-\; F^a_{\mu\nu} F^{a\mu\nu} \;-\; \lambda^2 \frac{\Phi^a \Phi^a}{v^2} \left(\Phi^b \Phi^b - v^2\right)^2 , \tag{3.85}$$

where D_μ is the $SU(2)$-covariant derivative with the gauge coupling strength $\tilde{g}$ and $F^a_{\mu\nu}$ is the field strength. We have chosen the Higgs potential as in [79]. The two degenerate vacua (modulo sign) are $\langle \Phi^a \rangle = 0$ and $\langle \Phi^a \rangle = \delta^a_3 v$. In the first one, the theory is in the $SU(2)$-phase. In the second one, the $SU(2)$-group is Higgsed down to a $U(1)$ subgroup which (perturbatively) is in the Coulomb phase. In order to create an effective $2+1$ dimensional theory, following [78], we are going to create a layer of $U(1)$-vacuum bounded by $SU(2)$ vacua from both sides. The layer has infinite extend in say the $x-y$-plane and has a width L in z-direction.

In order to create such a layer, we can consider a configuration in which the two phases are separated by a domain wall. The wall describes a classical solution for which the expectation value of the Higgs field interpolates between $\langle \Phi^a \rangle = 0$ and $\langle \Phi^a \rangle = \delta^a_3 v$. There exists an exact solution of the form $\Phi^a = f(z)\delta^a_3 v$ with

$$f(z) \;=\; \frac{\mathrm{e}^{\pm 2mz}}{1 + \mathrm{e}^{\pm 2mz}} \,. \tag{3.86}$$

Here $m \equiv \lambda v$ and the signs $\pm$ correspond to a wall and an anti-wall, respectively. To create a $2+1$-dimensional layer, we can place a wall and an anti-wall parallely at $z = 0$ and $z = L$, respectively.[13]

Then the picture is as follows. For $0 < z < L$ the $SU(2)$ is Higgsed down to $U(1)$, whereas for $z < 0$ and $z > L$ the Higgs VEV vanishes and $SU(2)$ is in the confining phase.

At the classical level the wall and anti-wall are transparent for the $U(1)$-photon. However, in the quantum theory this is no longer true. The $SU(2)$-phase becomes confining and develops a mass gap given by the QCD scale Λ. The photon that wants to escape from the layer must travel across the wall. But since the vacuum outside of the layer is confining, the photon can only penetrate the $SU(2)$-domain in form of a glueball of mass Λ. Correspondingly, the $U(1)$-photon is trapped in the space between the wall and anti-wall.

There are the following energy scales in the problem: The Higgs VEV v, the Higgs mass $m = \lambda v$, the mass of the gauge field $m_W = \tilde{g}v$ and the mass of the glueball Λ. We shall assume the hierarchy $m_W \gg \Lambda \gg L^{-1}$. Then the theory in the layer is in different regimes at different energies. In the energy interval $\Lambda > E > L^{-1}$ the observer (Alice) can resolve the thickness of the layer, and sees it as portion of the $3+1$-dimensional space bounded by the walls. At energies $E \ll L^{-1}$ the resolution is no longer possible and the effective theory of Alice is $2+1$-dimensional electrodynamics with compact $U(1)$. Since $\Lambda \gg L^{-1}$, the gauge coupling of the $2+1$-dimensional theory g is related to the original one (approximately) as $\frac{L}{\tilde{g}^2} = \frac{1}{g^2}$. In this theory there are Polyakov-type instantons [82] which generate the mass gap and confinement for $U(1)$.

By now, the $3+1$-dimensional origin of these instantons is very well understood [79,80]. In the $U(1)$-phase in which Higgs particles are condensed, there exist 't Hooft-Polyakov magnetic monopoles in form of solitons. In the $SU(2)$-phase, however, the magnetic charge is screened and monopoles are condensed. Thus, monopoles can only exist inside the layer in form of solitons, whereas on both sides of it the magnetic charges are in the vacuum.

As a consequence, for a static magnetic monopole placed in the middle of the layer at $z = L/2$, the magnetic field falls-off exponentially for $|x|^2 + |y|^2 \gg L$ even in the direction longitudinal to the layer. This happens due to the existence of the image magnetic charges outside of the layer (see figure 3.2) which screen the magnetic field of the monopole.[14] However, for distances $\ll L$, the magnetic monopole can be reliably approximated by the 't Hooft-Polyakov solution with the mass $M_{sol} = M_W/\tilde{g}^2$, where $\tilde{g}$ is the $3+1$-dimensional gauge coupling.

The instanton of the $2+1$-dimensional theory then corresponds to the process in which a magnetic monopole emerges from the condensate on one side of the layer, tunnels through it and discharges into the vacuum on the other side. This changes the topological number of the layer by one unit. The corresponding Euclidean action of the process can be estimated in the following way. Semi-classically, we can approximate it by evaluating the action of the monopole that evolves through the layer within the shortest Euclidean time, $\tau = L$.

[13] For $L \gg m^{-1}$ the wall-anti-wall system can be viewed as static.

[14] This explains in simple terms the generation of the magnetic photon mass and confinement of electric charges in $2+1$-dimensions.

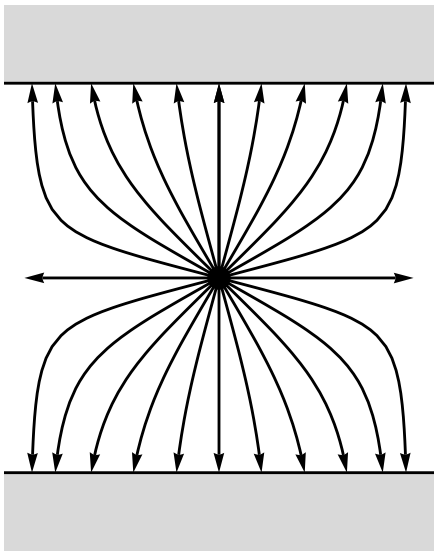

Figure 3.2: Magnetic field produced by a point-like magnetic charge placed in the middle of a layer of width L in the Higgs phase. This layer is surrounded by two confining phases where the Higgs vacuum expectation value vanishes. The magnetic field is screened at exponentially large distances even in the direction longitudinal to the layer due to existence of mirror magnetic charges on both sides of the layer.

This gives the action $S = M_{sol}L$. It is surprising that for M_{sol} taken to be the mass of an unperturbed $3+1$-dimensional monopole, this gives exactly the instanton action computed by Alice in the pure $2+1$-dimensional theory.

Analogously, in the coherent state language, we can evaluate the amplitude in terms of a virtual monopole surviving over the time interval L. This is given by equation (3.62), where M_{sol} is the mass of the monopole.

The fact that the $3+1$-dimensional time evolution of the virtual monopole matches exactly the pure $2+1$-dimensional instanton result, is rather non-trivial. Indeed, one would think that the two computations should become exact in the opposite limits. Alice's $2+1$-dimensional computation should work best in the $L \to 0$ limit, whereas the approximation of the tunneling-through 't Hooft-Polyakov monopole should work best in the limit of $L \to \infty$. However, the situation is more subtle, because the scale M_W which sets the inverse size of Alice's instanton, cannot become smaller than the glueball mass Λ, which sets the localization energy scale. In this way the $2+1$ dimensional theory is "aware" of its $3+1$-dimensional origin, because the instanton size in Alice's theory secretly probes physics of the UV-completion, i.e. of energies above which the $2+1$-dimensional theory is embedded into $3+1$-dimensions.

This probably indicates that the coherent state prescription that matches the instanton and the coherent state amplitudes via (3.63) is insensitive to the details of the embedding.

3.3.5 Scalar Field Theory

In this section we will go to even one more dimension and discuss the corpuscular picture of instantons in four Euclidean dimensions. This is again achieved by mapping it to a soliton evolving in $4+1$-dimensional space-time.

Before discussing the Yang-Mills instanton in the next section we shall consider a scalar toy model resembling some of the features of the BPST-instanton.

This analysis shall serve as a preparation for considering the instanton in gauge theory. The advantage is that in this case many properties of the gauge instanton are captured without need of considering the issues related to gauge redundancy. This enables to clearly isolate the quantum sub-structure behind the key properties such as the existence of size modulus.

Let us consider the following theory of a scalar field in $3+1$ dimensions,

$$\mathcal{L} = \partial_\mu \phi \partial^\mu \phi - g^2 \phi^4 \, . \tag{3.87}$$

It is well known [83] that this theory admits solutions to the Euclidean equations of motion of the following form

$$\phi(x) = \frac{2\rho}{g\,(\rho^2 + x^2)} \, . \tag{3.88}$$

Here ρ is the size modulus whose origin is the underlying scale invariance of the theory. One of the key points we would like to understand, is how this scale invariance translates in terms of the quantum-corpuscular resolution of the instanton.

In order to go to the quantum theory we follow our recipe and map the instanton onto a soliton of a lifted $4+1$ dimensional theory,

$$\mathcal{L} = \partial_\mu \tilde{\phi} \partial^\mu \tilde{\phi} - \tilde{g}^2 \tilde{\phi}^4 \, . \tag{3.89}$$

This theory admits a static soliton solution given by (3.88) in which all the $3+1$ entities must be replaces by the $4+1$-dimensional counterparts, $\phi \to \tilde{\phi}$, $g \to \tilde{g}$ and x has to be understood as 4-dimensional coordinate. The classical energy of the profile is given by $E_{sol} = 8\pi^2/\tilde{g}^2$.

Next, performing the Fourier expansion of the soliton,

$$\tilde{\phi}(x) = \int d^4k \frac{R^2}{4\pi^2\sqrt{2\omega(k)}} \Big(\alpha_k e^{-ikx} \, + \, \alpha_k^\dagger e^{ikx} \Big). \tag{3.90}$$

we determine the Fourier coefficients, which are given by

$$\alpha_k = \frac{\rho^2 \sqrt{2\omega(k)}}{R^2 \tilde{g}} \left(\frac{1}{k} K_1(\rho k) \right) \, , \tag{3.91}$$

where K_1 is the modified Bessel function of the first kind. We now follow our recipe and identify these Fourier coefficients with the expectation values of some Fock space creation

and annihilation operators $\hat{a}_k^\dagger, \hat{a}_k$ over a solitonic coherent state, $|sol\rangle$, via the relation similar to (3.9).

As a result we find the number of corpuscles in momentum mode k

$$N_k = \langle sol|\hat{a}_k^\dagger \hat{a}_k|sol\rangle = \frac{\rho^4 2\omega(k)}{R^4 k^2 \tilde{g}^2}\left[K_1(\rho k)\right]^2 \ . \tag{3.92}$$

The total number is

$$\begin{aligned} N &= R^4 \int d^4k \langle sol|\hat{a}_k^\dagger \hat{a}_k|sol\rangle = R^4 2\pi^2 \int d|k||k|^3 |\alpha_k|^2 \\ &= \frac{4\pi^2\rho}{\tilde{g}^2}\int du u\tilde{\omega}(u)\left[K_1(u)\right]^2 \ , \end{aligned} \tag{3.93}$$

where $u = k\rho$. Again, matching to the classical expression for the energy we find that the effective dispersion of the corpuscles is given by $\omega(k) = 3k$. As a consequence we see that the total number of a soliton coherent state constituents is finite and proportional to the size modulus ρ. Note that the finiteness of the number N tells us that there is no topological charge associated to the profile. Thus, the vacuum can decay via soliton formation.

Furthermore, the fact, that $N \propto \rho$ also has a clear physical meaning. It is due to the existence of the size modulus. Most of the contributions to the soliton mass come from the quanta of wavelength ρ, each contributing an energy $\sim 1/\rho$. So the total energy scales as $M_{sol} \sim N/\rho$. But since N scales proportional to ρ, the energy is independent of the soliton size.

Having mapped the instanton on the corresponding soliton, we can now again establish the connection between the instanton action and the soliton matrix element through the relation (3.63).

3.3.6 BPST-Instanton in $3+1$ Dimensions

We shall now proceed and apply the corpuscular picture to $SU(2)$ Yang–Mills instantons in $3+1$ Euclidean dimensions. In order to do so, we shall follow the recipe outlined in the previous sections and map it to a soliton in one more space dimension.

Let us briefly recall some features of that instanton (for more details, the reader in referred to the introduction). As usual, the Euclidean action can be written as

$$S = \int d^4x \frac{1}{4} G^a_{\mu\nu} G^a_{\mu\nu} = \frac{1}{8}\int d^4x \left(G^a_{\mu\nu} - \tilde{G}^a_{\mu\nu}\right)^2 + Q\frac{8\pi^2}{g^2}. \tag{3.94}$$

Here $G^a_{\mu\nu} = \partial_\mu A^a_\nu - \partial_\nu A^a_\mu + g\epsilon^{abc} A^b_\mu A^c_\nu$ is the non-abelian field strength, $\tilde{G}^a_{\mu\nu} = 1/2\epsilon_{\mu\nu\alpha\beta} G^a_{\alpha\beta}$ its dual, g is the Yang-Mills coupling and Q the topological charge. To be concrete, we will restrict our discussion to the self-dual instanton of $SU(2)$ with winding number one.

The classical profile is obtained as a solution to the classical BPS condition $G = \tilde{G}$ that follows from (3.94)

$$A_{a\mu} = \frac{2}{g}\eta_{a\mu\nu}\frac{x_\nu}{x^2+\rho^2}. \tag{3.95}$$

Here ρ is the size modulus of the instanton and $\eta_{a\mu\nu}$ are the 't Hooft symbols. Note that we have placed the instanton center at $x_0 = 0$.

As before we want to map the instanton to a soliton in an uplifted 5 dimensional theory. We shall call this soliton magnetic monopole. Therefore, we add an additional space-like dimension and promote the gauge field to a function of all five coordinates, $x_\mu, (\mu = 0, 1, 2, 3, 4)$. As before, we need to relate the coupling constants of the two theories according to (3.54) via a fundamental length scale L,

$$\frac{L}{\tilde{g}^2} = \frac{1}{g^2}. \tag{3.96}$$

In five dimensions we get a static configuration which describes a monopole and which is identical to the $4D$ instanton (3.95). The only difference is in re-naming the coordinates: μ index now runs over four space-like coordinates $\mu = 1, 2, 3, 4$. Thus, the monopole solution has the form,

$$\tilde{A}_{a\mu} = \frac{2}{\tilde{g}}\eta_{a\mu\nu}\frac{x_\nu}{x^2+\rho^2}\,. \tag{3.97}$$

The energy of such a monopole is

$$M_{mon} = \frac{8\pi^2}{\tilde{g}^2}\,. \tag{3.98}$$

Notice, that $\tilde{g}^2$ has the dimensionality of a length.

Now according to our correspondence, in order to reproduce the instanton action, we must consider a five-dimensional monopole evolving during the Euclidean time interval L. Thus, we have

$$S_{inst} = M_{mon}\,L = \frac{8\pi^2}{g^2}\,. \tag{3.99}$$

Let us now try to understand the monopole and subsequently the instanton in the quantum picture. As before, this can be achieved most directly by expanding (3.97) in Fourier space:

$$\tilde{A}_{a\nu} = \int d^4k \frac{R^2}{4\pi^2\sqrt{2\omega(k)}}\Big(\eta_{a\nu\alpha}\frac{k_\alpha}{k}\alpha_k e^{-ikx} + \eta_{a\nu\alpha}\frac{k_\alpha}{k}\alpha_k^\dagger e^{ikx}\Big). \tag{3.100}$$

The Fourier coefficients are given by

$$\alpha_k = \frac{\rho^2\sqrt{2\omega(k)}}{R^2\tilde{g}k}\Big[\frac{1}{2}\Big(K_0(\rho k) + K_2(\rho k)\Big) + \frac{1}{k\rho}K_1(\rho k)\Big], \tag{3.101}$$

where K_m, $m = 0, 1, 2$ are modified Bessel functions, $k \equiv \sqrt{k^2}$ and $\omega(k)$ is the dispersion relation of the corpuscles. Following our recipe, we promote these coefficients to expectation values of corpuscular annihilation and creation operators $\hat{a}_k$, $\hat{a}_k^\dagger$ evaluated in the coherent soliton state $|sol\rangle$ which is defined as in equations (3.11) and (3.35).

Let us now investigate how the total occupation number N depends on the modulus ρ. For that purpose, we introduce the dimensionless parameter $u = k\rho$. As before we define the total occupation number as

$$\begin{aligned} N &= R^4 \int d^4k \langle sol|\hat{a}_k^\dagger \hat{a}_k|sol\rangle = R^4 2\pi^2 \int d|k||k|^3 |\alpha_k|^2 \\ &= \frac{4\pi^2\rho}{\tilde{g}^2} \int du u\tilde{\omega}(u) \Big[\frac{1}{2}\Big(K_0(u) + K_2(u)\Big) + \frac{1}{u}K_1(u)\Big]^2 . \end{aligned} \tag{3.102}$$

Here we used that the only dimensionful quantity on which the dispersion relation can depend is ρ. Thus, we can introduce $\tilde{\omega}(u) = \omega(k)\rho$. From equation (3.102) one can directly see that N depends linearly on ρ. Since the modulus sets the size of the monopole, it is reasonable that the occupation number of constituents depends on this size. Therefore, the modulus becomes a physical parameter when we resolve the monopole quantum mechanically. In particular, already at this level our quantum picture reveals that scale invariance is broken by the total number of corpuscles. Nevertheless, to leading order in $1/N$ the energy of the corresponding profile cannot depend on ρ by construction. Note, that we could also have guessed the ρ dependence by dimensional analysis. Since N is dimensionless, while the coupling constant $\tilde{g}^2$ is not, $N \sim \rho/\tilde{g}^2$ is the only remaining possibility. In the following we will further investigate the dispersion relation.

Since the Hamiltonian is not diagonal on the BPS solution in the gauge field and subsequently in the corpuscular creation and annihilation operators, we cannot determine the dispersion relation for the corpuscles as easily as in the previous cases. Thus, the determination of N_k is not as straight forward as in the examples discussed before. Nevertheless, we can still analyze topological properties of the monopole from the corpuscular point of view.

For that purpose note that the origin of topology comes from the asymptotic scaling of the gauge field of the form $\tilde{A}_{a\nu}(x) = \frac{2}{\tilde{g}}\eta_{a\mu\nu}\frac{x_\nu}{x^2}$ which incorporates the scalings of derivatives of the angular coordinate. The typical $1/|x|$-decay of the angular derivatives is a signal of non-zero winding number and thus incorporates topology. In other words, since we consider the homotopy class $\pi_3(S_3)$ it is clear that all information about topology must be encoded in the angular derivatives of the gauge field.

Therefore, we can identify the quanta $\hat{t}_k$, $\hat{t}_k^\dagger$ which contribute to the topological charge. In particular, these are the corpuscles which lead to the pure gauge term $\tilde{A}_{a\nu}(x) = \frac{2}{\tilde{g}}\eta_{a\mu\nu}\frac{x_\nu}{x^2}$ at spatial infinity. As before, we use the Fourier transform to determine the expectation value of these topological annihilation and creation operators in the coherent soliton state,

$$\langle sol|\hat{t}_k|sol\rangle = t_k = \frac{1}{k^2}. \tag{3.103}$$

Similar to the 1 + 1-dimensional soliton case we can define the corpuscles $\hat{c}_k,\ \hat{c}_k^\dagger$ which contribute to the energy of the profile. Note, that the solitonic state can again be written as a product state of the form $|sol\rangle = |t\rangle \otimes |E\rangle$. Then $\hat{c}_k|E\rangle = c_k|E\rangle$ and $\hat{t}_k|t\rangle = t_k|t\rangle$. From $\alpha_k = t_k c_k$ we find

$$c_k = \frac{k^2\rho^2\sqrt{2\omega(k)}}{R^2\tilde{g}k}\Big[\frac{1}{2}\Big(K_0(\rho k) + K_2(\rho k)\Big) + \frac{1}{k\rho}K_1(\rho k)\Big]\ . \tag{3.104}$$

In order to show the topological stability of the solution it suffices to show that the total number of corpuscles is infinite. Since we have the explicit expression for the topological quanta, this is an easy task:

$$N^{top} = \int_{k_0} d^4k N_k^{top} = \int_{k_0} d^4k t_k^* t_k \ \sim\ \log(k_0)|_{k_o\to 0} \to \infty\ . \tag{3.105}$$

Just as in the example discussed in the previous section, the small k divergence is the underlying reason for conservation of topological charge in the corpuscular picture of the five dimensional monopole. This makes sense as the topological charge should be encoded in the large wavelength modes reflecting global structures in the corpuscular picture. Note, that the Hamiltonian is still not diagonal in the energy quanta $\hat{c}_k,\ \hat{c}_k^\dagger$ so that we cannot compute the dispersion relation. Nevertheless, we can explicitly show the topological stability of the soliton, since $\langle 0|sol\rangle \sim \exp(-N^{top}) \to 0$.

Due to the soliton instanton identification via the length scale L, this small k divergence is directly mapped to a similar divergence in the occupation number of instanton constituents. Therefore, we again uncover that topological properties of the instanton are in one-to-one correspondence with corpuscles of infinite wavelength.

3.3.7 Instanton-Induced Transitions

Having presented the dictionary which allows to map instanton physics on soliton coherent states in several examples, we shall now address the question how instanton induced amplitudes involving excited states can be obtained in our approach. For simplicity, we will once more consider the quantum mechanical double well potential. Notice that in the previous sections, we did not directly specify the instanton quantum state in order to compute the vacuum-to-vacuum transition elements. Rather, we gave a prescription which identifies this amplitude with a corresponding soliton evolving in more space dimension. Note, however, that this approach indicates that there should be some quantum state $|I\rangle$ representing the instanton. According to our previous discussion, this state should be directly related to the coherent state in terms of the lengthscale L. In turn, the existence of such a state immediately implies that this state (as well as multi-instanton states) should be contained in the Hilbert space of states of the theory.

Once we have defined the state $|I\rangle$ in that way we can proceed to define the coherent state representation of standard instanton amplitudes. For instance the amplitude $\langle 0+|0-\rangle$

for a double well potential will be given by $|\langle 0|I\rangle|^2$.[15] We can equally consider $\langle n+|n-\rangle$ amplitudes in the instanton background as

$$\langle n+|n-\rangle = |\langle n|I\rangle|^2 \, . \tag{3.106}$$

In what follows we shall use this formalism for the double well potential in quantum mechanics using results of the previous part concerning corpuscular resolution of the topological instanton in $0+1$ dimensions.

Let us now consider the formal $0+1$-dimensional scattering $n_+ \to n_-$, where n initial quanta are defined around the left minimum at time $t=-\infty$ lead to the same number of quanta around the right minimum at $t=+\infty$. All of these quanta have the same energy given by the frequency

$$\omega = \left.\frac{\partial^2 V}{\partial \phi^2}\right|_{\phi=m/g} = 2m \, . \tag{3.107}$$

Note that the instanton contribution to this amplitude gives us the instanton correction to the energy of the level n.

In order to define the coherent state prescription for the computation of this instanton amplitude we first need to identify the creation and annihilation operators associated with the in and out states. Defining them asymptotically in terms of field operators representing the instanton we get

$$\hat{a}(\hat{a}^\dagger)_\pm = 2 \lim_{t=\pm\infty} \sqrt{2\omega}\frac{m}{g}(\tanh(tm) \pm i\frac{m}{\omega}\mathrm{sech}^2(tm)) \, . \tag{3.108}$$

The factor of 2 in front of (3.108) is chosen to make contact with the standard semi-classical computation of the instanton induced transition matrix element. In particular, in the convention of [43], $\phi = m/g + \phi_0 \to \pm 2m/g$ as $t \to \pm\infty$.

Note that the coherent state $|I\rangle$ should only take into account the energetic component of the parent two dimensional soliton which we have used in order to define the corpuscular resolution of the $0+1$-dimensional instanton. In terms of this state the former definition of $\hat{a}$ and $\hat{a}^\dagger$ implies

$$a_\pm|I\rangle = \pm 2\sqrt{2\omega}\frac{m}{g}|I\rangle = 2\frac{m^{3/2}}{g} \, . \tag{3.109}$$

Thus, we observe that these creation and annihilation operators basically act on $|I\rangle$ as c_0. In particular, we have the relation $a = 2\sqrt{L\pi}c_{k=0}$. In this way we get for $\langle n_+|n_-\rangle$

$$e^{-N_{inst}}\frac{(N_{inst,(k=0)})^n}{n!} \, , \tag{3.110}$$

which gives us the result

$$e^{-\frac{4m^3}{3g^2}}\frac{1}{n!}\Big(16\frac{m^3}{g^2}\Big)^n \, . \tag{3.111}$$

[15] In principle, also multi-instanton events contribute. For simplicity, however, and in order to compare to the literature, we will restrict our discussion to the one-instanton sector.

Notice that (3.111) is in perfect agreement with results from the literature based on a semi-classical saddle-point analysis [41, 43][16]. In contrast, however, the corpuscular recipe we have used does not rely on the notion of classical saddle-point. Instead, it can be formally interpreted as

$$\langle n|I\rangle\langle I|n\rangle. \tag{3.112}$$

It is important to note that the transition amplitude (3.111) is only accurate as long as $n \ll m^3/g^2 \sim N_{inst}$. At the semi-classical level, the breakdown of the approximation is simply related to the fact that at this point the fluctuations become as important as the background. In other words, the saddle-point analysis is no longer valid.

The question we shall now address is whether the problem of unitarity violation can be easily circumvented in the corpuscular approach. Indeed, our construction of the operators (3.108) actually seems somehow artificial from the point of view of the corpuscular identification of instantons in d and solitons in $d+1$ dimension. Defining the in- and out-states instead directly in terms of the solitonic quanta we would instead find

$$\langle n_+|n_-\rangle_c = e^{-\frac{4m^3}{3g^2}}\frac{1}{n!}\Big(\frac{4}{\pi}\frac{m^3}{g^2}\Big)^n\,, \tag{3.113}$$

where the subscript c reminds us that we work solely with solitonic corpuscles evolving over the Euclidean time-interval L. Note that we have

$$e^{-\frac{4m^3}{3g^2}}\frac{1}{n!}\Big(\frac{4}{\pi}\frac{m^3}{g^2}\Big)^n < e^{-4\frac{m^3}{g^2}(1/3-1/\pi)} < 1\,. \tag{3.114}$$

We thus see that this amplitude is always bounded and therefore unitary. Of course, at this point, this approach seems to be rather speculative. Nevertheless, we think that it is interesting, that this amplitude just satisfies the unitarity bound.

3.3.8 Quantum Meaning of Resurgence

In the previous sections, we have argued, that the existence of a quantum coherent state description of the soliton implies that there should be a quantum description of an instanton in one less spatial dimension. We will now address the question, whether the existence of the corresponding quantum states describing solitons and instantons, respectively could shed new light on the physics of resurgent trans-series. As we have already explained in the introduction, resurgence is based on the idea that ambiguous imaginary contribution to physcal quantities generated after Laplace-Borel transforming the perturbative series around the vacuum of the theory should be canceled when non-trivial saddle points such as instantons or solitons are taken into account. While this idea is intriguing, there is so far no proof of the resurgent structure of a QFT. Rather, it was demonstrated in several examples. It is the purpose of this section to develop a full quantum understanding of the physics of resurgence. In other words, we try to explain that quantum mechanically,

[16] In order to get the full answer, we should multiply the previous expression by the translational zero mode contribution.

the resurgent structure of amplitudes follows as a simple consequence of the optical theorem. Furthermore, we understand that the phases of Borel summability as well as Borel non-summability can be understood easily from the point of view of the energy/topology decomposition which we have introduced before.

Let us first recall a few basic facts about Borel resummation. Consider a formal perturbative series

$$f(g) = \sum a_n g^n \tag{3.115}$$

with $a_n \sim A^n n!$. In this case we define the Borel transform

$$B(f)(x) = \sum \frac{a_n x^{n-1}}{(n-1)!} \tag{3.116}$$

$B(f)(x)$ is analytic in a neighbourhood of $x = 0$ in the x plane. Formally the Borel summation is defined by the Laplace transform of $B(f)(x)$

$$LB(f)(g) = \int_0^\infty e^{-\frac{x}{g}} B(f)(x) dx \tag{3.117}$$

The sum is then defined as $LB(f)(g) + c$ for c some constant. Note that the sum is well defined if and only if $B(f)(x)$ is analytic for x positive. In this case we say that the series is Borel summable. If on the contrary $B(f)(x)$ has *poles* for positive x we need a prescription to define the Laplace transform i.e. a choice of contour of integration[17].

For the simplest case of singularities on the positive x line we can use two different definitions for the sum $LB(f)(g)_\pm$ corresponding to the two paths of integration around the positive x axis. This leads to an ambiguity in the definition of the sum, namely for the case of a pole at $x = A$

$$LB(f)(g)_+ - LB(f)(g)_- = Se^{-\frac{A}{g}} \tag{3.118}$$

for S some imaginary number. This number can be understood as Stokes parameter assuming the positive real axis is a Stokes line.

In summary the first lesson we get from the Borel Laplace resummation is that in the case of a perturbative series which are not Borel summable the result can contain exponentially small imaginary parts.

Let us now imagine that $f(g)$ above is an amplitude defined perturbatively in some quantum field theory, let us say $M(A \to A)(g)$. This could for example be the the vacuum energy, or the level splitting of higher excited states. Obviously the Borel prescription above defines an imaginary part for this amplitude

$$\mathrm{ImM(A \to A)} = \mathrm{Se}^{-\frac{\mathrm{A}}{\mathrm{g}}} \ . \tag{3.119}$$

[17]Although the Borel summation is well defined if there are only poles on the negative real axis, there is still interesting physics to extract from those poles. In particluar, the singularities are directly related to ghost instantons, alternating series and IR renormalons.

Unitarity can be implemented by the optical theorem,

$$\mathrm{ImM(A \to A)} = \sum_{\mathrm{s}} |\langle \mathrm{A|s} \rangle|^2 \, . \tag{3.120}$$

Thus we can interpret the Borel imaginary part as the existence of a quantum state $|s\rangle$ with overlap with the state $|A\rangle$ exponentially small.

This strongly indicates that the state $|s\rangle$ is *a coherent state* with average number of quanta of the order $\frac{A}{g}$. This number of quanta is of the same order as the value n for which the original asymptotic series starts to diverge. From now on we shall assume the existence of this quantum state that we shall denote *The Borelon*.

In particular, from our discussion concerning the coherent state description of the soliton-anti-soliton interaction, it is clear that this interaction exactly generates the correct coefficient to cancel ambiguities in the perturbative sector on the trivial vacuum. Note that there cannot be any such contribution in the one-soliton (instanton) sector, because this state has topological charge 1. As a consequence, it does not contribute to (3.120) if A corresponds to a quantity defined with respect to the sector of vanishing topological charge. Notice furthermore, that (3.120) suggests that a similar cancellation must take place in all possible sectors, i.e. $Q = 1,\ 2,\ 3, \ldots$.

A priori, it is perfectly possible that we can find some classical saddle points that contribute to the amplitude we are working out. Once added to the perturbative series we get for the amplitude a trans-series of the type

$$f(g) = \sum a_n g^n + C(g) e^{-S} \, , \tag{3.121}$$

where S the classical action of the corresponding classical saddle point and $C(g)$ accounts for the perturbative expansion of quantum fluctuations around this saddle point. Generically, we can have many different saddle points i.e. $f(g) = \sum a_n g^n + \sum_s C_s(g) e^{-S_s}$.

In this case we can have two contributions to the imaginary part of the amplitude. The first one is due to the ambiguity in defining the Laplace transform while the second one is encoded in the non-perturbative sector of the theory.

$$\mathrm{ImM(A \to A)} = \mathrm{Se}^{-\frac{\mathrm{A}}{\mathrm{g}}} + \mathrm{ImC(g)e}^{-\mathrm{S}}. \tag{3.122}$$

The simplest physics criterion which allows to discover the imaginary part of the semi-classical configuration is to consider the translational mode. Indeed, if the saddle point depends only on one collective coordinate, imaginary parts can be anticipated if the derivative, i.e. the translational zero mode, of the profile has nodes. If this is the case, relying on standard quantum mechanics, we know that the associated state does not minimize the Hamiltonian. In other words, the profile is unstable with respect to decay into a lower energy eigenstate. Using the convolution representation of the saddle point it is easy to see the role of topology in eliminating these potential imaginary parts.

In general, imagine that you have $\phi_{sp} = f \star H$, where H the Heaviside function encoding the topology and f a smooth nodeless function representing the distribution of energy.

Note that the notation ϕ_{sp} suggests that we are considering a generic saddle point at the moment which could be a soliton or instanton, but also a more general solution of the classical equantions of motion. Using the derivative of the convolution

$$df \star g = df \star g = f \star dg \tag{3.123}$$

we discover that for configurations with non-trivial topology, i.e. with some H like function (in $1+1$ dimensions)

$$d\phi_{sp} = f \star \delta = f \ . \tag{3.124}$$

In other words, the translational mode has no zeros. This is of course not the case if we consider a non topological saddle point with $\phi = f \star \delta$. In this case

$$d\phi_{sp} = df \star \delta = df \tag{3.125}$$

which, of course, contains a node if the energy distribution described by f has a maximum at the location of the lump.

Thus, for a saddle ϕ_{sp} the existence of imaginary parts depends on the existence of nodes of $d\phi_{sp}$. We can use the convolution $\phi_{sp} = f \star g$ with f characterizing the energy and g the topology to distinguish several cases:

- A-Non topological: $\phi_{sp} = f \star \delta$. In this case $d\phi_{sp}$ is just given by df which has a node if the energy is located. This sort of lumps is not protected topologically. In run, it has a finite decay time leading to imaginary contributions. This decay is due to the interaction among the constituents of the energy lump. The decay rate is a consequence of the *quantum* decoherence of the corresponding coherent state.

- B-Topological: $\phi_{sp} = f \star H$. In this case $d\phi_{sp}$ is just f, i.e. nodeless. The lump of energy is stable.

- C-Non topological but with topological composition. In this case we generically have $\phi_{sp} = f \star B(a)$, where $B(a)$ is the box function of size 1. In this case $df = f_a - f_{-a}$ i.e. we get a node due to the topological constituency. Contrary to case A above the decay is due to the interaction among the topological components. This decay, in contrast to case A, is *classical*.

- D-Topological but with topological constituency. As an example we can consider $\phi_{sp} = f \star S(N)$, where $S(N)$ is the staircase function with N steps. In this case $df = \sum_N f$ i.e no nodes. As a consequence, the derivative of the profile does not vanish. Thus, the configuration is stable with respect to decay.

It is interesting to see that nodes of $d\phi_{sp}$ are related with infinite number of $k = 0$ modes i.e. poles in the Fourier transform of the topological part of the convolution.

After the previous discussion it is clear that for the case of non-topological solitons of type A (in the former classification) we can represent those systems as coherent states of

ordinary quanta. However, since they have instability we can associate to them a Lyapunov exponent and a quantum break time.

In order to understand the Borelon dynamics it is convenient to consider as a toy model a potential with two minima 1 and 2. Let us do perturbative physics about the point 1. We can tune the potential in such a way that we change the height of the second minimum 2. In this way we can consider two different phases

- Borel summable phase. It corresponds to the height of 2 bigger than zero. In this case the perturbative expansion around 1 is Borel summable and therefore we do not have a Borelon.
- Non Borel summable phase. It corresponds to the height of 2 to be smaller than zero. In this case the perturbative expansion is non Borel summable and a Borelon appears in the spectrum. The life time of this Borelon becomes smaller and smaller with the negative height of 2.
- Critical double well. In this case 1 and 2 are degenerate i.e. we have a double well like potential. This is the transition point between the Borel and non Borel phases. The Borelon in this critical point becomes a soliton-anti-soliton pair. They annihilate and the Borelon disappear.

Thus, we see that the physics of resurgence can be understood in terms of solitonic phase transitions. This can be understood very easily in terms of the topology/energy decomposition which we used to disentangle energetic and topological quanta. Furthermore, since we associate quantum coherent states entities which are usually introduced on purely classical grounds, we saw that the resurgent trans-series structure of the different phases follows from the simple fact, that these states must be included in the full Hilbert space of the theory. From this point of view, there is nothing special about the cancellation of ambiguous imaginary parts. Rather, this cancellation must take place as a consequence of the unitarity of the S-matrix.

Although we exemplified our reasoning concerning the different phases of Borel (non)-summability in the simple case of solitons (instantons) in $1+1$ $(0+1)$ dimensions, our arguments are much more general. Indeed, everything that we have said should be applicable to arbitrary solitons and instantons. As such, the work presented here could be viewed as a first step in understanding the necessity of the resurgent structure of a QFT.

3.4 Supersymmetry Breaking

We will now proceed with a discussion of corpuscular effects in the context of supersymmetric theories. Our main goal is to uncover deviations from a mean field description based on classical solutions in terms of corpuscular quantum effects. These effects are of particular interest when considering solitons in supersymmetric theories. We will show in detail that the corpuscular effects lead to deviations from the BPS condition which can never be uncovered in a semi-classical treatment even if backreaction on the classical soliton profile

is taken into account. These findings show that in the presence of a soliton, supersymmetry must be broken completely in the corpuscular theory. Detailed calculations demonstrating the phenomenon are performed in the case of a Wess-Zumino model in $(1+1)$ space-time dimensions.

The phenomenon of supersymmetry breaking can be understood in terms of corpuscles running in loops and the subsequent need for renormalization of the classical coherent state data[18].

Since we will carefully distinguish between corpuscular quantum effects and the ones originating from fluctuations on top of the background, we carefully need to distinguish between corpuscular algebras and algebras for fluctuations. Thus, in order to give a self-contained presentation, we will repeat some aspects of corpuscular creation and annihilation operators. In this part, however, we will confront the corpuscular algebra directly with the corresponding operators for the fluctuations in the background. Before discussing the concrete example of the Wess-Zumino model, we will first try to motivate our approach in rather general terms. This will in particular help the reader distinguishing corpuscular corrections and the role they play in defining a proper Hamiltonian form the usual loop expansion involving fluctuations on top of a classical background.

3.4.1 Motivation

There are two major sources giving rise to quantum corrections to classical results. The first one, which is commonly studied in the high energy literature, corresponds to loop corrections of small fluctuations in a given classical background. This background can either be the trivial vacuum or some non-trivial configuration such as a soliton in field theory or a black hole in gravity. The effect of these quantum corrections is to renormalize the classical background. For example, in the case of a soliton, these effects lead to a renormalization of the mass of the profile. The second source, usually not considered in the literature, is due to the quantum mechanical nature of the background itself. In other words, since the background should be viewed as a composite system of N quanta at the microscopic level there are in general corrections to classicality as long as N is finite.

Keeping ourselves in the weak coupling regime, i.e. in the regime where N is larger than one, it is pretty obvious that for the quantum coherent state, as a many quanta system, there are quantum $1/N$ effects that affect the quantum coherence of the system. The classical description of the soliton corresponds to the limit $N = \infty$ where we ignore quantum effects. This is the limit where we effectively put $\hbar = 0$ in what concerns the *inner structure* of the soliton. This should not be confused with ignoring quantum fluctuations of the classical soliton configuration. Those quantum fluctuations are defined as collective effects of a system of many quanta defining the soliton.

[18]Note that alternatively, switching back to the many-body language used to define the time evolution operator of the soliton state, the same physics can be understood in terms of the dynamics of quasi-particle excitations of the soliton. Obviously, since these particles account for deviations from the mean-field, they effectively correct the coherent state data as well. Thus, the phenomenon of supersymmetry breaking can also be understood in the many-body language.

To distinguish these effects it is convenient to use, at least at a formal level, two algebras of creation and annihilation operators. As usual there is an algebra A_q of creation annihilation operators $\hat{b}_k$ and $\hat{b}_k^\dagger$ representing *collective quantum fluctuations of the soliton*. This algebra is defined as usual by introducing a quantum field through

$$\phi(x) = \phi_{sol}(x) + \phi_q(x) \ , \tag{3.126}$$

where ϕ_{sol} is the classical c-number configuration and ϕ_q the quantum fluctuation. The algebra of A_q is defined by expanding the quantum field ϕ_q. The quantum soliton state is then formally defined by a state $|\phi_c\rangle$ satisfying

$$\hat{b}_k|sol\rangle = 0 \ . \tag{3.127}$$

A different algebra A_a which we shall denote *corpuscular algebra*, with creation and annihilation operators $\hat{a}_k$ and $\hat{a}_k^\dagger$ should be introduced. This algebra is associated with the quanta entering into the composition of the solitonic coherent state as explained in the previous sections. Thus, relative to this algebra the soliton quantum state $|sol\rangle$ behaves as a coherent state

$$\hat{a}_k|sol\rangle = \alpha_k|sol\rangle \equiv \sqrt{N_k}|sol\rangle \ . \tag{3.128}$$

In summary the complete quantum soliton system including fluctuations as well as the corpuscular structure is defined by the two algebras A_q and A_a via conditions (3.127) and (3.128). Once we have defined the two relevant algebras there are two obvious questions. The first one is the question of understanding classical properties such as topology and mass associated with the soliton as an emergent phenomenon to leading order in $1/N$ in quantum mechanical terms. This was already answered in the first part of this chapter. The second question which needs to be addressed is connected to unraveling higher order corpuscular effects and studying their implications. This will be the main focus of this section.

Already at this level of the discussion a natural puzzle appears. In supersymmetric theories we are used to a very special class of solitons, namely the BPS solitons. Classically, such solitons preserve half of the supersymmetries. The key consequence of this fact is that they are protected from quantum corrections involving $\hat{b}_k$ and $\hat{b}_k^\dagger$ quanta. However, if in the weak coupling we define such entities as many body systems of quanta, how can supersymmetry manage to protect the system with respect to $1/N$ effects for finite N?

The question is obviously puzzling because the soliton as a coherent state is purely bosonic and its representation as a coherent state seems to be a priori independent of the existence of any underlying supersymmetry, at least for those solitons with a well defined classical definition. The duality argument, at least in those cases where a dual theory can be identified, is telling us that when we move into strong coupling the soliton can become, relative to the dual theory, an elementary particle that behaves with respect to supersymmetry as a short representation. But what happens in between? Indeed, it is left unanswered how supersymmetry keeps the system protected from $1/N$ effects in the weak coupling regime by this general duality argument.

Obviously, understanding these questions is of utmost importance because if $1/N$ effects do not cancel out we are identifying a new mechanism of supersymmetry breaking once we put ourselves on solitonic backgrounds that are classically BPS.

In what follows we shall address this questions in a modest way using an example. This example indicates that the intrinsic *quantum noise* due to the composition of the soliton as a many quanta system generically breaks the BPS condition.

3.4.2 Normal Ordering in SUSY

Let us consider a generic supersymmetric (SUSY) system and let us denote by $\hat{H}$ the Hamiltonian[19]. In order to define normal ordering we need to introduce an algebra of creation and annihilation operators. We can do so using the Schrödinger picture in the standard way for some $\omega(k)$ that we do not need to fix a priori. The first thing we know about SUSY is that

$$\langle 0|\hat{H}|0\rangle = \langle 0| : \hat{H} : |0\rangle \tag{3.129}$$

for $|0\rangle$ the vacuum of the theory.

Quantum protected states $|\psi\rangle$ are those which share this property with the vacuum, i.e.

$$\langle \psi|\hat{H}|\psi\rangle = \langle \psi| : \hat{H} : |\psi\rangle \tag{3.130}$$

A prototype example of such a protected state is the BPS soliton. In order to understand this fact the first thing we need to do is to identify how to associate with a given classical configuration a quantum state. Given a classical configuration $\phi_{sol}(x)$ which is a saddle point, we normally define quantum fluctuations around it. This standard approach provides an algebra A_q of creation annihilation operators $\hat{b}_k$ and $\hat{b}_k^\dagger$ associated with the quantum fluctuations of the classical configuration. Relative to this algebra we define the state $|sol\rangle$ by the condition (3.127), $\hat{b}_k|sol\rangle = 0$.

In other words, this state is a "vacuum" relative to the quanta $\hat{b}_k$ and $\hat{b}_k^\dagger$. Moreover the decomposition of the field as $\phi_{sol} + \phi_q$ implies that

$$\langle sol|\hat{H}|sol\rangle = H_c + \langle sol|\hat{H}^q(\hat{b}_k, \hat{b}_k^\dagger)|sol\rangle \tag{3.131}$$

where the c-number H_c is simply the classical energy of the configuration ϕ_{sol}.

What happens if the classical configuration ϕ_{sol} satisfies the classical BPS condition and we are working in a supersymmetric theory? In this case we expect

$$\langle sol|\hat{H}|sol\rangle = H_c \ , \tag{3.132}$$

or equivalently

$$\langle sol|\hat{H}^q(\hat{b}_k, \hat{b}_k^\dagger)|sol\rangle = \langle sol| : \hat{H}^q(\hat{b}_k, \hat{b}_k^\dagger) : |sol\rangle = 0 \ . \tag{3.133}$$

The reason for this expectation is simply the following. Due to the fact that ϕ_{sol} is classically BPS, the Hamiltonian $\hat{H}^q$ defined after introducing $\phi = \phi_{sol} + \phi_q$ preserves by

[19]For convenience we choose to put "hats" on the quantum Hamiltonian in this section.

construction half of the supersymmetries as already explained in the introduction. Therefore, since $|sol\rangle$ is a vacuum with respect to the algebra A_q of $\hat{b}_k$ and $\hat{b}_k^\dagger$, we find that after normal ordering we simply get zero quantum corrections due to loops of $\hat{b}_k$ and $\hat{b}_k^\dagger$ quanta. The reason is the underlying unbroken supersymmetry of $\hat{H}_q$ which implies that loops of $\hat{b}$ quanta are canceled by the fermonic partners.

Note, however, that in this standard argument we have ignored the quantum nature of the soliton in the weak coupling as a coherent state composed of an average number of quanta N.

3.4.3 Corpuscular Resolution: Definition

Next we should consider the representation of the quantum soliton as a quantum coherent state as we have done in previous sections. We shall denote that representation the corpuscular resolution of the soliton. This resolution is based on promoting the c-number $H_c(\phi_{sol})$ into an operator

$$H_c(\phi_c) \to \hat{H}(\hat{a}_k, \hat{a}_k^\dagger) \tag{3.134}$$

with $\hat{a}_k$ and $\hat{a}_k^\dagger$ fulfilling the **corpuscular algebra** A_a relative to which the state $|sol\rangle$ is a coherent state

$$\hat{a}_k|\phi_c\rangle = \sqrt{N_k}|sol\rangle \tag{3.135}$$

Just as before, the N_k are Fourier data determined by ϕ_{sol}.

After introducing the algebra A_a we can promote the c-number energy $H_c(\phi_{sol})$ into an operator $H(\hat{a}_k, \hat{a}_k^\dagger)$,

$$\langle sol|\hat{H}|sol\rangle = \langle sol|\hat{H}(\hat{a}_k, \hat{a}_k^\dagger)|sol\rangle + \langle sol|\hat{H}^q(\hat{b}_k, \hat{b}_k^\dagger)|sol\rangle \tag{3.136}$$

where $\hat{H}(\hat{a}_k, \hat{a}_k^\dagger)$ is the original Hamiltonian written in terms of $\hat{a}_k$ and $\hat{a}_k^\dagger$ operators.

The previous equation makes explicit the key difference between *corpuscular effects* encoded in $\hat{H}(\hat{a}_k, \hat{a}_k^\dagger)$ and normal quantum effects due to collective quantum fluctuations of the soliton.

In the previous representation we are not including effects which couple $\hat{b}$ and $\hat{a}$ quanta. These effects can certainly exist and, in the case of BPS classical solitons, these can induce non supersymmetric corrections to the quantum Hamiltonian $\hat{H}_q$. These effects will be the analog of the many body interactions among phonons b quanta and electrons c quanta and can be of great importance. In particular, as we shall show below, these couplings will be a source of Fermi-Bose mass splitting via corpuscular effects.

3.4.4 Quantum Corpuscular Corrections

At the level of the coherent state representation of the soliton we can identify the simplest corpuscular effects as normal ordering effects. These are the simplest quantum effects we can think about and they are sourced by the quantum commutation relations among the $\hat{a}$ quanta.

In order to define these effects we simply use the definition of normal ordering using the Wick theorem for the corpuscular Hamiltonian.

As we shall see in an explicit example in the next subsection these normal ordering effects do not reduce simply to the addition of an infinite constant like it is the case for the vacuum energy. Indeed for a soliton state they generate infinities of a different type correcting the couplings of the theory. In that sense, although these divergences are of normal ordering type, they need to be taken into account to define properly the theory. This is similar to what happens for bosonic theories in two dimensions where the infinities are all of normal ordering type. In that case these infinities not only generate an additional constant to the energy but also they renormalize the coupling.

In general we can write

$$\hat{H}(\hat{a}_k, \hat{a}_k^\dagger) =: \hat{H}(\hat{a}_k, \hat{a}_k^\dagger) : + contractions \tag{3.137}$$

where the contractions are defined relative to the Green's function $G_a(k)$ of the $\hat{a}$ quanta and are associated with loops of $\hat{a}'s$ with just one vertex. Note that the coherent state construction guarantees that to leading order, the Hamiltonian simply reduces to its classical value (normal-ordered part in (3.137)). Quantum corpuscular, or $1/N$ corrections, are then simply encoded in the *contraction* term[20].

What we shall show next in a concrete example is that

$$\langle sol|\hat{H}(\hat{a}_k, \hat{a}_k^\dagger)|sol\rangle = H_c(\phi_{sol}) + divergences \tag{3.138}$$

where the divergences are due to the different contractions. In that sense these divergences can be eliminated by brute force normal ordering:

$$\langle sol| : \hat{H}(\hat{a}_k, \hat{a}_k^\dagger) : |sol\rangle = H_c(\phi_{sol}), \tag{3.139}$$

or in other words, at this level, all corpuscular effects are normal ordering effects. As we have already explained, this is similar to the two dimensional bosonic case where all loop divergences are normal ordering effects.

The key thing to be noticed is that the state $|sol\rangle$ is not BPS protected, i.e. the divergences coming from the contractions are not suppressed by supersymmetry, thereby effectively leading to a corpuscular renormalization of the superpotential. Let us try to understand this phenomenon from the point of view of the topology-energy split discussed before. Since the quanta which account for conservation of topological charge are of infinite wavelength, they are not subject to quantum fluctuations. The corpuscles which carry information about the energy, in contrast, have wavelength of the order of the typical size of the classical configuration. As a consequence, such particles are sensitive to quantum effects. This argument indicates that at the corpuscular level the equivalence of topological

[20] In the many-body language, the same effect is captured by the dynamics of quasi-particle excitations. Indeed, also in this approach the leading order Hamiltonian is simply the classical mass of the soliton. The *contraction* term (3.137) on the other hand, is replaced by bilinear terms coupling Bogoliubov modes to the classical mean-field.

charge and energy cannot be maintained. Indeed, corpuscular deviations from the BPS condition should appear at order $1/N_e$ with N_e the number of quanta contributing to the energy of the profile.

3.4.5 The Meaning of the Effect

Of course, if we define the corpuscular Hamiltonian by its normal ordering ignoring the effects of the loops due to the contractions we recover the standard results, i.e.

$$\langle sol|\hat{H}|sol\rangle = \langle sol| : \hat{H}(\hat{a}_k, \hat{a}_k^\dagger) : |sol\rangle + \langle sol|\hat{H}^q(\hat{b}_k, \hat{b}_k^\dagger)|sol\rangle = H_c + \langle sol|\hat{H}^q(\hat{b}_k, \hat{b}_k^\dagger)|sol\rangle \ , \tag{3.140}$$

and SUSY is unbroken relative to this Hamiltonian. Since the divergences originate from real physical effects coming from loops of $\hat{a}$'s in the Wick contractions, we should take them seriously. The physical meaning of these effects is quite clear. The coherent state is defined relative to classical data and corpuscular quantum normal ordering effects are renormalizing these classical data. In that sense the quantum coherent state defined by the classical data is effectively loosing coherence due to the "quantum noise" of the constituent quanta.

In the example we will consider in the next subsection these divergences appear as different powers of

$$\ln(\frac{\Lambda}{\mu}) \tag{3.141}$$

with Λ a UV cutoff and μ a scale of the problem. Thus, the BPS condition is only effectively satisfied when we work at length scales much larger than the typical width. From this point of view the normal ordering prescription is equivalent to set $\Lambda = \mu$ i.e, to set the corpuscular UV cutoff to be equal to the typical length scale of the soliton preventing its resolution.

3.4.6 Example: Wess-Zumino

In order to illustrate the ideas outlined above, we will now consider the explicit example of a kink in a $1+1$-dimensional Wess Zumino model. The classical Lagrangian is given by

$$\mathcal{L} = \frac{1}{2}\left[\partial_\mu\phi\partial^\mu\phi + \bar{\psi}i\gamma^\mu\partial_\mu\psi - \Big(\frac{\partial\mathcal{W}}{\partial\phi}\Big)^2 - \Big(\frac{\partial^2\mathcal{W}}{\partial^2\phi}\Big)\bar{\psi}\psi\right]. \tag{3.142}$$

Here ψ is a two-component Majorana spinor, $\gamma^0 = \sigma^2$ and $\gamma^1 = i\sigma^3$ with σ^μ, $\mu = 0, 1$ the Pauli matrices. The superpotential of the model has the following form,

$$W = \frac{m^2}{g}\Phi - \frac{g}{3}\Phi^3, \tag{3.143}$$

where m is a parameter of mass dimension and g is the coupling.

Classical, static BPS saturated kinks are found by minimizing the bosonic energy functional performing a standard Bogomol'nyi completion just as in the non-SUSY case (and setting $\psi = 0$):

$$H = \frac{1}{2}\int dx\Big[(\partial_x\phi) \pm \Big(m^2/g - g\phi^2\Big)\Big]^2 \mp \int dx\partial_x\phi\Big(m^2/g - g\phi\Big). \tag{3.144}$$

It is obvious that the Hamiltonian is minimized when the first term in (3.144) vanishes. Focusing on the minus-sign in (3.144) leads to the classical BPS condition,

$$\mathcal{O}_{BPS} \equiv \partial_x\phi - \Big(m^2/g - g\phi^2\Big) = 0. \tag{3.145}$$

Solving this equation one immediately finds the classical profile of the kink,

$$\phi_c(x) = \frac{m}{g}\tanh(xm), \tag{3.146}$$

which, of course, has the same form as its non supersymmetric counterpart analyzed in detail in the previous sections. Notice that on this profile the second term on the right-hand side of (3.144) reduces to $\int dx\partial_x\mathcal{W} = \mathcal{W}(x=\infty) - \mathcal{W}(x=-\infty)$ which is simply the topological charge Z of the kink. This implies that the Hamiltonian is given by the topological charge of the profile. Since the $\mathcal{N} = 1$ supersymmetry algebra in $(1+1)$-dimensions including a central extension schematically has the form $\{Q_1, Q_1\} = H - Z$ we can conclude that a part of supersymmetry is preserved by the kink profile. The second supercharge Q_2, however, does not annihilate the soliton state. Thus, the configuration preserves exactly half of the supersymmetries, i.e. it is 1/2 BPS.

Let us now proceed by briefly reviewing the standard semi-classical approach to quantum fluctuations around the kink profile. Expanding the field as in (3.126) and taking into account fluctuations of fermions as well, one can look at quantum corrections to the energy of the system. Although mass and central charge are renormalized, this renormalization still preserves the BPS condition [55]. In other words, supersymmetry protects the BPS condition, even if quantum fluctuations on top of the classical background are taken into account[21]. As we will discuss in the next subsection, this is no longer true if we take the corpuscular structure into account. Thus, as we already tried to explain in previous sections, what we will uncover are completely new quantum effects which can never be uncovered within the semi-classical approach to solitons.

In order to demonstrate these statements explicitly for the kink, we will now evaluate corrections to the BPS condition in the corpuscular theory of the kink. Since we will show that the central charge will not receive any corrections, a non-vanishing BPS operator immediately implies that the mass of the profile can no longer be given by its central charge. Equivalently, this suggests that all supersymmetries must be broken by the kink

[21] In $3+1$-dimensions, non-renormalization theorems ensure that there are no quantum corrections to the BPS condition at all. Thus, energy density and central charge of a domain wall are given by their classical values to all orders in perturbation theory.

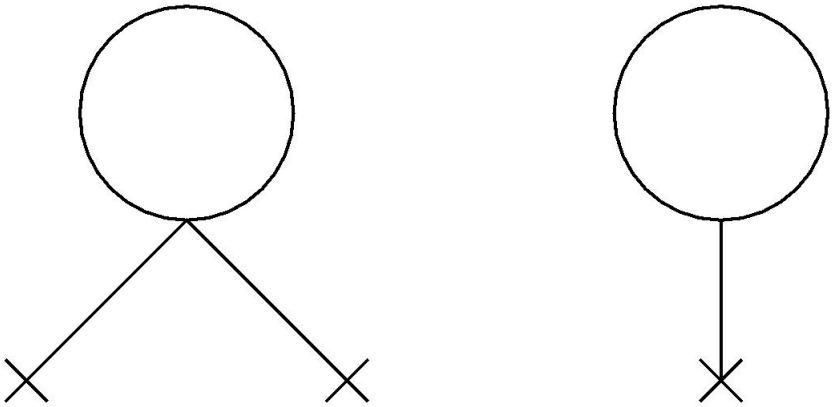

Figure 3.3: Diagrams contributing to the renormalization of the classical data N_k. Crosses correspond to the classical field and loops symbolize quantum contributions due to commutators. The first diagram represents the ϕ_c^2 contribution and the second one the term proportional to $\partial_x\phi$ in (3.147).

when resolved quantum mechanically implying the existence of a second goldstino zero mode on the background.

Using the techniques developed in the previous sections to resolve the kink as a coherent state, let us evaluate the BPS operator in the soliton state taking quantum corrections explicitly into account. Since the operator contributes as a perfect square into the Hamiltonian, let us consider $\langle\phi_c|\mathcal{O}^2_{BPS}|\phi_c\rangle$. The computation is straightforward and amounts to using commutation relations. Details of the calculation can be found in the appendix. Our final result is:

$$\mathcal{G}_{kink} \equiv \langle\phi_c|\mathcal{O}^2_{BPS}|\phi_c\rangle = \frac{1}{\pi}(g\partial_x\phi_c(x) + 3g^2\phi_c^2)\log\Big(\frac{\Lambda}{\mu}\Big), \tag{3.147}$$

where we introduced regulators in the UV (Λ) and IR (μ), respectively. A diagrammatic representation of this result is given in Figure (3.2).

The result explicitly shows that the classical BPS condition is violated in the corpuscular approach. In particular, one can see from (3.147) that these violations arise in the form of terms mixing the classical field with quantum contributions coming from commutators giving rise to logarithms. Since the corrections to the BPS condition explicitly contain information about the kink via its classical value, these terms cannot be attributed to the vacuum. In other words, the logarithm effectively corresponds to a renormalization of the data characterizing the kink. Thus, the classical data $\sqrt{N_k}$ corresponds to the bare value which is necessarily renormalized by commutators. Subsequently, working with physical parameters leads to the violation of the BPS condition. A plot of the quantum contribution to the BPS operator (after subtracting a pure vacuum contribution) is shown in figure (3.4).

From the Figure we see that quantum corrections to the BPS condition are localized on a scale given by the typical size of the soliton. Far away from the core of the kink,

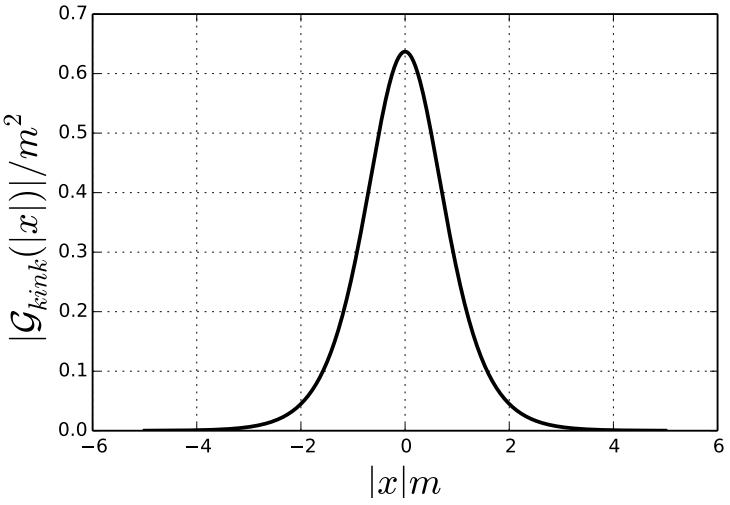

Figure 3.4: $\mathcal{G}_{kink}/m^2$ as a function of spatial distance xm for $\log(\Lambda/\mu) = 1$. The diagram gives a measure for BPS violation as well as the second goldstino's profile.

these effects vanish exponentially. Physically, we could have expected such a behaviour. Since the corpuscular structure is important on a scale set by the soliton size, we expect quantum corrections to become important on that lengthscale. Far away, however, the field tends to its vacuum value. Since in this situation vacuum fluctuations of bosons on top of the vacuum are canceled by their fermionic partners, supersymmetry should not be broken at large distances.

Notice, that since the BPS condition is violated while the central charge is not, the supersymmetry algebra is completely broken. In other words, also the second supercharge does no longer annihilate the soliton state. As a consequence, the kink supports a second goldstino zero mode with profile displayed is Figure (3.4).

Let us once more highlight the physical origin of supersymmetry breaking. While in the standard semi-classical treatment Fermi-Bose degeneracy of fluctuations on top of the kink ensures that the BPS condition holds to all orders in perturbation theory, corrections must arise in the corpuscular treatment. Roughly speaking, on top of the creation and annihilation operators for the fluctuations, we introduce a new set of corpuscular operators creating and destroying particles inside the kink. These operators are bosonic in nature and lack a fermionic counterpart. Therefore, the effects of these bosonic operators can in general not be canceled even in supersymmetric theories.

Notice that the corpuscular approach will in general induce interactions between the soliton constituents and the fluctuations as well. Since these effects are due to commutators involving the corpuscles, we expect them to be suppressed as $\hbar/N$. We can explicitly check that this is the case for the kink. For that purpose we expand the field as in (3.126) and also take the fermionic flucuations in the full quantum Hamiltonian into account. Here we

restrict our discussion to quadratic order in fluctuations[22]. Using this expansion, we find

$$\begin{aligned}\hat{H}-Z \quad &= \frac{1}{2}\int dx\Big(\mathcal{O}^2_{BPS}(\phi_{sol})+2\phi'_q\phi'_{sol}+\phi'^2_q+4g\phi'_{sol}\phi_{sol}\phi_q+2g\phi'_{sol}\phi^2_q\\ &+2g\phi^2_{sol}\phi'_q+4g\phi'_q\phi_q\phi_{sol}-2g\phi'_q m^2/g^2+6g^2\phi^2_q\phi^2_{sol}+4\phi^3_{sol}\phi_q\\ &-4m^2\phi_q\phi_{sol}-2m^2\phi^2_q-\bar{\psi}i\gamma^1\psi'+2g\phi_{sol}\bar{\psi}\psi\Big) \qquad (3.148)\end{aligned}$$

where all the fields are understood as operators in this expression and $'$ denotes derivative with respect to x.

Let us evaluate (3.148) in the solitonic coherent state $|sol\rangle$. Notice that terms linear in fluctuations vanish by virtue of equation (3.127). Furthermore, expanding all fields in terms of their respective creation and annihilation operators and using commutation relations, we arrive at

$$\begin{aligned}\langle sol|\hat{H}-Z|sol\rangle \quad &= \frac{1}{2}\int dx\Big(\langle\phi'^2_{sol}\rangle+I(2g\phi'_{sol}+6g^2\phi^2_{sol}-2m^2+g^2I+2g^2\langle\phi^2_q\rangle)\\ &+\langle\phi'^2_q\rangle+2g\phi'_{sol}J+6g^2\phi^2_{sol}J-2m^2J\\ &-\langle\bar{\psi}i\gamma^1\psi'\rangle-4g^2\phi^2_{sol}K\Big), \qquad (3.149)\end{aligned}$$

where I, J and K are divergent integral coming from commutators of corpuscles, bosonic fluctuations and fermions, respectively. Furthermore, we once more defined $\langle A\rangle\equiv\langle 0|A|0\rangle$ for any operator A and ϕ_{sol} is now understood as the classical profile of the kink. The explicit form of the integrals is as follows:

$$\begin{aligned}I &= \int\frac{dk}{4\pi\omega_k}\\ J &= \int\frac{dk}{4\pi\omega^b_k}\\ K &= \int\frac{dk}{4\pi\omega^f_k}, \qquad (3.150)\end{aligned}$$

with ω_k, ω^b_k and ω^f_k the corpuscular, bosonic and fermionic dispersion relations, respectively. Note furthermore that we used $\bar{u}(k)u(k)=2g\phi_{sol}$ with $u(k)$ a solution to the Dirac equation in the classical kink background. Note that in the semi-classical approach we have $\omega^b_k=\omega^f_k$ in the soliton background leading to a cancellation of loops of bosonic and

[22]Let us once more stress that alternatively, instead of working with the full quantum operators describing the solitonic fields, we could split them up into a classical background part plus fluctuations describing the $1/N$ corrections. This would be the standard approach which one usually uses in many-body physics. Although such a split makes manifest the fact that to leading order in $1/N$ the time evolution of the bosonic part of the theory is governed by the mass of the soliton, our results do not depend on such a split. In particular, in our approach, the classical part is simply encoded in the normal ordered part of the Hamiltonain. Quantum corrections are then accounted for in terms of commutators and the subsequent need for renormalizing the classical data.

fermionic fluctuations. In particular, in this case we have $J = K$ and, using the classical BPS condition the last two lines cancel due to supersymmetry. In the corpuscular approach, however, we see that quantum effects generate a mass splitting between bosons and fermions. Looking at the first line in (3.149) reveals that corpuscular effects generate a mass contribution for the bosonic fluctuations given by $2Ig^2\langle\phi_q^2\rangle$. Since this term does not contain any powers of the classical background, it is obviously suppressed as compared to the other terms in the first line which are also induced by corpuscular commutators. Notice that there is no such term for fermions. In other words, we see that the last two lines are not identically zero in the corpuscular treatment which again reveals that corpuscles lead to a breaking of supersymmetry.

Using the classical BPS equation our final answer for the corpuscular contribution becomes:

$$\begin{aligned}\langle\phi_c|\hat{H} - Z|\phi_c\rangle \quad &= \frac{1}{2}\int dx \Big(4g^2\phi_c^2(I + J - K) \\ &+\langle\phi_c'^2\rangle + \langle\phi_q'^2\rangle - \langle\bar{\psi}i\gamma^a\psi'\rangle + g^2I^2 + 2g^2IJ\Big)\end{aligned} \tag{3.151}$$

This form makes the structure of corpuscular corrections very transparant. Let us first discuss how to obtain the semi-classical result from (3.151). In that case we have $I = 0$ and $J = K$. Thus, all terms containing I, J or K vanish trivially. Furthermore, as already discussed above, $J = K$ implies Fermi-Bose degeneracy and therefore a cancellation between the expectation values of kinetic terms of bosonic and fermionic fluctuations. Finally, $I = 0$ when we do not resolve the soliton. Thus, we automatically recover $H = Z$ in the semi-classical limit.

Let us stress that although we demonstrated the physics of SUSY breaking due to corpuscular effects in the simple example of a Wess-Zumino theory in $1+1$ dimensions, our logic applies to more generic situations. Indeed, whenever we have a solitonic configuration (or an instanton), the introduction of a new algebra A_a of corpuscles will lead to corrections to the BPS condition. Within SUSY, there is no possibility of canceling these corrections simply because of the lack of fermionic partners for the corpuscles. In particular, our reasoning should be directly applicable in the case of SUSY Yang-Mills theories. In this situation, there will be corrections to the physics of the BPST instanton which again lead to SUSY breaking. Furthermore, our studies so far indicate that the corpuscular corrections will also break scale invariance of the instanton profile in 4 dimensions. A complete discussion of these and related issues, however, is left for future work.

3.5 Corpuscular Theory of AdS

Now that we have applied the coherent state picture to solitons and instantons in field theory, we want to turn to gravity again. In particular, we will apply the coherent state logic to the physics of AdS space-time. We choose to study AdS, because its property of being globally static as well as conformally equivalent to Minkowski space-time in Poincaré

coordinates, makes the analysis simple. Nevertheless, our results already indicate how corpuscular effects act within gravity in more general situations.

Our discussion concerning the corpuscular theory of AdS is divided into two major parts.

In the first part, we will present the basic idea and formalism which we are using in order to resolve AdS into constituent degrees of freedom using once more the language of coherent state. Having achieved such a coherent state representation of AdS, it is shown how to make contact with well established holographic notions such as central charge or the number of degrees of freedom of the CFT from the corpuscular point of view (to leading order in $1/N$). In order to check the consistency of our approach, we check that these properties hold in different dimensions and geometric set-ups. As a consequence of our description, it is furthermore explained how on the one hand the classical isometry group of AdS at leading order emerges even though we start from a flat space-time vacuum, and how the equivalence principle emerges in our description on the other hand.

In the second part, we will study higher order corpuscular correction in a way which parallels our discussion concerning solitons in SUSY theories. To be specific, we will consider how corpuscular corrections affect propagators in AdS space-time. In particular, it is shown that the corpuscular effects on propagators in AdS can be resummed in a Dyson-type series. The general form of the resummed propagator turns out to be geometry independent as long as one works in a static patch. Thus, the technique can be applied to other backgrounds as well when resolved quantum mechanically. Of course, the explicit form of the corrections will depend on the background we want to study. In particular, we will explicitly compute these corrections to all orders at the full non-linear level in an AdS space-time. Furthermore, AdS serves a playground to study possible deviations from thermality in the corpuscular approach. Considering an Unruh observer in AdS, it is shown, that the spectrum he/she measures is no longer exactly thermal. Therefore, our results might indicate that a similar mechanism could be at work in the case of Hawking radiation. As we have explained above, such deviations could be the key for a resolution of the information paradox. Furthermore, our results might have important implication for the AdS/CFT correspondence. One could for example ask whether corpuscular corrections to propagators imply deviation from duality, or whether there are similar effects on the CFT side. We will briefly comment on these issues below. A full analysis, however, is beyond the scope of this thesis. Nevertheless, we will investigate the role of corpuscular effects in the context of AdS/CFT in future research.

3.5.1 Corpuscular AdS

$\mathbf{AdS}_4$

In what follows, we will use the following conventions: We take mostly plus signature and work with the Poincaré patch of AdS

$$ds^2 = \frac{\rho^2}{z^2}\left(dz^2 + \eta_{\mu\nu}dx^\mu dx^\nu\right) \tag{3.152}$$

where z is the usual radial direction, ρ the AdS curvature radius and the boundary is $d = D - 1$ dimensional (with μ, ν indices; the bulk will be given M, N index structure). Any bosonic, canonically normalized field in the bulk then has dimension $\frac{d-2}{2} = \frac{D-1}{2}$. The metric, however, is usually introduced as a dimensionless quantity. We shall account for this fact by including appropriate factors of the Planck mass M_p in explicit expressions.

As a first step towards a corpuscular description, we write the classical metric field in Fourier space just as we did in the case of the coherent state description of solitons. That is

$$g_{MN} = \frac{L^d}{M_p^{(d-1)/2}} \int \frac{d^d k}{\sqrt{(2\pi)^d 2\omega_k L^d}} \left(\alpha(k)_{MN} e^{ikx} + h.c\right) \ . \tag{3.153}$$

A few remarks concerning this equation are in order. First of all, we introduced the regulating spatial length scale L. Using this normalization, ensures that the $\alpha(k)_{MN}$ are dimensionless. In turn, this will allow us to relate them to occupation numbers in the mode k as soon as we go to the quantum theory. Secondly the product kx only involves spatial components, because the metric is static in Poincaré coordinates. Of course, choosing this coordinate system suggests that also the $\alpha(k)_{MN}$ depend on this choice. As a consequence, the Fourier coefficients transform non-trivially under diffeomorphisms. Since we will consider only invariant quantities in this thesis, however, we can restrict ourselves for the moment to the coordinate system (3.152). In particular, since in this system the metric is conformally flat, we can express all components of the metric in terms of a single one. Subsequently, there is effectively only one expansion coefficient which we shall denote by $\alpha(k)$ in what follows. Finally, it is important to stress once more that the dispersion relation ω_k is not the one of free particles. Indeed, we shall fix it self-consistently below by requiring that the corpuscular approach correctly accounts for the energy of AdS to leading order in $1/N$.

Solving for the expansion coefficients in (3.153) we obtain

$$\alpha(k) = -\frac{L^{-d/2} M_p^{(d-1)/2}}{\sqrt{2\pi}} \frac{\sqrt{2\omega_k}|k|\rho^2}{2} \delta^{d-1}(k_i) \ . \tag{3.154}$$

The delta functions arise from the trivial integrations over the Minkowski coordinates at fixed values of z and the factor $|k| \equiv \sqrt{k_z^2}$ is due to the integration over the z coordinate.

Since we do not yet know ω_k we cannot make any claims about the behaviour of $\alpha(k)$ as a function of $|k|$. Nevertheless, when going to the quantum theory, we shall derive an explicit expression which allows for a transparent physical interpretation.

In order to move to the quantum theory, we follow the recipe used for the quantum description of solitons and promote the classical metric and thus the expansion coefficients (3.153) to quantum operators. The corresponding operators $\hat{a}(k)$, $\hat{a}^\dagger(k)$ then satisfy the usual creation and annihilation algebra (suppressing the polarization indices)

$$[\hat{a}(k), \hat{a}^\dagger(k')] = \frac{\delta^d(k - k')}{L^d} \ . \tag{3.155}$$

Using this algebra and requiring that the metric reduces to the classical solution when evaluated in the quantum state of AdS, fixes that state to be a coherent superposition of

number eigenstates of corpuscles $|n_k\rangle$ created when acting with $\hat{a}^\dagger(k)$ on the Minkowski vacuum:

$$|\text{AdS}\rangle = \prod_k e^{-N_k/2} \sum_{n_k} \frac{N_k^{n_k/2}}{n_k!} |n_k\rangle \ . \tag{3.156}$$

Here again N_k is defined via $\hat{a}(k)|\text{AdS}\rangle = \alpha(k)|\text{AdS}\rangle \equiv \sqrt{N_k}|\text{AdS}\rangle$.

We see that the advantage of Poincaré coordinates is that the absolute value of all the diagonal components is the same, $\frac{\rho^2}{z^2}$, and all the off-diagonal components are zero. Note that using Poincaré coordinates is not a loss because it gives one full causal patch of global AdS spacetimes. Thus, having the complete information about the Poincaré patch is enough to study further Cauchy evolutions and thus field dynamics in the full global geometry.

Let us now derive the expression for the dispersion relation $\omega(k)$. For this purpose we match the corpuscular energy to the classical result. For AdS, the Ricci scalar R and the cosmological constant Λ are respectively

$$R = -\frac{d(d+1)}{\rho^2} \quad \text{and} \quad \Lambda = -\frac{d(d-1)}{2\rho^2} \ . \tag{3.157}$$

The Einstein-Hilbert (EH) action is then

$$S_{EH} = \frac{1}{16\pi G_{d+1}} \int d^{d+1}X \sqrt{g} \, (R - 2\Lambda) \tag{3.158}$$

where G_{d+1} is the $d+1$-dimensional Newton's constant. Evaluating this action on the AdS solution in Poincaré coordinates gives

$$S_{EH} = \frac{1}{8\pi} \left(\frac{\rho}{l_p}\right)^{d-1} \left(\frac{r}{\epsilon}\right)^d , \tag{3.159}$$

where we introduced an UV cut-off at $z = \epsilon$. Furthermore, r denotes an IR cut-off of spatial slices of Minkowski at constant values of z and l_p is the Planck length.

Let us already mention at this point that, when choosing all the cut-off scales to be ρ we effectively consider the action evaluated over exactly one patch of volume ρ^d. In that case, the action scales as $(\rho/l_p)^{d-1}$ which corresponds to the holographic bound on the entropy in AdS, or, the central charge of the dual CFT [84].

Let us now try to understand how to give a quantum mechanical interpretation to the energy of AdS space. First notice, that we can define the energy invariantly as the product of spatial bulk volume and the vacuum energy at a classical level. In other words, a natural definition for the energy of AdS is in terms of a spatial integral over the constant vacuum energy density. Using similar cut-offs as before, we find

$$E = -\int \frac{2d(d-1)}{16\pi G_{d+1}\rho^2} \sqrt{g} d^d x = \frac{d-1}{8\pi} \left(\frac{\rho}{l_p}\right)^{d-1} \frac{r^{d-1}}{\epsilon^d} \ . \tag{3.160}$$

Quantum mechanically we want to understand this energy as a collective effect of N quanta contributing to the vacuum energy. In Poincaré coordinates such an interpretation is feasible in four space-time dimensions because the invariant volume scales like g_{zz}^2 in this case. Therefore in terms of creation and annihilation operators the corresponding Hamiltonian is diagonal. Of course, this statement is true in the expectation value up to $1/N$ corrections. In other dimensions a diagonalization is in principle possible by performing a proper Bogoliubov transformation or a diffeomorphism of the corpuscular operators. This will be done explicitly in the next subsection for AdS_5. In this section, however, we will restrict ourselves to AdS_4. In this case, the energy can be written as

$$E = \frac{L^3}{(2\pi)^3}\int d^3k\omega_k\langle AdS|\hat{a}_k^\dagger\hat{a}_k|AdS\rangle = \frac{r^2\rho^4M_p^2}{2(2\pi)^2}\int dk\omega_k^2|k|^2\,. \tag{3.161}$$

Here we regulated the product of δ functions which follows from (3.154) as usual by restricting to a finite volume ρ^2. If this is to be equal to (3.160), then we must have the following dispersion relation:

$$\omega_k^2 = 2\pi R^{-2} \tag{3.162}$$

From this expression we see that all corpuscles contribute the same amount of energy to the classical vacuum energy. Furthermore, the dispersion again shows that the particles we are dealing with are completely different from asymptotic S-matrix states. Finally, we want to emphasize that this result implies that the occupation of corpuscles at given momentum N_k scales as $|k|^2$. Thus, there is a divergence in this number at large values of $|k|$ which, in configuration space, follows from the pole at $z \to 0$. This gives a quantum mechanical manifestation of the fact that classically wavelengths are infinitely blue shifted at the boundary of AdS. Thus, we see that geometric concepts follow simply from the distribution of the constituents of space-time.

Using (3.162), one can also calculate the total number of corpuscles, which is

$$N = \frac{L^3}{(2\pi)^3}\int d^3k\langle AdS|\hat{a}_k^\dagger\hat{a}_k|AdS\rangle = \frac{\sqrt{2\pi}}{2(2\pi)^2}\left(\frac{r}{l_p}\right)^2\left(\frac{\rho}{\epsilon}\right)^3\,. \tag{3.163}$$

This result is interesting for several reasons. First of all, from the holographic point of view we see that the central charge N_{YM}^2 of the CFT side is recovered when we restrict ourselves to a patch of AdS of size ρ, i.e. when we take $r = \epsilon = \rho$. Thus, the central charge emerges as a collective effect of N_ρ corpuscles distributed over one patch in the bulk space-time:

$$N_{YM}^2 = \frac{\rho^2}{l_p^2} \sim N_\rho\,. \tag{3.164}$$

Alternatively, we notice that the factor r^2/ϵ^2 is simply the number of cells N_{cell} of size ϵ^2 in a portion of flat space-time of spatial size r^2. Notice that according to [84] the total

number of degrees of freedom on the field theory defined on the slice ϵ = constant with area r^2 can be expressed as $N_{\rm dof} = N_{YM}^2 N_{\rm cell}$. Thus, in terms of the number of degrees of freedom, (3.163) becomes $N = N_{\rm dof}\rho/\epsilon$. As a consequence one can see that the number of corpuscles in the bulk is a measure of the entropy of the corresponding field theory.

Let us now explain how classical, geometrical properties follow from our description. First, the stability of AdS with respect to decay into the vacuum can be understood easily from the properties of coherent states. For that purpose, consider the matrix element

$$\langle {\rm AdS}|0\rangle = e^{-N}|_{\epsilon\to 0} \to 0 \ . \tag{3.165}$$

Equation (3.165) therefore gives the quantum mechanical explanation that globally, AdS can never be recovered as a deformation of Minkowski space-time. Let us explain this point in more detail. Although the base space in our description is a $SO(3,1)$-invariant Minkowski vacuum, a consistent quantum description of AdS must be sensitive to the classical isometries AdS, i.e. $SO(3,2)$. In other words, the coherent state representing AdS can not be viewed as a small deformation of the Minkowski vacuum. This property is guaranteed in our approach as is encoded in equation (3.165). Thus, although we start with a Poincaré invariant vacuum and create number eigenstates of corpuscles transforming as definite representations of that group, these states secretly know about the isometries of AdS, because the resulting coherent state must be invariant under $SO(3,2)$ (at least in the semi-classical limit). Notice that a similar observation was made in the corpuscular theories of solitons and instantons where topology emerges as a collective effect of an infinite number of quanta of infinite wavelength.

At the same time, one might wonder how the principle of local equivalence to flat space-time emerges in our approach. This can be demonstrated straight forwardly. For that purpose we simply carry out our calculations in a small bulk neighborhood of size ϵ in boundary spatial directions and a small region of size δ in the z direction around the coordinate z_*. As above, the energy due to corpuscles in such small region is given by (with $d = 3$)

$$E_{\epsilon,\delta} \approx \frac{1}{l_p^{d-1}\rho^2}\int d^{d-1}x dz \frac{\rho^{d+1}}{z^{d+1}} = \frac{\rho^2}{l_p^2} V_\epsilon^{(2)} \frac{\delta}{z_*^4} \tag{3.166}$$

where again, $V_\epsilon^{(2)}$ is a small transverse (to z direction) spatial volume. Alternatively, evaluating this energy in terms of the creation-annihilation operators yields

$$E_{\epsilon,\delta} \approx \frac{V_\epsilon^{(2)}\rho^4}{l_p^2}\int_{1/z_*-\Delta E/2}^{1/z_*+\Delta E/2} dk|k|^2\omega_{loc}^2 = \frac{V_\epsilon^{(2)}\rho^4}{l_p^2}\frac{\omega_{loc}^2\Delta E}{z_*^2}. \tag{3.167}$$

Here by ω_{loc}, we mean the dispersion relation around a small energy range of value ΔE, which should be of order δ^{-1} due to our choice of the region around z_*. Using this and comparing the two energies (3.166) and (3.167), we find

$$\omega_{loc}^2 = \frac{2\pi}{\rho^2}\frac{\delta^2}{z_*^2} \ .$$

So we explicitly see how the dispersion relation scales with the small neighborhood. Furthermore, the scaling uncovered here corresponds to a red-shift factor measured by an observer in the local neighborhood. Moreover, we also recover the divergence structure when $z_* \to 0$ as above which simply reflects an unphysical coordinate singularity.

From here it should already be clear that the number of corpuscles will vanish as we take a vanishingly small neighborhood. To confirm, let's just compute[23]

$$N_{loc} = \int_k dk \alpha_k^* \alpha_k = \frac{\rho^3 \delta V_\epsilon^{(2)}}{l_p^2 z_*} \int_k dk_z k_z^2,$$

which goes to zero locally. This is nothing but the equivalence principle derived from the corpuscular portrait of AdS. In other words, local flatness of a space-time corresponds to a vanishing local occupation number of corpuscles from the quantum point of view.

To conclude this section, we have seen how well-known holographic and geometric properties easily arise quantum mechanically in our approach as a collective effect of constituent gravitons.

$\mathbf{AdS}_5$

In order to diagonalize the energy of AdS in 5 spacetime dimensions, we shall use the following coordinates:

$$ds^2 = e^{y/\rho} \eta_{\mu\nu} dx^\mu dx^\nu + dy^2, \tag{3.168}$$

where y ranges over the full real axis and ρ again denotes the curvature radius. We can then proceed as usual and define corpuscular creation/annihilation operators and the corresponding coherent state. Note, however, that in order to properly define the number of corpuscles in mode k we need to cut-off the y-integration. We shall denote this cut-off r_* in what follows. Following the logic of our previous section, we can define the energy basically as an invariant volume multiplied with M_p^3 and ρ^{-2} (which comes from the cosmological constant). Matching this energy with the corpuscular definition, one again finds $\omega_k \sim \rho^{-1}$ for the dispersion. Using this result, it is straightforward to show that the number of corpuscles in mode k and the total number are given by

$$N_k \sim \frac{M_p^3}{L^4} V_3 \delta^3(k_i) \frac{e^{2r_*/\rho}}{\rho k_y^2 + \rho^{-1}} \tag{3.169}$$

and

$$N \sim M_p^3 V_3 e^{2r_*/\rho}, \tag{3.170}$$

respectively. Here k_y the momentum along the holographic direction and $V_3 \equiv r^3$ is the spatial volume of slices of Minkowski at fixed values of y.

[23]The integral over k is once again important in a certain range, corresponding to the local choice in the position space.

There are several interesting things to note. First of all, restricting to a patch of volume ρ^4 in AdS amounts to taking $r_* = 0$ in this coordinate system and as usual $V_3 = \rho^3$. But then it is clear that the total number of corpuscles in one such patch again coincides with the central charge of the CFT (just as in the case of AdS_4 in Poincaré coordinates). In other words, while Poincaré coordinates diagonalize the energy in four dimensions, so do the coordinates used here in five dimensions. Since our result is coordinate invariant, matching with the central charge as demonstrated here holds for all coordinates.

Secondly, looking at N_k, one sees that it diverges as we send the cut-off to infinity for all k_y. In contrast, in Poincaré coordinates, the divergence at this level was encoded in the high momentum modes. There is no contradiction here though as N_k is not an observable. If we consider the total number of corpuscles in the two systems, we will find that they diverge only if we send the cut-off to infinity in both cases! Since this is the observable we are interested in, the result presented here is in perfect agreement with the one obtained in 4 dimensions using Poincaré coordinates.

As a consequence, geometric properties such as the stability of AdS_5 or the equivalence principle for AdS_5 follow in a similar way as before. Since the calculations are similar to the ones presented in the last subsection for AdS_4, we will not bother the reader with performing these simple computations again.

Randall-Sundrum Geometry

A slightly different situation where AdS and AdS/CFT naturally appears is in the Randall-Sundrum (RS) model [85], [86] which extended and modified the previous large extra dimensional models [87] to incorporate the hierarchy problem in light of warped spacetimes ending on either a brane in the UV or both in the UV and IR. In particular, the RS2 model is a closely related cousin of AdS/CFT except for the fact that the field theory on the brane in the UV generates gravity dynamically. That is, particles on the brane couple to bulk gravity. As a consequence, integrating out loops of such particles with external graviton lines attached, generate gravity on the brane dynamically.

Below we will study the bulk theory from the corpuscular point of view and show how geometric quantities such as the invariant bulk volume can be understood in this framework. Furthermore, relying on AdS/CFT, we shall give an alternative derivation of our earlier results connecting the central charge of the field theory with the number of corpuscles constituting the bulk. To do so, we note that in the RS model, the metric is given by[24]

$$ds^2 = g_{MN}dx^M dx^N = e^{-|y|/\rho}\eta_{\mu\nu}dx^\mu dx^\nu + dy^2 \ , \tag{3.171}$$

where the extra warped direction is y and μ, ν go from 0 to 3. We can write this metric in a conformal form like the Poincaré patch of AdS, but it is not necessary. Indeed, using the coordinate system (3.171) one observes that the invariant volume in this spacetime is

[24]In the original literature, the conventions for Einstein's equation, and hence the metric is slightly different from ours. We use here the conventions we used in the previous sections.

precisely

$$V_{inv} = \int d^5x\sqrt{g} = V_M \int dy e^{-2|y|/\rho} \ . \tag{3.172}$$

where V_M is the transverse (along the brane) volume of the 4 dimensional flat space-time. We notice that the integrand goes precisely as $g^2_{\mu\mu}$ (μ not summed). This makes it clear that if we quantize the solution in exactly the same way as we did in the case of AdS, the integrand is diagonal in the corresponding corpuscular creation and annihilation operators. This is also seen as follows. Expanding the metric in Fourier modes and promoting the coefficients to operators, consistency of the approach again requires to represent the RS2 solution as a coherent state. For the corresponding expansion coefficients we find

$$\alpha_k = L^{-2} M_p^{3/2} \sqrt{2\omega_k} \frac{\rho^{-1} - ik_y}{\rho^{-2} + k_y^2} 2\pi\delta^{(3)}(k_i) \ . \tag{3.173}$$

The total number of corpuscles in a given momentum mode is then simply $N_k = |\alpha_k|^2$ (again, the squares of δ functions due to the integration over slices of Minkowski should be regularized as in the case of AdS). From this expression we cannot directly obtain the precise form of the dispersion. We can, however, proceed as in the example of AdS and match the invariant energy of the bulk space-time to what one expects from a corpuscular description,

$$8\pi M_p^3 \Lambda V_{inv} = \frac{V_M \rho}{(2\pi)^4} \int d^4k \omega_k \alpha_k^* \alpha_k \ . \tag{3.174}$$

Since $V_{inv} \sim V_M \rho$ (e.g. for a time scale of size ρ), consistency of the corpuscular description implies again $\omega_k \sim \rho^{-1}$ just as in the case of AdS. In turn, the total number of corpuscles inside a patch of size R can be computed just as before. As a result we find $N_\rho \sim (\rho/l_p)^3$. Note that the invariant volume also defines the effective 4-dimensional Planck scale which in this case is related to the total number of corpuscles as

$$V_{inv} = \frac{\rho^2 N}{M_p^3} \tag{3.175}$$

Holographically, on the other hand, the same scale emerges effectively as a consequence of loops of all the particles on the brane. In Yang-Mills theory at large N_{YM}, this number goes as $N_{YM}^2 \sim \frac{\rho^3}{l_p^3} \sim N_\rho$. Thus, we again see that that the emergence of central charge can be understood as a collective effect of many gravitons from the corpuscular point of view of the bulk theory.

Holographic RG

It is well understood that the radial direction of the AdS spacetimes might be identified with an energy scale when viewed from the boundary field theory perspective [84]. Thus,

it is natural to identify the radial flow in AdS with a corresponding renormalization group (RG) flow in the field theory deformed by a multi-trace operator. This subject goes by the name of holographic RG and this is an interesting subject from the very beginning of the AdS/CFT correspondence starting with the work of e.g. [88–90] and others. This has also been a study of much recent discussions such as [91–93]. In these papers, the RG flow equations were calculated from the field theory sides and the c-type functions which decrease monotonically along an RG flow were derived. This can then be matched with the gravity calculations and one can also try to formalize a bulk beta-function equation in path integral language.

In this section, we will see such a c-function type behavior explicitly and speculate on a corpuscular description of bulk RG flow. Our statements here are far from complete as this type of holographic RG has many intuitive subtleties. All these problems stem from the fact that in the duality, an energy scale is identified with a spatial scale; whereas the RG equations treat the energy scale on a special footing. So if it were a standard Wilsonian RG in the bulk, one is then supposed to keep all the bulk fields from all of space-time, but just integrating out the higher momentum modes beyond the cut-off. But on the other hand, holographic RG compels one to throw away bulk fields for some radial values. Some of these bulk fields from this integrated out region may as well be massless. Similarly, by putting a cut-off at a radial distance, we are really not getting rid of all the high energy modes beyond a certain cut-off. There could as well be such modes populated in the IR region. So even though there is a quantity in the bulk which act as the c-type function and there could be an Wilsonian RG flow on the boundary, its bulk interpretation is still not clearly understood as it is in some sense a "spatial" RG flow.

However, below we will just be content with showing that there indeed exists a natural gauge invariant quantity like c which decreases along an RG flow.[25] This will turn out to be related to the total number of corpuscles that we derived before in (3.163) for AdS_4 and in (3.170) for AdS_5.[26] In fact, we can already see it in (3.170) as we vary r_*. To be formal, let us define the density of corpuscles per slice of Minkowski volume:

$$n = \frac{N}{V_3} \sim M_5 e^{2r_*/\rho}. \tag{3.176}$$

Now we can study the flow of this density as we vary the cut-off:

$$r_* \frac{\partial n}{\partial r_*} \sim \frac{M_5^3}{\rho} r_* e^{2r_*/\rho} \tag{3.177}$$

Notice that this function might be the corpuscular dual to the RG flow on the field theory side (there must be such a flow, because, introducing a cut-off we break the conformal

[25] Actually, in what follows, we will be mainly talking about AdS_5/CFT_4 dictionary, where the c-theorem of two dimensions [94] is generalized to an a-theorem [95, 96].

[26] Although the trace anomaly which supplies the c or a-functions vanishes in odd dimensional field theory, there are similar statements like F-theorem [97] and g-theorem [98] in other dimensions. It will be interesting to investigate whether our identification will continue to have such an interpretation in terms of F or g etc.

invariance of the dual field theory!). Notice furthermore, that N grows with r_* monotonically. So it is natural to expect that some functions of N could easily serve as the candidate for the corresponding a-function. We will make this identification more accurate in the next section.

Holographic RG in Domain Wall Ansatz

Typically, RG flow equations that we encounter in field theory consist of starting at a UV fixed point, and flowing down to an IR fixed point. At these fixed points one usually has scale invariant theories. This is a well-understood subject. In AdS/CFT contexts, this is achieved by a domain wall ansatz where at UV and IR the respective CFTs are dual to AdS spacetimes of one higher dimension and a priory with different cosmological constants. Such an example include an interpolation between free and critical CFT_3 (more specifically $O(N)$ vector models) which are dual to two different types of Vasiliev's higher spin theories in AdS_4 [99]. The c/a-theorems described in [94–96] were studied for such statements of traditional RG flows. For both two and four dimensional CFTs an alternative proof of c/a-theorems exists from field theory entanglement entropy and hence from holographic entanglement entropy [100] point of view which can also be generalized to higher dimensions [101].

In order to understand the RG flow in our language, we start with the domain wall ansatz metric, which at fixed points, boils down to the AdS_5 metric we used before

$$ds^2 = e^{2A(y)}\left(-dt^2 + d\mathbf{x}_3^2\right) + dy^2 \ ,$$

where $y \in [-\infty, \infty]$. The a-theorem function on the gravity side in such coordinates is [101]

$$C(y) = \frac{\pi}{G_5 A'(y)^3} \ , \tag{3.178}$$

with $A''(y) \leq 0$ coming from null energy conditions and prime denotes derivative with respect to y. Hence one constructs

$$C'(y) = -\frac{3A''(y)}{G_5 A'(y)^4} \geq 0.$$

Such form of $C(y)$ can be roughly understood as follows. For example, in $d = 4$, for $\mathcal{N} = 4$ super Yang-Mills theory (SYM), $a = C(y)|_{fp_i}$ (fp_i for i-th fixed point) is the coefficient appearing in front of the trace anomaly [102], [103]

$$\langle T^\mu_\mu \rangle = \frac{a}{8\pi^2}\left(R^{\mu\nu}R_{\mu\nu} - \frac{1}{3}R^2\right) \ ,$$

where $R_{\mu\nu}$ denotes the Ricci tensor and $a \sim \frac{\rho^3}{G_5}$ is known from holographic computations [104]. Now, at fixed points of the RG flow equations one has

$$A(y)|_{fp_i} = y/\rho_i \qquad \text{and} \qquad A'(y)|_{fp_i} = 1/\rho_i \ .$$

This suggests a natural way to generalize this a (this is equivalently the universal term of the entanglement entropy in 4 dimensional CFT [101]) to the $C(y)$ we have written above in (3.178).

In our case, we had from (3.175)[27]

$$V_{inv} = \frac{\rho^2 N}{M_p^3} \ ,$$

where N is the total number of corpuscles. Now at fixed points (V_3 denotes the transverse Minkowski spatial volume)

$$N = \frac{M_p^3 V_3}{\rho} \int dy e^{4A(y)|_{fp_i}} \ .$$

Then, parallel with the proposals of the holographic a-theorem, here we propose that during RG flow, i.e. away from the fixed point where N is in principle a function of y

$$\frac{dN(y)}{dy}\left(\frac{R}{M_p^3 V_3}\right) \sim e^{4A(y)} \ .$$

Hence, we can write

$$A'(y) \approx \frac{1}{4}\frac{N''}{N'} \ .$$

Thus, from the AdS/CFT perspective, it is natural to expect this behavior of $A(y)$ in terms of $N(y)$ and its derivatives even away from the fixed point. Plugging in the expressions for $C(y)$ and $C'(y)$, we recover that during RG flow, $N'N''' - N''^2$ has to be ≤ 0 and the role of the C-function is played by

$$C(y) \approx \frac{\pi}{G_5}\frac{N'^3}{N''^3} \tag{3.179}$$

Now at fixed points, for field theory duals such as e.g. $\mathcal{N} = 4$ SYM in four spacetime dimensions, one has $a = N_{YM}^2/4$ for $SU(N_{YM})$ gauge group at large N_{YM} with a as mentioned before [102], [103].

As it should be clear from our description of AdS_5 in section 3.5.1, we can now rerun our calculations of RS model in AdS_5 to obtain $N = N_{YM}^2$ where N is defined in terms of the invariant volume of AdS_5 and also when it is calculated directly in terms of $\sim \int dk a_k^\dagger a_k$ in a patch of AdS of radius R.

So we have a candidate of the a-function during the whole RG flow, both in terms of the invariant volume and the total number of corpuscles, which at the fixed point matches with SYM results. Note that the function $C(y)$ defined in (3.179) will boil down to a quantity of order N_{YM}^2 just by construction.

It is quite easy to provide a definition of $N(y)$ in the corpuscular picture in terms of the metric. Note that

$$N_k = \alpha_k^* \alpha_k = \int dy' dy'' e^{ik(y'-y'')} g(y') g(y'')$$

[27]Note that we can borrow the result (3.175) even for AdS calculations.

where $g(y)$ is effectively the y-dependent, non-radial component of the metric. Then a very natural definition of $N(y)$ is a Fourier transform of this quantity[28]

$$N(y) = \int dy'' g(y''-y)g(y'') \tag{3.180}$$

Note that as in the corpuscular language the semi-classical metrics have small $1/N$ quantum corrections, essentially this definition predicts and provides the possible quantum corrections to the anomaly term and the universal term of the entanglement entropy. Using this relation, one can even try to write down $A(y)$ and its y-derivatives in terms of $N(y)$ and plug that directly into (3.178). For example,

$$\frac{\partial N(y)}{\partial y} \approx -\frac{1}{R}\int dy'' g(y'')\frac{\partial}{\partial y}A(y''-y)g(y''-y)\ .$$

By construction, when substituted, this has to yield the expression of $C(y)$ as obtained in (3.179).

As in the previous subsection, we can also consider an RG flow equation characterized by $y\frac{\partial N(y)}{\partial y}$ which can serve as the beta function analog of Wilsonian RG flow.

3.5.2 Corpuscular Corrections

Based on the results of the last section we are now fully prepared to go one step further and discuss higher order quantum corpuscular corrections. To be specific, we will be interested in corrections to two-point functions such as the propagator or the Wightman function of a scalar in an AdS background. In other words, we will show that due to the compositeness of the background space-time the naive classical two-point functions do no longer solve the corresponding equation of motion. Instead, the corpuscular effects will reveal deviations which scale as $1/N$. This suggests to define quantum corrected two-point functions which, in turn, solve the corresponding quantum corrected equation of motion. This equation of motion will allow us to define a corpuscular effective action. As we will explain, this action should not be confused with the usual one-particle irreducible effective action which is a loop expansion rather than an expansion in the inverse number of corpuscles constituting the background. Based on these results we consider accelerated observers in AdS. Using the so-called Kubo-Martin-Schwinger (KMS) condition we show that the quantum corrected Wightman function cannot correspond to a thermal state. In other words, the corpuscular effects lead to a deviation from thermality of the spectrum an Unruh observer in AdS measures. We speculate that similar effects could lead to a purification of Hawking radiation in the case of black hole physics.

[28]Note that this relation doesn't touch the issue of whether the dispersion relation $\omega(k)$ at all points of the RG flow has a physical meaning or not.

Physical Motivation: Linearized AdS

Before computing corpuscular corrections to the full non-linear propagator in AdS space-time, we will first consider the leading order scattering process of a scalar on an AdS background linearized around Minkowski space-time. On the one hand, this exercise leads to a physical interpretation of the corpuscles constituting linearized AdS as we will explain. On the other hand, scattering processes unravel the physical origin of corpuscular corrections in a very transparent way. As we will discuss, these are due to the backreaction on the background due to the scattering. Since this section will serve only as a physical motivation, we will give a rather qualitative presentation of the basic ideas. Explicit computations are performed in the next sections when discussing the non-linear propagator and the Unruh effect in the corpuscular approach to AdS.

Let us start by considering AdS linearized around (d+1)-dimensional flat space-time in the static patch,

$$h_{00} = -\frac{\Lambda}{6} r^2, \; h_{0i} = 0, \; h_{ij} = -\frac{\Lambda}{6} x_i x_j. \tag{3.181}$$

Here Λ is the cosmological constant and $r^2 = x_i x_i$. This approximation, of course, is only valid for $r^2 \ll \rho^2$, where ρ is the curvature radius of AdS. In order to have a corpuscular interpretation of this solution, we expand it in Fourier space (note that we again choose to work with a normalization which guarantees that the expansion coefficients are dimensionless):

$$h_{\mu\nu}(z) = \frac{L^d}{M_{\rm p}^{(d-1)/2}} \int \frac{d^d k}{\sqrt{(2\pi)^d 2\omega_k L^d}} (e^{ikx} \alpha_k \epsilon_{\mu\nu}(k) + \text{h.c.}). \tag{3.182}$$

Here $M_{\rm p}$ denotes the $d+1$-dimensional Planck mass, L^d is the regulating spatial volume, $\epsilon_{\mu\nu}(k)$ the polarization tensor and ω_k the dispersion relation. Furthermore, the α_k's denote the classical Fourier coefficients of the metric. Note that the coefficient α_k gives the amplitude for the field to be in the mode k. Therefore, within the quantum mechanical treatment it should be identified with the typical occupation of quanta of momentum k constituting the background.

Let us explain how to resolve (3.181) in the corpuscular approach. Promoting the classical field into an operator, the coefficients α_k and α_k^* are replaced by annihilation and creation operators of corpuscles of the background, respectively. These operators satisfy the standard algebra, $[\hat{a}_k, \hat{a}_q^\dagger] = L^{-d}\delta^d(k-q)$. A proper classical limit is guaranteed when this operator is evaluated in a coherent state of corpuscles,

$$|\text{AdS}\rangle = \prod_k |N_k\rangle = \prod_k e^{-\frac{N_k}{2}} \sum_{n_k} \frac{N_k^{\frac{n_k}{2}}}{\sqrt{n_k!}} |n_k\rangle, \tag{3.183}$$

where $|n_k\rangle$ is an eigenstate of the number operator $\hat{a}_k^\dagger \hat{a}_k$ and $N_k \equiv |\alpha_k|^2$.

Note that these corpuscles are in general fully interacting. Thus, understanding their identity generically is a complicated problem. In the linearized description, however, we can attribute a precise meaning to the corpuscles.

One way is in terms of longitudinal, off-shell, massless gravitons of Einstein's theory with a cosmological constant expanded on Minkowski spacetime. This follows from the fact that the corpuscles obey a linearized wave equation with a source of the form of a cosmological constant. Alternatively, one could deform the theory by adding a Pauli-Fierz mass term. Then the deformed solution reduces to the metric above in the limit $m^2r^2 \ll 1$ [25, 106][29]. Here m is the mass deformation parameter. This theory now propagates five on-shell degrees of freedom. Thus, a second way to think about the coherent state is in terms of massive, on-shell gravitons. Since the metric is static globally, these gravitons should have zero frequency. From the dispersion relation of massive gravitons, we can conclude, that the gravitons in the coherent state can be interpreted as on-shell tachyons.

In order to get an intuition how corpuscular corrections arise, let us consider the scattering of a massive probe scalar on AdS to leading order. This process will serve as a motivation for the analogous full non-linear computation of the scalar propagator in the corpuscular description of AdS which we will discuss in the next section.

The interaction Lagrangian is given by

$$\mathcal{L} = \frac{1}{M_{\rm p}} h_{\mu\nu} T^{\mu\nu}(\phi), \tag{3.184}$$

where $T_{\mu\nu}(\phi)$ is the standard linearized energy momentum tensor of a massive scalar. To leading order, the amplitude takes the form

$$\begin{aligned} \mathcal{A}(q,p) \quad &= i\langle \mathrm{AdS}'| \otimes \langle 0|\mathrm{T}\hat{b}_q S_{int} \hat{b}_p^\dagger|0\rangle \otimes |\mathrm{AdS}\rangle \\ &= \frac{i}{M_{\rm P}} \int d^{(d+1)}x \langle \mathrm{AdS}'|h_{\mu\nu}|\mathrm{AdS}\rangle \langle 0|\mathrm{T}\hat{b}_q T^{\mu\nu}(\phi)\hat{b}_p^\dagger|0\rangle \end{aligned} \tag{3.185}$$

with $\hat{b}_q$ and $\hat{b}_p^\dagger$ the annihilation and creation operators of an asymptotic scalar field, respectively. Note that corrections to the classical result are encoded in the correlator $\mathrm{M}(x) = \langle \mathrm{AdS}'|h_{\mu\nu}|\mathrm{AdS}\rangle$. In particular, setting $|\mathrm{AdS}'\rangle = |\mathrm{AdS}\rangle$ one would recover the classical result by construction. In the corpuscular treatment, however, this is never the case. In particular, due to interactions with corpuscles in the coherent state, we should take backreaction into account. In other words, the scattered AdS state $|\mathrm{AdS}'\rangle$, can no longer be identified with the original state $|\mathrm{AdS}\rangle$. In general, it is not even clear that the scattered state can still be modeled as a coherent state. Taking the backreaction to be small, or equivalently the curvature radius much larger than the Planck length, however, it seems to be a good approximation to describe $|\mathrm{AdS}\rangle$ still as a coherent superposition, but with the occupations in different modes changed and disturbed dispersion relations.

[29]Notice that the authors show that this is the case for dS spacetime. It is easy, however, to show that similar results can be obtained for AdS as well.

According to these assumptions the matrix element takes the form

$$\frac{L^d\langle \mathrm{AdS}'|\mathrm{AdS}\rangle}{M_{\mathrm{p}}^{(d-1)/2}}\int\frac{d^dk}{\sqrt{(2\pi)^d 2\omega_k L^d}}\Big(e^{ikx}\sqrt{N_k}\epsilon_{\mu\nu}(k)+e^{-ikx}\sqrt{N'_k}\epsilon^*_{\mu\nu}(k)\Big). \tag{3.186}$$

This form makes the origin of the corrections very transparent. We see that the source of the corpuscular corrections is encoded in the difference between N'_k and N_k. Thus, first of all the integral in (3.186) will no longer give the classical field. Secondly, the overlap between $|\mathrm{AdS}\rangle$ and $|\mathrm{AdS}'\rangle$ is not exactly one. Although we will not compute the explicit form of the correction, let us be a bit more precise. Consider first the deviation of N'_k from N_k. Assuming that the backreaction is small, we can parametrize $N'_k = (N+\delta)_k$ where $|\delta_k| \ll N_k$. Then we can expand $\sqrt{N'_k} \simeq \sqrt{N_k}(1+\delta_k/(2N_k))$. Furthermore, the overlap between the coherent states is given by

$$\langle \mathrm{AdS}'|\mathrm{AdS}\rangle = e^{-\frac{1}{2}\int d^dk(N_k+N'_k-2\int d^dk\sqrt{N'_kN_k})} \simeq 1-\frac{1}{4}\int d^dk\frac{\delta_k^2}{N_k}. \tag{3.187}$$

On the one hand, these expressions are consistent with our earlier remark that to leading order we recover the classical result. On the other hand, corrections naturally appear as powers of $1/N$. Notice that these effects are entirely of corpuscular nature. In particular, the physics of such corrections can never be uncovered in a semi-classical treatment where instead one expects exponentially suppressed corrections.

Propagators, Wightman Function and Unruh Effect in AdS

Since we will be interested in quantum corrections to two-point correlation functions in AdS, let us briefly discuss some of the properties which we shall need later.

Let us first consider the defining equation for the classical propagator G_c of a scalar field Φ of mass m in an AdS background space-time[30],

$$\left\{\frac{1}{\sqrt{-g}}\partial_A(\sqrt{-g}g^{AB}\partial_B)+m^2\right\}G_c(X,Y) = \frac{1}{\sqrt{-g}}\delta^{(d+1)}(X-Y), \tag{3.188}$$

where g denotes the determinant of the metric, $X=\{x_\mu,z\}$ and A,B are $(d+1)$-dimensional indices. Let us for simplicity consider the case $d=3$. In Poincaré coordinates (3.188) becomes

$$\mathcal{O}_c(X)G_c(X,Y) = \delta^{(4)}(X,Y), \tag{3.189}$$

where we defined $\mathcal{O}_c(X) \equiv -g_{zz}^3\Box_M - 2g_{zz}^2(\partial^z g_{zz})\partial^z + g_{zz}^2m^2$ and $\Box_M = \partial^\mu\partial_\mu + (\partial^z)^2$. Note that the property of conformal flatness allowed us to express (3.189) in terms of a single component of the metric only. The general solution to equation (3.189) is known and can be found in the appendix.

[30] An equivalent definition of the propagator is given by the time-ordered two-point function of the scalar evaluated in an AdS vacuum state.

A related observable is given by the Wightman function W_c. It is defined as the non-time ordered two-point function of the field. Alternatively, the Wightman function is obtained as a solution of the equation of motion,

$$\mathcal{O}_c(X)W_c(X,Y) = 0. \tag{3.190}$$

This function will become crucial in our later analysis when corpuscular corrections to thermality of the spectrum of Unruh particles in AdS will be computed.

Thus, let us first of all review the Unruh effect in AdS and then discuss the properties the Wightman function has to obey in order to correspond to a thermal state. For a more detailed discussion, however, the reader is referred to the literature [105]. Just as in Minkowski space-time, the Unruh effect in AdS can be studied by looking at accelerated trajectories [107]. As we already know from our discussion of Hawking radiation, observers in general do not agree on the spectrum of measured particles. In particular, an inertial observer in AdS will define his vacuum as a state of no particles. For an accelerated observer, however, such a state can look like a thermal bath of particles. This is the essence of the Unruh effect. In AdS space-time, the analysis of the spectrum of emitted particles, however, is a little subtle.

In particular, an accelerated observer will only measure a thermal flux of particles if the acceleration a is above a certain threshold given by the inverse curvature radius ρ^{-1}. This becomes obvious when looking at the Bose distribution of emitted scalars an accelerated observer in AdS measures:

$$n_{(a,\rho)}(E) = \frac{1}{\exp\left(\frac{2\pi E}{\sqrt{a^2-\rho^{-2}}}\right) - 1}, \tag{3.191}$$

where E denotes the energy of the emitted particle. From this expression we can read off the temperature:

$$T = \frac{1}{2\pi}\sqrt{a^2 - \rho^{-2}}. \tag{3.192}$$

Thus, for $a^2 \leq \rho^{-2}$, there is no well-defined notion of temperature. Notice that no such condition must be fulfilled in the case of dS space-time. In this case an observer with $a > 0$ will measure a thermal spectrum no matter how small the acceleration is. This can be traced back to the fact that dS is positively curved in contrast to AdS. Furthermore, for $a^2 \gg \rho^{-2}$, effects of curvature can be neglected and one should reproduce the flat space-time result. We will later show, that this is still true in the corpuscular theory of Unruh radiation in AdS. In particular, in this limit all quantum corrections vanish thereby establishing a consistency check of our formalism. In other words, since only non-trivial space-times are understood as coherent states with respect to flat space-time, there should be no corrections if curvature effects become negligible. In other words, there are no corpuscles in Minkowski in our framework and subsequently no such effects[31].

[31]Note, however, that such a state of no particles cannot be distinguished from a state of an arbitrary

As a tool of investigating the thermality properties in the corpuscular approach we will later use a specific property of the Wightman function which is the so-called KMS condition stating the following. Suppose that the physical system under consideration corresponds to a thermal state. Then the Wightman function obeys the following property:

$$W_c(\tau_1, \tau_2) = W_c(\tau_2, \tau_1 + i\beta), \tag{3.193}$$

where τ_i, $i = 1, 2$ are time coordinates[32], $\beta = T^{-1}$ and we omitted spatial arguments. Notice that this condition simply expresses the periodicity of the bosonic path integral in Euclidean space.

Thus, in order to check whether an observer measures a thermal spectrum, it suffices to check (3.193). In the corpuscular theory, we will demonstrate that this property can no longer be fulfilled. Thus, quantum effects inevitably lead to deviations of thermality. For $a^2 \to \infty$, however, we recover the KMS condition which, as explained above, is a nice consistency check of our formalism.

Scalar Propagator

Having discussed the origin of the corpuscular effects in the context of scattering processes on linearized AdS and established the basic notions on propagators and Wightman functions, we will now proceed by considering corrections to the full non-linear propagator of a massive scalar field Φ in an AdS background. We will derive a general expression for the Green's function including corpuscular corrections. Furthermore, we explicitly evaluate these corrections in 4 dimensions in Poincaré coordinates.

Let us start by considering the line element of AdS in Poincaré coordinates,

$$ds^2 = \frac{\rho^2}{z^2}(dx^\mu dx_\mu + dz^2), \tag{3.194}$$

with $z = [\epsilon, \infty]$. Note that we introduced a short distance cut-off to regulate the behavior of the Green's function at $z = 0$ as usual. Furthermore, since the metric is conformally flat we have $g^c_{zz} = g^c_{ii} = -g^c_{tt}$. Here i labels the spatial Minkowski coordinates, t the time component and the superscript c stands for classical. Thus, in what follows we will express all components in terms of g_{zz}.

Just as before, we want to understand this metric as the expectation value of an operator evaluated in a coherent state. For that purpose, we follow the logic presented in the last section and expand the metric in Fourier space. Since the metric $g_{\mu\nu}$ depends only on the

number of gravitons of infinite wavelength. Indeed, in [108] it was shown that in gravity the Minkowski vacuum can be understood as a coherent state of an infinite number of gravitons with vanishing momentum. Since these particles have infinite wavelength, they will not introduce any quantum corrections.

[32]These are coordinates appropriate for an observer measuring a thermal spectrum. For example, these could correspond to the coordinates parametrizing an accelerated observers worldline in AdS in the regime $a^2 > \rho^{-2}$.

coordinate z, we are effectively considering a one-dimensional problem[33]. Consequently, the Fourier expansion can be written as

$$g^c_{zz} = \sqrt{L}\int \frac{dk_z}{\sqrt{(2\pi)2\omega_{k_z}}}(\alpha_{k_z}e^{ik_z z} + \text{h.c.}). \tag{3.195}$$

From this expression, one can easily derive the classical Fourier coefficients,

$$\alpha_{k_z} = -\sqrt{\pi}\sqrt{\frac{\omega_{k_z}}{L}}\rho^2|k_z|. \tag{3.196}$$

Notice that the dispersion relation in the case $d = 3$ which we shall investigate in detail below was determined in the previous section by matching with the classical energy of AdS. As a result we found that $\omega^2_{k_z} = 2\pi\rho^{-2}$ which again demonstrates that the corpuscles of AdS are very different from the ordinary S-matrix particles.

Promoting (3.195) to an operator equation and introducing a coherent state which resolves the background geometry[34],

$$|\text{AdS}\rangle = \prod_k |N_k\rangle = \prod_k e^{-\frac{N_k}{2}}\sum_{n_k}\frac{N_k^{\frac{n_k}{2}}}{\sqrt{n_k!}}|n_k\rangle, \tag{3.197}$$

a proper classical limit again leads to the interpretation of the corresponding operators $\hat{a}_k$ and $\hat{a}^\dagger_k$ as annihilation and creation operators of corpuscles in the AdS state with commutation relation similar to the ones introduced in the last section. In particular we have $\hat{a}^\dagger_k\hat{a}_k|n_k\rangle = n_k|n_k\rangle$ and $\hat{a}_k|N_k\rangle = \sqrt{N_k}|N_k\rangle$. Notice that since $\sqrt{N_k}$ corresponds to the classical Fourier coefficients in (3.195) we see that the occupation of corpuscles becomes large at high momenta. Physically, this should be clear. It simply reflects the fact that AdS acts like a finite sized box with the wavelengths infinitely blue-shifted as $z \to 0$.

Let us now consider the classical equation of motion for the classical propagator G_c of a scalar field of mass m in an AdS background space-time in the case $d = 3$,

$$\mathcal{O}_c(X)G_c(X,Y) = \delta^{(4)}(X,Y), \tag{3.198}$$

where we defined $\mathcal{O}_c(X) \equiv -g^3_{zz}\Box_M - 2g^2_{zz}(\partial^z g_{zz})\partial^z + g^2_{zz}m^2$ and $\Box_M = \partial^\mu\partial_\mu + (\partial^z)^2$. The explicit form of G_c is known and can be inferred from the appendix.

Let us now discuss the quantum corpuscular theory. In other words, we should replace (3.198) by an operator statement evaluated in the state (3.197). In particular, using the expansion (3.195) we see that we need to evaluate the action of powers of the creation and annihilation operators on the coherent state. Since $|\text{AdS}\rangle$ is not an eigenstate of $\hat{a}^\dagger_k$,

[33]Notice that in principle we could also take the other components into account. This would amount to a trivial delta-contribution in the expansion coefficients. Although these are important for understanding holographic properties from the corpuscular point of view as discussed in the last section, these contributions are not important for understanding the origin of corpuscular corrections.

[34]From now on we will drop the subscript z as it is clear that only this component contributes.

we can immediately understand the origin of corpuscular corrections. These are simply encoded in the commutators of $\hat{a}_k$ and $\hat{a}_k^\dagger$. Thus, we can rearrange the terms as a normal ordered part plus quantum corrections from commutators just as we did when analyzing corpuscular solitons in the Wess-Zumino model. Notice that by construction the normal ordered part simply reduces to its classical value. Quantum corrections, however, give departures from (3.198). Note that these quantum effects can be absorbed in a redefinition of the propagator. In other words, we demand that the full propagator G_f containing corpuscular corrections should satisfy the following equation;

$$\langle \text{AdS}|\mathcal{O}_f(X)G_f(X,Y)|\text{AdS}\rangle = \delta^{(4)}(X-Y). \tag{3.199}$$

where $\mathcal{O}_f = \mathcal{O}_c + \mathcal{O}_q$ and $G_f = G_c + G_q$, and $\mathcal{O}_q$ and G_q denote the quantum parts of the equation of motion operator and Green's function, respectively[35]. Equation (3.199) can be solved by iteration, $G_q = \sum_{j=1}^{\infty} G_{q,j}$. Hence,

$$G_f = G_c - G_c\mathcal{O}_q G_c + G_c\mathcal{O}_q G_c\mathcal{O}_q G_c - ..., \tag{3.200}$$

where we used $\mathcal{O}_c G_c = 1$ and it is understood that $\mathcal{O}_q$ is evaluated in the AdS state. Notice that (3.200) corresponds to a Dyson series which can be summed up explicitly. Thus, we find

$$G_f = \frac{G_c}{1+\mathcal{O}_q G_c}. \tag{3.201}$$

Let us stress that this derivation is not restricted to AdS space-time. Rather it applies to all Green's functions for arbitrary backgrounds which are resolved by means of coherent states. Furthermore, the result is consistent with the semi-classical limit, since in that case $\mathcal{O}_q = 0$. Finally, we can interpret $(\mathcal{O}_c+\mathcal{O}_q)^{-1}$ as propagator which can be derived from a corpuscular effective action $S = S_{\text{classical}} + S_{\text{corpuscular}}$ with $S_{\text{corpuscular}} \sim \int d^4X \Phi\mathcal{O}_q\Phi$. Notice that this action is truly of corpuscular origin. In particular, taking backreaction from quantum loops on a classical AdS into account we would still be blind to $S_{\text{corpuscular}}$. Therefore, we can only uncover this structure in a corpuscular approach. Let us elaborate a little bit more on the distinction between the one-particle irreducible effective action and the corpuscular action. The former correponds to an $\hbar$ expansion of loops on top of a classical background. As such, it renormalizes classical data characterizing the background order by order in $\hbar$. Note, that these effects are typically exponentially suppressed (an easy way to see this is when evaluating the functional determinant in the saddle point approximation using the functional integral). The latter action, in contrast, takes into account the quantum effects associated to the background itself. In other words, the classical data characterizing the solution are affected by the dynamics of corpuscles constituting the would-be classical solution. These effects are not exponentially, but rather $1/N$ suppressed. To summarize, there are two independent parameters, $\hbar$ and $1/N$. In particular, solving the complete theory would amount to computing the corresponding one-particle irreducible corpuscular

[35] From now on we will use operator notation.

effective action. Since both expansion parameters are in general independent, however, we can focus on the leading order in $\hbar$ and nevertheless investigate the corpuscular effects.

Let us now evaluate (3.201) explicitly for AdS. Since the computation is straight forward and works just as in the case of solitons in the Wess-Zumino model which is presented in the appendix, we only state the result here. For the quantum operator we find:

$$\mathcal{O}_q = \frac{\rho}{4\sqrt{2}\pi^{3/2}}\Big(- 2(\partial^z g^c_{zz})\partial^z - 3g^c_{zz}\Box_M\Big)\int dk. \tag{3.202}$$

Let us discuss this result in some detail. First of all we see that the quantum operator is linear in the metric field. Thus, it diverges as $1/z^2$ as $z \to 0$. The reader might be worried whether such a divergence could be inconsistent with classical results. In order to answer this question note that $G_f \sim (\mathcal{O}_c + \mathcal{O}_q)^{-1}$. Now for small z we have $\mathcal{O}_c \sim z^{-6}$. As a consequence $G_c \sim \mathcal{O}_c^{-1}$ for small z. Thus, even though the quantum part of the operator diverges, the classical part blows up much faster, thereby guaranteeing that at the boundary, the propagator reduces to its classical value. This seems to suggest that no corpuscular corrections to CFT correlation function are expected. Instead, the effects are important only in the interior of AdS.

Furthermore, we see that the quantum effects mix classical and quantum contributions. In particular, it can be seen that a function of the classical metric is multiplied by an integral which is due to commutator terms. Note that we cannot get rid of these terms by subtracting the corresponding vacuum contribution, because (3.202) explicitly contains information about the background due to the terms involving g^c_{zz}. Notice that there are divergences which we can interpret as follows: Since we used the classical data N_k to perform our computation, we can think of it as a bare distribution characterizing the geometry. Then, taking commutators is equivalent to considering loop effects. As usual, the infinities we encounter when performing such computations should be reabsorbed in a redefinition of the classical parameters. Thus, what we are uncovering could be interpreted as a corpuscular renormalization of the N_k and subsequently of the metric. In other words, on top of the usual wave function renormalization one encounters in perturbation theory, we uncover a novel, corpuscular source that renormalizes the classical gravitational field. In other words, we rediscover the same effect which we have already observered when we studied SUSY solitons in the coherent state description of gravity. Thus, the structure of $1/N$ effects seem to be independent of the explicit situation which we are considering. Rather, the phenomenon of corpuscular renormalization seems to be universal[36].

Finally, in order to complete our analysis, we have to act with $\mathcal{O}_q$ on the classical Green's function to find G_f. Our results are shown in the Figures (3.5 - 3.8). Unless otherwise stated the diagrams correspond to the choices $\rho = 1$ and $\Lambda = \sqrt{2\pi}\rho^{-1}$, where Λ denotes the UV cut-off on the momentum integration in (3.202). Note that the coordinate labels are as follows: $X = (t_1, x_1, y_1, z_1)$ and $Y = (t_2, x_2, y_2, z_2)$.

[36]Note that the phenomenon is not even tied to the coherent state description. Instead, it seems to be an effect which is shared by different approaches which aim at resolving the quantum substructure of classical solitons. Indeed, we already discovered a similar effect in the context of the auxiliary current description when we explained how to recover the Schwarzschild metric (see chapter 2).

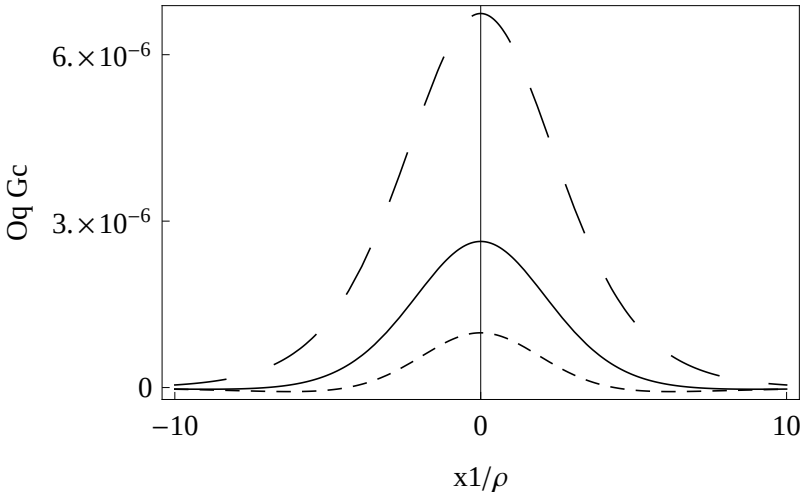

Figure 3.5: $\mathcal{O}_q G_c$ measured in units of the AdS curvature radius as a function of x_1 for the following choice of parameters $x_2 = y_1 = y_2 = 0$, $z_1 = 7$, $z_2 = 1$, $t_1 = 1$, $t_2 = 0$. The large dashed curve corresponds to $m^2 = -1$, the straight to $m^2 = 0$ and the dashed one to $m^2 = 1$.

All the diagrams indicate that the quantum corrections are extremely suppressed as long as we are far away from any poles. As we have explained before, the divergence at the point $z_1 = z_2$ is not inconsistent, because the classical part of the equation of motion operator diverges much faster at this point. Furthermore, the profile is completely well-behaved as a function of x_1 and drops quickly to zero for $x_1 \gg z_1$ as can be inferred from Figure (3.5). The second plot shows the behaviour of $\mathcal{O}_q G_c$ as a function of the coordinate x_1. Now the mass is fixed to $m^2 = 1$. The different curves illustrate the corpuscular effects for different choices of the curvature radius. It can be seen that quantum corrections are smaller for larger curvature radius as could be expected. Figure (3.7) uncovers the singularity structure of $\mathcal{O}_q G_c$ as a function of z_1. For large values of z_1, the corpuscular effect is rather small, but it grows rapidly if we take $z_1 \to z_2$ reflecting a singularity in the quantum contribution to the Green's function at z_2. Finally, in Figure (3.8) the behavior of $\mathcal{O}_q G_c$ is shown as a function of z_1 for AdS curvature radius $\rho = 1$ (straight curve) and $\rho = 1.5$ (large dashed curve). While the corpuscular corrections are small for large values of z_1, they become large for $z_1 \to 0$. This singular behavior, of course, simply reflects the singular structure of the Poincaré coordinates at the boundary.

In summary, the quantum corpuscular corrections seem to be well-behaved and small except for isolated singularities. Therefore, our approach as well as the resummation technique used seem to be justified.

Unruh Effect in AdS

Having discussed the physics of corpuscular corrections to the propagator, we will apply similar techniques to the Wightman function in this section. This computation is of par-

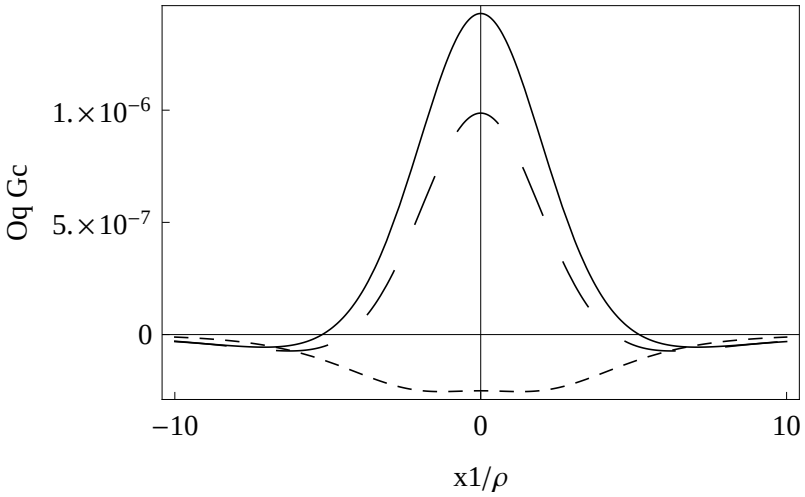

Figure 3.6: $\mathcal{O}_q G_c$ as a function of x_1 for the following choice of parameters $x_2 = y_1 = y_2 = 0$, $z_1 = 7$, $z_2 = 1$, $t_1 = 1$, $t_2 = 0$, $m^2 = 1$. The straight curve corresponds to $\rho = 0.8$, the large dashed one to $\rho = 1$ and the dashed one to $\rho = 2$.

ticular interest, because knowledge about the corpuscular Wightman function immediately translates into a statement about the Unruh effect in the corpuscular description of AdS. Before discussing the full quantum theory, we will first review the semi-classical analysis of the Unruh effect in AdS. For a more detailed discussion, however, the reader is referred to the literature [107].

Semi-Classical Analysis

Semi-classically, the Unruh temperature (in an arbitrary space-time) can be derived from the transition rate $\dot{\mathcal{F}}(E)$ which is defined as the temporal Fourier transform of the Wightman function $W_c(X, Y)$ introduced before. Let us now consider the Wightman function in AdS in $3 + 1$-dimensions. For a massless scalar in Poincaré coordinates it is given by the following expression:

$$W_c(X, Y) = \frac{1}{8\pi^2\rho^2}\Big(\frac{1}{\nu - 1} - \frac{1}{\nu + 1}\Big), \tag{3.203}$$

where

$$\nu = \frac{z_1^2 + z_2^2 + (x_1 - x_2)^2 + (y_1 - y_2)^2 - (t_1 - t_2 - i\epsilon)^2}{2z_1 z_2}. \tag{3.204}$$

In what follows, we will restrict our discussion to accelerated trajectories along the $z - t$ plane, so that we can set $x_1 = x_2 = y_1 = y_2 = 0$. Since we are ultimately interested in deviations from thermality, we will consider only the so-called supercritical regime where $a^2 > 1/\rho^2$ with a the observer's acceleration because for $a \leq 1/\rho^2$ a Rindler observer in

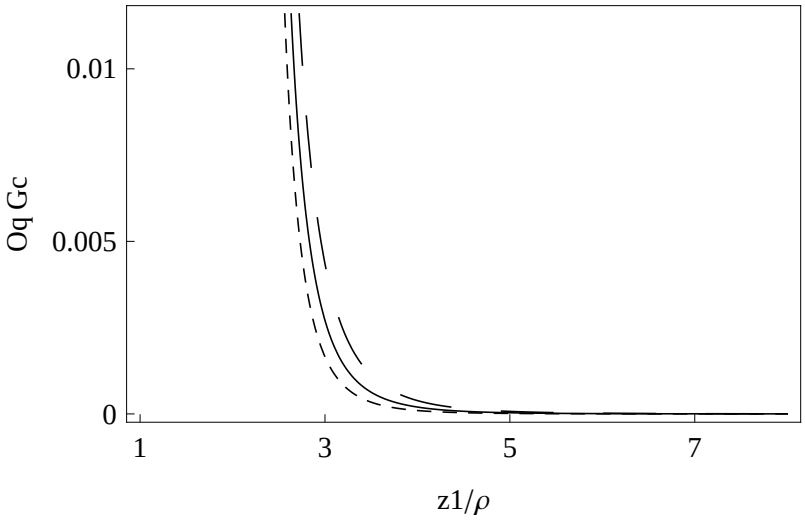

Figure 3.7: $\mathcal{O}_q G_c$ measured in units of the AdS curvature radius as a function of z_1 for the following choice of parameters $x_1 = x_2 = y_1 = y_2 = 0$, $z_2 = 1$, $t_1 = 1$, $t_2 = 0$. The large dashed curve corresponds to $m^2 = -1$, the straight to $m^2 = 0$ and the dashed one to $m^2 = 1$.

AdS will experience no thermal response[37]. In this regime, the worldline of an accelerated observer can be parametrized as follows [109].

$$\begin{aligned} t(\tau) &= \frac{a}{\sqrt{a^2 - 1/\rho^2}} z_o e^{\sqrt{a^2-1/\rho^2}\tau} \\ z(\tau) &= z_o e^{\sqrt{a^2-1/\rho^2}\tau}. \end{aligned} \tag{3.205}$$

Furthermore, the transition rate is given by

$$\begin{aligned} \dot{\mathcal{F}}(E) \quad &= \int ds e^{-is} W_c(s) \\ &= \left[\frac{E}{2\pi} - \frac{1}{4\pi a \rho^2} \sin\left(\frac{2E}{\sqrt{a^2 - 1/\rho^2}} \operatorname{arcsinh}(\rho\sqrt{a^2 - 1/\rho^2}) \right) \right] \\ &\times \frac{1}{\exp(2\pi E/\sqrt{a^2 - 1/\rho^2}) - 1}, \end{aligned} \tag{3.206}$$

where $s = \tau_1 - \tau_2$. From this expression, we can read off that an accelerated observer in AdS in the supercritical regime measures a flux of particles in thermal equilibrium with temperature given by

$$T = \frac{1}{2\pi}\sqrt{a^2 - 1/\rho^2}. \tag{3.207}$$

[37] In principle, the corpuscular effects could also correct the point of the phase transition. Taking a^2 well above ρ^{-2}, however, we can safely neglect such effects.

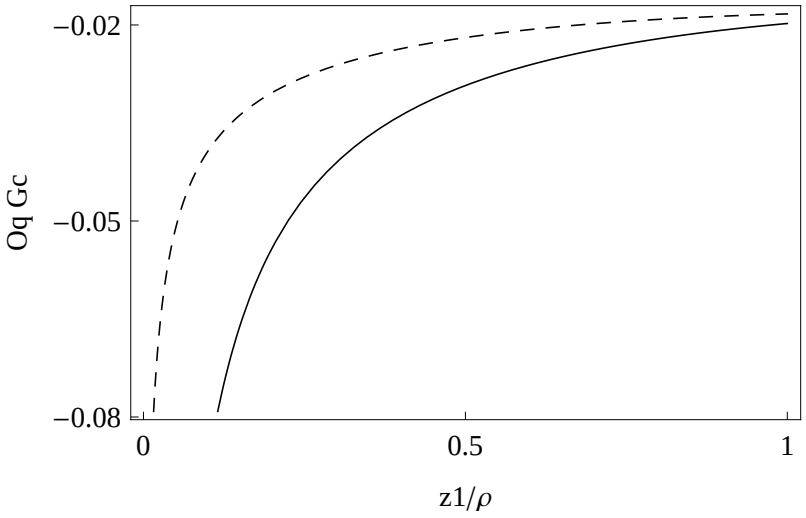

Figure 3.8: $\mathcal{O}_q G_c$ measured as a function of z_1 for the following choice of parameters $x_1 = x_2 = y_1 = y_2 = 0$, $z_2 = 0.1$, $t_1 = 1$, $t_2 = 0$, $m^2 = 1$. The straight curve corresponds to $\rho = 1$, the large dashed to $\rho = 1.5$.

Let us furthermore notice that the Wightman function expressed in accelerated coordinates is subject to the KMS (Kubo-Martin-Schwinger) condition explained above. Thus, without deriving an exact expression for the temperature a Rindler observer measures in AdS, we could in principle already anticipate that the observer is in thermal equilibrium with its environment simply by inspecting the Wightman function.

Corpuscular Effects

Having reviewed the semi-classical analysis, let us now proceed and describe the corpuscular effects on thermality. Let us first explain our strategy. In order to discuss the Unruh effect in AdS in the corpuscular theory, we first need to derive an expression for the full Wightman function W_f taking quantum effects into account. In order to discuss whether a Rindler observer measures a thermal spectrum, we must parametrize W_f according to (3.205). Finally, in order to check whether the system is thermal or not, we need to check the condition KMS condition for the full Wightman function expressed in terms of the parameter τ. Let us start be deriving an exact expression for W_f. Notice that classically we have

$$\mathcal{O}_c W_c = 0. \tag{3.208}$$

As explained in the last section, the classical equation of motion operator will receive corpuscular corrections. Thus, defining the full Wightman function such that it obeys the quantum corrected equation of motion,

$$(\mathcal{O}_c + \mathcal{O}_q) W_f = (\mathcal{O}_c + \mathcal{O}_q)(W_c + W_q) = 0, \tag{3.209}$$

with $\mathcal{O}_q$ given as before, we can again use a similar resummation as for the full propagator to find

$$W_f = W_c - G_f \mathcal{O}_q W_c. \tag{3.210}$$

Since the result is rather lengthy, we will illustrate the relevant physics in Figure (3.9). Note that for simplicity we set $\tau_2 = 0$ in our analysis. Thus, we have $\tau_1 = s \equiv \tau$. Furthermore, since (3.210) follows from a resummation of contributions containing the classical propagator, possible deviations from thermality are already encoded in terms of the form $W_{q_1} \equiv G_c \mathcal{O}_q W_c$. Thus, we can restrict our analysis to such contributions. In Figure (3.9)

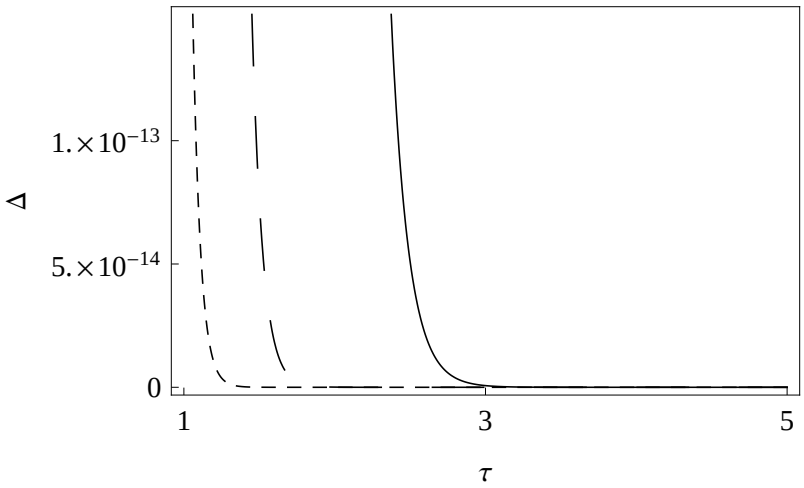

Figure 3.9: $\Delta \equiv W_{q_1}(\tau, 0) - W_{q_1}(0, \tau + i\beta)$ as a functions of τ for $z_0 = 1$ and $\rho = 1$. The straight line corresponds to $a = 2$, the large dashed to $a = 3$ and the dashed to $a = 4$.

we show $\Delta \equiv W_{q_1}(\tau, 0) - W_{q_1}(0, \tau + i\beta)$. Note that having $\Delta \neq 0$ implies that the KMS condition is violated. The plot thus clearly indicates deviations from thermality encoded in corpuscular corrections to the Wightman function. Furthermore, the effect becomes smaller for larger acceleration. Note that this larger acceleration effectively corresponds to curvature effects becoming less important. Thus, the result is consistent with our expectation that the corpuscular corrections vanish in flat spacetime, or equivalently if we take $a \gg \rho^{-1}$.

Notice that the full Wightman function is close to fulfilling the KMS condition for large values of τ. This result is in agreement with our earlier analysis of the propagator. In particular, in the last section we saw that quantum corrections quickly go to zero for large values of z_1. From (3.205) we can see that large values of z_1 correspond to large τ. In other words, when averaged over a large portion of AdS, quantum corrections effectively do not contribute. Nevertheless, as explained below the transition rate is sensitive to all scales due to the integration, corpuscular effects influence the physical observable, i.e. the spectrum of emitted particles. Thus, thermality is violated due to propagation scales probing local aspects of AdS. Notice that this result is in perfect agreement with the findings of the

previous chapter. There it was shown that the number of corpuscles defined in a local region around some point is always finite. In contrast, resolving the full AdS manifold, this number diverges towards the UV. Since our effects are naturally understood as $1/N$ corrections, we thus understand that the correction are visible only locally, or at a finite propagation scale, but not globally.

Technically, the result can be understood easily by inspecting (3.202). While G_c and W_c both fulfil the KMS condition, this cannot be the case for $\mathcal{O}_q$ simply because it does not depend either on z_2 or t_2. This fact once again is a manifestation of the corpuscular nature of the corrections.

Let us briefly elaborate how this result would affect the transition rate. For that purpose we note that (3.206) will receive a new contribution from the Fourier transform of W_{q_1}. While the classical contributions are all periodic in $i\beta$, this will not be true for the the quantum correction. In fact, the non-thermal behavior will be due to small values of τ, or equivalently large values of the energy E.

In conclusion, our analysis demonstrates that a corpuscular resolution of AdS is incompatible with a perfect thermal spectrum of Unruh radiation.

3.5.3 Discussion and Outlook

Let us briefly summarize our findings and possible new directions which could be addressed within the coherent state approach. We presented a general strategy aiming at a resolution of classical solutions in terms of coherent states. The coherent state was constructed self-consistently in such a way that the one-point function of the field operator reproduces the classical profile when evaluated in the coherent state. For that purpose, the coherent state was constructed as a superposition of number eigenstates of fully interacting particles or corpuscles constituting the profile.

The formalism was subsequently applied to solitons and instantons in field theory. It was shown that topological charge arises from an infinite occupation of zero frequency corpuscles supporting the momentum flow in one direction at the microscopic level. In contrast, we showed that the quanta contributing to the energy of a soliton have wavelengths of the order of the typical size of the profile. This distinction was made explicit by representing the soliton as a convolution of topological and energetic sector. For a non-topological soliton we observed that there is no pole in the occupation number of zero momentum modes. Due to basic properties of coherent states, this finiteness implied a non-vanishing overlap with the topologically trivial vacuum. In other words, finite occupation of corpuscles is the underlying reason for the instability of the vacuum with respect to bubble nucleation. As a next step, it was shown how the well-known interaction potential between soliton and anti-soliton arises as a simple consequence of our construction.

In the next section, we explained the physics of instanton constituency. Since an instanton in d dimensions can be mapped to a soliton in $d+1$ dimensions evolving in Euclidean time, we defined the corpuscular resolution of the former in terms of the one of the latter. We explicitly checked that our construction gives the correct instanton-induced transition matrix elements. This was demonstrated in various examples such as instantons in quan-

tum mechanics, Polyakov-instantons as well as in Yang-Mills theory. Having developed a quantum mechanical understanding of instantons, we argued that the physics of resurgence must follow simply as a consequence of the optical theorem. Indeed, cancellation of ambiguities in the perturbative expansions about trivial and non-trivial saddles can be naturally accounted for in the coherent state approach to instantons.

We proceeded with a discussion of solitons and instantons in supersymmetric theories. It was explicitly shown that the BPS condition cannot be maintained as soon as the corpuscular structure is taken into account properly. In other words, due to corpuscles running in loops, supersymmetry breaking can be understood as $1/N$ effect which can never be discovered in a semi-classical approach where $N = \infty$. Note that here N is associated to the quanta accounting for the energy of the soliton and not the ones which carry information about the topology. The program of corpuscular breaking of supersymmetry was developed in detail in the case of a Wess-Zumino model in 2 dimensions. We found an explicit expression for the Bose-Fermi mass splitting for the fluctuations due to corpuscular effects. Furthermore, we were able to understand the underlying physics of these effects in terms of the need for a corpuscular renormalization of data characterizing the classical profile due to corpuscles running in loops.

In the last section, we turned our attention again to gravity and, in particular, to a corpuscular resolution of AdS space-time. First, we presented the corpuscular portrait of AdS to leading order in $1/N$. This construction enabled us to reinterpret some well-known facts about AdS in pure quantum terms. In particular, holographic as well as geometric properties, are mapped to the occupation number of corpuscles constituting portions of the space-time. Subsequently, we considered corpuscular corrections to the scalar propagator in the fully resolved non-linear AdS space-time. It was possible to resum and explicitly compute the $1/N$ corrections to the propagator. In order to check the validity of our approach we performed several numerical checks concerning the corrections to the propagator. Finally, the Unruh effect in AdS was studied in detail from the coruscular point of view. Our main result was that as soon as corpuscular effects are considered, an Unruh observer in AdS does no longer measure a perfectly thermal spectrum. We argued that a similar mechanism in black hole physics could offer a microscopic explanation of purification of Hawking radiation.

Let us now give an overview over possible new research directions. Of course, just as in the case of the auxiliary current description, the list is not exhaustive.

- dS space-time:

  Having analyzed AdS a logical next step would be a corpuscular resolution of dS. In this case, however, one has to generalize our construction to time-dependent situations. An interesting question which should be addressed is the cosmological constant problem. In [25, 37] it was argued that a corpuscular resolution of dS sheds a completely new light on the nature of the cosmological constant. Indeed, the authors raise the question whether the cosmological constant problem posed as a naturalness issue as usual is well-defined when quantum effects are taken into account. The point

is that just as a black hole, dS is supposed to have a finite quantum break time [30]. In other words, there is no notion of eternal classical de Sitter and subsequently of a classical vacuum energy. Thus, it would be very interesting to study these ideas from a more quantitative point of view. The coherent state approach could offer a proper framework.

- Inflation:

  Another important application of the coherent state formalism could be inflation. In that case, one would need to introduce coherent states for gravitational as well as inflaton backgrounds. Subsequently, one could analyze corpuscular corrections to observables which can be measured in the CMB such as the spectral index or the scalar-to-tensor ratio. Notice that a first step in this was already done in [25].

- Black Holes:

  We already mentioned that an analysis of black hole evaporation from the corpuscular point of view could be of utmost importance. In particular, one should study the information paradox using a microscopic theory based on coherent states. Note that, as discussed in the previous section, according to the N Portrait, a black hole is supposed to become maximally quantum after the scrambling time $r_g \log N$ [30]. Therefore, at that time scale, coherent states cannot capture the physics of black holes anymore. Nevertheless, coherent states can be used when describing black holes at early time scales. Analyzing the early stages of evaporation in the coherent state picture might already give a clue how Hawking radiation is purified.

- Other Solitons and D-branes:

  Throughout the thesis, we analyzed the corpuscular theory of solitons using various concrete examples. As a next step, one could apply a similar reasoning to even more solitonic objects and instantons. Interesting questions could include dyons, sphalerons or Coleman-de Luccia-type instantons [77]. In the case of dyons, corpuscular effects might change the relation between electric and magnetic charge. In the context of sphaleron physics, one could compute quantum corrections to the physics of baryogenesis. Finally, an analysis of Coleman-de Luccia situations from the corpuscular point of view might shed a new light on the stability of a given space-time. Of course there are plenty of other interesting solitons one could study such as for example vortices or cosmic strings in field theory or certain D-brane configurations in string theory and supergravity.

Chapter 4

Summary

In this thesis we tried to develop a microscopic understanding of entities which are usually introduced on purely classical grounds within gravity and QFT. The basic idea was to replace classical solutions by bound states or coherent states of a large number of constituent quanta N. While such an approach should correctly reproduce semi-classical results in the limit $N \to \infty$ there should be corrections which scale as $1/N$ for any finite value of N. This way of thinking was originally put forward in [23] in the context of black hole physics. Indeed, it was argued that these $1/N$ effects are the key for understanding a resolution of the information paradox. Furthermore, following more recent ideas [31, 33], these effects offer a completely new and simple way of understanding the large amount of information capacity of black holes and Bekenstein entropy microscopically.

Following the logic that classical results only approximate a more fundamental quantum reality, similar arguments were applied to other space-times such as dS, AdS and inflationary backgrounds [25] as well as to solitonic configurations in supersymmetric theories [76]. Among other things, it was argued that this way of thinking could shed new light on AdS/CFT, the cosmological constant or supersymmetry breaking.

The main aim of this work was to build up on these ideas as well as to extend and formalize them. Indeed, we developed two independent, quantitative approaches which allow one to represent the quantum state of the system which is usually introduced classically, in terms of a large number of microscopic degrees of freedom.

The first approach, the so-called auxiliary current description, was inspired by techniques which are often employed in QCD when discussing bound states. Assuming that there is some bound state in the spectrum of the Hamiltonian of the theory, it is possible to represent its quantum state in terms of a Fock state expansion of number eigenstates constructed from the microscopic degrees of freedom appearing in the Lagrangian. In order to have a non-vanishing overlap with the true bound state, these Fock states must carry the same quantum number as the bound state itself. Having found such a set of states, it is possible to project the quantum bound state onto a given Fock state. In turn, one can directly express the quantum bound state in terms of the field operators of the Lagrangian.

The second approach was based on describing classical solutions in terms of quantum coherent states. In order to have a consistent description in the sense that the one-point

function of the field operator replacing the classical solution reduces to its classical value when evaluated in the coherent state, this state was constructed from fully interacting quanta constituting the profile. As a consequence, these quanta are completely different than the ordinary propagating degrees of freedom. In order to make the distinction, we thus referred to the former as to the corpuscular constituents, or simply corpuscles, of the classical profile.

In order to make our ideas transparent, we applied these constructions to concrete physical systems. In the case of the auxiliary current description, we were mostly interested in black hole physics. Understanding the black hole quantum state in terms of a multi-graviton state on flat space-time, we were able to compute observables connected to the black hole interior such as the density of gravitons in momentum space or their energy density at the parton level and in the large mass limit. Consistency of our results then implied that the total mass of the black hole must scale as the number of fields composing the auxiliary current. We found that the distribution of gravitons in the black hole is dominated by quanta of large wavelength which resonates with the ideas put forward in the Black Hole Quantum N Portrait. Based on these results, we explained that the distribution function of gravitons is directly accessible in S-matrix processes. As a consequence, an outside observer can in principle reconstruct the internal structure of the black hole. Thus, no loss of information as well as the existence of quantum hair are expected in our approach. Finally, we showed how the Schwarzschild metric emerges from our approach. The basic insight was to replace a classical black hole source characterized by the mass by the corresponding microscopic quantum source. This quantum source was identified with the energy density of gravitons inside the black hole. On the one hand, the mass arises as a collective effect of N gravitons. On the other hand, for any finite N, we argued that there are corrections to the classical notion of mass which can be absorbed in a wave function renormalization. Using this result combined with the finding of [67] it was straightforward to show that in our description, classical geometry indeed emerges in the limit $N \to \infty$.

Using the coherent state construction, we investigated issues in soliton physics, in the case of instantons as well as in the context of AdS. Representing solitons in terms of coherent states, we explained how well-known classical properties such as mass the profile or topology emerge as a collective effect of individual corpuscles. Discussing topological solitons, we showed that conservation of topological charge follows from an infinite occupation number of corpuscles of infinite wavelength. At the same time, the energy of the soliton is carried by corpuscles which have wavelengths that are set by the typical size of the classical profile. In order to make the distinction manifest, we represented the soliton as a convolution of the two sectors. This representation enabled us to clearly disentangle the quanta which are responsible for the topology from the one which account for the energy. Furthermore, we showed that in the case of non-topological solitons, there is no pole in the occupation number of corpuscles. As a consequence, the total number of corpuscles is finite. The property of instability of the vacuum then followed as a simple consequence of the basic properties of coherent states. Recognizing that there is a one to one correspondence between a soliton in $d+1$ dimensions evolving in Euclidean time and an instanton process in d dimension, we further argued that a corpuscular description of the former im-

plies that the latter should be composite as well. Using this mapping we explicitly showed how semi-classical instanton results are easily obtained in terms of the coherent state description of the corresponding soliton to leading order in $1/N$. This was done in detail in several cases such as instantons in quantum mechanics, Yang-Mills theory or 3-dimensional electrodynamics. In addition, in order to make the mapping manifest we constructed theories which naturally embed instanton physics in d dimensions into theories in one more dimension describing evolving solitons. Using the insight that instantons should have a quantum description, we further argued that the concept of resurgence should follow as a consequence of the basic principles of quantum mechanics such as unitarity. As a next step, we were concerned with higher order corpuscular effects in the case of solitons in SUSY theories. In the example of a Wess-Zumino model in $1+1$ dimensions we worked out in detail that these effects lead to a novel mechanism of SUSY breaking which can never be discovered in the semi-classical treatment. We argued that these correction can naturally be understood in terms a corpuscular renormalization of the classical profile induced by corpuscular loops. Alternatively, we explained that these effects can also be understood in the many-body language. Indeed, in Bogoliubov approximation, quantum corrections are encoded in the dynamics of small fluctuations (quasi-particle excitations) around the mean field data. Finally, we applied the coherent state picture to the physics of AdS space-time. To leading order in $1/N$, we explained how geometric properties such as local flatness or stability of AdS with respect to decay into Minkowski space-time are mapped to the occupation of corpuscles in AdS. In addition, we saw that the central charge of the dual CFT can be understood as a collective effects of corpuscles constituting a portion of AdS with volume set by the curvature radius. Based on these results, we proceeded with a discussion of higher order correction. In particular, we investigated how corpuscular effects correct propagators and Wightman functions in an AdS space-time. On the one hand, it was shown that the corpuscular effects on the propagator can be resummed in a Dyson-type series. On the other hand, using the KMS condition as a tool, we demonstrated that there are corrections to thermality of the spectrum that an accelerated observer measures in AdS which can never be uncoverer in the semi-classical treatment.

There are several important question which need to be addressed in the future using our constructions. Some of them were already indicated in the summary sections of the corresponding chapters. Let us nevertheless mention a few more open questions which are of theoretical importance. First of all, in order to truly capture the essence of the ideas put forward in the Black Hole Quantum N Portrait and subsequent works, we have to understand why a black hole should be special within the auxiliary current description. Notice, so far all of our results do not depend on the notion of a horizon, but rather apply to all spherically symmetric, gravitating objects irrespective of their geometric size. In order to distinguish a black hole from other spherical sources, we need to put in some extra ingredients. As a first step, one could implement the non-existence of a global time-like Killing vector on phenomenological grounds by implementing an explicit time dependence in the auxiliary current. This way, we could implement in principle the fact that black holes emit Hawking quanta and other gravitating sources do not. As a second step, one could analyze the evolution of graviton distribution for fixed geometric radius as a function

of the mass of the source. As already mentioned, one might suspect that the point where one classically expects a black hole could be identified with a fixed point of a related flow equation, i.e. with the point of graviton saturation. If this were the case, the black hole would be truly special, because it appears at a critical point. In turn, this point should be related to the quantum critical point of the Black Hole Quantum N Portrait. In the context of coherent states, it remains to be understood properly how time-dependent solutions can be treated. In particular, such an understanding is crucial for describing dS, inflationary or Friedmann-Robertsen-Walker space-times in the corpuscular approach. On top, it would be very interesting to relate the corpuscular quanta to the propagating degrees of freedom of the theory. Indeed, in terms of the latter, resurgence suggests that soliton or instanton effects become visible at high orders of perturbation theory. This naturally suggests that there should be some kind of Bogolyubov tranformation between the corpuscular and the asymptotic creation and annihilation operators. Working out this relation is an open problem. Finally, we think that the two approaches to compositeness of classical solutions presented in this thesis are not disconnected. Rather, it should be possible to translate the coherent state language into the auxiliary current description and vice versa. This should be rather clear, because the overlap between the coherent state and the state constructed by acting with the auxiliary current on the vacuum cannot be vanishing. Working out the precise dictionary that relates the two description remains an important challenge.

A somewhat related question which should be investigated in the future is motivated by the recent articles [110, 111]. While in the former the authors develop an understanding of Bekenstein entropy in terms of Stückelberg degrees of freedom which naturally live on the horizon of a black hole from the point of view of an outside observer, such an understanding is achieved in terms of BMS transformations in the latter (for a discussion about BMS symmetry we refer the reader to the original work [112, 113] as well as to recent developments [114,115]). Note that although both approaches seem to be complementary to the N portrait, there is a one to one mapping between the various descriptions. From the point of view of this thesis, it would be natural to investigate whether similar constructions could be applied to AdS space-time. From the point of view of the Stückelberg formulation, one could expect that there are degrees of freedom on the boundary of AdS which are needed in order to restore gauge invariance everywhere. Working out this connection in more detail might shed a completely new light on the AdS/CFT correspondence. Furthermore, comparing with the findings of [110], we might expect that the Stückelberg degrees of freedom can directly be mapped to the corpuscles composing AdS. In the case of BMS symmetry in AdS, the major difficulty is to generalize BMS transformation to space-times which are not asymptotically flat. Note, however, that the findings of [111] seem to suggest that the existence of a null hypersurface is sufficient in order to construct the corresponding BMS group. In AdS, however, the situation is even more comfortable because the conformal boundary has the topology of Minkowski space-time. Indeed, in this case, the asymptotic symmetry group can be explicitly constructed [116–118]. The corresponding algebra is naturally identified with a conformal algebra living on the boundary of AdS. The degeneracy of states obtained when acting with the BMS group might then be identified with the entropy of the dual CFT. Since we know from this thesis that this entropy can be

determined from the number of corpuscles constituting AdS it seems plausible that there is a mapping between the corpuscular algebra and the BMS-AdS group. Of course, these statements are still highly speculative. In order to check the validity of these claims, one needs to explicitly construct the Stückelberg degrees of freedom on the one hand and map the BMS-AdS group to the corpuscular picture on the other hand. Understanding these issues is under current investigation.

Appendix

A: Consituent Density in External Fields

For the sake of a self–contained presentation, in this appendix we derive the relation between the bi–local operator $\mathcal{O}$ representing the constituent occupation in the absence and presence of $\mathcal{G}$ to all orders in the derivative coupling on the light–cone. We follow [119].

The equation of motion (2.45) for the diagnostic device $\mathcal{O}$ can be solved iteratively. Including n derivative couplings to the gauge connection $\mathcal{G}$, the associated bi–local operator at this level is given by

$$\begin{aligned}\mathcal{O}^{(n)}(y;r/2) \quad &= \int \sigma((z)_n)\ (-1)^n \mathcal{O}^{(0)}(y_+,z_1)\mathcal{G}\cdot\partial\mathcal{O}^{(0)}(z_n,y_-) \\ &\times \prod_{a\in I(n-1)} \mathcal{G}\cdot\partial\mathcal{O}^{(0)}(z_a,z_{a+1}). \end{aligned} \tag{1}$$

Here, $y_\pm := y \pm r/2$, $I(n)$ denotes the index set $\{1,\ldots,n\}$, $\sigma(z) := \mathrm{d}^4 z$ and $\sigma((z)_n) := \sigma(z_1)\cdots\sigma(z_n)$.

Fourier–transforming the free constituent number operator $\mathcal{O}^{(0)}$,

$$\begin{aligned}\mathcal{O}^{(n)}(y;r/2) \quad &= \frac{(-\mathrm{i})^n}{(2\pi)^4}\int \sigma(k_0,k_n)\ \mathrm{e}^{\mathrm{i}(k_0-k_n)\cdot y}\mathrm{e}^{\mathrm{i}(k_0+k_n)\cdot r} \\ &\times \int \sigma((k)_{n-1})\ F(k_0,(k)_n) \prod_{a\in I(n)} k_a\cdot\mathcal{G}(k_{a-1}-k_a) \end{aligned} \tag{2}$$

where F denotes the usual propagator denominators for the specified momenta. Introducing the new momentum variables $2K := k_0 + k_n$, $2Q := k_0 - k_n$, which are Fourier–conjugated to y and r, respectively, and $q_a := k_{a-1} - k_a$, gives

$$\begin{aligned}\mathcal{O}^{(n)}(y;r/2) \quad &= \frac{(-\mathrm{i})^n}{(2\pi)^4}\int \sigma(K)\sigma(Q)\ \mathrm{e}^{\mathrm{i}2Q\cdot y}\mathrm{e}^{\mathrm{i}2K\cdot r} \\ &\times \int \sigma((q)_n)\delta^{(4)}\Big(Q - \sum_{a\in I(n)} q_a/2\Big)\ F\left(K,Q,(q)_{n-1}\right) \\ &\times \prod_{b\in I(n)} \Big(K+Q-\sum_{j=1}^{b} q_j\Big)\cdot\mathcal{G}(q_b). \end{aligned} \tag{3}$$

The scale r characterising the diagnostic process is an external scale and can be further qualified to simplify the expression for $\mathcal{O}^{(n)}(y;r/2)$. A common qualification is to make it light–like and to extract the leading light–cone contribution to $\mathcal{O}^{(n)}(y;r/2)$,

$$\begin{aligned}\mathcal{O}^{(n)}(y;r/2) \quad &= \frac{(-\mathrm{i})^n n!}{(2\pi)^4}\int \mathrm{d}u_0 \prod_{a\in I(n)} \mathrm{d}u_a\ \delta^{(1)}\Big(1-u_0-\sum_{b\in I(n)} u_b\Big)\\ &\times \prod_{c\in I(n)}\int \sigma(q_c)\ \exp\left\{\mathrm{i}\sum_{d\in I(n)} q_d\cdot\Big[y-\Big(1-2\sum_{l=1}^{d} u_l\Big)r\Big]\right\}\\ &\times \int \sigma(P)\ \exp\left(\mathrm{i}2r\cdot P\right)\prod_{m\in I(n)} P\cdot\mathcal{G}(q_c)/(P^2)^{n+1},\end{aligned}$$

where Feynman parameters have been used. The Fourier–transformation $P\to r$ requires regularisation. Employing the $\overline{\mathrm{MS}}$ scheme it is readily evaluated:

$$(2\pi)^4\frac{\mathrm{i}^n}{n!}\prod_{a\in I(n)} r^{\lambda_a}\ \mathcal{O}^{(0)}(y;r). \tag{4}$$

Performing the u_0–integration, we arrive at

$$\mathcal{O}(y;r/2)=\mathcal{P}\exp\left(-\oint_C \mathrm{d}z^\lambda \mathcal{G}_\lambda(z)\right)\mathcal{O}^{(0)}(y;r/2),$$

where C denotes the contour given by the path $z:[0,1]\to\mathbb{R}^4\,, u\to z(u):=y-(1-2u)r$, and $\mathcal{P}$ refers to path ordering along this contour.

B: Energy-Momentum Tensor

Using the defining equations for the black hole state and the energy-momentum tensor, respectively we find

$$\begin{aligned}\langle B|\mathrm{i}T_{\mu\nu}|B\rangle \quad &= \int \frac{\mathrm{d}^4P}{(2\pi)^4}\frac{\mathrm{d}^4P'}{(2\pi)^4}\frac{S_{\mu\alpha\nu\beta}}{2\Gamma_B^2}\tilde{\mathcal{B}}^*(P')\tilde{\mathcal{B}}(P)\int \mathrm{d}^4x\mathrm{d}^4y\mathrm{e}^{\mathrm{i}Px-\mathrm{i}P'y}\\ &\times \underbrace{\langle\Omega|\mathrm{T}h^N(x)\left(\partial^\alpha h(z)\right)\left(\partial^\beta h(z)\right)h^N(y)|\Omega\rangle}_{C^{\alpha\beta}(x,y,z)}\ .\end{aligned} \tag{5}$$

Let us now evaluate the correlator $C^{\alpha\beta}(x,y,z)$ at parton level. Note that due to composite operator normalization all the loop terms vanish as is explained in more detail in [8, 68]. Hence,

$$C^{\alpha\beta}(x,y,z)=2N^2\partial^\alpha\Delta(x-z)\partial^\beta\Delta(z-y)\langle\Omega|h^{N-1}(x)h^{N-1}(y)|\Omega\rangle\ , \tag{6}$$

where $\Delta(x-z)=\int\frac{\mathrm{d}^4q_i}{(2\pi)^4}\frac{\mathrm{i}}{q_i^2}\mathrm{e}^{\mathrm{i}q_i(x-z)}$ is the scalar graviton propagator. In principle, it is rather complicated to calculate this correlator exactly. It is, however, possible to evaluate

it in the limit of large black hole mass M. For that purpose we shift the momenta q and l occurring in the propagator by the black hole momenta P' and P, respectively. In particular, let us define $\tilde{q} = q - P'$ and $\tilde{l} = l - P$. As explained in Section 3, we can implement an on-shell condition on the black hole momenta in terms of the P_0 and P_0' integrations, respectively. This on-shell condition will be understood implicitly in what follows. Then, we have $P^2 = P'^2 = -M^2$ and $P_0^2 = M^2 + \mathbf{P}^2 \simeq M^2$ for large black hole mass (of course, the same approximation applies for P_0'). Using these relations, we can expand the propagators in inverse powers of M. Keeping the leading terms in this expansion[1], we arrive at

$$\begin{aligned}\langle B|\mathrm{i}T_{00}|B\rangle = \quad & \frac{N^2}{M^2\Gamma_B^2}\int\frac{\mathrm{d}^4P}{(2\pi)^4}\frac{\mathrm{d}^4P'}{(2\pi)^4}\tilde{\mathcal{B}}^*(P')\tilde{\mathcal{B}}(P)\int\frac{\mathrm{d}^4\tilde{q}}{(2\pi)^4}\frac{\mathrm{d}^4\tilde{l}}{(2\pi)^4}\mathrm{d}^4x\mathrm{d}^4y \\ & \times\left(1+\mathrm{i}\frac{\partial_{y_0}}{M}-\mathrm{i}\frac{\partial_{x_0}}{M}-\frac{2}{M^2}\left(2\partial_{x_0}\partial_{y_0}-\partial_{x_0}^2-\partial_{y_0}^2\right)\right) \\ & \times\mathrm{e}^{\mathrm{i}\tilde{q}(y-z)}\mathrm{e}^{\mathrm{i}\tilde{l}(z-z)}\mathrm{e}^{\mathrm{i}z(P-P')}\langle\Omega|h^{N-1}(x)h^{N-1}(y)|\Omega\rangle\ . \end{aligned} \tag{7}$$

Performing the integrations over $\tilde{q}$ and $\tilde{l}$, we observe that the terms linear in derivatives cancel. Finally, using unitary similarity transformations on the condensates as well as (2.48), we arrive at the desired expression.

C: Derivation of $\mathcal{G}_{kink}$

In order to determine $\mathcal{G}_{kink}$ we first have to express the BPS-Operator $\mathcal{O}_{BPS}$ in terms of of the creation annihilation operators of the scalar field ϕ_c. Notice that from now on the field is understood as an operator.

$$\begin{aligned}\mathcal{O}_{BPS} \quad & = \partial_x\phi_c - \left(m^2/g - g\phi_c^2\right) \\ & = \mathrm{i}\sqrt{R}\int\frac{dk}{\sqrt{4\pi|k|}}k\left(e^{ikx}\hat{a}_k\ -\ e^{-ikx}\hat{a}_k^\dagger\right) - m^2/g \\ & +gR\int\frac{dkdq}{4\pi\sqrt{|k||q|}}\left(e^{ikx}\hat{a}_k\ +\ e^{-ikx}\hat{a}_k^\dagger\right)\left(e^{iqx}\hat{a}_q\ +\ e^{-iqx}\hat{a}_q^\dagger\right) \end{aligned} \tag{8}$$

Here we simple expanded the Fourier expansion of the field operator. Now we have to evaluate $\mathcal{O}_{BPS}^2$. This, for example, gives rise to terms of the form $\hat{a}_k\hat{a}_q^\dagger\hat{a}_p\hat{a}_l^\dagger$. Using the commutation relation $\left[\hat{a}_k,\hat{a}_q^\dagger\right] = \delta(k-q)/R$ we can normal order all the terms which appear. The normal ordered products simply yield the classical result, while the terms

[1]It is important to mention that in principle we have to integrate over all momenta. Thus, for large but finite M, in general there will be contributions to the integrals where $\tilde{q} \sim M$ and similarly for $\tilde{l}$. This problem can be circumvented by introducing a physical cut-off $\Lambda \ll M$. Physically such a cut-off makes perfekt sense as we should not be sensitive to momenta which are larger than the Planck mass.

containing commutators give rise to quantum effects.

$$\begin{aligned}\mathcal{O}^2_{BPS} \quad &= :\Bigg[\mathrm{i}\sqrt{R}\int \frac{dk}{\sqrt{4\pi|k|}}k\,(e^{ikx}\hat{a}_k - e^{-ikx}\hat{a}_k^\dagger) - m^2/g \\ &\quad +gR\int \frac{dkdq}{4\pi\sqrt{|k||q|}}\,(e^{ikx}\hat{a}_k + e^{-ikx}\hat{a}_k^\dagger)(e^{iqx}\hat{a}_q + e^{-iqx}\hat{a}_q^\dagger)\Bigg]^2: \\ &\quad +6:g^2R\int \frac{dkdq}{4\pi\sqrt{|k||q|}}\,(e^{ikx}\hat{a}_k + e^{-ikx}\hat{a}_k^\dagger)(e^{iqx}\hat{a}_q + e^{-iqx}\hat{a}_q^\dagger):\int \frac{dk}{4\pi|k|} \\ &\quad +2\mathrm{i}\sqrt{R}\int \frac{dk}{\sqrt{4\pi|k|}}k\,(e^{ikx}\hat{a}_k - e^{-ikx}\hat{a}_k^\dagger)\int \frac{dk}{4\pi|k|} \end{aligned} \tag{9}$$

Here we neglected the terms which correspond to the vacuum contribution which do not contain any information about the soliton state. The first two lines correspond to the classical BPS operator which vanishes on the soliton. Line three and four correspond to quantum correction to the BPS equation. They would vanish on a non-solitonic vacuum state (due to normal ordering), but not on a solitonic, coherent state. The divergent integral emerges because the commutator results in a δ-function. Thus only one integral vanishes. Evaluating this integral and regulating it like explained above we arrive at

$$\begin{aligned}\langle\phi_c|\mathcal{O}^2_{BPS}|\phi_c\rangle \quad &= \underbrace{\Big[\partial_x\phi_c - \Big(m^2/g - g\phi_c^2\Big)\Big]^2}_{=0 \text{ because this is the classical BPS condition}} \\ &\quad +\frac{1}{\pi}(g\partial_x\phi_c(x) + 3g^2\phi_c^2)\log\Big(\frac{\Lambda}{\mu}\Big)\,, \end{aligned} \tag{10}$$

where we used $\langle\phi_c|c_k|\phi_c\rangle = \sqrt{N_k}$. Thus we exactly recover equation (3.149).

D: Scalar Propagator in AdS

In this appendix we want to collect formulas needed in our study of scalar propagators in AdS space-time. The Green's function solving equation (3.189) is given by

$$G_c(X,Y) = \frac{2}{C_\Delta}\Big(\frac{\xi}{2}\Big)^\Delta F\Big(\frac{\Delta}{2}, \frac{\Delta}{2}+\frac{1}{2}, \nu+1, \xi^2\Big), \tag{11}$$

with F the hypergeometric function. Δ denotes the scaling exponent of the scalar field in AdS in $(d+1)$ space-time dimensions,

$$\Delta = \frac{d}{2} + \nu, \quad \nu = \sqrt{\frac{d^2}{4} + m^2R^2}. \tag{12}$$

Furthermore, the constant C_Δ is given by

$$C_\Delta = \frac{\Gamma(\Delta)}{\pi^{d/2}\Gamma(\nu)} \tag{13}$$

where Γ is the gamma-function. Finally, the parameter ξ carries the dependence on the coordinates as follows:

$$\xi = \frac{2z_1 z_2}{z_1^2 + z_2^2 + (x_1 - x_2)^2}, \tag{14}$$

where the notation matches that of Section (3.5).

Bibliography

[1] ATLAS Collaboration, *Observation of a new particle in the search for the Standard Model Higgs boson with the ATLAS detector at the LHC*, Phys. Lett. **B 716** (2013) 1-29.

[2] WMAP Collaboration, *Nine-Year Wilkinson Microwave Anisotropy Probe (WMAP) Observations: Final Maps and Results*, *Astrophys.J.Suppl.* **2008** (2013) 20.

[3] J. Schwinger, *On gauge invariance and vacuum polarization* , *Phys.Rev.* **82** (1951) 664-679.

[4] S. Hawking, *Particle Creation by Black Holes*, *Commun.Math.Phys.* **43** (1975) 199-220.

[5] S. Hawking, *Breakdown of Predictability in Gravitational Collapse*, *Phys.Rev.* **D 14** (1976) 2460-2473.

[6] A. Strominger and C. Vafa, *Microscopic origin of the Bekenstein-Hawking entropy*, *Phys.Lett.* **B 379** (1996) 99-104.

[7] S. Mathur, *The Fuzzball proposal for black holes: An Elementary review*, *Fortschr.Phys.* **53** (2005) 793-827.

[8] S. Hofmann and T. Rug, *A Quantum Bound-State Description of Black Holes*, *Nucl.Phys.* **B902** (2016) 302-325.

[9] L. Gruending, S. Hofmann, S. Mueller and T. Rug, *Probing the Constituent Structure of Black Holes*, *JHEP* **1505** (2015) 047.

[10] G. Dvali, C. Gomez, L. Gruending and T. Rug, *Towards a Quantum Theory of Solitons*, *Nucl.Phys.* **B901** (2015) 338-353.

[11] S. Hofmann and M. Schneider, *Classical versus quantum completeness*, *Phys.Rev.* **D 91** (2015) 125028.

[12] J. Bekenstein, *Black holes and entropy*, *Phys.Rev.* **D 7** (1973) 2333-2346.

[13] G. 't Hooft, *Dimensional reduction in quantum gravity*, *Salamfest* (1993) 0284-296.

[14] L. Susskind, *The World as a hologram*, *J.Math.Phys.* **36** (1995) 6377-6396.

[15] J. Maldacena, *The Large N limit of superconformal field theories and supergravity*, *Int.J.Theor.Phys.* **38** (1999) 1113-1133, *Adv.Theor.Math.Phys.* **2** (1998) 231-252.

[16] E. Witten, *Anti-de Sitter space and holography*, *Adv.Theor.Math.Phys.* **2** (1998) 253-291.

[17] S. Gubser, I. Klebanov and A. Polyakov, *Gauge theory correlators from noncritical string theory*, *Phys.Lett.* **B 428** (1998) 105-114.

[18] G. Dvali, *Black Holes and Large N Species Solution to the Hierarchy Problem*, *Fortschr. Phys.* **58** (2010) 528-536.

[19] L. Susskind, L. Thorlacius and J. Uglum, *The Stretched horizon and black hole complementarity*, *Phys.Rev.* **D 48** (1993) 3743-3761.

[20] L. Susskind and L. Thorlacius, *Gedanken experiments involving black holes*, *Phys.Rev.* **D 49** (1994) 966-974.

[21] A. Almheiri, D. Marolf, J. Polchinski and J. Sully, *Black Holes: Complementarity or Firewalls*, *JHEP* **1302** (2013) 062.

[22] D. N. Page, *Information in black hole radiation*, *Phys.Rev.Lett* **71** (1993) 3743-3746.

[23] G. Dvali and C. Gomez, *Black hole's quantum N-portrait*, *Fortschr. Phys.* **61** (2013) 742.

[24] G. Dvali and C. Gomez, *Black hole's 1/N hair*, *Phys. Lett.* **B 719** (2013) 419.

[25] G. Dvali and C. Gomez, *Quantum Compositeness of Gravity: Black Holes, AdS and Inflation*, *JCAP* **1401** (2014) 023.

[26] T. Banks, W. Fischler, I. R. Klebanov and L. Susskind, *Schwarzschild Black Holes from Matrix Theory*, *Phys. Rev.* **B 80** (1998) 226.

[27] G. Dvali and C. Gomez, *Black Holes as Critical Point of Quantum Phase Transition*, *Europ.Phys.J* **C 74** (2014) 2752.

[28] D. Flassig, A. Pritzel and N. Wintergerst, *Black holes and quantumness on macroscopic scales*, *Phys.Rev.* **D 87** (2013) 8, 084007.

[29] F. Berkhahn, S. Muller, F. Niedermann and R. Schneider, *Microscopic Picture of Non-Relativistic Classicalons*, *JCAP* **1308** (2013) 028.

[30] G. Dvali, D. Flassig, C. Gomez, A. Pritzel and N. Wintergerst, *Scrambling in the Black Hole Portrait*, *Phys.Rev* **D 88** (2013) 12, 124041.

[31] G. Dvali, D. Flassig, C. Gomez, A. Pritzel and N. Wintergerst, *Nambu-Goldstone Effective Theory of Information at Quantum Criticality*, *arXiv:1507.02948 [hep-th]* (2015).

[32] G. Dvali and M. Panchenko, *Black Hole Type Quantum Computing in Critical Bose-Einstein Systems* , *arXiv: 1507.08952 [hep-th]* (2015).

[33] G. Dvali, C. Gomez, R. Isermann, D. Lüst and S. Stieberger, *Black hole formation and classicalization in ultra-Planckian 2N scattering*, *Nucl.Phys.* **B 893** (2015) 187-235.

[34] V. F. Foit and N. Wintergerst, *Self-similar Evaporation and Collapse in the Quantum Portrait of Black Holes*, *Phys.Rev.* **D 92** (2015) 6, 064043.

[35] G. Dvali, and C. Gomez, *Black Hole Macro-Quantumness*, *arXiv:1212.0765 [hep-th]* (2012).

[36] Y. Sekino and L. Susskind, *Fast Scramblers*, *JHEP* **0810** (2008) 065.

[37] G. Dvali, and C. Gomez, *Quantum Exclusion of Positive Cosmological Constant?*, *arXiv:1412.8077 [hep-th]* (2014).

[38] S. Weinberg, *THE QUANTUM THEORY OF FIELDS, VOLUME 2*, *CAMBRIDGE UNIVERSITY PRESS* (2001).

[39] M. Shifman, *ADVANCED TOPICS IN Quantum Field Theory*, *CAMBRIDGE UNIVERSITY PRESS* (2012).

[40] R. Jackiw and C. Rebbi, *Solitons with Fermion Number 1/2*, *Phys. Rev.* **D 13** (1976) 3398-3409.

[41] U. Jentschura and J. Zinn-Justin, *Multi-instantons and exact results I: Conjectures, WKB expansions, and instanton interactions* , *Annals Phys.* **313** (2004) 197-267.

[42] U. Jentschura and J. Zinn-Justin, *Multi-instantons and exact results II: Specific cases, higher-order effects, and numerical calculations* , *Annals Phys.* **313** (2004) 269-325.

[43] C. Bachas, G. Lazarides, Q. Shafi and G. Tiktopoulos, *Quantum mechanical tunneling at high-energy*, *Phys.Lett* **B 268** (1991) 401-407.

[44] G. V. Dunne and M. Ünsal, *Generating nonperturbative physics from perturbation theory*, *Phys.Rev.* **D 89** (2014) 4, 041701.

[45] G. V. Dunne and M. Ünsal, *Uniform WKB, Multi-instantons, and Resurgent Trans-Series*, *Phys.Rev.* **D 89** (2014) 10, 105009.

[46] G. V. Dunne and M. Ünsal, *Resurgence and Trans-series in Quantum Field Theory: The CP(N-1) Model*, *JHEP* **1211** (2012) 170.

[47] A. Cherman, D. Dorigoni, G. V. Dunne and M. Ünsal, *Resurgence in Quantum Field Theory: Nonperturbative Effects in the Principal Chiral Model*, *Phys.Rev.Lett.* **122** (2014) 021601.

[48] M. Marino, R. Schiappa and M. Weiss, *Nonperturbative Effects and the Large-Order Behavior of Matrix Models and Topological Strings*, *Comm.Num.Theor.Phys.* **2** (2008) 349-419.

[49] S. Pasquetti and R. Schiappa, *Borel and Stokes Nonperturbative Phenomena in Topological String Theory and c=1 Matrix Models* , *Annales Henri Poincare* **11** (2010) 351-431.

[50] A. Belavin, A. Polyakov, A. Schwartz and Y. Tyupkin, *Pseudoparticle Solutions of the Yang-Mills Equations*, *Phys.Lett.* **B 59** (1975) 85-87.

[51] S. Coleman and J. Mandula, *All Possible Symmetries of the S Matrix*, *Phys.Rev.* **159** (1967) 1251-1256.

[52] J. Wee and J. Bagger, *Supersymmetry and Supergravity*, *Princeton University Press* (1992).

[53] N. Seiberg, *The Power of holomorphy: Exact results in 4-D SUSY field theories*, *arXiv:9408013 [hep-th]* (1994).

[54] E. Witten, *Dynamical Breaking of Supersymmetry*, *Nucl.Phys.* **B 188** (1981) 513.

[55] M. Shifman and A. Vainshtein, *Instantons versus supersymmetry: Fifteen years later* ITEP lectures on particle physics and field theory, vol **2*** (1999) 482-647.

[56] M. Peskin and D. Schroeder, *An Introduction To Quantum Field Theory*, *Frontiers in Physics* (1995).

[57] G. Altarelli and G. Parisi. *Asymptotic Freedom in Parton Language*, *Nucl.Phys.* **B 126** (1977) 298.

[58] M. Shifman, A. Vainshtein and V. Zakharov, *QCD and Resonance Physics: Applications* , *Nucl. Phys.* **B 47** (1979) 448.

[59] W. Zimmermann, *On the bound state problem in quantum field theory*, *Nuovo Cim.***10** (1958) 199.

[60] K. Nishijima, *Formulation of Field Theories of Composite Particles* , emph-Phys.Rev.**111** (1958) 995.

[61] J. Berges, *Chiral Phase Transition from Non-Perturbative Flow Equations*, *arXiv:9708341 [hep-ph]* (1997).

[62] M. Shifman, *Quark hadron duality*, *At the frontier of particle physics*, 3 1447-1494 (2000) 42.

[63] G. Dunne, M. Shifman and M. Unsal, *Infrared Renormalons versus Operator Product Expansions in Supersymmetric and Related Gauge Theories*, *Phys. Rev. Lett.* **114** (2015) 19.

[64] E. Kuraev, L. Lipatov and V. Fadin, *Multi - Reggeon Processes in the Yang-Mills Theory*, *Sov. Phys. JETP* **44** (1976) 443.

[65] E. Kuraev, L. Lipatov and V. Fadin, *The Pomeranchuk Singularity in Nonabelian Gauge Theorie*, *Sov. Phys. JETP* **45** (1977) 199.

[66] F. Gelis, E. Iancu, J. Jalilian-Marian and R. Venugopalan, *The Color Glass Condensate*, *Ann. Rev. Nucl. Part. Sci* **60** (2010) 463.

[67] M. Duff, *Quantum Tree Graphs and the Schwarzschild Solution*, *Phys. Rev.* **D 7**, (1973) 2317.

[68] E. Witten, *Perturbative Renormalization*, *lecture notes, unpublished*.

[69] B. L. Ioffe, *Space–time picture of photon and neutrino scattering and electroproduction cross section asymptotics*, *Phys. Lett. B* **30** (1969) 123.

[70] V. Braun, P. Gornicki and L. Mankiewicz, *Ioffe–time distributions instead of parton momentum distributions in description of deep inelastic scattering*, *Phys. Rev. D* **51** (1995) 6036.

[71] J. C. Collins and D. E. Soper, *Parton Distribution and Decay Functions*, *Nucl.Phys. B* **194**, (1982) 445.

[72] T. Muta, *Foundations of Quantum Chromodynamics*, *World Scientific Lecture Notes in Physics: Volume* **78**.

[73] R. Glauber, *Coherent and incoherent states of the radiation field*, *Phys.Rev.* **131**, (1963) 2766-2788.

[74] S. Coleman, *The Quantum Sine-Gordon Equation as the Massive Thirring Model*, *Phys. Rev. D* **11**, (1975) 2088.

[75] S. Mandelstam, *Soliton operators for the quantized sine-Gordon equation*, *Phys. Rev. D* **11**, (1975) 3026.

[76] G. Dvali and C. Gomez, *Corpuscular Breaking of Supersymmetry*, (2014) arxiv:1406.6014 [hep-th] .

[77] S. Coleman, *Fate of the false vacuum: Semiclassical theory*, *Phys. Rev. D* **15** (1977) 2929.

[78] G. Dvali, M. Shifman, *Domain walls in strongly coupled theories*, *Phys. Lett. B* **396** (1997) 64-69, *Phys. Lett. B* **407**, (1997) 452.

[79] G. Dvali, H. Nielsen, N. Tetradis, *Localization of gauge fields and monopole tunneling*, Phys.Rev. D77 (2008) 085005.

[80] D. Flassig, A. Pritzel, *Localization of gauge fields and Maxwell-Chern-Simons theory*, Phys.Rev. D84 (2011) 125024.

[81] M. Dierigl, A. Pritzel, *Topological Model for Domain Walls in (Super-)Yang-Mills Theories*, Phys.Rev. D90 (2014) 10, 105008.

[82] A. Polyakov, *Quark Confinement and Topology of Gauge Theories*, *Nucl. Phys. B* **120**, (1977) 429.

[83] I. Affleck, *On Constrained Instantons*, *Nucl. Phys. B* **191**, (1981) 429.

[84] L. Susskind and E. Witten, *The Holographic bound in anti-de Sitter space*, (1998) arXiv:9805114 [hep-th].

[85] L. Randall and R. Sundrum, *A Large mass hierarchy from a small extra dimension*, *Phys. Rev. Lett.* **83**, (1999) 3370.

[86] L. Randall and R. Sundrum, *An Alternative to compactification*, *Phys.Rev.Lett.* **83** (1999) 4690-4693.

[87] N. Arkani-Hamed, S. Dimopoulos and G. Dvali, *The Hierarchy problem and new dimensions at a millimeter*, *Phys. Lett. B* **429**, (1998) 263.

[88] E. Alvarez and C. Gomez, *Geometric holography, the renormalization group and the c theorem*, *Nucl. Phys. B* **541**, (1999) 441.

[89] L. Girardello, M. Petrini, M. Porrati and A. Zaffaroni, *Novel local CFT and exact results on perturbations of N=4 superYang Mills from AdS dynamics*, *JHEP* **9812**, (1998) 022.

[90] D. Freedman, S. Gubser, K. Pilch and N. P. Warner, *Renormalization group flows from holography supersymmetry and a c theorem*, *Adv. Theor. Math. Phys.* **3**, (1999) 363.

[91] I. Heemskerk and J. Polchinski, *Holographic and Wilsonian Renormalization Groups*, *JHEP* **1106**, (2011) 031.

[92] T. Faulkner, H. Liu and M. Rangamani, *Integrating out geometry: Holographic Wilsonian RG and the membrane paradigm*, *JHEP* **1108**, (2011) 051.

[93] D. Sarkar, *(A)dS holography with a cutoff*, *Phys. Rev. D* **90**, (2014) 086005.

[94] A. Zamolodchikov, *Irreversibility of the Flux of the Renormalization Group in a 2D Field Theory*, *JETP Lett.* **43**, (1986) 730.

[95] Z. Komargodski and A. Schwimmer, *On Renormalization Group Flows in Four Dimensions*, *JHEP* **1112**, (2011) 099.

[96] Z. Komargodski, *The Constraints of Conformal Symmetry on RG Flows*, *JHEP* **1207**, (2012) 069.

[97] D. Jafferis, I. Klebanov, S. Pufu and B. Safdi, *Towards the F-Theorem: N=2 Field Theories on the Three-Sphere*, *JHEP* **1106**, (2011) 102.

[98] I. Affleck and A. Ludwig, *Universal noninteger 'ground state degeneracy' in critical quantum systems*, *Phys. Rev. Lett.* **67**, (1991) 161.

[99] I. Klebanov and A. Polyakov, *AdS dual of the critical O(N) vector model*, *Phys. Lett. B* **550**, (2002) 213.

[100] S. Ryu and T. Takayanagi, *Holographic derivation of entanglement entropy from AdS/CFT*, *Phys. Rev. Lett.* **96**, (2006) 181602.

[101] R. Myers and A. Sinha, *Holographic c-theorems in arbitrary dimensions*, *JHEP* **1101**, (2011) 125.

[102] D. Capper and M. Duff, *Conformal Anomalies and the Renormalizability Problem in Quantum Gravity*, *Phys. Lett. A* **53**, (1975) 361.

[103] S. Christensen and M. Duff, *Axial and Conformal Anomalies for Arbitrary Spin in Gravity and Supergravity*, *Phys. Lett. B* **76**, (1978) 571.

[104] M. Henningson and K. Skenderis, *Holography and the Weyl anomaly*, *Fortsch. Phys.* **48**, (2000) 125.

[105] N. Birrel and P. Davies, *Quantum Fields in Curved Space*, *Cambridge Monographs on Mathematical Physics* (1984).

[106] G. Dvali, S. Hofmann and J. Khoury, *Degravitation of the cosmological constant and graviton width Phys.Rev. D* **76** (2007) 084006.

[107] S. Deser and O. Levin, *Accelerated detectors and temperature in (anti)-de Sitter spaces*, *Class.Quant.Grav.* **14** (1997) L163-L168.

[108] G. Dvali, C. Gomez and D. Lust, *Classical Limit of Black Hole Quantum N-Portrait and BMS Symmetry*, *Phys. Lett. B* **753** (2016) 173 - 177.

[109] D. Jennings, *On the response of a particle detector in Anti-de Sitter spacetime*, *Class.Quant.Grav.* **27** (2010) 205005.

[110] G. Dvali, C. Gomez and N. Wintergerst, *Stückelberg Formulation of Holography* , (2015) 1511.03525 [hep-th].

[111] A. Averin, D. Dvali, C. Gomez and D. Lust, *Gravitational Black Hole Hair from Event Horizon Supertranslations*, (2016) arXiv:1601.03725 [hep-th].

[112] H. Bondi, M. van der Burg, A. Metzner, *Gravitational waves in general relativity VII. Waves from isolated axisymmetric systems*, *Proc.Roy.Soc.Lond. A* **269**, (1962) 21.

[113] R. K. Sachs, *Gravitational waves in general relativity VIII. Waves in asymptotically flat space-time*, *Proc.Roy.Soc.Lond. A* **270**, (1962) 103.

[114] A. Strominger, *On BMS Invariance of Gravitational Scattering* , *JHEP* **1407**, (2014) 152.

[115] T. He, V. Lysov, P. Mitra and A. Strominger, *BMS supertranslations and Weinbergs soft graviton theorem*, *JHEP*, **1505**, (2015) 151.

[116] J. Brown and M. Henneaux, *Central Charges in the Canonical Realization of Asymptotic Symmetries: An Example from Three-Dimensional Gravity*, *Commun.Math.Phys.* **104** (1986) 207 - 226.

[117] M. Henneaux and C. Teitelboim, *Asymptotically anti-De Sitter Spaces*, *Commun.Math.Phys.* **98** (1985) 391 - 424.

[118] A. Ashtekar and S. Das, *Asymptotically Anti-de Sitter space-times: Conserved quantities*, *Class.Quant.Grav.* **17** (2000) L17 - L30.

[119] D. Gross and S. Treimann, *Light-Cone Structure of Current Commutators in the Gluon-Quark Model*, *Physical Review* **D 4** (1971) 1059.

Acknowledgements

First of all I want to thank Gia Dvali for his support and guidance over the past years. I am grateful for all the interesting physical discussions we had and the insights he shared we me. I want to thank him for sharpening my intuition concerning various physical questions ranging from quantum field theory to quantum gravity. Collaborating with Gia was one of the most instructive and exciting experiences I had.

Furthermore, I want to thank Stefan Hofmann as well as Cesar Gomez for all the interesting questions we discussed (and partially answered) during the last years. It is truly amazing how much I learned about physics by collaborating with the two of you. I appreciate that both of you agreed to be part of my PhD committee.

It is a pleasure to thank all people I collaborated with during the last years: Gia Dvali, Lukas Gruending, Cesar Gomez, Stefan Hofmann, Sophia Mueller, Maximilian Koegler and Debayoti Sarkar. A lot of material covered in this thesis originated from the countless hours we spent working on physical problems.

Thanks go out to all my colleagues at the Arnold Sommerfeld Center and the Max-Planck Institute for the good times we had and for the various interesting discussions about physics: Daniel, Nico, Sarah, Alex P., Alex G., Andre, Clausius, Oscar, Deb, Cristiano, Lukas, Sebastian K., Sebastian Z., Korbi, Lena, Misha, Artem, Rainke, Flo, Rob, Sophia, Marc, Cora, Thomas, Michi, Alexis, Tobias, Raoul, Max K., Max W., David, Valentino and many others.

It is a pleasure to thank Lukas, Sophia, Sebastian Z., Maximilian K. Florian, Rob and Marc for proofreading and improving parts of this thesis.

Thanks to Gabi and Hertha as well as Monika for their support in administrative questions at the ASC and the MPI, respectively. In this context, I want to thank the MPI for the financial support over the last three years.

A special shoutout goes to all of my friends. I thank you for all the funny evenings and nights that we spent together. There were countless crazy adventures which I will never forget. In addition, I appreciate that I can rely on all of you in case there is something important that I need to talk about. Whenever there is a hard decision which I have to make, I know that I can count on you advice. For these among many other things I am truly grateful.

The last lines of this thesis are dedicated to my family and in particular my mother. Through all my life you were the one person I knew I could always rely on. No matter how difficult times were, I could count on you. You raised me, Sarah and Yasin with so much

dedication and love. No words can describe how thankful I am for that. I love you.